Indian J. Chem. Vol. 27A No. 11 pp. 923-1012
November 1988
CODEN : IJOCAP ISSN : 0019-5103
27(A)(11) 923-1012 (1988)

Indian Journal of
CHEMISTRY

SECTION A
(Inorganic, Physical, Theoretical & Analytical)

Published by
PUBLICATIONS & INFORMATION DIRECTORATE, CSIR, NEW DELHI
in association with
THE INDIAN NATIONAL SCIENCE ACADEMY, NEW DELHI

A RANGE OF HIGH PRECISION, HIGH QUALITY RECORDING INSTRUMENTS FOR THE DISCRIMINATING RESEARCH SCIENTIST

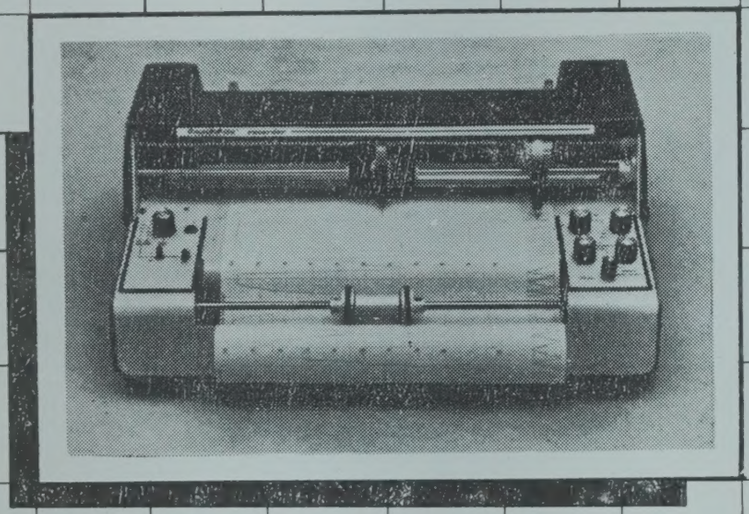

Series 5000 Strip Chart Recorder

The series 5000 Strip Chart Recorder and the series 2000 XY Recorder are well proven instruments incorporating State of the Art Circuitry. A wide range of models offer tremendous flexibility to the user. With over 5000 installations, these instruments are the preferred choice of discriminating users all over India.

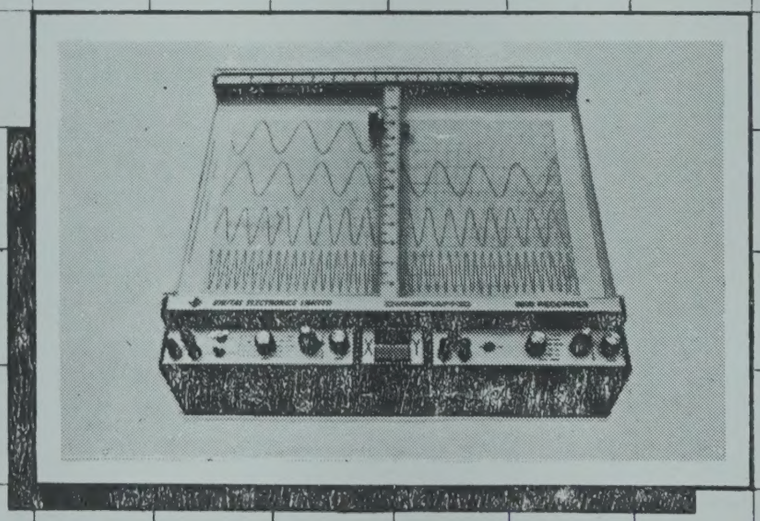

Series 2000 XY Recorder

Another quality product from

DIGITAL ELECTRONICS LIMITED

Reliability in Recording Instruments.

Digilog House 74/II, Marol Industrial Area MIDC, Andheri (East), Bombay- 400 093 Tel: 634 09 01, 632 86 76 Grams: 'DIGILOG'

A Company in collaboration with houston instrument

Special Effects/DE/25/86

RENEWAL NOTICE

Your subscription which expires with the despatch of December 1988 issue of the journal, stands for renewal. We request you to be so good as to return the enclosed order form duly filled early, so as to ensure continuity in despatch.

Sales & Distribution Officer

DATED:

The Sales & Distribution Officer
PUBLICATIONS & INFORMATION DIRECTORATE
HILLSIDE ROAD, NEW DELHI-110012 (INDIA)

Dear Sir,

Please renew my subscription/enrol me as subscriber to:

			Rs.	$	£
1	Journal of Scientific & Industrial Research	(Monthly)	200.00	70.00	45.00
2	Indian Journal of Chemistry, Section A	(Monthly)	300.00	100.00	70.00
3	Indian Journal of Chemistry, Section B	(Monthly)	300.00	100.00	70.00
4	Indian Journal of Experimental Biology	(Monthly)	250.00	85.00	55.00
5	Indian Journal of Technology	(Monthly)	250.00	85.00	55.00
6	Indian Journal of Pure & Applied Physics	(Monthly)	250.00	85.00	55.00
7	Indian Journal of Biochemistry & Biophysics	(Bimonthly)	125.00	42.00	28.00
8	Indian Journal of Radio & Space Physics	(Bimonthly)	125.00	42.00	28.00
9	Indian Journal of Marine Sciences	(Quarterly)	125.00	42.00	28.00
10	Indian Journal of Textile Research	(Quarterly)	125.00	42.00	28.00
11	Research & Industry	(Quarterly)	125.00	42.00	28.00
12	Current Literature on Science of Science	(Monthly)	100.00	30.00	12.00
13	Medicinal & Aromatic Plants Abstracts	(Bimonthly)	225.00	75.00	50.00

(Please tick off the periodicals you would like to subscribe).

for one year from January 1989 for which I/we have remitted to you a sum of Rs .....£ ..... $ ..... by Cheque/Demand Draft No. ..... dated ..... in favour of PUBLICATIONS & INFORMATION DIRECTORATE, NEW DELHI.

COMPLETE MAILING ADDRESS

Name .....

Address .....

Country/State .....

(Signature)

Note:

1. Subscribers at annual rates for all the periodicals are enlisted for the full volumes, i.e. for the period from January to December only.
2. The Cheque Demand Draft may plese be drawn in favour of "PUBLICATIONS & INFORMATION DIRECTORATE, NEW DELHI". Banking charges shall be borne by the subscriber. For inland outstation cheques please add Rs. 3.50. For foreign cheques please add $ 1.00 or £ 0.45.
3. The supply will commence on receipt of subscription in advance.

INDIAN JOURNAL OF CHEMISTRY

Section A: Inorganic, Physical, Theoretical & Analytical Chemistry

Published by the Publications & Information Directorate (CSIR), Hillside Road, New Delhi 110 012

Editor-in-Chief: S.P. Ambasta

The Indian Journal of Chemistry is issued monthly in two sections: A and B. Communications regarding contributions for publication in the journal should be addressed to the Editor, Indian Journal of Chemistry, Publications & Information Directorate, Hillside Road, New Delhi 110 012.

Correspondence regarding subscriptions and advertisements should be addressed to the Sales & Distribution Officer, Publications & Information Directorate, hillside Road, New Delhi 110 012.

The Publications & Information Directorate (CSIR) assumes no responsibility for the statements and opinions advanced by contributors. The Editorial Board in its work of examining papers received for publication is assisted, in an honorary capacity by a large number of distinguished scientists, working in various parts of India.

Annual Subscription: Rs. 300.00 £ 70.00 $ 100.00; 50% discount admissible to research workers and students and 25% discount to non-research individuals on annual subscription.

Single Copy: Rs. 30.00 £ 7.00 $ 10.00

Payments in respect of subscriptions and advertisements may be sent by cheque, bank draft, money order or postal order marked payable to Publications & Information Directorate, Hillside Road, New Delhi 110 012.

Claims for missing numbers will be allowed only if received within 3 months of the date of issue of the journal plus the time normally required for postal delivery of the journal and the claim.

AUTHOR INDEX

Indian Journal of Chemistry

Sect. A : Inorganic, Physical, Theoretical & Analytical

VOLUME 27A NUMBER 11 NOVEMBER 1988

CONTENTS

Continued overleaf

CONTENTS

Notes

Authors for correspondence are indicated by (*)

Indian Journal of Chemistry
Vol. 27A, November 1988, pp. 923-931

Correlation between Topological Features & Physicochemical Properties of Alkylbenzenes

D V S JAIN*, SUKHBIR SINGH & VIJAY K GOMBAR†
Department of Chemistry, Panjab University, Chandigarh 160 014

Received 8 *June* 1987; *revised and accepted* 8 *February* 1988

Quantitative relationships are developed between some physicochemical properties and topological features of alkylbenzenes. Valence connectivity indices of different orders and types ($^{m}\chi_t^v$) are employed to encode molecular topology and the properties regressed are enthalpy of atomisation (ΔH_a) and vaporisation (ΔH_v) at 298.15K, boiling point (t_b), molar volume (v_M) and molar refraction [R] at 293.15K and diamagnetic susceptibility (χ_M). A high degree of correlation ($r > 0.99$) in all the cases indicates the role of molecular size and shape in these properties. The relationships are statistically significant and can be employed to predict the properties with confidence within the experimental limits.

Connectivity indices $^{m}\chi_t^1$ of different order (m), type (t) and complexity level (1) have been shown to effectively quantify molecular topology[1-3]. We have been interested in developing quantitative relationship between topological features and physicochemical properties. Some of the earlier papers from these laboratories included correlations of connectivity indices with positronium annihilation cross sections[4], boiling points of saturated aliphatic monocarboxylic acids[5], molar and excess volumes of mixtures of *n*-alkanes[6], critical constants[7] and the second virial coefficient[8] of alkanes, alkylbenzenes and aliphatic acylic monoalkanols. The present work concerns the correlation of connectivity indices with boiling points (t_b) enthalpies of vaporisation (ΔH_v), enthalpies of atomisation (ΔH_a), molar volumes, v_M, molar refractions [R] and diamagnetic susceptibilities, (χ_M) of a series of alkyl substituted benzenes.

Methods

Calculation of connectivity indices

The calculation of connectivity indices associated with a molecule (Fig. 1a), begins by drawing a hydrogen suppressed graph (HSG) (Fig. 1b), whose vertices and edges represent non-hydrogen atoms and bonds, respectively, in the molecule. Each vertex is then assigned a numerical value δ^v, called valence δ-value, which for alkylbenzenes is related to the number of hydrogens (h_i) suppressed at a given vertex (i) by Eq. (1). For 1,3,5-trimethylbenzene, for instance, the vertices

$$\delta_i^v = 4 - h_i \qquad \ldots (1)$$

1 to 9 have δ^v values 4, 3, 4, 3, 4, 3, 1, 1 and 1, respectively (Fig. 1). In order to compute valence connectivity index ($^{m}\chi_t^v$) order m and type t, $^{m}\chi_t^v$, where m and t refer to the number and arrangement of vertices, all the subgraphs $^{m}g_t$ are identified and contribution C_j calculated for each of these using Eq. (2) and summed up, Eq. (3).

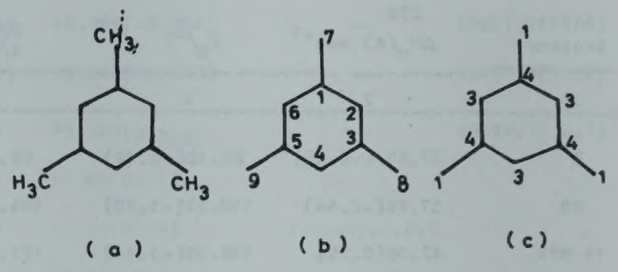

Fig: 1 Structure (a), HSG (b) and δ^v (c) values for 1,3,5, trimethylbenzene.

$$C_j = \prod_{R=1}^{m+1} (\delta_R^v)_j^{-1/2} \qquad \ldots (2)$$

$$^{m}\chi_t^v = \sum_{j=1}^{^{m}g_t} C_j \qquad \ldots (3)$$

Since identification of all possible subgraphs, particularly of higher order and path/cluster type, is difficult by visual perception of an HSG, a computer programme VGO385 was used[9]. The input required for the programme is primarily the adjacency matrix and output is all possible types of connectivity indices up to seventh order.

Data set

The values of physicochemical properties used as the dependent variables in the regression analysis were taken from the literature. The boiling points and enthalpies of vaporization for 47 alkylbenzenes compiled by Wilhoit and Zwolinski[10] were used.

†Present address: Dept of Pharmaceutical Sciences, Panjab University, Chandigarh 160 014

The values of molar refraction at 293.15K for 120 alkylbenzenes[2,11] were used directly whereas the molar volumes of these compounds were derived from the reported densities[11,12]. The values of enthalpy of atomization, ΔH_a, in respect of 33 alkylbenzenes have been obtained from the experimental values of enthalpy of formation, (ΔH_f) using Eq. (4).

$$\Delta H_a = 716.68\, n_c + 218.0\, n_H - \Delta H_f \quad \ldots (4)$$

The experimental values of magnetic susceptibility for a sample of 12 alkylbenzenes were taken from literature[13].

Regression analysis

The machine procedure described by Dixon[14] was translated into a computer programme VGO184 for step-wise regression analysis. The variables are included in the regression depending upon relative partial F-values.

The independent variables included all valence type connectivity indices up to fourth order and six transgenerated variables, viz. $({}^0\chi^v)^2$, $({}^0\chi^v)^3$, $({}^1\chi^v)^2$, $({}^1\chi^v)^3$, $1/{}^0\chi^v$ and $1/{}^1\chi^v$. The intercorrelation among various independent variables was not considered for the present work. However, the inclusion of variables into regression was terminated either after the best three variables were selected or when the observation-to-variable ratio fell below six.

Data processing

For a set of 122 alkylbenzenes (Table 1) the calculated values of all the independent variables were

Table 1—Experimental Values and Deviations between Experimental and Calculated Values of Physicochemical Properties of Alkylbenzenes[a]

Alkyl Benzene	ΔH_v^{298}/KJ mol^{-1}	t_b/°C	V^{293}/Cm^3 mol^{-1}	$[R]^{293}$/Cm^3 mol^{-1}	χ_M/Cm^3 mol^{-1}	ΔH_a/KJ mol^{-1}
1	2	3	4	5		
B	33.85 (-0.89)[b]	80.10(-3.19)	88.86(3.54)	26.188(0.017)	54.84(-0.25)	5559.1(-3.5)
MB	37.99(-0.54)	110.63(-1.70)	106.28(1.22)	31.058(-0.108)	66.11(-0.24)	6748.8(-0.5)
14 MMB	42.38(0.20)	138.35(-1.14)	123.29(-0.59)	36.005(-0.309)	76.75(0.37)	7937.9(3.1)
13 MMB	42.66(-0.15)	139.10(-1.96)	122.85(-0.13)	35.961(-0.261)	76.56(0.51)	7938.9(3.0)
12 MMB	43.43(-0.20)	144.41(-5.65)	120.61(0.47)	35.800(-0.135)	77.78(-0.52)	7937.9(-8.4)
EB	42.25(-0.41)	136.19(3.26)	122.44(1.01)	35.761(0.010)	77.20(0.31)	7925.9(5.8)
135 MMMB	47.48(0.38)	164.72(-1.74)	138.91(-0.85)	40.813(-0.361)	--	9129.7(6.8)
124 MMMB	47.94(0.74)	169.35(-4.71)	137.23(-0.80)	40.691(-0.277)	--	9128.0(-4.9)
123 MMMB	49.06(0.29)	176.08(-9.91)	134.39(0.76)	40.451(-0.070)	--	9124.8(-13.3)
(i 3)B	45.14(0.47)	152.39(5.78)	139.46(0.17)	40.422(0.035)	--	9107.3(13.4)
14 EMB	46.61(0.86)	161.99(2.81)	139.56(-1.01)	40.699(-0.182)	--	9116.0(8.4)
13 EMB	46.90(0.50)	161.31(3.42)	139.02(-0.36)	40.652(-0.132)	--	9114.9(10.4)
12 EMB	47.70(0.24)	165.15(0.93)	136.47(1.12)	40.447(0.049)	--	9113.0(2.9)
(3) B	46.23(-0.70)	159.22(1.97)	139.42(1.03)	40.450(0.001)	89.24(-0.04)	9104.5(-11.0)
1235 MMMMB	55.81(-0.82)	198.05(-7.61)	150.75(-0.27)	4531(-0.18)	--	10317.3(-11.3)
1234 MMMMB	57.15(-1.41)	205.09(-13.07)	148.27(0.80)	45.10(0.00)	--	10325.2(-31.8)
(9i) B	50.12(-0.15)	183.31(-1.34)	155.04(0.84)	45.095(-0.005)	--	10283.3(-39.8)
(t4) B	49.08(-0.78)	169.15(0.80)	154.89(1.83)	44.986(0.145)	--	--
14M(i 3)B	50.29(1.15)	177.13(5.14)	155.55(-1.82)	45.33(-0.13)	--	10297.2(13.2)
13M(i 3)B	49.96(1.42)	175.18(7.02)	155.89(-1.05)	45.30(-0.09)	--	10297.0(17.3)
12M(i 3)B	50.63(1.20)	179.18(5.25)	153.10(0.94)	45.09(0.11)	--	10294.9(11.4)
135 MME B	52.38(0.72)	183.78(4.84)	155.15(-1.20)	45.50(-0.23)	--	10306.1(13.8)
124 MEM B	52.33(1.10)	185.94(3.09)	153.00(-0.21)	45.33(-0.09)	--	10304.1(5.5)

(contd.)

Table 1—Experimental Values and Deviations between Experimental and Calculated Values of Physicochemical Properties of Alkylbenzenes[a]—*Contd.*

Alkyl Benzene	$^{298}\Delta H_v$/KJ mol^{-1}	t_b/°C	^{293}V/Cm^3 mol^{-1}	$[R]^{293}$/Cm^3 mol^{-1}	χ_m/Cm^3 mol^{-1}	ΔH_g/KJ mol^{-1}
1	2	3	4	5		
124 MME B	53.93(-0.02)	189.78(0.47)	153.47(-1.11)	45.38(-0.15)	--	10304.1(2.4)
134 MME B	53.30(0.42)	188.44(1.58)	153.16(-0.36)	45.34(-0.09)	--	10304.1(5.5)
123 MEM B	53.89(0.32)	190.04(1.25)	150.73(1.18)	45.13(0.09)	--	10301.9(-0.8)
123 MME B	54.85(-0.45)	193.96(-2.44)	150.45(1.04)	45.12(0.09)	--	10301.9(-4.0)
(i 4) B	49.45(-0.71)	172.79(2.90)	157.30(0.60)	45.198(-0.098)	--	10288.7(-8.0)
13M(3)B	52.09(-0.74)	181.84(3.07)	155.88(-0.22)	45.35(-0.15)	--	10294.2(-7.0)
14M(3)B	51.92(-0.50)	183.34(1.54)	155.35(-0.80)	45.35(-0.15)	--	10294.4(-8.2)
12M(3) B	52.58(-0.77)	184.83(1.41)	153.49(1.08)	45.13(0.05)	--	--
(i 4) B	49.50(1.88)	173.34(10.39)	155.69(-1.06)	45.027(0.097)	101.31(0.03)	10285.3(-19.4)
14 EEB	52.47(0.31)	183.79(6.09)	155.71(-1.21)	45.394(-0.056)	--	10291.9(15.8)
13 EEB	52.51(0.21)	181.14(8.57)	155.35(-0.76)	45.344(-0.003)	--	10291.8(16.9)
12 EEB	52.76(0.34)	183.45(7.46)	152.52(1.36)	45.122(0.205)	--	10289.7(12.7)
13M(t 4)B	--	--	171.24(0.68)	49.88(0.00)	--	--
(2 M 4)B	--	--	172.57(0.89)	49.60(0.14)	113.33(-0.29)	--
14 M(t 4) B	--	--	172.13(-0.31)	49.92(-0.04)	--	--
(22 MM 3) B	--	--	172.77(1.72)	49.80(-0.03)	--	--
124 MM(i 3)B	--	--	170.41(-1.87)	50.06(-0.14)	--	--
12 M(4)B	--	--	170.19(0.81)	49.70(0.12)	--	--
124 M(i 3)MB	--	--	169.55(-0.41)	49.98(-0.04)	--	--
13 M(4) B	--	--	172.57(-0.48)	50.00(-0.16)	--	--
123 M(i 3) MB	--	--	166.56(2.06)	49.70(0.22)	--	--
14 M(4) B	--	--	172.37(-0.39)	50.00(-0.16)	--	--
123 MM(i 3)B	--	--	166.93(1.00)	49.80(0.10)	--	--
12 M(t 4) B	--	--	166.62(3.64)	49.63(0.24)	--	--
(t 5) B	--	--	169.45(-0.39)	49.48(0.29)	--	--
MMMMMB	--	--	161.66(1.44)	49.80(0.02)	--	--
13 M i 4 B	--	--	173.66(-0.56)	50.10(-0.25)	--	--
14 E(4) B	--	--	172.49(-0.99)	50.05(-0.03)	--	--
14M(i 4) B	--	--	174.05(-1.05)	50.09(-0.24)	--	--
123 MM(3) B	--	--	167.24(1.24)	49.81(0.08)	--	--
12 M (i 4) B	--	--	171.39(0.62)	49.85(0.03)	--	--
124 MM(3)B	--	--	170.10(-0.74)	50.03(-0.12)	--	--
(12 MM 3) B	--	--	170.39(-0.49)	48.30(0.85)	--	--
123M(3) MB	--	--	167.39(1.49)	49.76(0.14)	--	--

(contd.)

Table 1—Experimental Values and Deviations between Experimental and Calculated Values of Physicochemical Properties of Alkylbenzenes[a]—*Contd.*

Alkyl Benzene	298 ΔH_v/KJ mol^{-1}	t_b/°C	293 V/Cm^3 mol^{-1}	[R]^{293}/Cm^3 mol^{-1}	χ_m/Cm^3 mol^{-1}	ΔH_g/KJ mol^{-1}
1	2	3	4	5		
124M(3) MB	--	--	170.05(-0.28)	50.03(-0.11)	--	--
135 MM(3) B	--	--	172.23(-1.24)	50.24(-0.29)	--	--
134 MM(3) B	--	--	169.94(-0.15)	49.97(-0.05)	--	--
134 MM(i 3) B	--	--	169.80(-0.54)	49.90(0.04)	--	--
14 M(S 4) B	--	--	171.18(-1.45)	49.80(0.07)	--	--
135 MM(i 3)B	--	--	171.97(-1.81)	50.20(-0.24)	--	--
13 M(s 4) B	--	--	172.77(-2.94)	50.00(-0.13)	--	--
125 MEEB	--	--	169.26(-0.52)	50.07(0.00)	--	--
12 M(s 4) B	--	--	169.80(-0.79)	49.70(0.15)	--	--
126 MEE B	--	--	166.43(1.41)	49.83(0.21)	--	--
14E(i 3) B	--	--	172.57(-1.99)	50.12(-0.10)	--	--
1235 MEMMB	--	--	167.98(-0.64)	50.00(-0.02)	--	--
13 E(i 3) B	--	--	172.57(-1.80)	50.10(-0.07)	--	--
1234 MMEMB	--	--	165.63(0.17)	49.80(0.14)	--	--
(15) B	--	--	173.18(0.61)	49.50(0.12)	--	--
1234 MMM EB	--	--	164.36(1.06)	49.81(0.12)	--	--
12 E(i 3) B	--	--	166.94(3.36)	49.80(0.22)	--	--
1235 MMME B	--	--	167.25(-0.86)	50.03(-0.08)	--	--
135 MEEB	--	--	171.77(-1.86)	50.26(-0.17)	--	--
1245 MMMEB	--	--	167.88(-1.27)	50.00(-0.04)	--	--
124 MEEB	--	--	169.45(-0.72)	50.07(0.00)	--	--
1246 MMMEB	--	--	166.62(0.19)	49.98(-0.01)	--	--
134 MEEB	--	--	169.18(-0.09)	49.83(0.25)	--	--
123 MEEB	--	--	166.37(1.81)	49.80(0.25)	--	--
(S 5)B	--	--	172.67(-1.13)	49.71(0.08)	--	--
(1 E 3) B	--	--	172.37(-1.91)	49.60(0.24)	--	--
13 E(3) B	--	--	172.23(-0.63)	50.05(-0.03)	--	--
12E(3) B	--	--	169.53(1.34)	49.79(0.22)	--	--
(5) B	55.05(-0.48)	205.45(-3.94)	172.67(0.64)	49.73(0.00)	--	--
13(i 3)(i3)B	--	--	189.58(-2.54)	54.616(0.097)	--	--
12(i3)(i3)B	--	--	185.01(1.69)	54.229(0.479)	--	--
(6) B	60.00(-0.00)	226.1(-5.0)	189.23(0.50)	54.37(0.00)	124.23(0.08)	--
MMMMMMB	--	--	--	--	122.50(0.09)	--
14(i 3)(i3)B	--	--	186.39(-2.53)	54.772(-0.062)	--	--

(contd.)

Table 1—Experimental Values and Deviations between Experimental and Calculated Values of Physicochemical Properties of Alkylbenzenes[a]—*Contd.*

Alkyl Benzene	298 ΔH_v/KJ mol^{-1}	t_b/°C	293 V/Cm^3 mol^{-1}	$[R]^{293}$/Cm^3 mol^{-1}	χ_m/Cm^3 mol^{-1}	ΔH_f/KJ mol^{-1}
1	2	3	4	5		
(7) B	64.94(-0.75)	246.0(-7.7)	205.78(0.38)	59.01(0.00)	--	--
(8) B	69.96(-0.93)	264.4(-8.5)	222.28(0.31)	63.25(0.40)	--	--
(9) B	74.91(-0.68)	282.0(-8.79)	238.77(0.25)	68.29(0.00)	--	--
(10)B	79.75(-0.58)	297.89(-7.68)	255.24(0.20)	72.920(0.010)	--	--
(4 6 6 MMM 7)B	--	--	--	--	173.90(-0.06)	--
(11) B	84.58(-0.42)	313.2(-6.2)	271.71(0.17)	77.57(0.00)	--	--
(12) B	89.62(-0.18)	327.6(-4.5)	288.18(0.12)	82.21(0.00)	--	--
(13) B	94.6(-0.1)	341.2(-1.2)	304.62(0.11)	86.85(0.00)	--	--
(14) B	99.6(0.1)	354. (2.)	321.06(0.10)	91.49(0.00)	--	--
(15)B	104.6(0.3)	366. (7.)	337.50(0.09)	96.13(0.00)	--	--
(16) B	109.2(0.8)	378. (11.)	353.95(0.07)	100.77(0.00)	--	--
(17)B	--	--	370.41(0.03)	105.42(-0.01)	--	--
(18)B	--	--	386.82(0.05)	110.06(-0.01)	--	--
(19) B	--	--	403.28(0.02)	114.70(-0.01)	--	--
(20)B	--	--	419.69(0.04)	119.34(-0.01)	--	--
(21) B	--	--	436.11(0.05)	123.98(-0.01)	--	--
(22) B	--	--	452.58(0.01)	128.62(-0.01)	--	--
(23) B	--	--	468.99(0.02)	133.26(-0.01)	--	--
(24) B	--	--	485.41(0.03)	137.90(-0.01)	--	--
(25) B	--	--	501.82(0.05)	142.54(-0.01)	--	--
(26) B	--	--	518.30(0.00)	147.18(-0.01)	--	--
(27) B	--	--	534.72 (0.01)	151.82(-0.01)	--	--
(28) B	--	--	551.14(0.02)	156.46(-0.01)	--	--
(29) B	--	--	567.56(0.02)	161.10(-0.01)	--	--
(30) B	--	--	583.97(0.04)	165.74(-0.01)	--	--
(31) B	--	--	600.39(0.05)	170.38(-0.01)	--	--
(32) B	--	--	616.81(0.06)	175.02(-0.01)	--	--
(33) B	--	--	633.23(0.07)	179.66(-0.01)	--	--
(34) B	--	--	649.65(0.07)	184.30(-0.01)	--	--
(35) B	---	--	666.06(0.09)	188.95(-0.02)	--	--
(36) B	--	--	682.56(0.02)	193.59(-0.02)	--	--

[a] In the symbolic representation of the names of various compounds, the symbols B, M, E, i, t, s stand for the words Benzene, Methyl, Ethyl, iso, tertiary and secondary respectively. The inclusion of the figure/figures within the parentheses represent the appropriate alkyl group. The presence of integers 1, 2, 3 etc. in the beginning of each symbolic representation indicate the position of various substituents in the benzene ring. Integer in the parentheses indicate the alkyl group substituted at the benzene ring. (t4)B, 123 MMEB, 14M(t4)B, (1,2 MM 3)B respectively stand for t-Butyl benzene, 1,2 dimethyl 3 ethyl benzene, 1,Methyl 4 ter butyl benzene, (1,2 Dimethyl propyl) benzene.

[b] The number in the parentheses = Calculated Value-Experimental Value.

stored along with the name and experimental values of each property, in the form of an alphanumeric matrix on the disc of a 36-bit machine, DEC-2050 operating under TOPS-20, at the Regional Computer Centre, Chandigarh. The input to a front-end programme, VGO184, preparing formatted input to VGO385, was generated by entering, in an interactive mode, the property code and the sequence numbers of compounds of the subset possessing that property.

Results and Discussion

Enthalpy of vaporization (ΔH_v)

The experimental values ΔH_v at 298.15K for 47 alkylbenzenes (Table 1) vary from 33.8 kJmol^{-1} to 109.2 kJmol^{-1} with an uncertainty[1] ranging between 0.04 to 4 kJmol^{-1}. The best one-variable correlation between ΔH_v and connectivity indices was obtained with $^0\chi^v$ (Eq. 5; Table 2). Though highly significant ($P < 0.01$), Eq. (5) cannot be used to predict the enthalpy of vaporisation because the structure quantifier ($^0\chi^v$) is an atom-derived index and many isomeric alkylbenzenes have the same calculated value. The quality of correlation steadily improves if $^3\chi_c^v$ and $(^1\chi^v)^{-1}$ are included in the regression (Eqs 6 and 7; Table 2). A significant improvement in all the statistical parameters is observed on inclusion of $^2\chi^v$ at the fourth step of the step-wise regression analysis procedure. However, with the inclusion of $^2\chi^v$, $^3\chi_c^v$ included at the second step is rendered insignificant as its partial F-value (0.95) falls below the threshold and its coefficient has a large standard error. Probably both, $^2\chi^v$ and $^3\chi_c^v$ encode similar structural information. Consequently, $^3\chi_c^v$ is excluded from the regression at the fifth step yielding a three-variable correlation (Eq. 8; Table 2) which results in a standard deviation of 0.75 kJmol^{-1} and an absolute maximum deviation of 1.90 kJmol^{-1}. Amongst the 47 compounds only two, viz. 2-ethyl-1,4-dimethylbenzene and 4-ethyl-1,3-dimethylbenzenes, have the same set of values for $^0\chi^v$, $1/^1\chi^v$ and $^2\chi^v$. Therefore, all the isomers with the same number of carbon atoms, but for these two, can be distinguished with this three variable correlation. The agreement between the values of ΔH_v calculated from Eq. (8) and the experimental values is excellent (Table 1) with more than 70% alkylbenzenes.

Boiling point (t_b)

The sample of 47 alkylbenzenes (Table 1) was investigated for correlation between t_b and $^m\chi_t^v$. The step-wise development of the correlations is given in Table 3. Equation (1) yields a standard deviation of 5.82°C which is well within the experimental uncertainty ($\pm$0.002-20°C). It can distinguish all isomeric compounds except 2-ethyl-1,4-dimethylbenzene and 4-ethyl-1,3-dimethylbenzene.

Since boiling point (t_b) and enthalpy of vaporisation (ΔH_v) are best correlated with the same structure quantifiers it can be concluded that the two properties are representative of a common physical phenomenon.

Molar volume (v_M)

The molar volumes derived from densities at 293.15K for a set of 120 alkylbenzenes are given in Table 1. The values show large variance from 88.86 cm^3 mol^{-1} to 682.56 cm^3 mol^{-1} with a standard deviation of 1.12 cm^3 mol^{-1}. The step-wise develop-

Table 2—Regression Coefficients and Statistical Parameters for Correlation between Enthalpy of Vaporisation and Valence Connectivity Indices for 47 Alkylbenzenes

Step	Regression Coefficients[a]					Stetisticel Parameters[b]				Eqn.
	$^0\chi^v$	$^3\chi_c^v$	$1/^1\chi^v$	$^2\chi^v$	Intercept	r	S	F	$\lvert\Delta max\rvert$	
1.	6.857 (0.083)				5.837	0.9967	1.44	6774	4.26	(4)
2.	6.745 (0.067)	-4.408 (0.782)			8.020	0.9981	1.11	5720	3.25	(5)
3.	7.282 (0.141)	-4.172 (0.6697)	18.426 (4.417)		-0.800	0.9986	0.95	5241	3.06	(6)
4.	10.251 (0.593)	-0.825 (0.846)	25.126 (3.752)	-5.508 (1.081)	-8.487	0.9992	0.76	6215	2.12	(7)
5.	10.707 (0.366)		26.305 (3.548)	-6.327 (0.680)	-9.879	0.9991	0.75	8308	1.90	(8)

a The quantities in parentheses are standard errors of the coefficients.

b r : multiple correlation coefficient, s: standard deviation of the estimate, F: F-ratio, $\lvert\Delta max\rvert$: maximum absolute deviation between experimental and calculated values.

Table 3—Regression Coefficients and Statistical Parameters for Correlations between Boiling Point and Valence Connectivity Indices for 47 Alkylbenzenes

Step	Regression Coefficients[a]				Statistical Parameters[b]				Eqn
	$^{0}\chi^{v}$	$1/^{1}\chi^{v}$	$^{2}\chi^{v}$	Intercept	r	S	F	$\lvert\Delta max\rvert$	
1	26.241 (0.4929)			4.626	0.9922	8.53	2834	20.26	(9)
2	21.393 (0.9735)	-168.108 (30.9917)		84.230	0.9953	6.68	2327	16.49	(10)
3	31.633 (2.8289)	-150.277 (27.3910)	-20.318 (5.2520)	65.241	0.9965	5.62	2049	10.65	(11)

a see footnote a to Table 2.
b see footnote b to Table 2.

Table 4—Regression Coefficients and Statistical Parameters for Correlations between Molar Volumes and Valence Connectivity Indices for 120 Alkylbenzenes

Step	Regression Coefficients[a]				Statistical Parameters[b]				Eqn.
	$^{1}\chi^{v}$	$^{2}\chi^{v}$	$^{4}\chi^{v}_{PC}$	Intercept	r	S	F	$\lvert\Delta max\rvert$	
1	32.6398 (0.0623)			29.6374	0.99978	2.99	274140	9.60	(12)
2	27.2137 (0.2711)	8.0726 (0.4009)		27.1300	0.99995	1.42	606378	4.29	(13)
3	25.2917 (0.3236)	10.6982 (0.4584)	-3.3120 (0.4177)	29.4635	0.99997	1.12	646761	3.64	(14)

a see footnote a to Table 2
b see footnote b to Table 2

ment of correlation between molar volume and valence connectivity indices is shown in Table 4. The one-variable correlation in $^{1}\chi^{v}$ (Eq. 12; Table 4), is highly significant but cannot be employed for predicting molar volumes of alkylbenzenes. The step-wise regression analysis procedure resulted in Eq. (14) as the best three-variable equation which distinguishes all the isomeric alkylbenzenes and yields a standard deviation of 1.12 $cm^3\ mol^{-1}$ with absolute maximum deviation of 3.64 $cm^3\ mol^{-1}$ for 1-methyl-2-*t*-butylbenzene. The molar volumes calculated from Eq. (14) are compared with the experimental values. The agreement between the two is once again excellent (Table 1). It can be seen that the values of higher alkylbenzenes are very accurately predicted.

Molar refraction [*R*]

Kier and Hall[1] have studied a set of 70 alkylbenzenes for such a correlation. We have included 50 additional alkylbenzenes (Table 1). The experimental values of the updated samples vary from 26.188 $cm^3\ mol^{-1}$ to 193.59 $cm^3\ mol^{-1}$. The step-wise development of the correlations is described in Table 5. Equation (17) is highly significant indicating almost a complete correlation between [R] and $^{1}\chi^{v}$, $^{0}\chi^{v}$ and $^{2}\chi^{v}$ values of alkylbenzenes. The equation is better than the best reported by Kier and Hall[1]. The values of [R] calculated by Eq. (17) show excellent agreement the experimental values (Table 1), the agreement being best for higher alkylbenzenes.

Table 5—Regression Coefficients and Statistical Parameters for Correlation between Molar Refraction and Valence Connectivity Indices of 120 Alkylbenzenes

Step	Regression Coefficients[a]				Statistical Parameters[b]				Eqn
-	$^1\chi^v$	$^0\chi^v$	$^2\chi''$	Intercept	r	s	F	$\lvert\Delta_{max}\rvert$	
1	9.1393 (0.0200)			10.3775	0.99972	0.96	209602	2.33	(15)
2	5.1927 (0.1011)	2.8925 (0.0740)		5.5973	0.99998	0.26	1457896	0.85	(16)
3	5.5600 (0.0480)	2.1679 (0.0501)	0.9247 (0.0490)	6.5071	1.00000	0.11	5151241	0.85	(17)

a See foot note a : Table 2
b See foot note b : Table 2

Table 6—Regression Coefficients and Statistical Parameters for Correlations between Diamagnetic Susceptibility and Valence Connectivity Indices for 12 Alkylbenzenes

Step	Regression Coefficients[a]				Statistical Parameters[b]				Eqn
	$^1\chi^v$	$^2\chi^v$	$^3\chi^v$	Intercept	r^2	s	F	$\lvert\Delta_{max}\rvert$	
1	25.6637 (0.7367)			2.9978	0.9959	3.13	1214	6.35	(18)
2	18.0131 (0.9697)	7.6104 (0.9274)		10.1617	0.9995	1.13	4666	2.74	(19)
3	17.0042 (0.3209)	7.2293 (0.2914)	2.4834 (0.2693)	10.5796	1.0000	0.35	32178	0.52	(20)

a See footnote a to table 2
b See footnote b to Table 2

Diamagnetic susceptibility (χ_M)

Diamagnetic susceptibility values for only 12 alkylbenzenes (Table 1) were available in the literature. The best one-variable, 2-variable and three-variable correlations of χ_M with connectivity indices are given in Table 6. Equation (19) can distinguish all the isomers in the given sample and is statistically significant ($P<0.005$). Though Eq. (20) has lower observation-to-variable ratio as compared to that of Eq. (19) the improvement in all the statistical parameters does not appear to be the result of statistical artifact and $^3\chi_p^v$ is an important topological feature in determining χ_M. The agreement between the values of χ_M calculated from Eq. (20) and the experimental values is excellent (Table 1). The maximum absolute deviation is 0.52 $cm^3\ mol^{-1}$.

Enthalpy of atomisation (ΔH_a)

For a set of 33 alkylbenzenes (Table 1) the ΔH_a values as derived from Eq. (4) range between 5559.1 $kJmol^{-1}$ and 10325.2 $kJmol^{-1}$. The stepwise development of correlation between $^m\chi_t^v$ and ΔH_a for this set is given in Table 7. Equation (23) is found to be the best three-variable correlation. It is highly significant and gives a standard deviation of 14.16 $kJmol^{-1}$. It can be seen from Table 1 that average absolute deviation between calculated (Eq. 23) and experimental ΔH_a values is 0.16% with 0.39% and

Table 7—Regression Coefficients and Statistical Parameters for Correlations between Enthalpy of Atomization and Valence Connectivity Indices for 33 Alkylbenzenes

Step	Regression Coefficients[a]				Statistical Parameters				
	$^{0}\chi^{v}$	$^{1}\chi^{v}$	$^{2}\chi^{v}$	Intercept	r	s	F	$\lvert\Delta_{max}\rvert$	Eq$_n$
1	1399.6470 (43.7291)			675.5437	0.9852	209.14	1024	498.71	(21)
2	737.3440 (24.4254)	1227.5850 (42.5808)		552.0548	0.9995	39.68	14645	119.44	(22)
3	556.7468 (15.2923)	1317.8187 (16.4422)	275.6155 (19.1750)	673.0752	0.9999	14.16	76721	39.71	(23)

a see footnote a to Table 2

b see footnote b to Table 2

0.007% deviations as absolute maximum and minimum, respectively. The structure descriptors used in Eq. (23) can distinguish all the isomeric molecules.

References

1 Kier L B & Hall L H, *Molecular connectivity in chemistry and drug research* (Academic Press, New York) 1976.

2 Jain D V S, Sukhbir Singh & Gombar V, *Proc Indian Acad Sci* (Chem Sci), **93** (1984) 927.

3 Kier L B & Hall L H, *Molecular connectivity in structure-activity analysis* (Research Studies Press Ltd, England) 1986.

4 Gombar V, Kapoor V K & Jain D V S, *Indian J Chem*, **19A** (1980) 715.

5 Gombar V, *The Pharmacos*, **25** (1981)? 45.

6 Jain D V S & Gombar V, *J chem Soc Faraday* I (1979) 1132.

7 Jain D V S, Sukhbir Singh & Gombar V, *Indian J Chem*, **24A** (1985) 545.

8 Jain D V S, Sukhbir Singh & Gombar V K, *Fluid Phase Equilibria*, **27** (1986) 341.

9 Gombar V, Surjit Singh, Jain D V S (unpublished work).

10 *Handbook of vapour pressures and heats of vaporisation of hydrocarbons and related compounds*, edited by R C Wilheit & B J Zwolinki (Texas A & M University, Texas) 1971.

11 Dreisback R R, *Physical properties of chemical compounds: Advances in chemistry* 15, (American Chemical Society, Washington D C) 1955.

12 Kier L B, Hall L H, Murray W J & Randic, *J Pharm Sci*, **65** (1976) 1226.

13 *Handbook of physics and chemistry – A ready reference book of chemical and physical data*, edited by R C Weast (CRC-Press, Ohio) 1975-76, pp E 127-135.

14 *BMD-Biomedical computer programs No.* 2, edited by W J Dixon (University of California Press, Berkeley) 1970, 233.

Indian Journal of Chemistry
Vol. 27A, November 1988, pp. 932-936

A Unified Empirical Treatment of Carbon-13 NMR Chemical Shifts: Part II—Correlation Analysis of Data on Carbonyl Compounds

IRAGAVARAPU SURYANARAYANA*† & JOHANN GASTEIGER
Organische Chemisches Institut der Technischen Universitat, Munchen, D 8046 Garching, Federal Republic of Germany

Received 25 *June* 1987; *revised and accepted* 18 *December* 1987

The ^{13}C NMR chemical shifts of carbonyl carbons of 90 different carbonyl compounds are reproduced by a linear two parameter equation with a correlation coefficient of 0.9857 and a standard deviation of 3.07 ppm. The two parameters are the total charges (both σ and π) on the carbonyl carbon atom as calculated by the iterative partial equalization of orbital electronegativity (PEOE method) and the effective polarizability as represented by a molecular connectivity number.

^{13}C NMR chemical shifts of the carbonyl carbons of various compounds are of interest for theoretical as well as experimental work. Stothers and Lauterbur[1] discussed the influence of alkyl substitution, conjugation and hydrogen bonding on the ^{13}C NMR chemical shifts of carbonyl carbons in a number of compounds. They explained the observed downfield shift of carbonyl carbon with increasing methyl substitution in terms of the hyperconjugation effect of methyl groups. This is in contrast to the opinion of Spiesecke and Schneider[2], and Grant and Paul[3], who attributed the downfield shift to the diamagnetic anisotropy of the alkyl group. Jackmann and Kelly[4] attributed the downfield shift to the negative inductive effect of methyl groups. Delseth and Kentzinger[5] proposed an additivity relationship with six parameters for 28 alkyl ketones, with a standard deviation of 2.5 ppm, and related the six parameters to the hyperconjugation effect of methyl groups on the polarity of the $>C=O$ group. Assuming constant excitation energy-invariant non-polar sigma net work and neglecting neighbouring anisotropic effects and intermolecular dispersion effects, Maciel[6] derived an equation relating the chemical shift to the π-bond polarity of the $C=O$ bond in terms of Taft substituent parameters for 14 carbonyl compounds. Sasvitsky *et al.*[7] proposed a correlation between the ^{13}C NMR chemical shifts and the $n\rightarrow\pi^*$ absorption maximum for a set of 10 alkyl substituted cyclic and bicyclic ketones with a correlation coefficient of 0.912 and a standard deviation of 1.78 ppm. Yalpani *et al.*[8] attributed the upfield shift of the carbonyl signal on substitution of halogens to the conformational effects or the field effects of the halogens on the $>C=O$ dipole in addition to the electronegativity effect, the latter contributing to a small extent. Couperus *et al.*[9] and Velichko *et al.*[10] reported the ^{13}C spectra for a number of esters to get information on conformational and stereochemical aspects of esters.

In view of the conflicting explanations for the variation of the ^{13}C chemical shifts of carbonyl carbons, and in order to understand the factors influencing the ^{13}C chemical shifts in general, we have attempted to correlate the available ^{13}C chemical shifts of aliphatic carbonyl carbons of different aldehydes, ketones, carboxylic acids, acid halides and esters with the physically significant and explainable parameters like the partial atomic charge on the carbonyl carbon atom as calculated by the iterative partial equalization of orbital electronegativity[11] and the effective polarizability[12] as represented by a molecular connectivity number, which can be calculated by inspection.

Data Set

The data set consists of the experimental ^{13}C chemical shifts of aliphatic saturated carbonyl compounds, e.g., aldehydes, ketones, acids, acid halides and esters. These different types of compounds were chosen so that the influence of all saturated bonding (σ) situations around carbonyl group can be covered to get a balanced statistical analysis. The sources of the experimental data from literatures are indicated as footnotes in Table 1. The variation of chemical shifts with change of solvent and temperature is considered negligible as the chemical shift variation observed

† Permanent address: Analytical Chemistry Division, Regional Research Laboratory, Jorhat 785 006, Assam

Table 1 — The Calculated and Experimental ^{13}C NMR Chemical Shifts of Carbonyl Compounds

S.No.	Compound	δ_{exp}[a]	δ_{calc}[b]	$\Delta(\delta_{exp}-\delta_{calc})$	Q_σ[c]	Q_π[c]	Q_{total}[c]	N
1	H.CO.H	194.3	192.32	1.98	0.107	0.003	0.110	4.00
2	CH_3.CO.H	199.6	196.70	2.90	0.117	0.002	0.119	5.50
3	Et.CO.H	201.8	199.26	2.54	0.120	0.002	0.122	6.25
4	*n*-Pr.CO.H	201.6	200.91	0.69	0.120	0.002	0.122	6.625
5	*n*-Bu.CO.H	202.2	201.70	0.50	0.120	0.002	0.122	6.813
6	*i*-Pr.CO.H	204.0	201.82	2.18	0.123	0.002	0.125	7.000
7	*t*-Bu.CO.H	203.9	204.60	−0.70	0.126	0.001	0.127	7.750
8	*i*-Bu.CO.H	201.1	202.60	−1.50	0.120	0.002	0.122	7.000
9	neo-Pen.CO.H	201.1	204.00	−2.86	0.121	0.002	0.123	7.375
10	Et_2CH.CO.H	203.5	205.10	−1.61	0.123	0.002	0.125	7.750
11	$ClCH_2$.CO.H	193.3	190.55	2.75	0.135	0.000	0.135	5.500
12	Cl_3C.CO.H	175.9	184.60	−8.69	0.171	−0.003	0.168	5.500
13	Br_3C.CO.H	175.9	187.60	−11.66	0.158	−0.002	0.156	5.500
14	Me.CO.Me	205.1	200.8	4.27	0.127	0.002	0.129	7.00
15	Me.CO.Et	206.3	203.6	2.67	0.130	0.001	0.131	7.75
16	Me.CO.nPr	206.6	205.3	1.30	0.130	0.001	0.131	8.125
17	Me.CO.nBu	206.8	206.1	0.70	0.130	0.001	0.131	8.313
18	Me.CO.iPr	209.1	206.2	2.90	0.133	0.001	0.134	8.500
19	Me.CO.tBu	211.8	208.7	3.10	0.136	0.001	0.137	9.250
20	Me.CO.iBu	205.8	206.7	−0.90	0.131	0.001	0.132	8.500
21	Me.CO.neo-Pen	205.5	208.3	−2.80	0.131	0.001	0.132	8.875
22	Me.CO.$C(Me)_2C(Me)_3$	211.4	213.7	−2.30	0.136	0.001	0.137	10.375
23	Et.CO.Et	209.3	206.2	3.10	0.133	0.001	0.134	8.500
24	Et.CO.iPr	211.8	208.7	3.10	0.136	0.001	0.137	9.250
25	Et.CO.tBu	213.0	211.8	1.30	0.138	0.001	0.139	10.000
26	Et.CO.nPr	209.3	207.8	1.50	0.133	0.001	0.134	8.875
27	Et.CO.iBu	208.0	206.2	1.80	0.134	0.001	0.135	8.500
28	Et.CO.$C(Et)_3$	213.1	216.5	−3.40	0.139	0.000	0.139	11.125
29	*i*-Pr.CO.iPr	215.1	211.8	3.30	0.138	0.000	0.138	10.000
30	*i*-Pr.CO.tBu	217.1	214.4	2.70	0.141	0.000	0.141	10.750
31	*i*-Pr.CO.iBu	212.4	212.0	0.40	0.136	0.001	0.137	10.000
32	*n*-Bu.CO.nBu	208.6	211.3	−2.50	0.133	0.001	0.134	9.625
33	*t*-Bu.CO.tBu	217.1	216.9	0.20	0.144	0.000	0.144	11.500
34	*t*-Bu.CO.nPr	213.6	213.2	0.40	0.139	0.000	0.139	10.375
35	*i*-Bu.CO.iBu	208.4	212.5	−4.10	0.134	0.001	0.135	10.000
36	Me.CO.CH_2Cl	200.7	196.9	3.80	0.145	0.000	0.145	7.000
37	Me.CO.$CHCl_2$	193.6	192.9	0.70	0.163	−0.002	0.161	7.000
38	Me.CO.CCl_3	186.3	188.7	−2.40	0.181	−0.003	0.178	7.000
39	Me.CO.$CClBr_2$	186.8	190.9	−4.10	0.172	−0.003	0.169	7.000
40	Me.CO.CCl_2Br	186.6	190.0	−3.40	0.176	−0.003	0.173	7.000
41	Me.CO.CHClBr	193.9	193.9	0.00	0.158	−0.001	0.157	7.000
42	Me.CO.CH_2Br	199.0	197.9	1.10	0.141	0.000	0.141	7.000
43	Me.CO.CH.MeJ	202.7	200.7	2.00	0.143	0.000	0.143	7.750
44	Me.CO.$CHMeBr_2$	200.3	200.7	−0.40	0.143	0.000	0.143	7.750
45	Me.CO.CHMeCl	201.2	199.7	1.50	0.148	−0.001	0.147	7.750
46	Me.CO.CMeBr	193.9	197.5	−3.60	0.157	−0.001	0.156	7.750
47	Me.CO.CMeClBr	193.8	196.7	−2.90	0.161	−0.002	0.159	7.750
48	Me.CO.$CMeCl_2$	194.2	195.7	−1.50	0.165	−0.002	0.163	7.750
49	*t*-Bu.CO.$CHCl_2$	201.1	200.8	0.30	0.172	−0.002	0.160	9.250
50	*t*-Bu.CO.$CHBr_2$	201.4	203.0	−1.60	0.171	−0.002	0.169	9.250
51	*i*-Pr.CO.CH_2Cl	205.8	202.5	3.30	0.150	−0.001	0.149	8.500
52	*i*-Pr.CO.$CCLMe_2$	211.0	207.6	3.40	0.156	−0.001	0.155	10.000
53	$ClCH_2$.CO.CH_2Cl	194.9	193.2	1.70	0.162	−0.002	0.160	7.000
54	Cl_2HC.CO.$CHCl_2$	183.4	185.0	−1.60	0.198	−0.005	0.193	7.000
55	Cl_3C.CO.CCl_3	175.9	176.9	−1.00	0.234	−0.008	0.226	7.000
56	Me.CO.Cl	171.0	173.5	−2.50	0.219	−0.006	0.213	5.500
57	Et.CO.Cl	174.7	176.3	−1.60	0.221	−0.006	0.215	6.250
58	$ClCH_2$.CO.Cl	167.7	169.8	−2.10	0.236	−0.008	0.228	5.500
59	Cl_2CH.CO.Cl	165.5	165.6	−0.10	0.254	−0.009	0.245	5.500

(*Contd.*)

Table 1—The Calculated and Experimental ^{13}C NMR Chemical Shifts of Carbonyl Compounds — *Contd.*

S.No.	Compound	δ_{exp}[a]	δ_{calc}[b]	$\Delta(\delta_{exp}-\delta_{calc})$	Q_σ[c]	Q_π[c]	Q_{total}[c]	N
60	$Cl_3C.CO.Cl$	163.5	161.4	2.10	0.273	−0.011	0.262	5.500
61	H.CO.OH	166.7	162.9	3.80	0.246	−0.008	0.238	4.500
62	Me.CO.OH	171.1	167.3	3.80	0.256	−0.009	0.247	6.000
63	Et.CO.OH	173.4	169.8	3.60	0.259	−0.009	0.250	6.750
64	*i*-Pr.CO.OH	177.1	172.6	4.50	0.262	−0.010	0.252	7.500
65	*t*-Bu.CO.OH	178.9	175.1	3.70	0.265	−0.010	0.255	8.250
66	$CH_2Cl.CO.OH$	166.8	163.3	3.50	0.274	−0.011	0.263	6.000
67	$CHCl_2.CO.OH$	163.3	158.9	4.40	0.293	−0.012	0.281	6.000
68	$CCl_3.CO.OH$	160.1	154.9	5.20	0.311	−0.014	0.297	6.000
69	H.CO.OMe	160.7	165.7	−5.00	0.249	−0.009	0.240	5.250
70	Me.CO.OMe	170.0	169.8	0.20	0.259	−0.009	0.250	6.750
71	Et.CO.OMe	173.3	172.4	0.90	0.262	−0.009	0.253	7.500
72	Pr.CO.OMe	173.0	174.0	1.00	0.262	−0.009	0.253	7.500
73	Pen.CO.OMe	172.1	175.5	−3.40	0.262	−0.010	0.252	8.156
74	Hex.CO.OMe	173.4	175.7	−2.30	0.262	−0.010	0.252	8.203
75	*i*-Pr.CO.OMe	175.7	175.4	0.30	0.264	−0.010	0.254	8.250
76	$CH_2Cl.CO.OMe$	167.8	165.9	1.90	0.277	−0.011	0.266	6.750
77	$CHCl_2.CO.OMe$	164.4	161.7	2.70	0.295	−0.012	0.283	6.750
78	$CCl_3.CO.OMe$	160.0	157.5	2.50	0.314	−0.014	0.300	6.750
79	$CH_2Br.CO.OMe$	166.6	166.9	−0.30	0.272	−0.010	0.262	6.750
80	$CHBr_2.CO.OMe$	164.3	163.9	0.40	0.286	−0.012	0.274	6.750
81	$CBr_3.CO.OMe$	161.8	160.7	1.10	0.300	−0.013	0.287	6.750
82	MeHBrC.CO.OMe	169.2	169.7	−0.50	0.275	−0.011	0.264	7.500
83	$MeBr_2C.CO.OMe$	166.2	172.4	−5.90	0.264	−0.010	0.254	7.500
84	$CH_2BrCHBr.CO.OMe$	167.0	169.4	−2.40	0.276	−0.011	0.265	7.500
85	Me.CO.OEt	170.4	171.5	−1.10	0.259	−0.009	0.250	7.125
86	$Cl_3C.CO.OEt$	161.1	159.1	−2.00	0.314	−0.014	0.300	7.125
87	Me.CO.OPr	169.9	172.3	−2.4	0.259	−0.009	0.250	7.313
88	Me.CO.OiPr	167.1	173.5	−6.00	0.259	−0.009	0.250	7.500
89	Me.CO.OiBu	169.9	173.9	−4.00	0.259	−0.009	0.250	7.688
90	Me.CO.OtBu	170.2	174.8	−4.60	0.259	−0.009	0.250	7.875

(a) The expt. values are taken from the ref. indicated in the bracket against the compound number: 1(6); 2-10 & 14-35 (5); 36,37,39-48(8); 13,49-54 (values obtained by us); 69-75,85,87-90 (9); 76-84(10); 86(17); 11,12,38,55-61, and 62-68 with H.bonding correction δ - 7 ppm (12)

(b) values calculated by Eq.2.

(c) in electron volts.

Table 2—Results of Multilinear Regression Analysis of ^{13}C NMR Chemical Shifts of Carbonyl Carbons

[n = Number of points, R = regression coefficient, s = standard deviation, C_0, C_1 and C_2 are the coefficients of Eqs 1 and 2]

	Parameters	n	R	C_0	C_1	C_2	
	Q_σ	99	0.9162	7.11	236.37	−240.64	
	Q_π	99	0.9142	7.19	201.83	2928.74	
all carbonyl	Q_{total}	99	0.9161	7.11	239.33	−262.07	
compounds	Q_σ, N	99	0.9679	4.39	198.27	−213.53	4.29
	Q_π, N	99	0.9665	4.48	168.28	2614.63	4.23
	Q_{total}, N	99	0.9679	4.39	200.40	−232.40	4.30
all with	Q_σ, N	99	0.9790	3.65	199.05	−222.79	4.36
H. bonding	Q_π, N	99	0.9776	3.77	167.75	2727.61	4.29
correction	Q_{total}, N	99	0.9790	3.65	201.80	−242.48	4.37
without	Q_σ, N	90	0.9859	3.06	199.16	−227.17	4.39
fluoro	Q_π, N	90	0.9858	3.07	167.36	2797.64	4.31
compounds	Q_{total}, N	90	0.9857	3.07	201.90	−247.10	4.40

for acetone between CCl_4 and $CDCl_3$ is only 1 ppm which is less than the standard error. Similar is the case with temperature variation of 10°C.

Results and Discussion

Multiple linear regression analysis (MLRA) was performed on the ^{13}C chemical shifts of different carbonyl compounds with partial atomic charges to derive Eq.1, since the charge values contain structural information. Charge (Q) as a single parameter gave a correlation coefficient (R) = 0.9161 and standard deviation (s) = 7.1 ppm for all the carbonyl carbons.

$$\delta = C_0 + C_1 Q \quad \ldots (1)$$

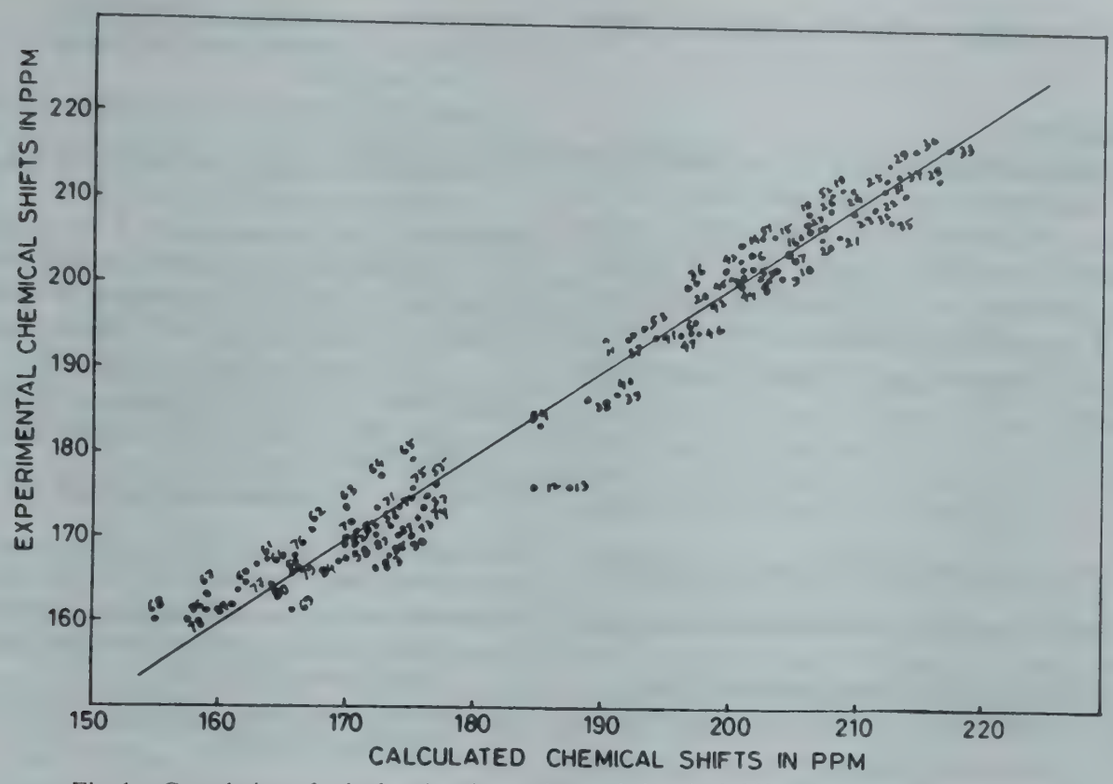

Fig. 1—Correlation of calculated and experimental chemical shifts of carbonyl compounds

Addition of connectivity number, which represents effective polarizability, as a second parameter markedly improved the correlation to R = 0.9679 with s = 4.39 ppm (Table 2). Among the 99 compounds which were studied originally, carboxylic acids and fluoro substituted carbonyl compounds were found to deviate to an extent of 7-10 ppm.

All carboxylic acids deviate almost constantly to an extent of 7.0 ppm and this deviation was considered earlier by Lauterbur *et al.*[1] to be due to the dimerization of acids through hydrogen bonding. By correcting the carboxylic acid chemical shifts for hydrogen bonding, the correlation improved significantly and gave a correlation coefficient of 0.9790 with a standard deviation of 3.65 ppm. In this correlation, the fluoro compounds show the most deviation. Deletion of the fluoro compounds reduced the standard deviation to 3.07 ppm with a regression coefficient of 0.9859. The plot of the calculated chemical shifts with the experimental shifts is shown in Fig.1. The deviation of the fluoro compounds may be due to either the high electronegativity of the fluorine or the back donation of the fluorine lone pair of electrons to carbon as attributed by Ditchfield and Ellis[13], giving partial double bond character, and thereby causing an upfield shift of the carbonyl carbon. The same problem was encountered in our earlier studies of halogen substituted methanes[14].

The ^{13}C chemical shifts of carbonyl carbons can be calculated using Eq.2:

$$\delta = 201.90 - 247.10Q + 4.40\,N \qquad \ldots(2)$$

The charge on the carbonyl carbon can be calculated by the partial equalization of electronegativity method, in which the atoms are characterized by their orbital electronegativity and the topology of the molecule. N, the effective polarizability was calculated by a bond counting ansatz. The number of bonds per sphere were summed to give N, while allowing for an attenuation by a factor of 0.5 for each sphere further from the reactive centre.

Thus, this equation reproduces the ^{13}C chemical shifts of 90 carbonyl carbons of different aldehydes, ketones, acid halides, carboxylic acids and esters (Table 1), just with two parameters, the partial atomic charge on the carbonyl carbon and the effective polarizability. As mentioned in our earlier work[14], these results further support the view that polarizability influences ^{13}C chemical shifts considerably as it has an intrinsic relationship with magnetic anisotropy.

The slope of the dependence of the ^{13}C chemical shift on the charge of the carbon (-220 ppm/electron), is in the expected range. The negative sign and the magnitude of the coefficient of the charge is in agreement with the results of Fliszar[15], arrived at using *ab initio* calculations. The negative sign of the coefficient indicates that the

increase in the charge shifts the signal to down field.

Acknowledgement

One of the authors (I S N) is grateful to Deutsche Akademische Austauschdienst for a Post-doctoral Fellowship and CSIR, New Delhi for depuation from RRL, Jorhat. The computer access was provided by Leibniz-Rechenzentrum, Munchen. Programming assistance by Dr M G Hutchings, B Christoph and H Saller is gratefully acknowledged.

References

1 Stothers J B & Lauterbur P C, *Can J Chem*, **42** (1964) 1563.
2 Spiesecke N & Schneider W G, *J chem Phys*, **35** (1971) 722.
3 Grant D M & Paul E G, *J Am chem Soc*, **86** (1964) 2984.
4 Jackmann L M & Kelly D P, *J chem Soc*, **8** (1970)102.
5 Delseth C & Kintzinger J P, *Helv chim Acta*, **59** (1976) 466.
6 Maciel G E, *J chem Phys*, **42** (1965) 2746.
7 Savitsky G B, Namakawa K & Zweifel G, *J phys Chem*, **69** (1965) 3105.
8 Yalpani M, Modavai B & Koshdal E, *Org Magn Res*, **12** (1972) 254.
9 Couperus P A, Claugue A D H & Von Daugen J P C M, *Org Magn Res*, **11** (1978) 590.
10 Velichko F K, Dostovalova V I, Vinogradova L V & Freidlina R H, *Org Magn Res*, **13** (1980) 442.
11 Gasteiger J & Marsili M, *Tetrahedron*, **36** (1980) 3219.
12 Gasteiger J & Hutchings M G, *Tetrahedron Lett*, (1983) 2537; *J chem Soc, Perkin II*, (1984) 559.
13 Ditchfield R & Ellis P D, *Topics in ^{13}C NMR spectroscopy*, Vol 1, Edited by G C Levy (Wiley Interscience, New York) 1974, 31.
14 Gasteiger J & Suryanarayana I, *Magn Res in Chem*, **23** (1985) 156.
15 Beraldin M T, Vantheir E & Fliszar S, *Can J Chem*, **60** (1982) 106.
16 *Spectral data for structural determination of organic compounds*, edited by Petsch Clerc Seibl Simon (Springer Verlag, Berlin) 1983, C170.
17 *^{13}C NMR spectroscopy*, edited by G C Levy (John Wiley, New York) 1980, 140.

Indian Journal of Chemistry
Vol. 27A, November 1988, pp. 937-941

Viscosity B-Coefficients of Amines in Dilute Aqueous Solutions

M V KAULGUD*, M R AWODE & D S PATIL
Department of Chemistry, Nagpur University, Nagpur 440 010

Received 26 *December* 1986; *revised* 27 *September* 1987; *accepted* 31 *December* 1987

Viscosity B-coefficients (B_η) in dilute aqueous solutions of NH_3, $MeNH_2$, $EtNH_2$, *n*-$PrNH_2$, *n*-$BuNH_2$, *t*-$BuNH_2$, Me_2NH and Me_3N have been reported at 5°, 15° and 25°C after correcting for hydrolysis (The procedure of hydrolysis correction is also described). A method for obtaining B_η^{str}, which represents the effect of solute on the structure of solvent, is described. The non-polar part of the molecule enhances water structure, whereas the $-NH_2$ group has an opposite effect of loosening water structure.

In the previous work[1] from this laboratory, viscosity B-coefficients (B_η) of aliphatic amines, in the concentration range of 0.05 to 1.0 molar were reported. This concentration range, however, is not low enough to rule out solute-solute interaction. Consequently B_η values in this concentration range may not give a true picture of the solute-solvent interaction.

We are reporting here B_η values of amines obtained from measurements of viscosity of very dilute solutions (0.005 *M* to 0.1 *M*). Though measurements in this low concentration range eliminate or minimise the uncertainty due to solute-solute interactions, the B-coefficient of unhyrolysed amines will have contributions from the species XH^+ and OH^- as a result of the hydrolysis of the amine (X): $X + H_2O \rightleftharpoons XH^+ + OH^-$. In dilute solutions the degree of hydrolysis could be as high as 25-30%.

This difficulty is usually avoided by carrying out measurements in a dilute solution (0.05 *M*) of a strong alkali (like KOH) as solvent to supress hydrolysis, a procedure adopted by Conway *et al.*[2] for obtaining partial molal compressibilities of unhydrolyzed amines. An alternative to the use of alkali would be to apply appropriate correction for the contribution of the ionic species, XH^+ and OH^- to the total observed property. Cabani *et al.*[3] were the first to work out successfully a procedure for such a hydrolysis correction to determine the true limiting volumes of amines. This was modified and adapted to obtain true limiting partial compressibilities and also limiting volumes for measurements at lower concentrations[4,5]. Davies and Malpass[6] applied correction for dissociation of some aliphatic acids for obtaining the B_η of the undissociated acid molecules. In the present work true B_η of amines have been obtained by applying suitable correction for hydrolysis to the relative viscosities of solutions of amines at very low concentration. An appropriate procedure for hydrolysis correction has also been described. The present treatment though similar in approach to that of Davies and Malpass differs in important aspect that after correcting for the ionic species the method yields the B-coefficient for the hypothetical aggregate $X.H_2O$ yielding the hydrolytic products from which one has to subtract the $B_\eta(H_2O)$ to be obtained by a separate experiment.

Relative viscosities of dilute solutions of the following eight amines, viz. NH_3, $MeNH_2$, $EtNH_2$, *n*-$PrNH_2$, *n*-$BuNH_2$, *t*-$BuNH_2$, Me_2NH and Me_3N have been measured at 5°, 15° and 25°C. A new parameter, B_η^{str}, the structural part of the B_η has been defined and evaluated to enable a meaningful interpretation of viscosity parameters.

As the values of the viscosity B-coefficients of alcohols at different temperatures were available[7] an attempt has also been made to compare the effect of $-NH_2$ and $-OH$ groups of amine and alcohol respectively on the structure of water.

Materials and Methods

n-$PrNH_2$ (Riedel), *n*-$BuNH_2$ (Merck) and *t*-$BuNH_2$ (Fluka) were dried over KOH for 48 hr and distilled twice over fresh KOH pellets. The purity of the liquid amines was established by density measurements. The stock solutions of gaseous amines were prepared by dissolving the purified vapours in doubly distilled water. The concentration of the stock solutions was determined by titrating against 0.2 *M* HCl (AR). Bromocresol purple was used as indicator for titration of all amines except ammonia for which bromophenol blue was used.

The relative viscosities of the aqueous solutions were determined by Eq. (1)

$$\frac{\eta}{\eta_0} = \left(\frac{\tau\rho}{\tau^0\rho^0}\right) K \qquad \ldots (1)$$

Table 1—Viscosity B-Coefficients of NaCl and NaOH in Water at 5°, 15° and 25°C

	B-coefficients (dm^3/mol) at		
	5°	15°	20°C
NaCl	0.046†	0.066*	0.079*
NaOH	0.184†	0.194†	0.205*

*Ref. 8
†This work

where, η, τ and ρ are respectively viscosity, time of flow and density of the solution and η_0, τ^0 and ρ^0 are respectively the viscosity, time of flow and density of solvent; K is the kinetic energy correction factor[8]. Differential method[8] was used in which two almost identical Ubbelohde viscometers fabricated with calibrated capillaries (tolerance $\pm 0.4\%$) were simultaneously suspended by special levelling device in a thermostatic bath. The bath was driven by MK-70 cryostat (± 0.02°C) for 5° and 15° and U-10 thermostat for 25°C. Because of the large volume(27 dm^3) of the viscosity bath it was possible to control its temperature within ± 0.005°C. The reproducibility in the flow time of about 1000s was ± 0.1 s. Kinetic energy corrections[8] were applied. Relative viscosities of NaCl solutions measured at 15° and 25°C, were in agreement with the literature[8] values within $\pm$ 0.02%.

The amine hydrochlorides were prepared according to the procedure given by Campbell and Lam[10]. The purity of the salts, checked by conductometric estimation of the halide was found to be 99.9%. The concentration of the solutions was varied *in situ* by adding weighed quantity of solution of known concentration to a known mass of water in the viscometer.

To prevent carbonisation of amines due to atmospheric CO_2 an atmosphere of N_2 was maintained over the solution in the viscometer using sodalime traps.

All solutions were filtered through sintered disc (No. 4) before use to eliminate particulate matter if any.

Densities[4] were measured with an accuracy of 3 in sixth place of decimal using a differential bouyancy balance with float volume of about 180 ml.

Procedure for hydrolysis correction

It is assumed that the hydrolysis takes place from a hypothetical[3] aggregate $X.H_2O$ as follows:

$$X + H_2O \rightarrow X.H_2O \rightleftharpoons \underset{(1-\alpha)c}{XH^+} + \underset{\alpha c}{OH^-} \qquad \ldots (2)$$

In Eq. (2) X is the amine molecule, α is the degree of hydrolysis and c the stochiometric concentration. According to the Jones-Dole equation[11] the observed relative viscosity η/η_0 can be written as

$$\left(\frac{\eta}{\eta_0}\right)_{obs} = 1 + A_\eta(XH^+OH^-)\sqrt{\alpha c} + B_\eta(XH^+OH^-)\alpha c + A_\eta(X.H_2O)\sqrt{(1-\alpha)c} + B_\eta(X.H_2O)(1-\alpha)c \qquad \ldots (3)$$

where $A_\eta(XH^+OH^-)$ and $A_\eta(X.H_2O)$ are respectively the viscosity A_η-coefficients of XH^+OH^- and $X.H_2O$. Also $B_\eta(XH^+OH^-)$ and $B_\eta(X.H_2O)$ are viscosity B-coefficients of XH^+OH^- and $X.H_2O$ respectively. $A_\eta(X.H_2O) = 0$ by definition[12] since $X.H_2O$ is a non-electrolyte, we thus get:

$$\left(\frac{\eta}{\eta_0}\right)_{obs} = 1 + A_\eta(XH^+OH^-)\sqrt{\alpha c} + B_\eta(XH^+OH^-)\alpha c + B_\eta(X.H_2O)(1-\alpha)c \qquad \ldots (4)$$

Rearranging Eq. (4) we get

$$\left[\left(\frac{\eta}{\eta_0}\right)_{obs} - 1\right] - \phi = B_\eta(X.H_2O)(1-\alpha)c \qquad \ldots (5)$$

where $\phi = A_\eta(XH^+OH^-)\sqrt{\alpha c} + B_\eta(XH^+OH^-)\alpha c$

The A_η-values for XH^+OH^- were calculated from the limiting equivalent conductances using the equation given by Falkenhagen *et al.*[8,13]. The values of the limiting conductances of XH^+ and OH^- were taken from literature[14-16]. $B_\eta(XH^+OH^-)$ were evaluated using the additivity equation (Eq. 6), valid for strong electrolytes in dilute solutions.

$$B_\eta(XH^+OH^-) = B_\eta(XH^+Cl^-) + B_\eta(Na^+OH^-) - B_\eta(Na^+Cl^-) \qquad \ldots (6)$$

where $B_\eta(XH^+Cl^-)$, $B_\eta(Na^+OH^-)$ and $B_\eta(Na^+Cl^-)$ are the viscosity B-coefficients of amine hydrochloride, NaOH and NaCl respectively. The viscosity B-coefficients of the amine hydrochlorides were determined in this work[17]. The values of viscosity B-coefficients of NaCl and NaOH used in Eq. (6) are given in Table 1.

For the evaluation of $B_\eta(X)$, the viscosity B-coefficients of the hypothetical aggregate $X.H_2O$ were first evaluated as slopes of the plots of left hand side of Eq. (5) versus $(1-\alpha)c$ which were all linear passing through the origin (Fig. 1). Since similar plots at 5° and 15°C were all linear passing through the origin these have not been reproduced here. The α-values were determined iteratively[3,4].

In the case of hydrolysis corrections applied for obtaining limiting compressibilities and volumes in the previous work[4,5] the respective quantities for pure water, i.e. ϕ_{ks}^0 (H_2O) and ϕ_v^0 (H_2O) were sub-

Table 2—B_η^{str} and $B_\eta(X)$ Values of Amines and Alcohols* at Different Temperatures

Compound	5°		15°		25°	
	$B_\eta(X)$	B_η^{str}	$B_\eta(X)$	B_η^{str}	$B_\eta(X)$	B_η^{str}
NH_3	0.014	−0.021	0.003	−0.032	−0.004	−0.039
H_2O		−0.004		−0.002		
$MeNH_2$	0.144	0.083	0.119	0.056	0.087	0.026
	(0.170)		(0.147)		(0.130)	
MeOH	0.121	0.067	0.095	0.040	0.080	0.025
$EtNH_2$	0.249	0.162	0.238	0.151	0.184	0.097
	(0.307)		(0.260)		(0.215)	
EtOH	0.245	0.164	0.210	0.129	0.185	0.104
n-$PrNH_2$	0.372	0.259	0.311	0.198	0.251	0.138
	(0.380)		(0.325)		(0.275)	
n-PrOH	0.350	0.243	0.290	0.183	0.250	0.143
n-$BuNH_2$	0.440	0.257	0.344	0.201	0.305	0.162
	(0.480)		(0.415)		(0.355)	
n-BuOH	0.439	0.302	0.360	0.223	0.305	0.168
t-$BuNH_2$	0.450	0.313	0.364	0.270	0.303	0.166
	(0.505)		(0.440)		(0.377)	
t-BuOH	0.515	0.384	0.425	0.294	0.365	0.234
Me_2NH	0.293	0.204	0.254	0.165	0.167	0.087
	(0.290)		(0.250)		(0.220)	
Me_3N	0.439	0.326	0.394	0.281	0.318	0.205
	(0.470)		(0.435)		(0.375)	

Values in parantheses are from ref. 1 and 14

*B_η^{str} of alcohols corresponding to the amines (column 1) calculated from viscosity B_η-coefficients (extrapolated at 15° and 25°C) from ref. 7.

tracted from the composite quantities ϕ_k^0 ($X.H_2O$) and ϕ_v^0 ($X.H_2O$) in order to obtain ϕ_{ks}^0 (X) and ϕ_v^0 (X) of unhydrolysed amine molecules. Similarly, in the present case the B_η of the unhydrolysed species X was obtained using Eq. (7):

$$B_\eta(X) = B_\eta(X.H_2O) - B_\eta(H_2O) \quad \ldots (7)$$

Equation (7) is based upon the postulate that the effective volume of the hypothetical aggregate $X.H_2O$ is additively made up of the corresponding volume of X and H_2O, which is reasonable in the context of the present work.

Unlike ϕ_{ks}^0 (H_2O) and ϕ_v^0 (H_2O) which are well known quantities, the B_η (H_2O) cannot be determined by direct measurements. $B_\eta(H_2O)$ which represents the effective hydrodynamic volume of water molecules in liquid water cannot be evaluated by using the Stokes-Einstein diffusion equation since water molecules are not sufficiently large to allow the treatment of liquid water as continuum. There is also no established method of obtaining $B_\eta(H_2O)$. In the work of Conway *et al.*[2] measurements of compressibility of amines dissolved in dil KOH solution enabled them to evaluate limiting compressibilities of unhydrolysed amine molecules. The results obtained were interpreted in terms of amine-water hydration interactions. Presence of KOH is thus to be understood as totally suppressing hydrolytic chemical interaction with water (Eq. 2) without affecting the hydrophobic hydration effects, if any. It was hence thought that a similar procedure could be adopted for evaluating $B_\eta(X)$ for $MeNH_2$ and $EtNH_2$. Substracting this $B_\eta(X)$ from $B_\eta(X.H_2O)$ obtained from Eq. (5) would then enable evaluation of the parameter $B_\eta(H_2O)$. The correctness of this line of thinking is further confirmed by the fact that the difference $[B_\eta(X.H_2O) - B_\eta(X)]$ found experimentally is always positive, as it should be, if this difference has to represent $B_\eta(H_2O)$. The mean values of $B_\eta(H_2O)$ obtained from measurements of viscosity of $MeNH_2$ and $EtNH_2$ dissolved in KOH and after subtracting $B_\eta(X)$ from the $B_\eta(X.H_2O)$ (Eq. 5) were found to be 0.030 and 0.028 at 25° and 15°C, respectively. The value at 5°C obtained by extrapolation was 0.026 $dm^3\ mol^{-1}$. These values were hence used in Eq. (7) to estimate $B_\eta(X)$ for all the other amines at different temperatures.

However, this method of using KOH for the determination of $B_\eta(X)$ cannot be extended to higher amines (*n*-propylamine onwards) because of the possible increase in the degree of amine-amine-ion interactions with increase in size of the solute. These values of $B_\eta(H_2O)$ so obtained from measurements on methyl and ethyl amines were used subsequently in the case of other amines to obtain $B_\eta(X)$.

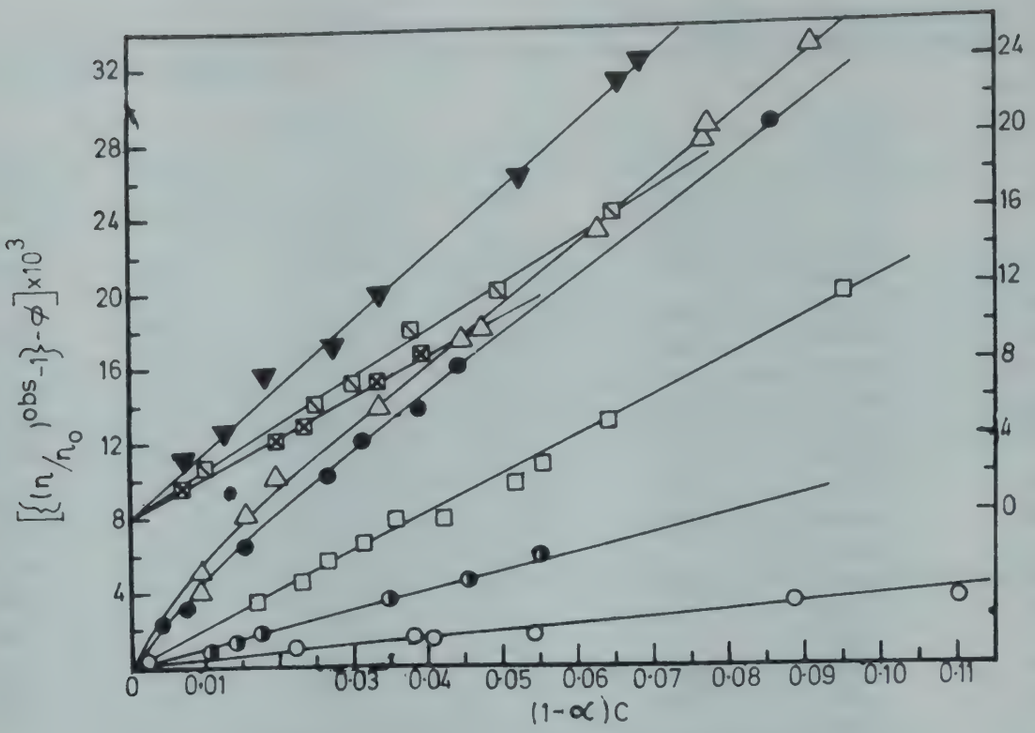

Fig. 1—Variation of $[\{(\eta/\eta_0)_{obs}-1\}-\phi]$ with $(1-\alpha)c$ at 25°C, ○, NH_3; ◑, $MeNH_2$; □, $EtNH_2$; ●, t-$BuNH_2$; △, n-$BuNH_2$ (Left hand scale) ⊠, Me_2NH; ⊡, n-$PrNH_2$; ▼, Me_3N (Right hand scale)

For n-$BuNH_2$ and t-$BuNH_2$ at 25° the plots between left hand side of Eq. (5) versus $(1-\alpha)c$ had slight curvature at low concentration (0 to 0.01 *M*) (Fig. 1). Hence $B_\eta(X.H_2O)$ of these amines at 25°C were determined from the plots in the amine concentration range of 0.015-0.1 *M* within which the plots were linear.

Results and Discussion

In Table 2 are given the coefficients, $B_\eta(X)$, of amines at 5°, 15° and 25°C, obtained after correction for hydrolysis. For comparison, the B_η-coefficients obtained earlier at high concentration1 are also given. The B_η-coefficients obtained presently after applying correction for hydrolysis are slightly smaller. The trends in variation with respect to temperature of the present $B_\eta(X)$ and earlier values are, however, similar. In Table 3 are presented the values of $(dB_\eta/dT)_{5°}$ $[\equiv B'_\eta(5°)]$ for amines. For comparison the $B'_\eta(5°)$ of alcohols are also given.

The B_η-coefficients are usually interpreted in the light of the Einstein[11,19] equations.

$$\left(\frac{\eta}{\eta_0}-1\right)=\nu^E\phi_W \qquad \ldots (8)$$

or

$$\left(\frac{\eta}{\eta_0}-1\right)=\nu^E Vh.c \qquad \ldots (9)$$

Table 3—Values of $B'_\eta(5°)\times10^3$ at 5°C for Amines and Alcohols

Amine		Alcohol*	
Ammonia	−1.1		
Methyl	−2.5	MeOH	−3.3
Ethyl	−1.1	EtOH	−4.0
n-Propyl	−6.1	n-PrOH	−6.3
n-Butyl	−10.4	n-BuOH	−11.0
t-Butyl	−10.0	t-BuOH	−12.5
$(CH_3)_2NH$	−3.9		
$(CH_3)_3N$	−4.5		

*From ref. 7

where ϕ_W is the volume fraction, ν^E is a constant depending upon the size and shape of the solute particles in a solution of concentration c and Vh is the hydrodynamic volume of the solute. The net effect of the solute on the structure of a solvent can be understood appropriately if the shape and size effect B^E_η is subtracted from the experimental viscosity B-coefficients. We define a new parameter, B^{str}_η by Eq. (10)

$$B^{str}_\eta=B^{Tot}_\eta-B^E_\eta \qquad \ldots (10)$$

where B^E_η is evaluated from Eq. (11)

$$B^E_\eta=\nu^E\ V_w=\nu^E.V^h \qquad \ldots (11)$$

In Table 2 are given the values of B^{str}_η computed from the van der Waal's volumes $(V_w)^{20}$ and the values of ν^E given by Herskovits[21], for alcohols assuming that the axial ratio of the amines and correspond-

ing alcohols will not differ much. B_η^{str} increases with increase in the chain length of the molecule (Table 2). This is expected since non-polar groups enhance[22] water structure due to hydrophobic hydration. The ability of structure promotion therefore increases with increase in chain length as is to be expected. In the case of isomeric amines (Table 2), the B_η^{str} values of the branched isomers Me_2NH and Me_3N are greater than those of the straight chain isomers $EtNH_2$ and *n*-$PrNH_2$ respectively, especially at lower temperatures. Similarly the B_η^{str} of *t*-$BuNH_2$ is greater than that of *n*-$BuNH_2$. This suggests that the branching of the hydrocarbon chain has greater influence on water structure. The negative B_η^{str} for ammonia and for water at 5° and 15° should not be interpreted as showing structure breaking tendency, but rather it may be looked upon as indicating the inadequacy of the Einstein relation for molecules which are of size comparable to the molecules of the medium in which they move.

In Table 2 are also given the B_η^{str} of alcohols evaluated by us using the B-coefficients of alcohols determined by Alexander[7]. The values of B_η^{str} of the amines do not differ significantly from those of the corresponding alcohols (Table 2) indicating that the difference in the degree of structure promotion of water by the $-OH$ and the $-NH_2$ groups is too subtle to be differentiated on B_η^{str} values alone.

The temperature dependence of viscosity B_η-coefficients can be more useful for understanding the solvent interaction. In Table 3 are given the B'_η (5°) at sufficiently low temperature where thermal disordering effects do not obliterate the structural stabilisation, if any, induced by the solute in its neighbourhood. Negative B'_η (5°) can be meaningfully attributed to the structural melting and the degree of structure promotion by the solute. It is seen that though the B'_η (5°) of amines and alcohols become more negative as the hydrophobic chain length increases the B'_η (5°) of amines are always less negative than the B'_η (5°) of the corresponding alcohols (Table 3). This suggests that $-OH$ group causes greater water structure stabilisation than the $-NH_2$ group. This corroborates the observation of Kaulgud[23], who has shown on the basis of the relation between compressibilities (of alcohols and of amines) and the change in temperature of maximum density of water caused by the solutes that $-NH_2$ group has a loosening effect on water structure while $-OH$ group, because of its ability to enter into cooperative bonding with water molecules, promotes it. Similar conclusion has been drawn from the study of volumetric properties[5] of dilute solutions of amines and alcohols.

The B_η-coefficients obtained from measurements at higher concentration are systematically higher than those obtained from present measurements at very low concentration (Table 2). This can be due to solute-solute interactions at higher concentration causing an increase in the effective volumes of solutes.

Acknowledgement

Two of us (MRA) and (DSP) are thankful to UGC, New Delhi for the award of fellowship under Faculty Improvement Programme.

References

1 Patel R I, Patil K J & Kaulgud M V, *Z phys Chem (NF)*, **86** (1973) 67.
2 Conway B E & Verral R E, *J phys Chem*, **70** (1966) 3953, 3961.
3 Cabani S, Conti G & Lepori L, *J phys Chem*, **76** (1972) 1338, **78** (1974) 1030.
4 Kaulgud M V, Awode M R & Shrivastava A, *Indian J Chem*, **19A** (1980) 144.
5 Kaulgud M V, Bhagde V S & Shrivastava A, *J chem Soc Faraday Trans I*, (1982) 313.
6 Davies C & Malpass V E, *Trans Faraday Soc*, **60** (1964) 1081.
7 Alexander D M, *Aust J Chem*, **35** (1982) 465.
8 Kaminsky M, *Z Phys Chem (NF)*, **5** (1955) 154.
9 Stokes R H & Mills R, *Viscosity of electrolytes and related properties* (Pergman Press, New York) 1965.
10 Campbell A N & Lam S Y, *Can J Chem*, **5** (1973) 551.
11 Tyrrell H J V, *Essay in structural chemistry* (Macmillan, London) 1971, Chapter 10.
12 Jones G & Talley S K, *J Am chem Soc*, **55** (1933) 624.
13 Falkenhagen H & Vernon E L, *Z Physik*, **33** (1932) 140.
14 Sommerville W C, *J phys Chem*, **35** (1931) 2412.
15 Moore T S & Winmill T F, *J chem Soc*, **101** (1912) 635.
16 Robinson R A & Stokes R H, *Electrolyte solutions* (Butterworths, London) 1959.
17 Awode M R, *Studies on the transport properties of aqueous solutions*, Ph D Thesis, Nagpur University (1981).
18 Patil D S, *Studies of viscosity B-coefficients of neutral amines in aqueous solutions*, M Phil Project, Nagpur University (1984).
19 Einstein A, *Am Physik*, **19** (1906) 289.
20 Bondi A, *J phys Chem*, **68** (1964) 441.
21 Herskovitz T T & Kelly T M, *J phys Chem*, **77** (1973) 381.
22 Frank H S & Evans M W, *J chem Phys*, **13** (1945) 507.
23 Kaulgud M V, *J chem Soc Faraday Trans I* (1979) 2246.

Indian Journal of Chemistry
Vol. 27A, November 1988, pp. 942-946

Enthalpies of Dimerization of Some Polar & Nonpolar Gases

CHRISTOPHER J BIERMANN
Department of Forest Products, Oregon State University, Corvallis, Oregon 97331, USA

Received 24 *June* 1987; *revised and accepted* 8 *March* 1988

Deviations from ideal gas behaviour due to dimerization may be solved in terms of the virial equation. The two parameters, the slope and intercept of the van't Hoff plot, have been successfully used to determine a correction factor (generally with less than 2% error below one atmosphere pressure, corresponding to less than 0.1% error in compressibility factor, Z) from ideal behavior for temperatures up to 1.5 times the boiling point of a compound. This method should be useful in computer applications to replace tables or interpolation for calculating deviations from ideal gas behavior at relatively low pressures. It is also a link between cluster theory and gas behavior. By determining the equilibrium constant as a function of temperature the following enthalpy of dimerization values have been obtained: ethanol, 4300; pentane, 2394; perfluoropentane, 2609; argon, 533; and krypton, 708 cal/mol.

The concept of dimerization in the gaseous state has been used to explain large negative deviations from ideal behavior reflected in values of the compressibility factor (Z) below unity at temperatures in the vicinity of the boiling points of compounds. As early as 1928 Coolidge[1] studied the vapor pressure of formic acid in terms of dimerization. The phenomenon of dimerization to explain the behavior of carboxylic acids is well documented[2]. Hydrogen bonding (H-bonding) in carboxylic acids is much stronger than most other examples of H-bonding. Various gas phase properties of compounds, such as heat capacity, PVT behavior, and thermal conductivity, have been investigated in terms of dimerization and higher interactions[3-7].

In the past nonpolar forces were not thought to contribute to dimerization. The concept of association has usually been applied only if one of the following is true[8]: the law of corresponding states does not hold, the molecular structure allows the formation of a definite dimer with either a H-bond or a covalent bond, or dimeric species have been detected by an independent means such as spectroscopy. More recently clusters have been observed for nonpolar compounds[9,10]. Future work with clusters should make it possible to confirm and quantitate dimers and higher clusters in gases at various temperatures and pressures. Data presented for carbon dioxide show that lower temperatures and higher pressures favor the formation of large clusters with techniques recently introduced[10], exactly the behavior one predicts from PVT data and association theory[11-13].

Based on these more recent developments it is quite logical to determine enthalpies of dimerization of polar and nonpolar compounds from virial coefficient data. The enthalpy of dimerization is a fundamental property of a compound as is the enthalpy of vaporization. Based on the understanding of dimerization and vaporization, the enthalpy fo dimerization is expected to be a fraction of the enthalpy of vaporization. One noticeable exception is the case of carboxylic acids where the enthalpy of dimerization is stronger than the enthalpy of vaporization since the vapor exists largely in the form of dimers.

One study[14] estimated dimerization constants based on second virial coefficients of nonpolar compounds assuming a molar excluded volume of 1.75 times the molar critical volume. The present study reconstructs the PVT data or uses PVT data directly for greater accuracy, as explained presently, and considers only temperatures sufficiently low so that the excluded volume represents a small error and is considered as zero. Furthermore, better data are available in the literature since the previous study[14]. Other than this study, negligible information is available on the dimerization of nonpolar gases in the gas phase.

Mathematical Development

With the concept of dimerization in mind the behaviour of gases will be examined with only two premises: (i) gas molecules tend to form dimers (Eq. 1) with an equilibrium constant of K_p defined in Eq. (2); and (ii) individually the molecular species obey the ideal gas law (Eq. 3).

$$m + m \rightarrow m - m \qquad \ldots (1)$$

$$K_p = \frac{P_{m-m}}{(P_m)^2} \qquad \ldots (2)$$

$$\frac{P_{eff}V}{RT} = N_{eff} = N_m + N_{m-m} \qquad \ldots (3)$$

Table 1- Deviation of Truncated Virial Approximation of B From Actual B due strictly to Dimerization

Pressure (atm)	K $(atm)^{-1}$	B_{dimer}[a] cm^3/mol	$B_{truncated}$ cm^3/mol	Deviation Percent
1.00	0.04	984.7	858.6	12.8
0.50	0.04	984.7	913.8	7.2
0.10	0.04	984.7	969.2	1.5
0.01	0.04	984.7	983.1	0.16
1.00	0.01	246.2	236.8	3.8
0.50	0.01	246.2	241.4	2.0
0.10	0.01	246.2	245.2	0.4

[a]B is solved at an arbitrary temperature of 300 K

From Eq. (1) it follows that there is a net decrease in one mole for every mole of dimer formed. Using the second premise it then follows that the difference between the experimental pressure and the classical ideal pressure is equal to the pressure of the dimer:

$$P_{m-m} = P_{id} - P_{eff} \quad \ldots (4)$$

Also from Eq. (1) there is a decrease of two moles of monomer per mole of dimer formed. Thus, assuming Eq. (3) to be true:

$$P_m = P_{id} - 2(P_{id} - P_{eff})$$

$$P_m = 2P_{eff} - P_{id} \quad \ldots (5)$$

And, by definition:

$$K_p = (P_{id} - P_{eff})/(2P_{eff} - P_{id})^2 \quad \ldots (6)$$

The virial equation of state in terms of K_p has been derived by both Woolley[11] and Stogryn and Hirschfelder[12]. The equation is given as Eq. (7) and is valid for $P_{id} \leq 1/8K_p$.

$$Z_d = P_{eff}/P_{id}$$
$$= 1 - K_pP_{id} + 4K_p^2P_{id}^2 - 20K_p^3P_{id}^3 + \quad \ldots (7)$$

In Eq. (7) the term Z_d designates the contribution of dimerization to the overall Z. P_{id} could be substituted with RTN/V to give it in the form of molar volume. P_{eff} is strictly the ideal pressure reduced according to the effective number of moles relative to the ideal number of moles assuming no interactions between the dimers and monomers.

Results and Discussion

Error of virial approximation

At low pressures, the virial equation is often approximated to the second virial coefficient with the mistaken impression that the third virial coefficient does not depend on binary interactions (which Eq. 7 proves is not true). Z then becomes:

$$Z = 1 - B_vN_{id}/V \quad \ldots (8)$$

If dimerization significantly influences the deviation from ideal behavior, and if the virial equation is approximated to one term then the virial coefficient determined is a function of pressure, since the virial approximation is only true as pressure tends to zero. This explains much of the disagreement in the value of second virial coefficients at relatively low temperatures in literature. Table 1 gives the calculated error, which can be substantial under the conditions virial coefficients are often measured in literature, for various equilibrium constants and pressures.

Due to the substantial error of the truncated approximation for most data in literature, if the virial coefficient is given as an approximation then Z may be determined from Eq. (8), provided the approximate pressure, and therefore molar volume, is known; one chooses an approximate molar volume as exact for the purposes of calculation. The effective and ideal pressure may then be calculated and K_p solved by Eq. (6). It is preferable to use the original PVT data if available.

One additional point to consider is the possibility for trimerization. The higher the pressure the larger the relative error introduced by trimerization and higher interactions. For values of Z greater than 0.97 the concentration of dimer is less than 3% of the concentration of monomer. Assuming the equilibrium constant for trimerization (based on the concentration of dimer and monomer) is approximately the same or less than the equilibrium constant for dimerization, the error of the correction will be less than 3%. From the data presented in this paper and assumption appears to be valid.

Enthalpy of dimerization of ethanol

Recently Bich *et al.*[15] have published excellent data on the pressure-volume-temperature relationship of ehtanol at pressures from 40 to 170 kPa and at temperatures from 340 to 680K. These data are the model type from which to calculate thrmodynamic data for the enthalpy of dimerization.

Where pressure-molar volume-temperature data are given for a gas of a single molecular species at relatively low pressures one can determine the ideal pressure (assuming ideal behavior) and the actual pressure (the effective or experimental pressure). From these data the equilibrium constant for dimerization may be determined from Eq. (6).

This has been done for all the data at temperatures below 525K. Above this temperature, the equilibrium constant is too small to be determined accurately by experimental data in this pressure range and also excluded volume (which tends to increase Z) becomes significant. Additionally the second

Table 2 - Equilibrium Constant of Ethanol Dimerization in the Gas State

T (K)	K_p(exptl)	ln K_p Experimental	ln K_p Least Squares	Deviation
n = 0.0019938 mols, 144.37 cm^3				
348.34	0.03914	-3.241	-3.253	-0.012
389.60	0.01964	-3.930	-3.912	+0.028
415.36	0.01418	-4.256	-4.257	-0.001
443.92	0.01004	-4.601	-4.593	+0.009
486.60	0.00668	-5.009	-5.021	-0.011
n = 0.0030909 mols, 144.35 cm^3				
360.91	0.03165	-3.453	-3.472	-0.019
383.94	0.02124	-3.852	-3.832	+0.020
412.52	0.01443	-4.238	-4.224	+0 014
439.24	0.01083	-4.526	-4.543	-0.017
469.66	0.00766	-4.871	-4.863	+0.008
502.63	0.00575	-5.159	-5.166	-0.007
n = 0.0040460 mols, 139.24 cm^3				
390.07	0.02004	-3.910	-3.905	-0.005
415.31	0.01440	-4.241	-4.241	0.000
443.81	0.01034	-4.571	-4.574	-0.003
477.19	0.00743	-4.902	-4.915	-0.013
506.97	0.00555	-5.193	-5.181	+0.010
n = 0.0045016 mols, 138.30 cm^3				
376.57	0.02499	-3.689	-3.705	-0.016
395.80	0.01839	-3.996	-3.984	+0.012
413.82	0.01454	-4.231	-4.222	-0.009
450.43	0.00961	-4.645	-4.646	-0.001
486.40	0.00675	-4.999	-5.001	-0.002
517.33	0.00517	-5.264	-5.267	-0.003

point of the first set and the first point of the third set was discarded, but K_p has been determined for the remaining data based on the pressure in atmospheres. The equilibrium constant is related to temperature by Eq. (9), a derivation of the van't Hoff equation:

$$d(\ln K_p)/d(1/T) = \Delta H/R \qquad \ldots (9)$$

Thus the slope of the plot of ln K_p versus $(1/T)$ at a given temperature multiplied by R is equal to the enthalpy of reaction at that temperature. The equilibrium constant was plotted as a function of temperature according to Eq. (9), linear regression (least squares fit) was applied to the data and the results are listed in Table 2.

The results indicate that it is possible to determine precise enthalpies of dimerization under appropriate conditions. The deviation amounts to less than 1% on the average. This corresponds to less than 0.01% error in the original pressure-volume-temperature data. Because the enthalpy of dimerization is constant over the temperature range it may be used to accurately predict dimerization at temperatures below the range of the data. Furthermore, K_p is independent of pressure, at least over the modest levels encountered in this data, which would not be true of the second virial coefficient of the truncated virial equation. It may also be assumed that trimerization of the gas molecules is negligible, except at the lowest temperature for each set of data where the least squares fit predicts a slightly smaller equilibrium constant than is actually observed. This is due to trimerization which increases the apparent value of K_p. In any case two parameters (the slope and intercept) accurately predict the behavior of Z over a modest temperature and pressure range.

Table 3 - Summary of Intercept and Slope Data For Ethanol.

Set	Intercept	Slope	-ΔH cal/mol	Sum of (errors)^2
1	-9.474	2167	4306	0.00068
2	-9.479	2168	4308	0.00136
3	-9.437	2158	4287	0.00036
4	-9.446	2162	4296	0.00050
Ave	-9.459	2164	4300	
Std Dev.	0.02	5	10	

Table 4- Derived Equilibrium Constants for Pentane and Perfluoropentane

Temp (K)	-B_v Corr. cm^3/mol	-B_p 1/atm	ln K_p (ln B_p)	ln K_p Least Sq.	Deviation
Pentane					
307.55	1082	0.0429	-3.149	-3.143	0.006
329.25	896	0.0332	-3.406	-3.401	0.005
337.65	851	0.0307	-3.483	-3.492	-0.009
351.15	783	0.0272	-3.606	-3.630	-0.024
352.95	747	0.0258	-3.658	-3.647	0.011
372.05	662	0.0217	-3.831	-3.822	0.009
383.65	623	0.0198	-3.923	-3.920	0.003
ln K_p = -7.061 + 1205.0(1/K) ΔH = -2394 cal/mol					
Perfluoropentane					
307.55	1360	0.0539	-2.921	-2.908	0.013
329.15	1125	0.0417	-3.178	-3.188	-0.010
337.35	1036	0.0374	-3.285	-3.285	-0.000
350.85	914	0.0324	-3.428	-3.435	-0.007
372.75	811	0.0265	-3.630	-3.655	-0.025
382.75	717	0.0228	-3.780	-3.750	0.030
ln K_p = -7.177 + 1312.9(1/K) ΔH = -2609 cal/mol					

The results, summarized in Table 3, show that the enthalpy of dimerization can be measured within 0.5% error at the 95% confidence level. By extrapolating K_p to zero pressure at constant temperature this error could be significantly reduced. The enthalpy of dimerization, -4300 cal/mol, is a reasonable proportion of the enthalpy of vaporization which is -9675 cal/mol at the boiling point, and agrees well with the results of -3700 cal/mol determined by thermal conductivity[5] and -4000 cal/mol determined by Kretschmer and Wiebe[4]. Thermal conductivity data also suggest the presence of a small amount of trimers at the higher pressures.

Table 5. Derived Equilibrium Constants for Argon and Krypton.

Temp	$-B_v$ Corr.	$-B_p$	ln K_p		Deviation
(K)	cm^3/mol	1/atm	(ln B_p)	Least Sq.	
		Argon			
84.791	249.34	0.03584	-3.329	-3.312	0.017
88.336	229.89	0.03172	-3.451	-3.444	0.007
92.303	211.79	0.02796	-3.577	-3.580	-0.003
95.058	200.87	0.02575	-3.659	-3.667	-0.008
101.398	178.73	0.02148	-3.841	-3.850	-0.009
102.014	177.65	0.02122	-3.853	-3.867	-0.014
105.513	166.06	0.01918	-3.954	-3.957	-0.003
108.146	160.27	0.01806	-4.014	-4.021	-0.007
113.318	149.58	0.01609	-4.130	-4.139	-0.009
117.501	140.58	0.01458	-4.228	-4.226	0.002
123.990	127.99	0.01256	-4.377	-4.350	0.027
ln K_p = -6.596 + 278.44(1/K)		ΔH = -553 cal/mol			
		Krypton			
107.547	386.67	0.04382	-3.128	-3.129	-0.001
108.894	374.23	0.04188	-3.173	-3.170	0.003
109.938	365.03	0.04046	-3.207	-3.201	0.006
112.279	349.75	0.03796	-3.271	-3.269	0.002
115.351	330.80	0.03495	-3.354	-3.353	0.001
118.498	314.83	0.03238	-3.430	-3.436	-0.006
121.467	301.59	0.03026	-3.498	-3.509	-0.011
121.641	297.47	0.02980	-3.513	-3.513	0.000
128.137	270.49	0.02573	-3.660	-3.662	-0.002
132.126	255.62	0.02358	-3.747	-3.746	0.001
138.071	236.73	0.02089	-3.868	-3.862	0.006
ln K_p = -6.443 + 356.43(1/K)		ΔH = -708 cal/mol			

Enthalpy of dimerization of pentane and perfluoropentane

Data for the compressibility of *n*-pentane and perfluoropentane are available[16] in the temperature range of 307 to 384K. The second virial coefficients of the molar volume series given were extrapolated to zero pressure so they directly represent the equilibrium constant for dimerization after division by the term RT. The results for pentane and perfluoropentane are given in Table 4.

The enthalpy of dimerization of −2394 cal/mol for pentane compares well with the enthalpy of vaporization of −6182 cal/mol at the boiling point. The enthalpy of dimerization of −2609 cal/mol for perfluoropentane is, as expected, higher than that for pentane; the enthalpy of vaporization for this compound is not available.

Enthalpy of dimerization of argon and krypton

Argon and krypton have low enthalpies of vaporization and low enthalpies of dimerization. Consequentl;y, it is necessary to determine the enthalpy of dimerization at low temperatures. The second virial coefficients of the molar volume virial equation have been determined for argon and krypton at various temperatures by Fender and Halsey[17]. The second virial coefficients were corrected for adsorption of the species as well as for the effect of the third virial coefficient by the authors. All that is necessary is to divide the virial coefficient by the term RT to express it in terms of the ideal pressure series. The second virial term is then the equilibrium constant. This has been accomplished for argon and krypton and the results are presented in Table 5.

For argon the enthalpy of dimerization of −553 cal/mol was obtained throughout the temperature range. The enthalpies of vaporization in the same temperature range are −1540 cal/mol (at 85°) and −1150 cal/mol (at 124°) (ref. 18). Similarly for krypton the enthalpy of dimerization is −708 cal/mol with enthalpies of vaporization of −2250 cal/mol (at 107.5°) and −2000 cal/mol (at 237°) (ref. 18). For all of the compounds studied so presently the enthalpies of dimerization are constant, whereas, the enthalpies of vaporization decrease with increase in temperature.

Appendix

List of Variables

B_v = Second virial coefficient of the volume series
B_p = Second virial coefficient of the pressure series
ΔH = Heat of dimerization
K_p = Equilibrium constant (pressure)
N_{eff} = The effective number of moles
N_{id} = The ideal number of moles (assuming no dimerization)
N_m = Moles of monomer
N_{m-m} = Moles of the dimer
P_{m-m} = Pressure of the dimer (all pressures are in atmospheres)
P_m = Pressure of the monomer
P_{eff} = Effective pressure (experimental pressure)
P_{id} = Ideal pressure (classical ideal pressure)
R = Ideal gas constant 82.0575 atm cm^3/mol K, 1.987 cal/mol K
T = Temperature in Kelvin
V = Volume of gas
Z = Compressibility factor ($Z = P_{eff}V/NRT$)

References

1 Coolidge A S, *J Am chem Soc*, **50** (1928) 2166.
2 Buettner R & Maurer G, *Ber Bunsenges Phys Chem*, **87** (1983) 877.
3 Weltner Jr. W & Pitzer K S, *J Am chem Soc*, **73** (1951) 2606.
4 Kretschmer C B & Weibe R, *J Am chem Soc*, **76** (1954) 2579.
5 Frurip D L, Curtiss L A & Blander M, *Therm Conduct*, **16** (1979) 565.
6 Prausnitz J M & Carter W B, *A I Ch E Journal*, **6** (1960) 611.
7 Lambert J D, Roberts G A H, Rowlinson J S, Wilkinson V J, *Proc Roy Soc*, **A196** (1949) 113.
8 Beattie J A& Stockmayer W H in *A treatise in physical chemistry, Vol 2, States of matter*, edited by H S Taylor & S Glasstone (Van Nstrand, New York) 1951; p 339-341.
9 Jortner J, *Ber Bunsenges Phys Chem*, **88** (1984) 188.

10 Recknagel E, *Ber Bunsenges Phys Chem*, **88** (1984) 201.
11 Woolley H W, *J chem Phys*, **21** (1953) 236.
12 Stogryn D E & Hirschfelder J O, *J chem Phys*, **31** (1959) 1531.
13 Spurling T H & Mason E A, *J chem Phys*, **51** (1969) 1684.
14 Hirschfelder J O, McClure F T & Weeks I F, *J chem Phys*, **10** (1942) 201.
15 Bich E, Ramsdorf M & Opel G, *Z Phys Chem*, (*Leipzig*), **265** (1984) 401.
16 Garner M D G & McCoubrey J C, *Trans Faraday Soc*, **55** (1959) 1524.
17 Fender B E F & Halsey G D, *J chem Phys*, **36** (1962) 1881.
18 Vargaftik N B, *Tables of thermophysical properties of liquids and gases*, (John Wiley, New York) 1975.

Indian Journal of Chemistry
Vol. 27A, November 1988, pp. 947-950

A Study of Intramolecular Hydrogen Bonding in *o*-Nitroaniline

G PARIMALA SOMESWAR
Department of Chemistry, Govt. City College, Hyderabad 500 002

Received 18 *September* 1985; *revised* 12 *March* 1986; *rerevised and accepted* 7 *March* 1988

The presence of intramolecular hydrogen bond in *o*-nitroaniline has been investigated by studying the IR spectrum of the compound in different proton accepting solvents. For the purpose of comparison, a similar study has been made on *p*-nitroaniline also. Frequency shifts of the asymmetric and symmetric N – H stretching bands show formation of associated species with the solvents. Analysis of the shift patterns shows the presence of hydrogen bond in *o*-nitroaniline.

The presence of intramolecular hydrogen bonding in *o*-nitroaniline has been a matter of greater controversy[1-6]. Pimental *et al.*[1] pointed out that the differences in the N – H stretching frequencies of *o*-nitroaniline in nitrobenzene are due to the presence of a weak hydrogen bond.

Medhi and Kastha[2] studied the influence of proton acceptor solvents like ether, acetone, tetrahydrofuran and pyridine on the IR spectra of some *o*-substituted anilines and concluded that the shifts in the NH frequencies have no systematic dependence either on the dielectric constants or on the dipole moments of solvent molecules. According to them the smaller shifts in *o*-nitroaniline compared to those in its *p*-isomer are due to steric effects. Kruger[3], however, attributed the increase in the apparent HNH angle of *o*-nitroaniline (121.7°) compared to that of aniline (110.9°) to intramolecular hydrogen bonding.

In view of the controversy about the presence of intramolecular hydrogen bond in *o*-nitroaniline, it was thought worthwhile to re-examine the behaviour of *o*-nitroaniline and to see whether solvent effect could be helpful in the diagnosis of intramolecular hydrogen bonding. The IR spectrum of the compound has been recorded in a wide range of proton accepting solvents of varying dielectric constants so as to get a clear picture of the solvent effect which might throw some light on the presence of intramolecular H-bond in *o*-nitroaniline. For the purpose of comparison, *p*-nitroaniline, in which there is no intramolecular hydrogen bonding, has also been included in the present study.

The IR data are presented in Tables 1 and 2 and the spectra are presented in Figs 1-5.

Materials and Methods

The infrared spectra were recorded on a Perkin-Elmer 337 grating spectrophotometer (wave number linear) at a temperature of 28 ± 2°C, at a slow speed. Matched sodium chloride cells of 0.5 mm path length were used. The concentrations of the so-

Table 1—Frequencies (cm^{-1}) of the Asymmetric and Symmetric N – H Stretching Bands of *o*- and *p*-Nitroanilines

Sl. No.	Solvent	*p*-Nitroaniline				*o*-Nitroaniline			
		ν_a	$\Delta\nu_a$	ν_s	$\Delta\nu_s$	ν_a	$\Delta\nu_a$	ν_s	$\Delta\nu_s$
1	Carbon tetrachloride	3500	—	3402	—	3525	—	3400	—
2	Chloroform	3505	−5	3420	−18	3525	0	3400	0
3	Dichloromethane	3500	0	3402	0	3520	5	3400	0
4	Dioxane	3430	70	3355	47	3475	50	3345	55
5	Ether	3440	60	3365	37	3480	45	3345	55
6	Anisole	3480	20	3390	12	3500	25	3390	10
7	Diphenyl ether	3490	10	3395	7	3515	10	3395	5
8	Acetone	3445	55	3365	37	3495	30	3375	25
9	Acetophenone	3450	50	3365	37	3500	25	3375	25
10	DMF	3480	50	3350	52	3480	45	3335	65
11	Acetonitrile	3455	45	3377	25	3495	30	3375	25
12	TEA (binary solvent mix)	(a) 3490 (b) 3455	45	(c) 3395 (d) 3305	97	(a) 3510 (b) 3450	75	(c) 3397 (d) 3300	100
13	Pyridine (binary solvent mix)	(a) 3495 (b) 3465	35	(c) 3400 (d) 3325	77	(a) 3515 (b) 3470	55	(c) 3400 (d) 3305	95

Table 2—Deviations of νNH_s Values of *o*- and *p*-Nitroanilines from Bellamy's Equation in Different Solvents

Sl. No.	Solvent	*o*-Nitroaniline				*p*-Nitroaniline			
		νNH_a (cm^{-1})	νNH_s (cm^{-1})		Deviation ($\pm$) (cm^{-1})	νNH_a (cm^{-1})	νNH (cm^{-1})		Deviation ($\pm$) (cm^{-1})
			obs.	expected			obs.	expected	
1	Carbon tetrachloride	3525	3400	3432	32	3500	3402	3412	9
2	Acetonitrile	3495	3375	3406	31	3455	3377	3371	−6
3	Acetone	3495	3375	3406	31	3445	3365	3363	−2
4	Dioxane	3475	3345	3389	44	3430	3355	3349	−6
5	TEA	3450	3300	3367	67	3455	3305	3371	66

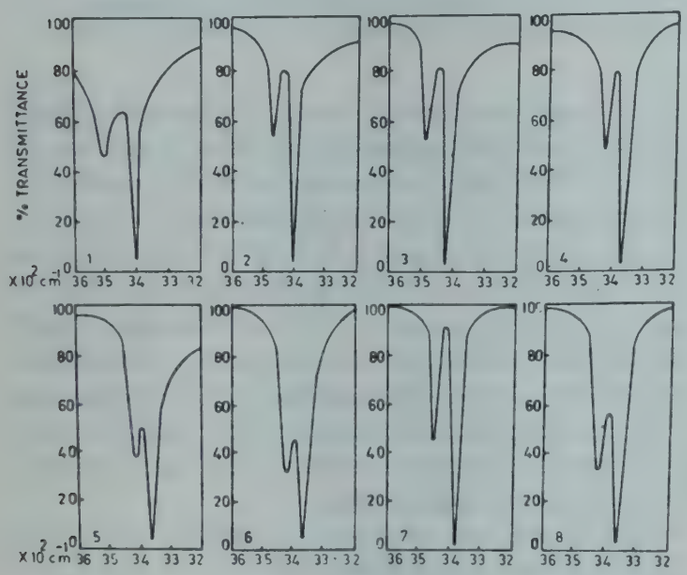

Fig. 1—NH_2 bands of *p*-nitroaniline in different solvents [1, carbon tetrachloride; 2, dichloromethane; 3, chloroform; 4, acetonitrile; 5, dioxane; 6, ether; 7, anisole; 8, acetone]

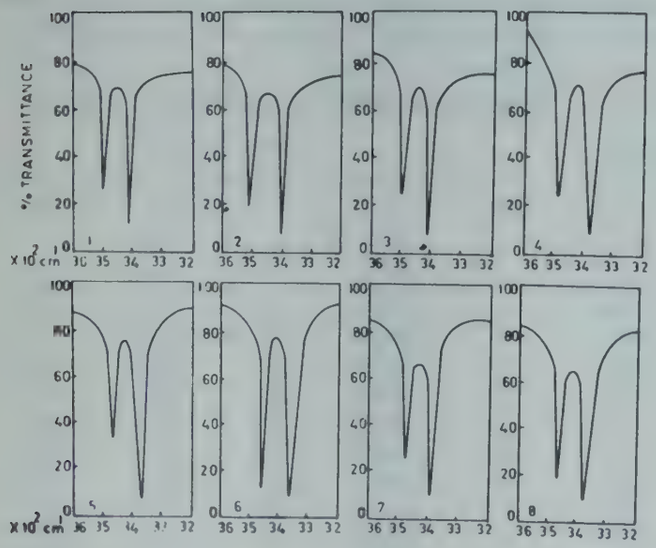

Fig. 2—NH_2 bands of *o*-nitroaniline in different solvents [1, carbon tetrachloride; 2, dichloromethane; 3, chloroform; 4, acetonitrile; 5, dioxane; 6, ether; 7, anisole; 8, acetone]

lutions were of the order 0-1 *M*. For identifying the original bands and the bands due to associated species simultaneously, binary solvent mixtures containing varying amounts of proton acceptor solvents in dichloromethane have been used. Solvent mixtures of the same composition were placed in the reference cell to compensate for the solvent absorption. The solvents were purified and dried as described in literature[7].

Results and Discussion

Effect of halohydrocarbons

In carbon tetrachloride, the two N−H stretching bands are found at 3500 and 3402 cm^{-1} in the case of *p*-nitroaniline and at 3525 and 3400 cm^{-1} in the case of *o*-nitroaniline (Figs 1 and 2). The larger value of νNH_{as}-νNH_s in *o*-nitroaniline (125 cm^{-1}) compared to that in *p*-nitroaniline (98 cm − 1) indicates the presence of a sufficiently strong intramolecular hydrogen bond in *o*-nitroaniline. This is in agreement with Kruger's report that in *o*-nitroaniline there is 56% hydrogen bonding.

In dichloromethane the two bands of *o*- and *p*-nitroanilines suffer little or no change.

In chloroform solution, *o*- and *p*-nitroanilines exhibit sharp singlets for the symmetric and asymmetric vibrations in contrast to clear doublets shown by *o*- and *p*-anisidines and *o*- and *p*-chloroanilines (Fig. 3). This shows lack of association between the NH_2 group and $CHCl_3$ molecules which may be due to the powerful electron withdrawing effect of the NO_2 group. In contrast, $-OCH_3$ and $-Cl$ groups are electron releasing groups and increase the electron density on nitrogen of the NH_2 group in anisidines and chloroanilines.

In dioxane the two bands of *p*-nitroanilines are found at 3430 and 3355 cm^{-1} and in *o*-nitroaniline these are found at 3475 and 3345 cm^{-1}. In order to find out the identity of these bands, the compounds were studied in binary solvent mixtures. For instance, the spectrum of *o*-nitroaniline was recorded in CH_2Cl_2 containing different concentrations of di-

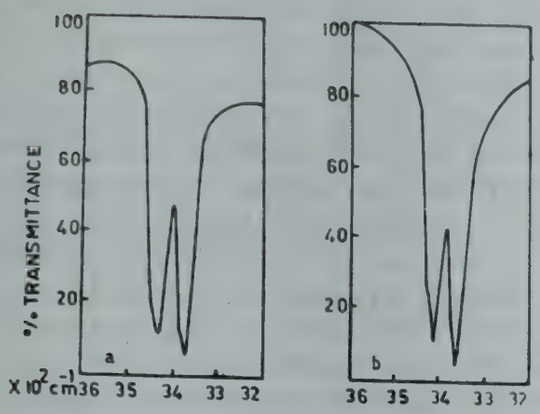

Fig. 3(a)—NH_2 bands of *o*- and *p*-anisidines in chloroform [a, *o*-anisidine; b, *p*-anisidine]

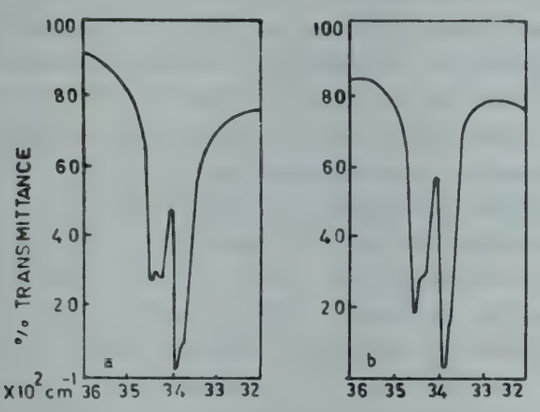

Fig. 3(b)—NH_2 bands of *o*- and *p*-chloroanilines in chloroform [a, *p*-chloroaniline; b, *o*-chloroaniline]

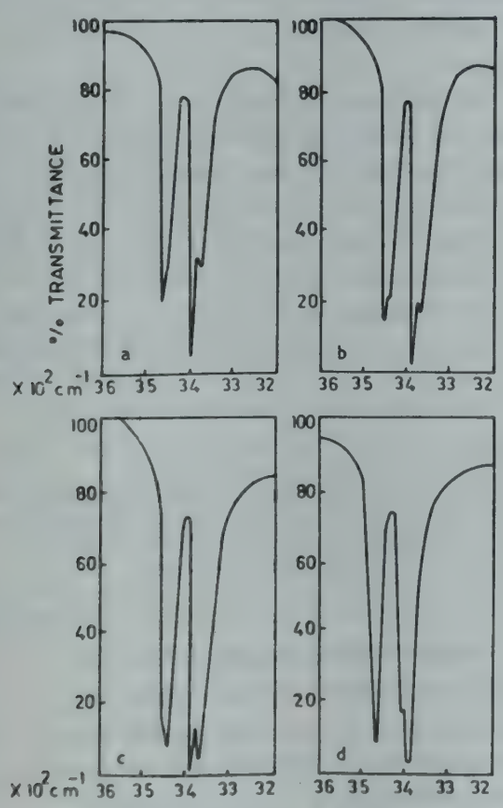

Fig. 4—NH_2 bands of *o*-nitroaniline in acetophenone + dichloromethane [a, 0.05 ml acetophenone + 0.95 ml CH_2Cl_2; b, 0.1 ml acetophenone + 0.9 ml CH_2Cl_2; c, 0.2 ml acetophenone + 0.8 ml CH_2Cl_2; d, 0.4 ml acetophenone + 0.6 ml CH_2Cl_2]

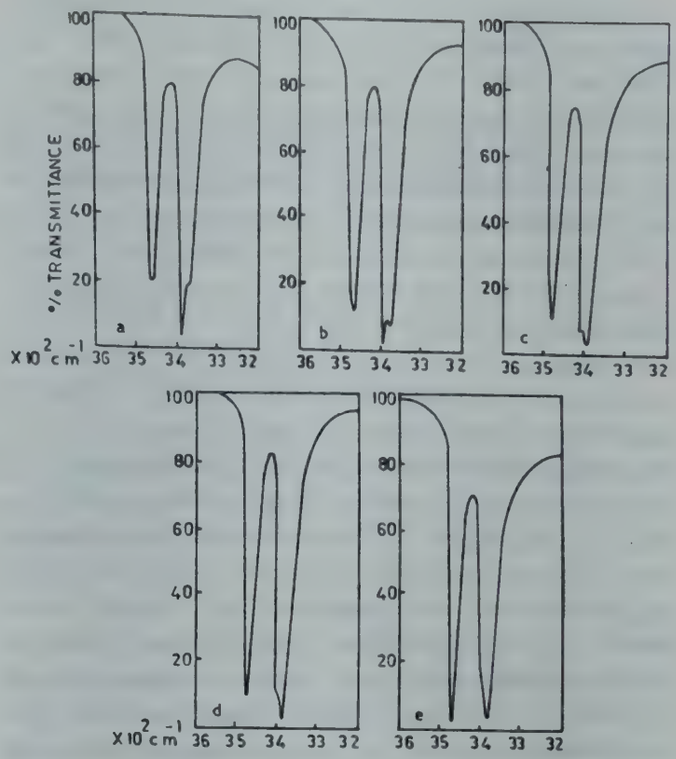

Fig. 5—NH_2 bands of *o*-nitroaniline in acetonitrile + dichloromethane [a, 0.05 ml acetonitrile + 0.95 ml CH_2Cl_2; b, 0.1 ml acetonitrile + 0.9 ml CH_2Cl_2; c, 0.2 ml acetonitrile + 0.8 ml CH_2Cl_2; d, 0.3 ml acetonitrile + 0.7 ml CH_2Cl_2; e, 0.4 ml acetonitrile + 0.6 ml CH_2Cl_2]

oxane. When the spectrum of the compound was recorded in dichloromethane containing very small quantity of dioxane, besides the two original bands found in CH_2Cl_2 (at 3520 and 3400 cm^{-1}), two new bands were found at 3475 and 3345 cm^{-1}. On gradually increasing the concentration of dioxane, the intensities of the two N − H bands in CH_2Cl_2 (3520 and 3400 cm^{-1}) started gradually decreasing and those of the new bands (3475 and 3345 cm^{-1}) started gradually increasing. This process continued till the original bands disappeared and the new bands persisted. This clearly shows that on adding dioxane to CH_2Cl_2, in addition to the two N − H bands of *o*-nitroaniline (in CH_2Cl_2) two association bands are exhibited whose intensities increase with the increasing concentration of the dioxane with the simultaneous decrease in the intensities of the bands due to CH_2Cl_2. In dioxane it was also found that the symmetric band was broader than the asymmetric band. This is attributed to the overlapping or merging of the two bands (− one due to the original symmetric band and the other due to association with the solvent molecules). Thus, binary solvent mixture study gives evidence for the formation of association bands with dioxane. In ether, the frequencies of the bands are slightly higher than those in dioxane. The bands of both the isomers are broader than those in

CCl_4. In anisole and diphenyl ether the two bands of *p*-nitroaniline are found at 3480 and 3390 cm^{-1} and 3490 and 3395 cm^{-1} respectively. In both the cases the shifts are small and binary solvent mixture study does not reveal the formation of new bands. But the N – H bands are considerably broad indicating the merger of the associated and unassociated bands. In *o*-nitroaniline also similar observations were made.

In acetone the two bands of *p*-nitroaniline and *o*-nitroaniline are found at 3445 and 3365 cm^{-1} and at 3495 and 3375 cm^{-1} respectively. Binary solvent mixture study revealed that these bands are due to association. By adding a very small quantity of acetone to a solution of dichloromethane, formation of association bands could be observed clearly. By increasing the concentration of acetone the intensities of the association bands increased with simultaneous decrease in the intensities of the original bands. Finally, the original bands disappeared and association bands persisted in pure acetone as was observed in dioxane. This clearly shows that in acetone also intramolecular hydrogen bond is broken and both the N – H modes are affected by the association with solvent molecules. In acetone, just like that in dioxane, the symmetric band is broader than the asymmetric band showing that in the former the original band is overlapping with the association band. In acetophenone also binary solvent mixture study revealed formation of associated species (Fig. 4).

In acetonitrile the N – H band of *p*-nitro- and *o*-nitro-anilines were found at 3455, 3366 and 3495, 3375 cm^{-1} respectively. The bands of *o*-nitroaniline in this medium are slightly broader than those in CCl_4. The symmetric band is broader than the asymmetric band. The shifts in the asymmetric bands of both the isomers are larger than those in the symmetric bands. Binary solvent mixture study has shown that the shifts are due to association (Fig. 5).

In binary solvent mixture of triethylamine and CH_2Cl_2, four bands were observed for both the isomers. Two of them (a & c) are same as the original bands and the other two (b & d) are association bands (Table 1). In both the isomers frequency shifts are very large for the symmetric band.

In pyridine-CH_2Cl_2 mixtures both the isomers exhibited four bands as observed in triethylamine-CH_2Cl_2 mixtures. The new bands are due to association. The shifts in the symmetric bands of both the isomers are quite large compared to the shifts in the asymmetric band.

Spectra of *o*- and *p*-nitroanilines in different solvents indicate that there is no regular order in the frequency shifts of the asymmetric and symmetric N – H stretching bands; but the total shifts in the *o*-isomer are smaller than those in the *p*-isomer and a random survey of the deviations using Bellamy's equation[8] in the case of the two isomers in different solvents (Table 2) revealed some interesting results. In the case of *p*-nitroaniline the deviation from Bellamy's equation in carbon tetrachloride, a non-interfering solvent, is very small or negligible showing the absence of any intramolecular hydrogen bond. The deviation remained small in other proton accepting solvent also (except in triethylamine) showing that the molecule forms 1:2 complexes with the solvents. But in the case of *o*-nitroaniline the deviation from Bellamy's equation is very large in CCl_4 giving a clear indication of the presence of intramolecular hydrogen bond. The magnitude of deviation is more or less same in proton accepting solvents (except in TEA) showing that the intramolecular H-bonding in *o*-nitroaniline is not strong enough to resist the action of these solvents, and after breaking of the chelation in these solvents the molecule forms 1:2 complexes with the solvent molecules just like the *p*-isomer. The similarity of the deviations of *p*- and *o*-nitroanilines in triethylamine shows that in the case of the latter isomer the intramolecular hydrogen bond is completely broken and hence it behaves exactly like the *p*-isomer. Both the isomers show very large deviations from Bellamy's equation which indicates that the stoichiometry of the complex is 1:1 in this solvent.

Thus, on the basis of studies in solvents having a wide range of proton accepting abilities, it could be concluded that there is a moderately strong intramolecular hydrogen bond in *o*-nitroaniline. The bond remains intact in halohydrocarbons, is slightly affected in anisole and diphenyl ether, but is completely broken in dioxane, ether, acetone, acetophenone, acetonitrile, dimethylformamide, triethylamine and pyridine.

References

1 Pimental G C & Sedernolm C H, *J chem Phys*, **24** (1950) 639.

2 Medhi K C & Kastha G S, *Indian J Phys*, **37** (1963) 275.

3 Kruger P J, *Can J Chem*, **40** (1962) 2300.

4 Dyall L K & Kamp J K, *Spectrochim Acta*, **22** (1966) 467.

5 Dyall L K, *Spectrochim Acta*, **25A** (1969) 1423.

6 Dyall L K, *Spectrochim Acta*, **25A** (1969) 1727.

7 Vogel A I, *A text book of practical organic chemistry*, 3rd Edn (English Language Book Society and Longman Group Ltd., London) 1971.

8 Bellamy L J & Williams R L, *Spectrochim Acta*, **9** (1957) 341.

Indian Journal of Chemistry
Vol. 27A, November 1988, pp. 951-955

Kinetics of Formation of Copper(I) by Reduction of Silver (I) Solutions by Metallic Copper & of Copper(II) Solutions by Metallic Nickel in Water + Acetonitrile Mixtures and their Applications in Hydrometallurgy

DIP SINGH GILL*, MANDEEP SINGH BAKSHI & BALBIR SINGH
Department of Chemistry, Panjab University, Chandigarh 160014

Received 3 *September* 1987; *revised* 18 *January* 1988; *accepted* 1 *February* 1988

The rates of formation of copper(I) in the reactions: $Ag^+ + Cu^0 \rightarrow Cu^+ + Ag^0$ and $2Cu^{2+} + Ni^0 \rightarrow 2Cu^+ + Ni^{2+}$ have been evaluated under different conditions in water + acetonitrile (H_2O + AN) mixtures to establish the optimum conditions of these reactions for the formation of copper(I). Both the reactions are typical of H_2O + AN solvent system. Pure copper and silver powders are recovered as products from solutions. The reactions are thus useful for the hydrometallurgical recovery of copper and silver in pure state.

The choice of a solvent system, other than water in which copper(I) salts are unstable, is important for the formation and stabilization of copper(I) in solution. Metals like iron and zinc reduce copper(II) solution in water to copper metal without the formation of copper(I). Recently it has been shown[1,2] that copper(II) solution can be reduced to copper(I) by metallic copper in acetonitrile (AN) or in H_2O + AN mixtures. Nickel metal like copper has also a tendency in H_2O + AN mixtures to reduce copper(II) to copper(I). Similarly silver(I) solution can also be reduced by metallic copper in H_2O + AN mixtures to produce copper(I). The present paper reports the rate of formation of copper(I) in the reactions (1) and (2) in H_2O + AN mixtures under different conditions.

$$Ag^+ + Cu^0 \rightarrow Cu^+ + Ag^0 \quad \ldots (1)$$
$$2Cu^{2+} + Ni^0 \rightarrow 2Cu^+ + Ni^{2+} \quad \ldots (2)$$

Materials and Methods

Doubly distilled water, 99.5% H_2SO_4 and 99% AN (E. Merck) were used for the preparation of solutions. Extra pure copper sulphate pentahydrate (99.8%; Sarabhai M. Chemicals), ExcelaR silver nitrate (99.9%; Glaxo), nickel powder (180-200 mesh; 99.5%; Löba) and pure copper turnings (30-35 mesh) were used without further purification.

All the kinetic measurements were made in H_2O + AN mixtures under identical conditions using 5, 10, 15, 20 and 25% (v/v) AN [also 50% aq AN in the case of reaction (1)], varying concentrations of $AgNO_3/CuSO_4$ and copper turnings/nickel powder (1 g) at 25, 35, 45 and 55°C in a double jacketed pyrex glass vessel shown in Fig. 1. The inner reaction tube of the vessel was a flat bottomed tube (6 cm in diameter and 13 cm in length), narrowed at the top to fit a B-24 standard joint with a stopper. The outer jacket (8 cm in diameter) enclosed the reaction tube and acted as a vessel for circulating thermostated water for maintaining constant temperature. The reaction solution was stirred with a magnetic stirrer revolving at 700 rpm. For each kinetic measurement 200 ml of the reaction solution were used. The amount of copper(I) formed as a function of time (t) was determined by $KMnO_4$ titration method[3]. Kinetics of reaction (2) were studied in

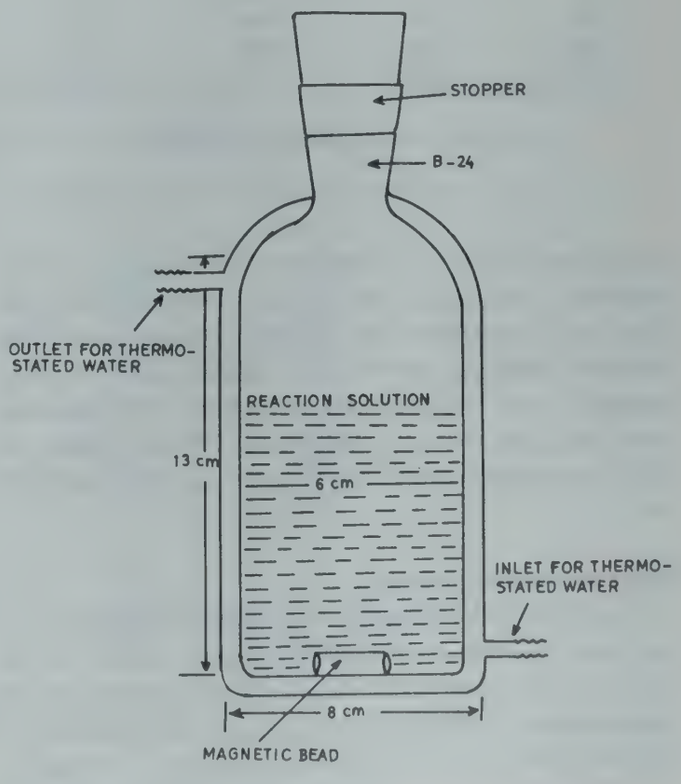

Fig. 1 – Cell used for kinetic measurements.

Table 1 – Rate (R) of Formation of Copper(I) in the Reaction: $Ag^+ + Cu^0 \rightarrow Cu^+ + Ag^0$ in H_2O + AN Mixtures at Different Temperatures.

% (v/v) AN in aq. AN	$10^3 \times$ Rate (mol dm^{-3} min^{-1})[a] at different [$AgNO_3$](mol dm^{-3})		
	0.02941	0.05882	0.08823
	Temp. = 25°C		
5	0.20	0.33	0.45
10	0.40	0.86	1.17
15	0.54	1.07	1.60
20	0.70	1.63	2.26
25	0.97	2.39	3.30
50	1.70	3.70	5.71
	35°C		
5	0.41	0.75	1.00
10	0.90	1.72	2.30
15	1.10	2.22	3.21
20	1.41	2.81	3.80
25	1.74	3.50	4.50
50	2.50	4.71	7.03
	45°C		
5	0.45	0.91	1.30
10	1.01	2.00	2.50
15	1.60	2.94	3.70
20	1.80	3.40	4.91
25	2.30	4.20	6.00
50	2.83	5.57	7.57
	55°C		
5	0.80	1.55	1.85
10	1.40	2.77	3.60
15	2.14	4.15	6.02
20	2.50	4.64	7.10
25	2.81	5.65	7.50
50	4.60	8.01	9.98

(a) All these rate values have an uncertainty of ± 5%.

Table 2 – Rate (R) of Formation of Copper(I) in the Reaction: $2Cu^{2+} + Ni^0 \rightarrow 2Cu^+ + Ni^{2+}$ in H_2O + AN Mixtures[a] at Different Temperatures.

% (v/v) AN in aq. AN	$10^3 \times$ Rate (mol dm^{-3} min^{-1})[b] at different [$CuSO_4$](mol dm^{-3})		
	0.1002	0.1503	0.2004
	Temp. = 25°C		
5	0.94	0.82	0.68
10	0.62	0.44	0.32
15	0.31	0.24	0.21
20	0.19	0.17	0.16
25	0.15	0.13	0.12
	35°C		
5	2.78	2.12	1.18
10	1.40	1.22	0.70
15	0.60	0.58	0.54
20	0.46	0.42	0.40
25	0.35	0.27	0.25
	45°C		
5	5.30	2.70	2.30
10	4.35	2.03	1.25
15	2.30	1.15	0.86
20	1.81	0.75	0.57
25	1.24	0.65	0.45
	55°C		
5	7.82	4.10	3.90
10	5.01	3.75	2.90
15	3.57	2.75	1.80
20	3.03	1.45	1.28
25	1.67	1.20	1.05

(a) AN concentration higher than 25% (v/v) was not used because the solubility of $CuSO_4$ was not good in H_2O + AN mixtures containing higher percentages of AN.
(b) All these rate values have an uncertainty of ± 5%.

the presence of 0.15 mol dm^{-3} H_2SO_4 to avoid hydrolysis of copper or nickel salts and those of reaction (1) without the addition of any acid. The reaction kinetics were mostly followed at two-min intervals, but in some cases, where the reaction was slow, at five-min intervals. Other details of the measurements were the same as reported earlier[3].

Results and Discussion

The plots of amount of copper(I) formed as a function of time were almost linear at the initial stages of the reaction which became parabolic at longer times. All these plots passed through origin at zero time. The rate of formation of copper(I) ($R = \partial M/\partial t$) was determined in all the cases by the empirical differentiation method, i.e. by evaluating the slopes of the linear parts of the plots of [M] versus t at the initial stages of the reaction. The values of the rate at different temperatures alongwith the concentrations of $AgNO_3/CuSO_4$ and AN used are reported in Tables 1 and 2.

The results presented in Table 1 show that the rate of formation of copper(I) in reaction (1) increases with the increase in temperature and [AN] and [$AgNO_3$]. The increase in the rate of reaction (1) with the increase in [AN] can be explained as due to medium effects[4]. The medium effects influence the rate of the reaction either by changes in the dielectric constant of the medium or by solvation effects[5,6]. With increase in [AN] the dielectric constant of H_2O + AN mixtures decreases[7] and one expects the formation of more ion-pairs be-

tween Ag^+ and NO_3^- leading to a decrease in free Ag^+ ions concentration. This would lead to a decrease in the rate of reaction (1) with the increase in [AN]. This implies that the actual increase in the rate of reaction (1) with increase in [AN] is due to the increased solvation effects on Cu^+ (ref. 8, 9) which impart more stability to this ion in solution.

The rate of formation of copper(I) in reaction (2) increases with increase in temperature but decreases with increase in $[Cu^{2+}]$ and [AN] (Table 2). In more concentrated $CuSO_4$ solutions, the stronger ion-pairing between highly charged Cu^{2+} and SO_4^{2-} ions seems to be responsible for the slowness of this reaction with increase in $[Cu^{2+}]$. The stability of copper(I) alone is not responsible for reaction (2) but the stability of Ni^{2+} also plays an important role. Since the stability of Ni^{2+} decreases with increase in [AN], the rate of reaction (2) decreases with increase in [AN].

Reactions (1) and (2) do not proceed with measurable rates in aquo-organic mixtures other than AN. Therefore, both the reactions (1) and (2) are typical of $H_2O + AN$ solvent system. The effect of some added organic solvents (5 ml and 10 ml) on the rate of reaction (1) in 200 ml of the reaction solution in $H_2O + AN$ mixtures containing 20% (v/v) AN, 0.02941 mol dm^{-3} $AgNO_3$ and copper turnings (1 g) at 45°C has been investigated. Such studies have also been made for reaction (2) in $H_2O + AN$ mixtures containing 5% (v/v) AN,

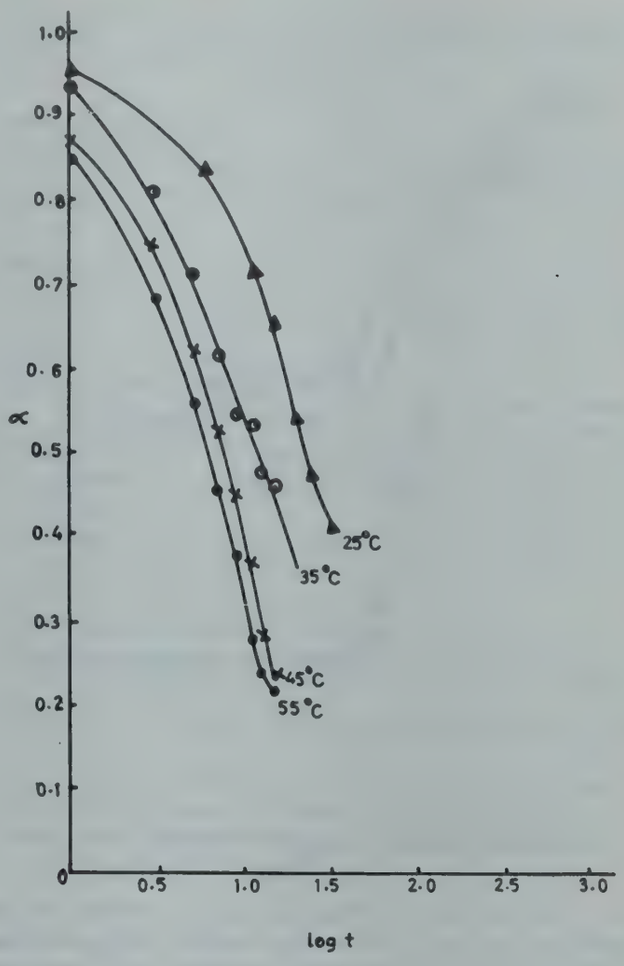

Fig. 2 – Fraction of Ag^+ remaining (α) as a function of time parameter (log t) in 200 ml of the reaction solution consisting of 0.02941 mol dm^{-3} $AgNO_3$, 1 g of copper turnings (30-35 mesh) and 25% (v/v) AN at different temperatures.

Table 3 – Effect of Added Organic Solvents on Rates[a] (R) of Reactions (1) and (2) in $H_2O + AN$ Mixtures at 45°C.

Solvent[b]	Volume added (ml)	$R \times 10^3$ (mol dm^{-3} min^{-1})	
		Reaction (1)	Reaction (2)
—	—	2.77	5.30
N,N-Dimethylformamide	5	2.08	4.25
N,N-Dimethylformamide	10	1.82	3.50
N,N-Dimethylacetamide	5	1.62	4.45
N,N-Dimethylacetamide	10	1.34	3.45
Acetone	5	2.50	5.20
Acetone	10	2.25	4.20
Methanol	5	3.23	5.20
Methanol	10	3.63	5.10
Ethanol	5	5.05	5.25
Ethanol	10	5.83	4.70
Ethyl methyl ketone	5	3.02	4.20
Ethyl methyl ketone	10	3.33	3.35
Pyridine	5	1.45	Reaction becomes
Pyridine	10	1.21	extremely slow.

(a) All these rate values have an uncertainty of ± 5%.

(b) The organic solvents which did not interfere with the determination of Cu^+ by $KMnO_4$ titration were only used.

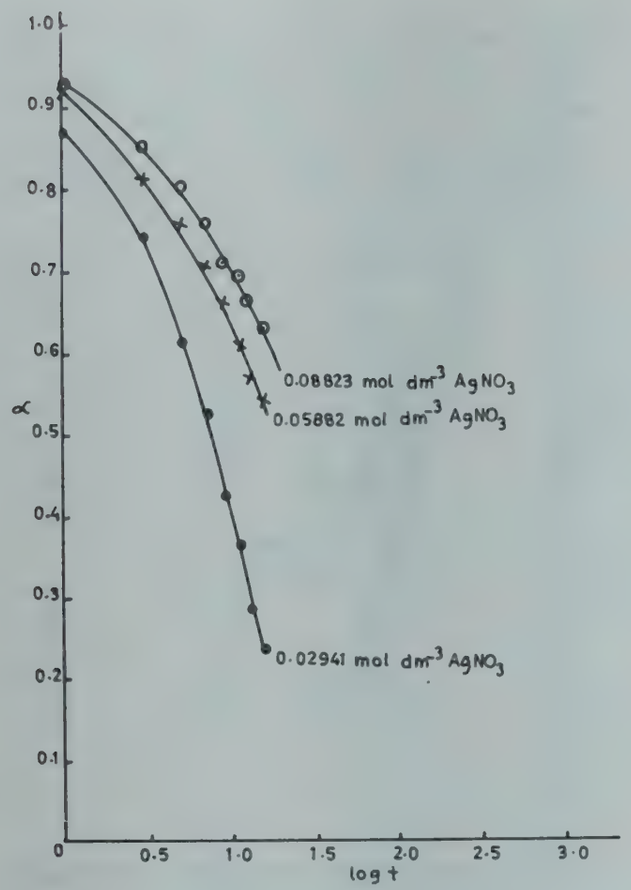

Fig. 3 – Fraction of Ag^+ remaining (α) as a function of time parameter (log t) in 200 ml of the reaction solution consisting of 25% (v/v) AN, 1 g of copper turnings (30-35 mesh) and different concentrations of $AgNO_3$ at 45°C.

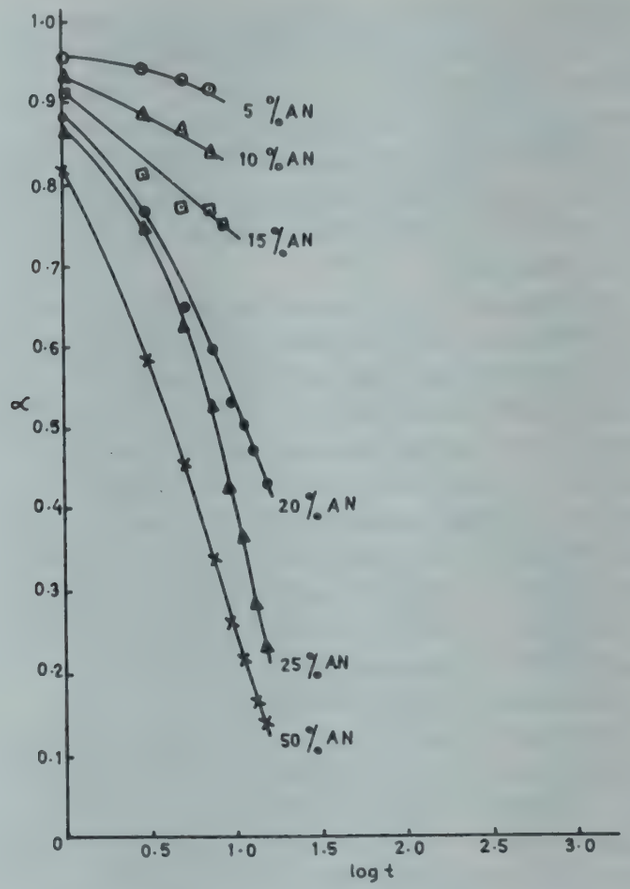

Fig. 4 – Fraction of Ag^+ remaining (α) as a function of time parameter (log t) in 200 ml of the reaction solution consisting of 0.02941 mol dm^{-3} $AgNO_3$, 1 g of copper turnings (30-35 mesh) and 5, 10, 15, 20, 25 and 50% (v/v) AN at 45°C.

0.1002 mol dm^{-3} $CuSO_4$, nickel powder (1 g) and 0.1 mol dm^{-3} H_2SO_4 at 45°C. The results are reported in Table 3. In most of the cases the rates of reactions (1) and (2) significantly decrease by the addition of organic solvent in $H_2O + AN$ mixture (Table 3). The rates of both the reactions were significantly affected by the addition of 10 ml of organic solvent than by the addition of 5 ml of organic solvent. The addition of methanol, ethanol and ethyl methyl ketone to $H_2O + AN$ mixture, however, increases the rate of reaction (1). The $H_2O + AN$ solvent mixtures with small amounts of one of these three solvents thus form even more potential solvents for reaction (1).

It is usually difficult to find out the order of a heterogeneous reaction. Plots using dimensionless parameters give some information about the tentative order of such reactions. The rate of reaction (2) decreases with increase in $[Cu^{2+}]$. Therefore, the order for reaction (2) has no meaning. The plots using dimensionless parameters in the form recommended by Powell and extended by Frost and Pearson[12] were, however, made in all the cases for reaction (1). These plots under different conditions were of the same type and comparable to the theoretical curve for the first order reaction[12]. The illustrative dimensionless parameter plots under different conditions for reaction (1) are given in Figs 2-4. For constructing these plots relative concentration (α) of Ag^+ for the dimensionless parameter plots was calculated in each case from the ratio of $[Ag^+]$ remaining at a particular time, i.e. $C_0 - X$, to the initial $[Ag^+]$, i.e. C_0. The value of X was calculated at various times from the amounts of Cu^+ formed using the relation $[Ag^+] = [Cu^+]$.

Taking reaction (1) as a first order reaction, the specific rate constants (k) under different conditions were calculated from the rate values of Table 1. In a particular $H_2O + AN$ mixture and at a given temperature, the k-values at three $[AgNO_3]$ were found to be reasonably invariant and the average of these k-values was used for the calculation of activation energy. The average k-values in different $H_2O + AN$ mixtures at 25°, 35°, 45° and 55°C alongwith the activation energy values are listed in Table 4. The results presented in Table 4 show a decrease in activation energy with increase in [AN].

Reaction (1) produces pure silver powder di-

Table 4 – Average Values of Specific Rate Constants (k) and Activation Energy (E_a) for Reaction (1) in H_2O + AN Mixtures at Different Temperatures.

% (v/v) AN in aq AN	E_a (kJ mol^{-1})	$k \times 10^2$ (min^{-1})			
		25°	35°	45°	55°
5	37.8	0.60	1.25	1.50	2.50
10	35.9	1.40	2.85	3.20	4.50
15	35.2	1.80	3.70	4.88	7.05
20	28.5	2.55	4.65	5.80	8.15
25	27.1	3.70	5.65	7.25	9.20
50	21.4	6.05	8.15	9.20	13.50

rectly which can be separated from the solution. Pure copper powder can be obtained from the copper(I) solution by the method already reported in detail by Gill and coworkers[3,10,11]. Reactions (1) and (2) are thus useful for the hydrometallurgical recovery of copper and silver in pure state. More concentrated solutions of silver nitrate, high [AN] and relatively high temperature are the optimum conditions of reaction (1), while low [$CuSO_4$], low [AN] and relatively high temperature are the optimum conditions of reaction (2).

Acknowledgement

MSB thanks the CSIR, New Delhi for the award of a research fellowship.

References

1 Hathaway B J, Holah D G & Postlethwaite J D, *J chem Soc*, (1961) 3215.
2 Parker A J, *Search*, **4** (1973) 426.
3 Gill D S & Srivastava R, *J chem Soc Faraday Trans* 1, (1982) 1533.
4 Bates R G, *The chemistry of non-aqueous solvents*, Vol 1, edited by J J Lagowski (Academic Press, New York) 1966.
5 Hammett L P, *Physical organic chemistry* (McGraw Hill, New York) 1970.
6 Parker A J, *Chem Rev*, **69** (1969) 1.
7 D'Aprano & Fuoss R M, *J phys Chem*, **73** (1969) 400.
8 MacLeod I D, Muir D M, Parker A J & Singh P, *Aust J Chem*, **30** (1977) 1422.
9 Gill D S & Nörding R, *Z phys Chem*, (N.F.), **136** (1983) 117.
10 Gill D S & Srivastava R, *Indian J Chem*, **22A** (1983) 140.
11 Gill D S & Srivastava R, *Indian J Chem*, **22A** (1983) 479.
12 Frost A S & Pearson R G, *Kinetics and mechanism* (Wiley Eastern, New Delhi) 1970.

Indian Journal of Chemistry
Vol. 27A, November 1988, pp. 956-958

Regeneration of Carbonyl Compounds from Semicarbazones by Manganese(III) Acetate

K R SANKARAN, KALYANI RAMAKRISHNAN† & VANGALUR S SRINIVASAN*
Department of Chemistry, Ramakrishna Mission Vivekananda College, Madras 600 004

Received 14 *September* 1987; *revised* 27 *January* 1988; *accepted* 11 *February* 1988

The kinetics of manganese(III) triacetate dihydrate oxidation of semicarbazones have been studied in 76% (v/v) aq acetic acid at 28 ± 0.2°C. The reaction exhibits total second order kinetics—first order in each reactant. The rates of these reactions are susceptible to electronic influence of substituents on the phenyl ring. To account for the negative Hammett reaction constant ($\rho = -1.57$) in the case of benzaldehyde and substituted benzaldehydes, a rate-determining cleavage of N-Mn^{III} bond has been proposed. As the Hammett reaction constant obtained in the case of acetophenone/benzophenone semicarbazones is positive, an alternate scheme involving rate-determining addition of $Mn(OAc)_3$ across of C = N is proposed. At ambient temperature, manganese(III) acetate regenerates the corresponding carbonyl compound in about 80% yield.

Thallium triacetate regenerates[1] benzaldehyde from its semicarbazone in about 90% yield at ambient temperature. However, the same reagent regenerates carbonyl compounds[2] from semicarbazones of acetophenone and substituted acetophenones, after long reflux times in 65-90% yield along with an acylated product. Potassium bromate has also been shown to regenerate carbonyl compounds quantitatively at ambient temperature. Presently we have shown that manganese(III) triacetate regenerates carbonyl compounds quantitatively from semicarbazones of aldehydes and ketones at ambient temperature. The kinetics of the oxidation reaction have been studied in 76% (v/v) aq acetic acid.

Materials and Methods

The semicarbazones of benzaldehyde, substituted benzaldehydes, acetophenones, substituted acetophenones, benzophenone and substituted benzophenones were prepared from extra pure compounds by literature procedures and their purities checked. Manganese(III) acetate dihydrate, prepared in the laboratory was of 99% purity. As the decomposition of manganese(III) acetate at room temperature was considerable, the solution was prepared as and when necessary in 100% acetic acid, left overnight and filtering off the resultant solution. The other reagents used were of reagent grade (BDH).

The rate of reaction was measured following decrease in absorbance of Mn(III) at 350 nm using a Carl-Zeiss VSU 2-P spectrophotometer. When Mn(III) was in excess, the absorbance value was corrected using about 70% of that concentration of Mn(III) in the reference compartment, so that the change in absorbance could be measured precisely. The specific rates calculated using integrated rate equations from duplicate runs agreed within ± 7% and these values also agreed with those obtained from the slopes of linear plots of log of change in absorbance versus time.

Product analysis and stoichiometry

Reaction mixture containing semicarbazone (1.0 to 2.0 mmol) and manganese(III) acetate (10 to 20 mmol) in 76% (v/v) aq acetic acid at 28°C, after nine half-lives, was diluted with equal volumes of ice-water and extracted with $CHCl_3$ (3 × 5 ml). The combined chloroform extract was dried ($MgSO_4$), filtered and acetic acid was neutralised by adding saturated $NaHCO_3$ solution and extracted with ether. The organic layer gave the product. From UV and IR spectra, the product was identified as the corresponding aldehyde or ketone. The amount of benzaldehyde, benzophenone or acetophenone formed was determined by measuring the absorbance of the organic layer at 250 nm ($\varepsilon = 11{,}400\ dm^3mol^{-1}cm^{-1}$), 257 nm ($\varepsilon = 18{,}500\ dm^3mol^{-1}cm^{-1}$) or 246 nm ($\varepsilon = 12{,}600\ dm^3mol^{-1}cm^{-1}$)[4,5] respectively. The amount of benzaldehyde or acetophenone or benzophenone formed from the respective semicarbazones was between 73% to 85%, when [semicarbazone] = 1.04 to 3.5×10^{-3} mol dm^{-3} and [Mn(III) = 10.0 to 35×10^{-3} mol dm^{-3}. The inorganic products were not identified.

Taking manganese(III) acetate in 10-30 fold excess, stoichiometric runs for the Mn(III) oxidation of semicarbazones were carried out. After nine half-lives, the

† Department of Chemistry, Meenakshi College for Women, Madras 600 024, India.

Table 1—Kinetic Data for Mn(III) Acetate Oxidation of Semicarbazones[a,b]

$[C_6H_5-C(R_1)=N-NHCONH_2]$

10^4[semicarbazone] (mol dm^{-3})	10^3[Mn(III)] (mol dm^{-3})	$10^3 k_1$ (s^{-1})	k_2 ($dm^3 mol^{-1} s^{-1}$)
	$R_1 = H$		
2.0	1.08	—	0.73
4.0	1.08	—	0.67
2.0	2.0	—	0.73
3.0	2.0	—	0.70
	$R_1 = CH_3$		
2.0	1.2	—	3.6
3.2	1.2	—	3.8
4.0	1.2	—	3.2
6.0	1.2	—	3.6
	$R_1 = C_6H_5$		
20	0.20	0.53	0.27
40	0.20	1.01	0.25
60	0.20	1.62	0.27
20	0.10	0.53	0.27
20	0.30[c]	0.42[c]	—

(a) Reactions were carried out at 28 ± 0.2°C in 76% aq acetic acid at constant ionic strength.
(b) Decomposition/disproportionation of Mn(III) is minimum (less than 5%) only in 76% (v/v) aq acetic acid.
(c) When [Mn(III)] was more than 3.0×10^{-4} mol dm^{-3}, the specific rate, k_1(s^{-1}) was lower than 0.53, probably due to nature of oxidant which is known to exist in different forms such as $[Mn_3O(OAc)_6(OAc)HOAc].5H_2O$ (cf. Fristad, W.E. Peterson, J.R. & Ernst A, *J org Chem*, **50** (1985) 3143.

unreacted Mn(III) was determined spectrophotometrically. It was found that one mol of semicarbazone consumed 2 mol of Mn(III).

Results and Discussion

Table 1 summarises the kinetic data for Mn(III) oxidation of semicarbzones. As manganese(III) reactions with semicarbazones of benzaldehyde and acetophenone proceed faster, these reactions have been followed with oxidant in excess. The reaction exhibits total second order kinetics, one each in reactant (Table 1).

Substituent effects :

The rate of Mn(III) acetate oxidation of semicarbazones of benzaldehydes and substituted benzaldehydes are susceptible to electronic influence of substituents in the phenyl ring. Electron donating groups enhance the rate while electron withdrawing groups retard the rate (Table 2). The Hammett reaction constant, ρ, calculated using the substituent constants (σ) is − 1.57 indicating an electron deficient transition state. The *ortho* substituent, *o*-Cl seems to retard the rate due to its − *I* and steric effects.

Table 2—Substituent Effect on Rate of Manganese(III) Acetate Oxidation of Semicarbazones[a,c]

$[R_2C_6H_4-C(R_1)=N-NH-CO-NH_2]$

R_1	R_2	k_2 ($dm^3 mol^{-1} s^{-1}$)
H	H	0.73
H	*p*—CH_3	1.00
H	*p*—Cl	0.30
H	*m*—NO_2	0.40
H	*o*—Cl	0.21
CH_3	H	3.6
CH_3	*p*—Cl	4.3
CH_3	*p*—CH_3	0.70
CH_3	*o*—Cl	5.0
C_6H_5	H	0.26[b]
C_6H_5	*p*—NO_2	0.66[b]
C_6H_5	*p*—Cl	0.38[b]
C_6H_5	*p*—CH_3	0.50[b]

(a) Reactions of benzaldehyde and acetophenone semicarbazones were carried out with the oxidant in 10-fold excess, viz. [Mn(III)] = 2.0×10^{-3} mol dm^{-3} and [semicarbazone] = 2.0×10^{-4} mol dm^{-3} at 28 ± 0.2°C in 76% (v/v) aq acetic acid,
(b) Reactions of benzophenone semicarbazones were carried out as above with [semicarbazone] in 10-fold excess, viz. [semicarbzone] = 2.0×10^{-3} mol dm^{-3} and [Mn(III)] = 2.0×10^{-4} mol dm^{-3}.
(c) Specific rate for the maganese(III) acetate oxidation of semicarbazide in concentration range, [semicarbazide] = 1.92×10^{-3} mol dm^{-3}, [Mn(III) = 2.1×10^{-4} mol dm^{-3} at 28 ± 0.2°C is 5.1×10^{-3} s^{-1}.

In contrast, the rates of oxidation of semicarbazones of acetophenone and substituted acetophenones, are retarded by electron donating groups (*p*—CH_3) and enhanced by substituent like *p*-Cl (Table 2). The plot of log [specific rate] versus Hammett substituent constant (σ), which is a fairly linear, gives Hammett reaction constant (ρ) = + 0.41 (correlation coefficient γ = 0.98). This ρ-value indicates an electron rich transition state. Similar electronic influence has been observed in Mn(III) oxidation of semicarbazones of benzophenone and substituted benzophenones (Table 1), with ρ = + 0.44. As the magnitude of reaction constant, ρ, is low, probably these reactions are less susceptible to electronic influence than the semicarbazones of benzaldehydes.

As acetopheone semicarbazone gets oxidised by Mn(III) faster than that of benzaldehyde, possibly electron donation to α-carbon by $-CH_3$ group facilitates the reaction; benzophenone semicarbazone reacts at the slowest rate, possibly, because of steric influence of phenyl group at α-carbon in benzophenone (Table 2).

Mechanism

To account for the high yield (≃ 80%) of benzaldehyde at all [Mn(III)] and nearly same amount (≃ 80%)

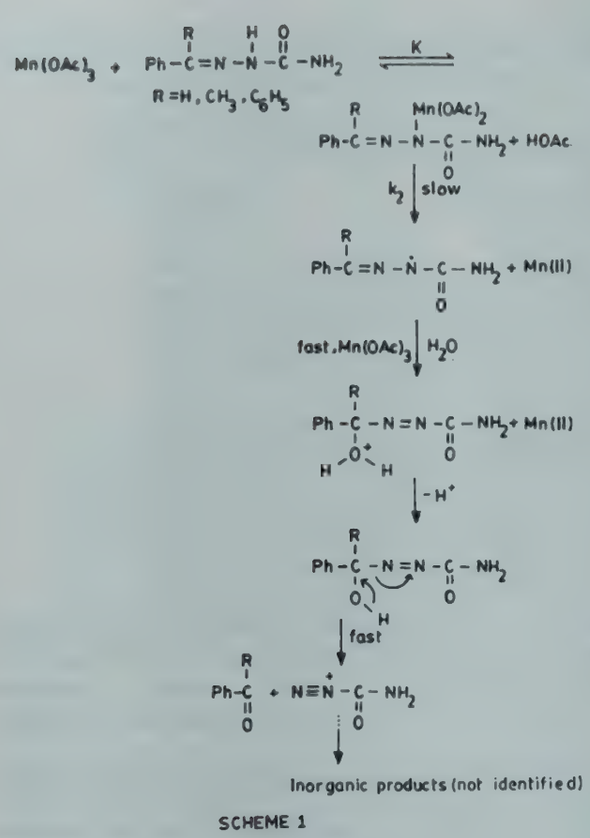

SCHEME 1

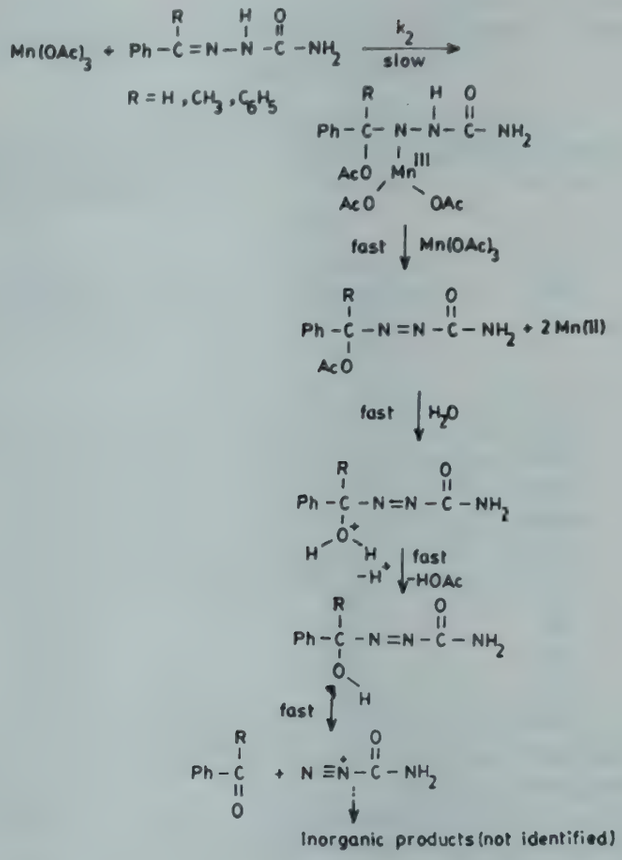

SCHEME 2

of ketones at lower [Mn(III)] from the respective semicarbazones and the stoichiometry, [1 mol of semicarbazone requiring nearly 2 mol of Mn(III)], the reaction Scheme 1 is proposed. Scheme 1 envisages the formation of N-manganese(III) intermediate which then decomposes in a slow step with electron transfer to Mn(III). Such an electron transfer to Mn(III) will be facilitated by electron donating groups and retarded by electron withdrawing groups. This trend is observed in the Mn(III)-benzaldehyde semicarbazones only. Hence an alternate mechanism involving the addition of $Mn(OAc)_3$ to C = N has been proposed (Scheme 2).

The presence of electron withdrawing group at the *para* position of phenyl ring ($p-CH_3$) may make the nitrogen of C = N electron rich, hindering the addition of $Mn(OAc)_3$ to C = N, while an electron withdrawing p-NO_2 group will favour the electron flow in the opposite direction towards the carbon of C = N facilitating addition of $Mn(OAc)_3$. This trend in reactivity is observed in the case of Mn(III) oxidation of semicarbazones of acetophenones and benzophenones. Hence it can be said that Scheme 1 is a probable mode of conversion of benzaldehyde semicarbazone to benzaldehyde while the reaction of semicarbazones of acetophenone/benzophenone with Mn(III) seems to prefer alternate reaction Scheme 2.

Acknowledgement

One of the authors (KRS) is thankful to UGC, New Delhi, for the award of a junior research fellowship.

References

1 Balakrishnan R & Srinivasan V S, *Proc Indian Acad Sci*, **93** (1984) 171.

2 Butler R N, Morris G J & O'Donohue A M, *J chem Res(S)*, (1981) 61.

3 Narayanan S & Srinivasan V S, *J chem Soc Perkin II*, (1986) 1557.

4 Dyer J R, *Applications of absorption spectroscopy of organic compounds* (Printice Hall, Englewood Cliffs) 1965, p.18.

5 Streitwieser A Jr & Heathock C H, *Introduction to organic chemistry* (Macmillan, New York) 1973 p. 596.

6 (a) Hine J, *Physical organic chemistry* (McGraw Hill, New York) (1962), (b) Brown H C & Okomoto *J Am chem Soc*, **80** (1958) 4979.

Indian Journal of Chemistry
Vol. 27A, November 1988, pp. 959-962

Micellar Influence on Hydroxylation of Rosaniline Hydrochloride by Sodium Hydroxide

(MISS) P K MISHRA, L N PANDA, B K MISHRA & G B BEHERA*
Centre of Studies in Surface Science and Technology, Department of Chemistry,
Sambalpur University, Jyoti Vihar 768 019

Received 14 *July* 1987; *revised* 8 *January* 1988; *accepted* 19 *February* 1988

Hydroxylation of rosaniline hydrochloride by NaOH in the presence of cetyltrimethylammonium bromide (CTAB), sodium lauryl sulphate (NaLS) and Triton-X-100 solutions has been studied. The rate enhancement (2.25 fold) in CTAB and rate inhibition (11.76 fold) in NaLS and (1.7 fold) Triton-X-100 have been explained by assuming that the surfactant molecules exist in the form of Menger's micelle. The thermodynamic perameters have been calculated in CTAB solution only. The influence of electrolytes in the presence of CTAB has also been analysed.

Catalysis by aqueous micelle parallels the behaviour of biological ensemble, the globular proteins and biomembranes[1]. Organic reactions in aqueous solutions of surfactants undergo either rate acceleration or inhibition and this behaviour has been attributed to electrostatic and hydrophobic interactions between the substrate and surfactant aggregates. The present investigation reports the effect of cetyltrimethylammonium bromide (CTAB), sodium lauryl sulphate (NaLS) and Triton-X-100 (T-X-100) on the hydroxylation of rosaniline hydrochloride (**1**) by sodium hydroxide.

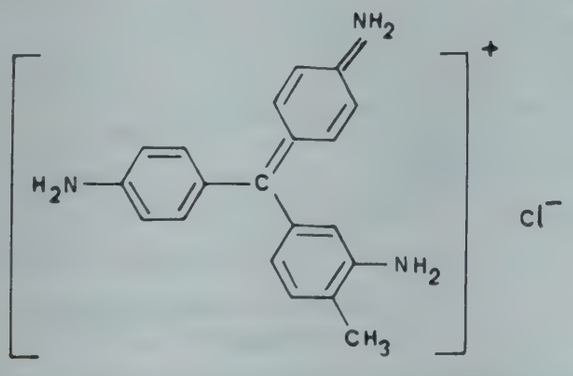

1

Materials and Methods

The surfactants, CTAB and NaLS (BDH) were purified before use. Triton-X-100 and rosaniline hydrochloride (BDH) were used as such. All inorganic salts (AR grade) were dried before use. All solutions were prepared in triply distilled water and used within seven days of their preparation.

The reaction between rosaniline hydrochloride (2.5×10^{-6} mol dm^{-3}) and sodium hydroxide (3×10^{-3} mol dm^{-3}) was monitored spectrophotometrically in the absence and presence of varying concentrations of surfactants employing a Carl-Zeiss-Jena VSU-2P spectrophotometer equipped with thermostated cell holder and fitted with matched 1 cm quartz cells. The temperature of the cell compartments could be controlled within ± 0.1°C. Plot of log $(A_0 - A_\infty)$ versus time were linear within experimental error. The pseudo-first order rate constants were computed by the least squares method.

Results and Discussion

The absorption maximum of rosaniline hydrochloride at 540 nm in water is shifted to 546 nm in the presence of 0.01 mol dm^{-3} NaLS and to 543 nm in the presence of 1% T-X-100 micelle. No shift in λ_{max} is, however, observed in the presence of CTAB.

Surfactant concentration-rate profile

The pseudo-first order rate constants in water, CTAB, NaLS and T-X-100 are given in Table 1. The plot of k_{obs} versus [CTAB] describes a curve with a broad maximum at [CTAB] = 0.0015 mol dm^{-3} (Fig. 1). The k_{obs} values in the case of NaLS and T-X-100 decrease with increase in [surfactant] and become assymptotic at 0.003 mol dm^{-3} NaLS and 0.4% (v/v) T-X-100 (Fig. 2).

In the case of NaLS the decrease in k_{obs} with increase in [surfactant] can be explained in terms of incorporation of the dye into the anion aggregate and non-approachability of nucleophilic OH− to the micelle bound dye cation due to electrostatic repulsion. In the case of T-X-100 the rate retardation is due to the fact that although the surface of T-X-100 micelle is neutral, the oxygen of polyoxyethylene group creates a negative surface which attracts the positively charged dye cation and repels the OH ion. In the case of CTAB micelle, the surface is po-

Table 1—Specific Reaction Rates and Activation Parameters for Hydroxylation Reaction of Rosaniline Hydrochloride in CTAB, NaLS and Triton-X-100

$10^3 \times$ [CTAB] mol dm^{-3}	CTAB								NaLH		Triton-X-100	
	$10^3 \times k_{obs}$ (s^{-1})				$-E_a$ (kJ/ mol)	$\Delta H^{\ddagger}$ (kJ/ mol)	$-\Delta S^{\ddagger}$ (30°C) (JK^{-1} mol^{-1})	$\Delta F^{\ddagger}$ kJ/ mol)	$10^2 \times$ [NaLS], (mol dm^{-3})	$10^3 \times k_{obs}$, (s^{-1}) (30°C)	T-X-100 in vol %	$10^3 \times k_{obs}$ (s^{-1}) (30°C)
	30°C	25°C	20°C	15°C								
0.000	11.20	10.50	9.60	9.00	10.46	7.95	0.305	100.4	0.000	11.20	0.000	11.20
0.025	11.30	10.70	9.75	9.10	10.46	7.95	0.305	100.3	0.124	9.45	0.125	10.15
0.050	11.45	10.82	9.83	9.20	10.59	8.08	0.304	100.2	0.250	8.00	0.250	9.50
0.075	11.60	10.91	9.92	9.30	10.67	8.16	0.303	100.2	0.375	6.50	0.500	8.95
0.100	11.70	11.00	10.00	9.40	10.59	8.04	0.304	100.1	0.500	5.50	0.750	8.35
0.200	15.50	12.30	11.00	9.80	21.51	19.02	0.262	98.5	0.750	3.95	1.000	8.15
0.300	18.00	14.30	12.70	11.00	22.77	20.22	0.255	97.6	1.000	2.95	1.500	7.60
0.400	20.00	17.10	15.00	13.40	18.71	16.16	0.267	97.0	1.250	2.25	2.000	7.40
0.600	22.00	20.20	18.40	16.70	12.85	10.34	0.284	96.4	1.500	2.25	3.000	7.00
0.800	23.40	21.60	19.90	18.20	11.68	9.17	0.287	96.1	1.750	1.80	4.000	6.85
1.000	24.20	22.50	20.80	19.40	10.34	7.83	0.291	95.9	2.000	1.60	5.000	6.70
1.200	24.80	23.00	21.50	20.10	9.75	7.24	0.292	95.8	2.250	1.40	6.000	6.70
1.400	25.00	23.50	22.00	20.70	8.83	6.32	0.295	95.7	2.500	1.22	7.000	6.60
1.600	25.20	23.70	22.40	21.40	8.04	5.52	0.298	95.6	2.750	1.15		
1.800	25.10	23.80	22.30	21.20	7.99	4.48	0.298	94.6	3.000	1.05		
2.000	25.00	23.70	23.30	21.10	7.95	5.44	0.298	95.7	3.250	1.00		
2.400	24.90	23.50	22.10	21.00	7.99	5.48	0.298	95.7	3.500	0.95		
2.800	24.70	23.20	22.00	20.80	7.95	5.44	0.298	95.8	3.750	0.95		

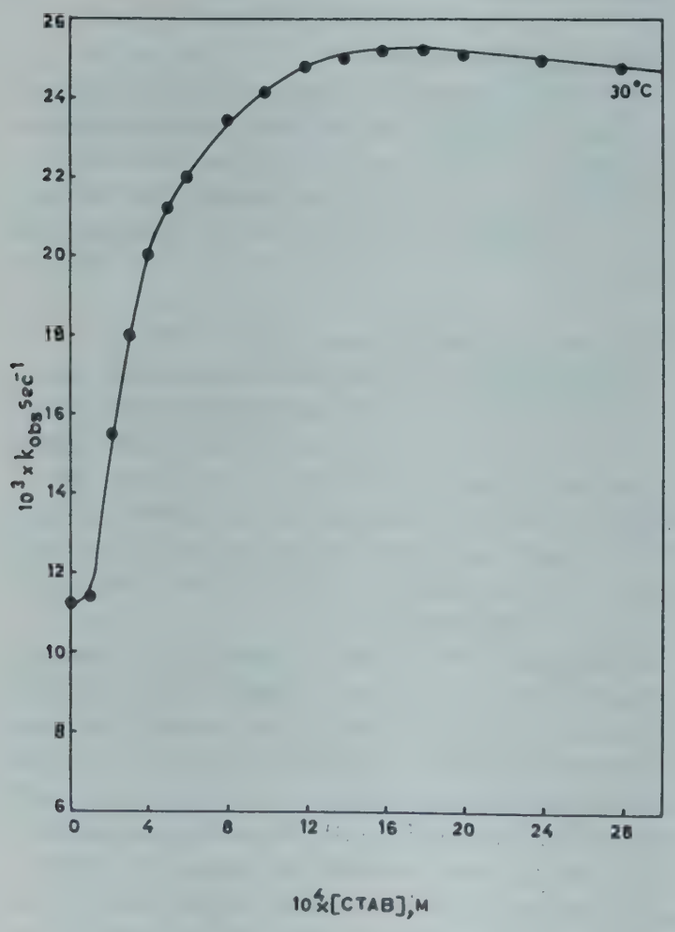

Fig. 1—Influence of [CTAB] on hydroxylation of rosaniline hydrochloride by sodium hydroxide at 30°C.

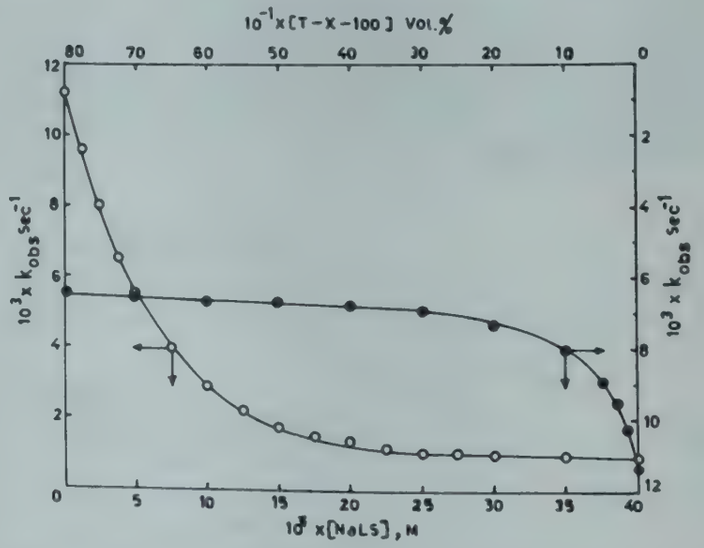

Fig. 2—Influence of [surfactant] on the hydroxylation of rosaniline hydrochloride by sodium hydroxide at 30°C [(○)-NaLS, (●)-Triton-X-100]

sitively charged which attracts the OH^- and is expected to repel the dye cation. However, rate acceleration with increase in [CTAB] is unexpected. Cordes *et al.*[2] and Katiyar *et al.*[3] have also made similar observations. The enhancement of rate by CTAB micelles does not indicate a NaLS/T-X-100 type of partioning effect. Obviously the dye cations are also found on the micellar surface enabling the OH^- ions to react more easily. This type of interaction can not be explained by Hartley's micelles[4] but

can be conveniently explained by Menger's micelles[5]. The Menger's micelles have both polar and hydrophobic surfaces. The dye molecule has also both hydrophobic and polar portions. Thus CTAB micelles can bind the large hydrophobic groups of the dye and the OH^- on its ionic coat. In this way both the reactants are brought into close proximity and the rate is enhanced. This model also explains the retardation due to NaLS and T-X-100 micelles. In NaLS and T-X-100 micelles, the OH^- naturally has no site to occupy. The dye molecule occupies both the hydrophobic and the ionic sites of the micellar surface in both these cases. Because of this added interaction the retardation of NaLS is 11.76 fold whereas the acceleration is only by 2.25 fold. The influence of temperature on rate acceleration also supports our model for dye binding since the weak short range interaction is expected to decrease with increase in temperature. The retardation in the case of T-X-100 is only 1.7 fold since its Menger's surface is not able to accommodate both hydrophobic and polar portions of the substrate. The probability of hydrophobic interaction is less due to its short hydrophobic chain which is buried inside and surrounded by the longer hydrophilic polyoxyethylene chain.

Effect of varying [reactant]

The effect of varying $[OH^-]$ has been studied in the presence of [CTAB] = 0.0015 mol dm^{-3} (where $k_{obs} = k_{max}$) at a fixed [substrate] (2.5×10^{-6} mol dm^{-3}) and 30°C. The plot of k_{obs} versus [NaOH] (Fig. 3) shows that the overall catalysis factor slowly increases initially, followed by a sharp increase and finally attaining a plateau. This indicates that in micellar system there is also optimal [reactant] at which the maximal effect on the rate would be observed. This finding is similar to the behaviour of enzymes at optimal *p*H[6] and [substrate].

Effect of added anions on rate

The effect of added anion on overall catalytic effect of CTAB (0.0015 mol dm^{-3}) has been studied. It is found that the rate retardation is maximum at an [anion] = 0.15 mol dm^{-3} and the order of retardation with respect to anion is $NO_3^- > Br^- > Cl^- > SO_4^{2-}$ (Table 2). This behaviour can be rationalised by assuming a competition between the reactant and the anion for the bonding site in the micelle. This phenomenon is explicable in terms of the greater affinity of the low charge density anions for the micelle[3].

Effect of temperature

The effect of temperature on the reaction has been studied in the absence and presence of CTAB.

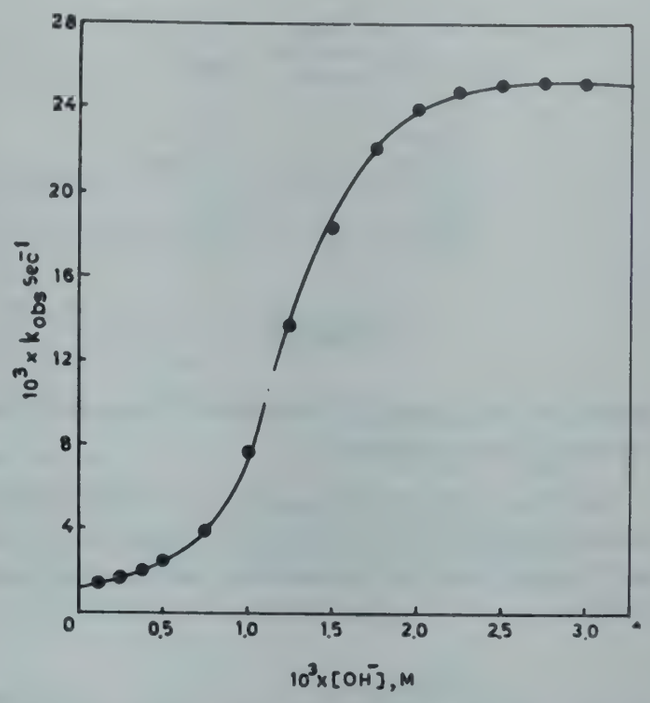

Fig. 3—Influence of [reactant] on CTAB catalysed hydroxylation of rosaniline hydrochloride by sodium hydroxide at 30°C ([CTAB] = 0.0015 mol dm^{-3}, [rosaniline hydrochloride] = 2.5×10^{-6} mol dm^{-3})

Table 2—Influence of Electrolytes on CTAB Catalysed Hydroxylation of Rosaniline Hydrochloride by Sodium Hydroxide

[CTAB] = 0.0015 mol dm^{-3}; [NaOH] = 0.003 mol dm^{-3}; temp. = 30°C; [Rosaniline hydrochloride] = 2.5×10^{-6} mol dm^{-3}.

[Salt], (mol dm^{-3})	$10^3 \times k_{obs}$ (s^{-1})			
	KCl	KBr	KNO_3	K_2SO_4
0.000	25.2	25.2	25.2	25.2
0.025	9.0	10.2	7.5	8.2
0.050	7.6	7.0	6.0	7.5
0.075	6.6	5.6	4.9	6.8
0.100	6.2	4.6	4.0	6.0
0.150	5.4	4.0	3.4	5.9
0.200	5.2	3.8	3.2	5.8
0.250	5.2	3.8	3.2	5.8

The reaction is found to obey Arrhenius equation. The values of the activation parameters are summarised in Table 1. The high negative values of $\Delta S^{\ddagger}$ indicate that the reaction is occurring between ionic species.

Mechanism

The micelle catalysed hydroxylation reaction of the dye cation can be explained by Scheme 1, where K_s is micelle-substrate binding constant, D_n is the micelle, S is the substrate (dye cation), D_nS is the micelle-substrate complex, k_m and k_w are the rate con-

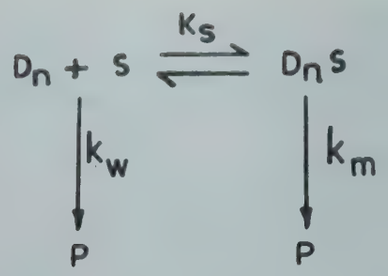

Scheme 1

stants for the product formation in micellar and aqueous phase respectively.

The observed rate constnat for the product formation is given by Eq. (1) (ref. 7) where m^S_{OH} is the mol ratio of micellar bound OH^- to micellar head groups.

$$k_{obs} = \frac{k_w + k_m m^S_{OH} K_s D_n}{1 + K_s D_n} \quad \ldots (1)$$

The values of m^S_{OH} have been calculated using Eq. (2) (ref. 7) where β is micellar binding parameters[8].

$$(m^S_{OH})^2 + m^S_{OH}\left\{\frac{[OH^-] + K^{OH}_{Br}[Br^-]_T}{(K^{OH}_{Br} - 1)[D_n]} - \beta\right\} - \frac{\beta[OH^-]_T}{(K^{OH}_{Br} - 1)[D_n]} = 0 \quad \ldots (2)$$

Values of K^{OH}_{Br} for CTAB micelle obtained by different methods[8] are reported to be 10, 12, 13 and 21. The β is often treated as an adjustable parameter. Bunton *et al*[8] had fitted their data using the values of β in the range of 0.75 to 0.8. We have chosen the values of K^{OH}_{Br} and β as 10.0 and 0.75 respectively. Equation (1) on rearrangement gives Eq. (3).

$$\frac{k_{obs} - k_w}{m^S_{OH} D_n} = k_m K_S - K_s \frac{k_{obs}}{m^S_{OH}} \quad \ldots (3)$$

The plot of $k_{obs} - k_w / m^S_{OH} D_n$ versus k_{obs}/m^S_{OH} for runs at $[CTAB] = 1 \times 10^{-3}$ to 1.6×10^{-3} mol dm^{-3} and $[OH^-] = 3 \times 10^{-3}$ mol dm^{-3} is linear and yielded $K_S = 1.921 \times 10^4$ mol dm^{-3} and $k_m = 16.76 \times 10^{-2}$ s^{-1}. At 100% binding of dye cation onto micelle, the rate would have been 16.76×10^{-2} s^{-1}. But the observed maximum rate is found to be 0.025 s^{-1}. This finding has prompted us to calculate the percentage of micelle-bound dye at different [surfactant].

Table 3—Percentage of Micelle-bound Dye

$[Dye]_T = 2.5 \times 10^{-6}$ mol dm^{-3}

10^3 [Surfactant] (mol dm^{-3})	10^7 [dye] in water (mol dm^{-3})	10^7 [dye] in micelle (mol dm^{-3})	% of micelle-bound dye
1.0	22.900	2.100	8.40
1.2	22.825	2.175	8.70
1.4	22.793	2.207	8.83
1.6	22.762	2.238	8.95

The concentration of dye molecule in water has been calculated in the following way. The observed rate V_{obs} is due to the rate in micelle (V_m) and in water (V_w).

$$V_{obs} = V_m + V_w \quad \ldots (4)$$

or

$$k_{obs}[R]_T = k_w[R]_w + k_m[R]_m \quad \ldots (5)$$

$[R]_T$ stands for the total concentration of the dye, and $[R]_w$ and $[R]_m$ are the concentrations of the dye in aqueous and micellar phases respectively.

Equation (5) on rearrangement gives Eq. (6). The percentage of dye molecule adsorbed on CTAB micelle has been calculated and are given in Table 3.

$$R_w = \frac{k_{obs} - k_m \times [R]_T}{k_w - k_m} \quad \ldots (6)$$

It may be concluded therefore that almost 9% of the surface of Menger's micelles are hydrophobic in nature.

Acknowledgement

Support of this work in part through the award of a junior research fellowship by the UGC, New Delhi to one of the authors (PM) is gratefully acknowledged.

References

1 Bunton C A, *Micellar reactions in application to biomedical systems in chemistry*, Part III, Edited by J B Janes (John Wiley, New York) 1976, Chapter 4.
2 Albrizzio J, Archilla J, Rodulfo T & Cordes E H, *J org Chem*, **37** (1972) 871.
3 Reddy I A K & Katiyar S S, *Solution behaviour of surfactants*, Edited by K L Mittal & E J Fendler (Plenum Press, New York), **2** (1982) 1017.
4 Hartley G S, *J chem Soc*, (1938) 1968.
5 Menger F M, *Surfactants in solution*, Edited by K L Mittal & B Lindman (Plenum Press, New York), **1** (1984) 347.
6 Funaski N, *J Colloid Int Sci*, **62** (1977) 336.
7 Dash A C, *Indian J Chem*, **23A** (1984) 421.
8 Al-Lohedan H, Bunton C A & Romsted L S, *J phys Chem*, **85** (1981) 2123.

Indian Journal of Chemistry
Vol. 27A, November 1988, pp. 963-967

Kinetics of Oxidation of Lactic, Mandelic & Benzilic Acids by Trichloroisocyanuric Acid in Aqueous Acetic Acid Media

P S RADHAKRISHNAMURTI*, NABEEN KUMAR RATH & RAM KRISHNA PANDA

Chemistry Department, Berhampur University, Berhampur 760007

Received 15 *September* 1987; *revised* 21 *December* 1987; *accepted* 15 *February* 1988

Oxidation of lactic, mandelic and benzilic acids by trichloroisocyanuric acid (TCICA) in aqueous acetic acid-acid media is pseudo-first order in $[TCICA]_0$ both in the absence and presence of added Cl^-. The rate constants show a linear dependence on [substrate]. The reaction remains unaffected at lower $[H^+]$ (0.1×10^{-2}-2×10^{-2} mol dm^{-3}); but increases linearly at higher $[H^+]$ (10×10^{-2}-40×10^{-2} mol dm^{-3}). Increase in dielectric constant of the medium has a negligible effect on the reaction rate. Although k_{obs} consistently increases with increase in $[Cl^-]_{ad}$, the magnitude of increase is rather small. The reaction most probably proceeds through a concerted oxidative decarboxylation mechanism leading to a carbonyl derivative and CO_2 as the primary oxidation products.

Numerous reports are available on kinetics of oxidation of α-hydroxy carboxylic acids (HA) by a variety of oxidants[1,2]. While oxidation of HA by one-electron oxidants generally proceeds through one of the several possible initial radical formation steps[3], oxidation by two-electron[4] oxidants usually proceeds either by a ionic mechanism involving transfer of α-hydrogen or by a concerted oxidative decarboxylation involving cleavage of $C_1 - C_2$ bond.

While a group of authors[5-7] suggested a hydride ion mechanism leading to α-keto acid as the product of oxidation, parallel reports[1,8-11] suggested aldehyde or ketone as the product. The choice of mechanistic route, envisaged to be operative, would thus depend to a great deal on several factors, such as structural parameters of the substrates (HA), the nature and the oxidising capacity of the oxidant, the reaction conditions employed and the actual products isolated. For quite sometime we have been interested in the study of oxidation kinetics of organic substrates by trichloroisocyanuric acid (TCICA). The title investigation forms a part of this broad programme.

Materials and Methods

The experimental procedure was briefly described earlier[12]. The substrates, viz lactic acid (LA), mandelic acid (MA) and benzilic acid (BA) were of GR grade and were recrystallised or redistilled before use. Trichloroisocyanuric acid (TCICA) was of Fluka grade. The kinetics were monitored by estimating the disappearance of TCICA iodometrically at regular time intervals.

Stoichiometry and product analysis

Stoichiometric runs with $[TCICA] > [HA]_0$ at $[HClO_4] = 0.4$ mol dm^{-3}, $[Cl^-] = 0.5$ mol dm^{-3} in 30% acetic acid medium, did not give meaningful results as the self-decomposition of TCICA in these cases was appreciably large. However in the oxidation of mandelic acid and benzilic acid, benzaldehyde and benzophenone were the oxidation products, respectively. The product of lactic acid oxidation is acetaldehyde.

Results

The disappearance of TCICA followed a pseudo-first order kinetics for more than four half-lives, as seen from the perfect linearity of log $[TCICA]_t$ versus time plots. The pseudo-first order rate constants (k_{obs}) showed a linear dependence on $[HA]_0$ in the range studied. There was no perceptible change in k_{obs} at lower $[H^+]$ range (0.1×10^{-2} to 2.0×10^{-2} mol dm^{-3}) while change in k_{obs} was linear at higher $[H^+]$ (10×10^{-2} to 40×10^{-2} mol dm^{-3}).

Rate law and mechanism

The important steps connected with the various reactant species in the present reaction are shown in Scheme 1.

$$TCICA + H_2O \overset{K_1}{\rightleftarrows} DCICA + HOCl,$$

$$HOCl + H^+ \overset{K_2}{\rightleftarrows} H_2OCl^+$$

$$H_2OCl^+ + Cl^- \overset{K_3}{\rightleftarrows} Cl_2 + H_2O$$

$$HA \overset{K_a}{\rightleftarrows} H^+ + A^-$$

$$A^- + HOCl \xrightarrow[k_{2x}]{H^+} \text{Products}$$

$$A^- + H_2OCl^+ \xrightarrow[k_{3x}]{H^+} \text{Products}$$

$A^- + Cl_2 \xrightarrow[k_{1x}]{H^+}$ Products

$HA + HOCl \xrightarrow[k_{2x}]{H^+}$ Products

$HA + H_2OCl^+ \xrightarrow[k_{3x}]{H^+}$ Products

$HA + Cl_2 \xrightarrow[k_{4x}]{H^+}$ Products

Scheme 1

If as a first approximation the reactivity of the TCICA species is neglected in comparison to those of the other reacting species, then the rate law (1) could be derived for the reaction in the absence of added Cl^-.

$$-\frac{d[TCICA]/dt}{[TCICA]} = k_{obs} = \frac{(k'_{2x}K_1K_a + k_{2x}K_1[H^+] + k'_{3x}K_1K_aK_4[H^+] + k_{3x}K_1K_4[H^+]^2)[HA][H^+]}{([DCICA] + K_1 + K_4[H^+])([H^+] + K_a)} \quad \cdots (1)$$

Assuming [DCICA] in the denominator as negligible compared to the other terms, Eq. (1) would reduce to Eq. (2).

$$k_{obs} = \frac{(k'_{2x}K_a[H^+] + k_{2x}[H^+]^2 + k'_{3x}K_aK_4[H^+]^2 + k_{3x}K_4[H^+]^3)[HA]}{([H^+] + K_a)(1 + K_4[H^+])} \quad \cdots (2)$$

where the concentration terms refer to those taken initially and the k'_{nx} and k_{nx} are termolecular reaction constants involving one unit each of [HA], [oxidant] and $[H^+]$.

Using the reported[13] values of K_a at 35°C for various substrates and data in Tables 1-3 various constants could be obtained the average values of which are presented in Table 4. While k'_{2x} and k_{3x} values are unambiguous, k_{2x} and k'_{3x} values are the estimates; the latter were obtained from the mixed terms assuming the contribution of each of the two terms to be approximately equal.

In the presence of added Cl^- Eq. (3) can be used to compute the pertinent constants, the average values of which are also listed in Table 4.

$$k_{Cl_2} = \frac{(k'_{4x}K_aK_4K_5[H^+]^2 + k_{4x}K_4K_5[H^+]^3)[HA][Cl^-]}{([H^+] + K_a)(1 + K_4[H^+] + K_4K_5[H^+][Cl^-])} \quad (3)$$

The average values of K_4 and K_4K_5 obtained here are in agreement with those obtained earlier; e.g. $K_4 = 73$ dm^3mol^{-1} (in 20% aq HOAc at 35°C);

Table 1—Pseudo-first-order Rate Constants for Oxidation of Lactic Acid (LA), Mandelic Acid (MA) and Benzilic Acid (BA) by TCICA in Aqueous Acetic Acid-Acid Media.

$[TCICA]_0 = 5 \times 10^{-4}$ mol dm^{-3}, $[H^+] = 1 \times 10^{-2}$ mol dm^{-3}[a], HOAc = 30%[b]

$10^2[MA]_0$ (mol dm^{-3})	$10^4 k_{obs}$ (s^{-1})		
	LA[c]	MA[d]	BA[d]
0.5	0.925	2.109	0.807
1.0	1.806[c]	4.411[d]	1.618[d]
	0.243[d]	5.442[e]	1.914[e]
	0.422[f]	7.637[f]	3.039[f]
1.5	2.731	—	—
2.0	—	8.807	3.24
2.5	4.514	—	—
4.0	9.03	18.18	6.325
6.0	18.12	26.33	9.506
$(\Delta H^{\neq}$/kJ $mol^{-1})$[g]	69	65	65
$(-\Delta S^{\neq}$/J K^{-1} $mol^{-1})$[g]	27	25	27

(a) $HClO_4$ was used; (b) acetic acid-water: 30%-70% (v/v); (c, d) at 55° and 35°C respectively; (e, f) at 40° and 45°C respectively; and (g) values of the net activation parameters.

Table 2—Pseudo-first Order Rate Constants for Oxidation of Benzilic Acid by TCICA in Aqueous Acetic Acid-Acid Media.

$[TCICA]_0 = 5 \times 10^{-4}$ mol dm^{-3}, HOAc = 30%[b], [benzilic acid]$_0 = 1 \times 10^{-2}$ mol dm^{-3}; temp. = 35°C

$10^2[Cl^-]_{ad}$ (mol dm^{-3})	$10^4 k_{obs}$ (s^{-1})			
	$10^2[H^+]$ mol dm^{-3}[a] = 1	4	10	40
Nil	1.618	1.806	2.506	11.3
1	1.703	2.025	3.037	13.08
5	1.834	2.431	3.718	15.11
10	1.927	2.604	4.108	17.34

(a) $HClO_4$ was used; and (b) acetic acid-water: 30%-70% (v/v)

Table 3—Pseudo-first Order Rate Constants for Oxidation of LA, MA and BA by TCICA in Aqueous Acetic Acid-Acid Media

$[TCICA]_0 = 5 \times 10^{-4}$ mol dm^{-3}; $[HA]_0 = 1 \times 10^{-2}$ mol dm^{-3}, $[H^+] = 1 \times 10^{-2}$ mol dm^{-3}; temp = 35°C

(S)	$10^4 k_{obs}$ (s^{-1}) in medium containing HOAc (%)			
	15	30	45	60
Lactic acid[a] (LA)	1.309	1.806	1.845	1.732
Benzilic Acid[b] (BA)	1.521	1.618	1.728	1.527
Mandelic acid[b] (MA)	4.036	4.411	4.614	3.907

(a, b) At 55° and 35°C respectively.

Table 4—Average Values of Resolved Constants[a] Associated with Oxidation of LA, BA and MA by TCICA in Aqueous Acetic Acid-Acid Media.

[HOAc = 30%]

Constant	Lactic acid* (LA)	Mandelic acid* (MA)	Benzilic acid* (BA)
K_4 dm^{3}mol^{-1} [b]	73	73	73
K_4K_5 dm^6 mol^{-2} [b]	1.8×10^3	1.8×10^3	1.8×10^3
K_a mol dm^{-3} [b] (at 35°C)	$10^{-3.9}$	$10^{-3.4}$	$10^{-3.0}$
k'_{2x} dm^{6}mol^{-2}s^{-1}	1.8×10^2	1.5×10^2	0.24×10^2
k_{2x} dm^{6}mol^{-2}s^{-1}	0.4	1.0	0.3
k'_{3x} dm^{6}mol^{-2}s^{-1}	40	30	2.7
k_{3x} dm^{6}mol^{-2}s^{-1}	0.28	0.52	0.27
k'_{4x} dm^{6}mol^{-2}s^{-1}	—	—	2.0
k_{4x} dm^{6}mol^{-2}s^{-1}	—	—	0.2

(a) cf Eqs (2) and (3); (b) temperature dependence in the range 35°-55°C is assumed to be negligible.

$K_4K_5 = 1.8\times10^3$ dm^{6}mol^{-2} (in 20% aq HOAc at 35°C); $K_4K_5 = 1.4\times10^3$ dm^{6}mol^{-2} (in 15% aq HOAc at 35°C). The average value of $1/(K_4K_5)$ in the present study works out to be 5.5×10^{-4} mol^{2}dm^{-6}) in aqueous medium for the equilibrium: $Cl_2 + H_2O \rightleftarrows H^+ + Cl^- + HOCl$.

The pseudo-first order rate constants calculated using the various constants of Table 4 are in good agreement with the experimental k_{obs}.

Inspite of the apparent complexity of the rate law(s), some reasonably simple inferences on the reactivity pattern emerge from the study. A glance at Table 4 suggests that for all the reaction steps the reactivities of the substrates follow the orders: mandelic acid > lactic acid and mandelic acid > benzilic acid. For all the reducing substrates studied, $k'_{nx} > k_{nx}$ implying that anion A^- reacts significantly faster than the undissociated hydroxy acid (HA). Moreover, the reactivity orders: $k'_{2x} > k'_{3x} \gtrsim k'_{4x}$ and $k_{2x} \gtrsim k_{3x} \gtrsim k_{4x}$ suggest that the relative oxidising capacity of the oxidant species decreases in the order: $HOCl > H_2OCl^+ \gtrsim Cl_2$. It may be recalled that when chlorination of substrates is considered the relative chlorinating ability of these species follows a reverse order; $Cl_2 > H_2OCl^+ \gg HOCl$, in aqueous acetic acid-acid media. The reported redox potentials (E^0), involving two-electron processes for the couples $HOCl/Cl^-$ and $Cl_2/2Cl^-$ are -1.49 V and -1.36 V, respectively[12]. Since $H_2OCl^+ + Cl^-$ reaction gives Cl_2 (e.g. $K_5 \approx 25$ dm^3 mol^{-1}), the redox potential for the couple H_2OCl^+/Cl^- would not be much different from that of $Cl_2/2Cl^-$ (viz. -1.36 V). Thus with an estimated value of $E^0 = -1.38$ V for the couple H_2OCl^+/Cl^- the reactivity pattern $k'_{2x} > k'_{3x} \gtrsim k'_{4x}$ agrees in magnitude as well as in reaction order with the relation, $\Delta \log k_{obs} = \Delta E^0 +$ constant, for the reaction of the A^- with HOCl, H_2OCl^+ and Cl_2. However, this agreement is not so strictly satisfied for the reactivities of HA species with HOCl, H_2OCl^+ and Cl_2 which are approximately the same (since $k_{2x} \gtrsim k_{3x} \gtrsim k_{4x}$). The latter observation leads to the assumption that in the medium of $[H^+]$ where HA is the predominant species, viz. H_2OCl^+ and Cl_2 (in the presence of added Cl^-) are also predominant and probably contribute as significantly as is possible by a less abundant (but more reactive) HOCl species.

Discussion

The present reactions do not appear to involve a radical mechanism (lack of polymerisation of acrylonitrile). Moreover, in predominantly aqueous acid conditions employed, all the oxidant species contain positive chlorine and under this condition irreversible transfer of two electrons from the substrate will be a facile and thermodynamically feasible process.

A two-electron transfer might occur through the two pathways shown in Scheme 2 (1) A rate-determining formation of a hypohalite ester to give the product (formed in two pathways)[14].

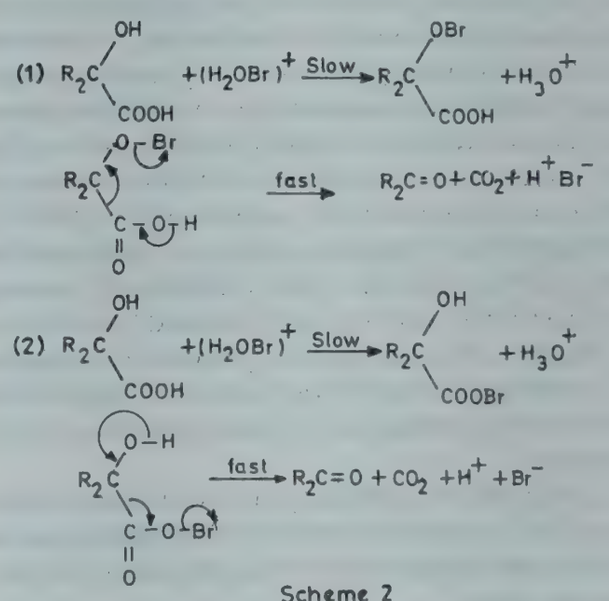

Scheme 2

(2) A concerted mechanism leading to carbonyl derivative as products. It appears to us that the concerted mechanism is possibly the best pathway for these TCICA oxidations.

Benzilic acid (BA) with no α-hydrogen should react much slower than those HAs containing α-hydrogen, since the energy required for the $C_1 - C_2$ bond cleavage would obviously be relatively higher than that required for the $C_2 - H$ transfer.

Table 5—Comparison of Rates of Oxidation of α-Hydroxy Acids with Those of Other Relavant Compounds

$[TCICA]_0 = 5 \times 10^{-4}$ mol dm^{-3}, $[S]_0 = 1 \times 10^{-2}$ mol dm^{-3}, $[H^+] = 1 \times 10^{-2}$ mol dm^{-3}, HOAc = 30%, temp. = 35°C

Substrates	$10^4 k_{obs}$ (s^{-1})	Substrates	$10^4 k_{obs}$ (s^{-1})
Lactic acid	0.243	Benzaldehyde	0.22(0.4)[a]
Pyruvic acid	14.03	Benzyl alcohol	—
Acetaldehyde	Fast	Benzilic acid	1.618
Ethyl alcohol	1.105	Benzhydrol	1.047
Mandelic acid	4.411	Benzophenone	Nil
Phenylglyoxalic acid	> 200		

(a) $HClO_4$ was used

Evidences in favour of a rate-determining oxidative decarboxylation involving heterolytic cleavage of $C_1 - C_2$ bond

A rate-determining oxidative decarboxylation involving heterolytic cleavage of $C_1 - C_2$ bond is supported on the basis of the following arguments.

(a) The predominant product of LA or MA oxidation isolated in this work is not an α-keto carboxylic acid, but a carboxyl derivative containing one carbon atom less than the number of carbons in the substrate HA, this carbon being lost as CO_2 (e.g. acetic acid produced rapidly from acetaldehyde in the reaction of LA; benzaldeyde, and probably some benzoic acid by slow oxidation of benzaldehyde, in the reaction of MA; benzophenone in the reaction of BA; Table 5). We believe that even in the oxidations by oxidants like CAT, CAB, NCS etc. (which effectively produce HOCl, H_2OCl^+ and/or Cl_2 by the acid hydrolysis of the reagent), the predominant products of oxidation of α-hydroxy acids are those formed through oxidative decarboxylation, but not the keto acids as reported earlier.

(b) A pointer to similarity in mechanism of oxidation of BA, LA and MA is that the same kinetic pattern and the same range of net activation parameters have been observed.

(c) The data in Table 5 show that keto acids like pyruvic acid and phenylglyoxalic acid react much faster than LA and MA, respectively, under identical conditions; and hence keto acids can not be thought of as predominant products of oxidation of α-hydroxy acids. The magnitudes of the measurably faster rates of oxidation of pyruvic acid and phenylglyoxalic acid do not permit the assumption that keto acids are produced in the initial step. If this were true then the oxidation would have a complicated kinetics and not smooth one as observed presently.

The discussion on the exact site of electron transfer and the nature of the transition state would rest on whether the decarboxylation is slightly more advanced than oxidation (or vice-versa). A clear description of this is difficult on the basis of kinetic data alone; nevertheless, a reasonable mechanistic pathway can be suggested, which is shown in Scheme 3. We envisage a concerted oxidative decarboxylation process involving most probably a cyclic transition state of the type shown in Scheme 3 in which there is simultaneous development of partial charges at $C_1^{\delta-}$ and $C_2^{\delta+}$ before the actual transfer of electrons.

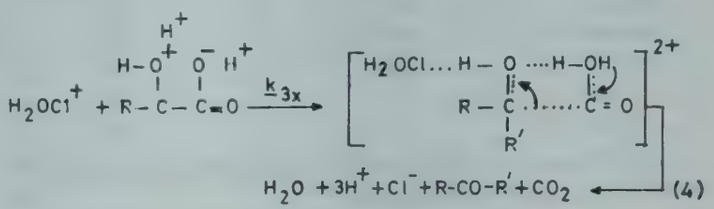

Scheme 3

That the $C_2 - OH$ group in the HA substrate is involved in the product formation suggests that the transition state should have a considerable product character and that it is the $C_2 - OH$ group (or rather the OH bond at C-2) which is effectively involved in the two-electron transfer process. This appears to be compatible with the observed reactivity patterns: (i) $HOCl > H_2OCl^+ \geq Cl_2$ (ii) $A^- > HA$, (iii) MA > LA; (iv) BA < MA. The transition state depicted in Scheme 3 also explains the need for extra H^+ in the reaction even though HOCl and A^- are the most effective reacting species. We have not been able to get the activation parameters for the various reaction steps. However, the net ΔH^+ values, although not very high for a termolecular transition state are not so low to rule out the concerted process[10]. The higher reactivity of α-hydroxy acid than that of the corresponding primary alcohol (Table 5) is also compatible with this transition state as the hydroxy acid contains an electron withdrawing ($-COOH$) group in the place of an H in the simple primary alcohol.

Acknowledgement

One of the authors (NKP) is grateful to the authorities of Berhampur University and Khallikote College for permission and facilities to carry out the work.

References

1 Banerji K K, *Indian J Chem*, **15A** (1977) 675; **17A** (1979) 90.
2 *Comprehensive chemical kinetics*, Vol. 7 edited by C H Bamford & C F H Tipper (Elsevier, London) 1972.
3 Waters W A & Kemp, *J chem Soc*, (1964) 339, 1192, 3101, 3193.
4 Wiberg K B, *Oxidation in organic chemistry*, Part A (1965) p. 65, 282.

5 Mushran S P, *J chem Soc(B)* (1971) 1712, Jha Sailendra, Sharma P D & Gupta Y K, *Inorg Chem*, **22**(9) (1983) 1393.
6 Jain A L & Banerji K K, *J Indian chem Soc*, **59** (1982) 654.
7 Mathur A K & Banerji K K, *Indian J Chem*, **20B** (1981) 529.
8 Venketasubramanian N, *Indian J Chem*, **22A** (1983) 292.
9 Barakat M Z & Abdul Wahab M F, *J Am chem Soc*, **75** (1953) 5731. Venkatasubramanian N & Natarajan R, *Indian J Chem*, **13** (1975) 261.
10 Pink J M & Stewart R, *Can J Chem*, **49** (1971) 649, 654, Barker & Aukett, *J chem Soc, Perkin II*, (1973) 965.
11 Beebe T R, Adkins R L, Balcher A I, Choy T, Fuller A E, Morgan V L, Senchery B B, Russell L J & Yates S W, *J org Chem*, **47** (1982) 3006.
12 Radhakrishnamurti P S, Rath N K & Panda R K, *J chem Soc Perkin II*, (1987) 517.
13 *Hand book of analytical chemistry*, edited by L Meites (McGraw Hill, London) 1963; Sec. 1, p. 8, 20.
14 Bishnoi M L, Negi S C & Banerji K K, *Indian J Chem*, **25A** (1986) 660.

Indian Journal of Chemistry
Vol. 27A, November 1988, pp. 968-973

Kinetics of Oxidation of Hydrazinium Ion by Iodine Monobromide in Presence of Aquamercury(II) in Acetic Acid—Acetate Media

P S RADHAKRISHNA MURTY*, LAXMI N PALO & RAMA KRUSHNA PANDA*
Department of Chemistry, Berhampur University, Berhampur 760 007

Received 19 *October* 1987; *revised* 29 *December* 1987; *accepted* 18 *January* 1988

Kinetics of oxidation of hydrazinium ion (LH^+) by IBr in the presence of Hg(II) aqueous follow pseudo-first order disappearance in oxidant in the *p*H range of 2.4-3.9 (in aqueous acetic acid/acetate media) at 30°C and an ionic strength of 0.5 mol dm^{-3}. The results are interpreted in terms of a probable mechanism which envisages an equilibrium formation of [$Hg^{II} - LH^+$] complex (from the $IBrHg^{II}$ and LH^+ species present in the medium), which reacts with another substrate LH^+ unit in a rate-determining step to form the [$Hg^{II}(LH^+)_2$] species; the latter reacts with the oxidant or IBr-Hg^{II} derived complex in very rapid and kinetically indistinguishable steps giving products. The formation of nitrogen gas as the oxidation product of hydrazine (L) is compatible with the observed stoichiometric ratio $\Delta[IBr]/\Delta[L] \approx 2$.

Iodine monobromide (IBr) acts as an efficient electrophilic halogenating agent[1]. However, certain complications arise by the use of this reagent because of competing reactions of comparatively more reactive molecular bromine and a less reactive molecular iodine produced due to a slow dissociation of IBr[2]. In addition, complications also arise due to other species which might be derived from the produced halogens under a variety of conditions[3a]. These complications are, however, effectively circumvented by the use of Hg(II) salts, which form complexes with molecular halogen species. We have recently reported[4] the kinetics of oxidation of hydrazine using I_3^- in aqueous acid and acetate medium. The present study attempts to delineate the mechanism of oxidation of hydrazine (L) by IBr in the presence of Hg(II) salt in aqueous acetic acid/acetate media at 30°C (± 0.1) and an ionic strength (μ) of 0.5 mol dm^{-3}.

Materials and Methods

Hydrazinium sulphate, anhydrous IBr, glacial acetic acid and mercury(II) diacetate (all of GR grade) were used. The [L], [IBr] and [Hg(II)] in the reaction mixture were monitored by bromatometric titration in strong acid medium, iodometric titration in strong acid medium, and by indirect Na_2EDTA titration at *p*H ~ 10, respectively[5]. The [H^+] was calculated from the mean recorded *p*H (measured both before and after the reactions and found to be reproducible with ± 0.01 *p*H units) using an Elico LC-II digital *p*H meter, after applying corrections due to ionic strength effect[6].

For kinetic runs equal volumes of the colourless (IBr-Hg^{II}) solution mixture and the substrate solution of desired strength preequilibrated at the desired temperature, were mixed and the disappearance of the oxidant monitored at different initial [IBr]. The rate constants calculated were reproducible within $\pm 5\%$. The effect of Hg(II) acetate on the reaction could not be studied because of the low solubility of the salt. In the concentration ranges of the reactants employed, the reactions were perfectly homogeneous; larger concentration ranges could not be employed either because of the appearance of an opalscence or because of relative rapidity of reactions. The oxidant solutions in the presence of Hg(II) were very stable and perfectly colourless.

In order to avoid any possible precipitation, stoichiometric runs were carried out under the following conditions: $[IBr]_0 > 5[L]_0$ ($[IBr]_0 = 0.5 \times 10^{-3}$ to 3.0×10^{-3} mol dm^{-3}, $[L]_0 = 0.1 \times 10^{-3}$ to 0.5×10^{-3} mol dm^{-3}), $[Hg^{II}]_0 = 5.0 \times 10^{-3}$ mol dm^{-3}, *p*H = 3 and solvent medium = aq. acetic acid 10% (v/v)). Unreacted [IBr] at the end of the reaction was measured iodometrically after acidification of the reaction mixture. One mol of the substrate was found to react with 2.0 ± 0.2 mol of oxidant (Eq. 1); the $[Hg^{II}]_0$ was found to remain almost unchanged.

$$N_2H_5^+ + 2IBr \xrightarrow{(Hg^{II})} N_2 + 5H^+ + 2I^- + 2Br^- \quad \ldots (1)$$

The evolved nitrogen gas was qualitatively identified. Tests for ammonia by Nessler's reagent gave negative results. Nitrogen gas was also obtained as the exclusive product of oxidation of hydrazine by this oxidant in acid medium in almost all earlier known investigations.

Results

The disappearance of IBr, which was monitored for at least four half-lives, followed a pseudo-first

Table 1—Average Pseudo-first Order Rate Constants for Oxidation of Hydrazine by IBr in Presence of Hg^{II}

$[L]_0 = 5.0 \times 10^{-3}$ mol dm^{-3}; HOAc = 10%[a]; temp. = 30°C

pH[b]	10^3 $[Hg^{II}]_0$ mol dm^{-3}	10^4 k_{obs} (s^{-1}) at 10^4 $[IBr]_0$ (mol dm^{-3})			
		1.2	5.0	7.5	10
2.8	1.25	7.8	5.7	4.8	4.2
	1.8	8.2	6.5	5.6	5.1
	2.5	8.4	7.0	6.3	5.7
	3.7	8.5	7.5	6.8	6.5
	5.0	8.6	7.8	7.3	7.0
	[$k_r = 0.18$ dm^3 mol^{-1} s^{-1}, $K = 6.7$ dm^3 mol^{-1}, $K_1 = 22$; cf Eq. (7)]				
2.9	1.25	7.0	4.9	—	3.5
	2.5	7.5	6.0	—	4.8
			(6.1)[c]	—	
			(6.0)[d]	—	
			(6.2)[e]		
			(6.1)[f]		
			(6.0)[g]		
			(6.0)[h]		
	3.7	7.7	6.5	—	5.4
	[$k_r = 0.16$ dm^3 mol^{-1} s^{-1}, $K = 78$ dm^3 mol^{-1}, $K_1 = 1.8$]				
3.2	1.25	4.0	2.2	—	1.4
	2.5	4.5	2.8	—	1.9
	3.7	4.6	3.1	—	2.2
	[$k_r = 0.11$ dm^3 mol^{-1} s^{-1}, $K = 3.2 \times 10^2$ dm^3 mol^{-1}, $K_1 = 0.25$]				
3.9	1.25	1.7	1.1	—	0.9
	2.5	1.8	1.4	—	1.0
	3.7	2.0	1.8	—	1.6
	[$k_r = 0.04$ dm^3 mol^{-1} s^{-1}, $K = 2.7 \times 10^3$ dm^3 mol^{-1}, $K_1 = 0.2$]				

a = Water-acetic acid: 90-10% (v/v) (in all tables).
b = *p*H adjusted with HOAc-NaOAc buffers. Corrected *p*H (±0.01 *p*H units).
c, d = In the presence of 5.0×10^{-4} and 10×10^{-4} mol dm^{-3} of added Cl^-, respectively,
e,f = In the presence of 5.0×10^{-4} and 10×10^{-4} mol dm^{-3} of added Br^-, respectively,
g,h = In the presence of 5.0×10^{-4} and 10×10^{-4} mol dm^{-3} of added I^-, respectively.

order kinetics in individual runs as seen from the linear plots of log $[IBr]_t$ versus time. While the pseudo-first order nature of the IBr disappearance in individual runs was still perfectly maintained at different $[IBr]_0$, the $t_{1/2}$ values increased and the k_{obs} values decreased with increase in $[IBr]_0$ in the range of 1.2×10^{-4} to 10.0×10^{-4} mol dm^{-3} (Table 1). The decreasing trend in k_{obs} tended to attain a limiting value at higher relative $[IBr]_0$. Furthermore, plots of

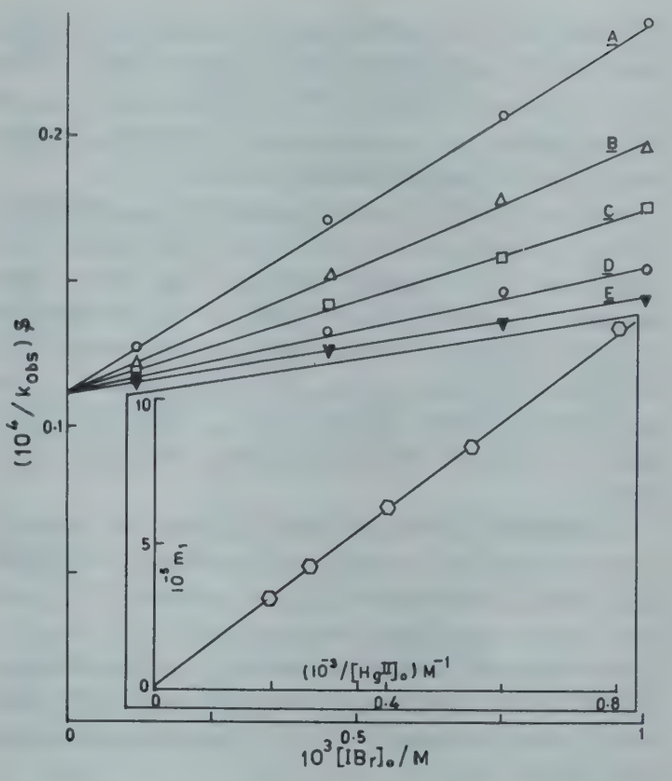

Fig. 1—Plots of $(k_{obs})^{-1}$ versus $[IBr]_0$ ($[L]_0 = 5.0 \times 10^{-3}$ mol dm^{-3}; solvent = Water-HOAc (10%, v/v); *p*H = 2.8; 10^3 $[Hg^{II}]_0$ = (*A*) 1.25, (*B*) 1.8, (*C*) 2.5, (*D*) 3.7 and (*E*) 5.0 mol dm^{-3}, (Inset: The plot of m_1 versus $([Hg^{II}]_0)^{-1}$; cf text))

$1/k_{obs}$ versus $[IBr]_0$ were linear for different $[Hg^{II}]_0$; while the intercepts on the $(1/k_{obs})$-axis of such plots were almost constant (at a particular *p*H) and independent of $[Hg^{II}]_0$, the gradients (m_1) were independent on $1/[Hg^{II}]_0$ and furnished significant slopes (on the M_1-axis). Relevant and representative plots (e.g. at *p*H 2.8) are presented in Fig. 1 (Since all the log $[IBr]_t$ versus time plots were perfectly linear for at least four half-lives of the IBr disappearance in individual runs, the reactions exhibited a perfect pseudo-first order nature). Assuming that the rates of the IBr disappearnace, might be composed of pseudo-first order and pseudo-zero order components, the experimental rates were fitted to an integrated Eq. (2) for possible resolution of these components. Equation (2) can be rewritten as (2A):

$$-\frac{d[IBr]}{dt} = k_1[IBr] + k_0 \qquad \ldots (2)$$

$$\left[\frac{\{[IBr]_{t_n} - [IBr]_{t_{(n+1)}}\}}{t_{(n+1)} - t_n}\right] = k_1\left[\frac{\{[IBr]_{t_n} + [IBr]_{t_{(n+1)}}\}}{2}\right] + k_0 \qquad \ldots (2A)$$

In Eq. (2A) $[IBr]_{t_n}$ and $[IBr]_{t_{(n+1)}}$ refer to the measured concentrations of the disappearing IBr at time t_n and

$t_{(n+1)}$ respectively, and k_1 and k_0 to the pseudo-first order and pseudo-zero order components[7]. However, the fit of the data in Eq. (2A) showed that the k_0 component was non-existent and that k_1 component decreased with increase in $[IBr]_0$.

Increase in $[Hg^{II}]_0$ led to increase in k_{obs}, which attained a limiting value at higher relative $[Hg^{II}]_0$; moreover, this limiting tendency was more pronounced at lower $[IBr]_0$. The data on the variation of k_{obs} with $[Hg^{II}]_0$ at different $[IBr]_0$ and different $[H^+]$ and the dependence of k_{obs} on $[Hg^{II}]_0$ at *p*H 2.8 are presented in Table 1. Plots of $1/k_{obs}$ versus $1/[Hg^{II}]_0$ were also linear with significant intercepts and slopes.

Increase in $[L]_0$ increased the k_{obs}, but the increase was not linear and became very prominent at higher $[L]_0$ (Table 2). The plot of $[L]_0/k_{obs}$ versus $1/[L]_0$ was linear with a significant intercept and slope (Fig. 2).

The effect of varying $[H^+]$ on k_{obs}, in the *p*H range of 2.4-3.9 and at constant $[IBr]_0$, $[L]_0$ and $[Hg^{II}]_0$, did not appear to be linear (Table 3), but appeared to be somewhat zigzag.

Added Cl^-, Br^- and I^- in representative runs did not have any significant effect on k_{obs} under the conditions employed (Table 1).

The following observations (in the *p*H range 2-4, unless otherwise mentioned) were also qualitatively noted.

(a) A whitish precipitate was formed when Hg^{II} and IBr were mixed under the conditions: $[IBr]_0 \gtrsim [Hg^{II}]_0$ ($[Hg^{II}]_0 \gtrsim 2 \times 10^{-2}$ mol dm^{-3}) in the absence of L; the precipitate dissolved in acid medium ($[H^+] \gtrsim 1$ mol dm^{-3}) giving a reddish brown solution.

(b) Addition of Hg^{II} ($[Hg^{II}]_0 \gtrsim 2 \times 10^{-2}$ mol dm^{-3}) to L furnished a white precipitate; there was no evolution of N_2 gas under the condition of $[Hg^{II}]_0 \gtrsim [L]_0$. However, N_2 was slowly liberated when a large excess of L over Hg^{II} was added to this white precipitate at $[H^+] > 1$ mol dm^{-3}, but addition of IBr to the white precipitate in the *p*H range 2-4 immediately led to the evolution of N_2.

(c) An attempt to monitor the kinetics of reaction between Hg^{II} and L (in the absence of IBr) under limiting concentrations of the reactants failed because of immediate appearance of opalscence.

Mechanism and rate law

At fixed *p*H the reaction followed steps (3) to (6). The rate law (7) based on Scheme 1 was consistent with the kinetic results.

$$IBr + Hg^{II} \underset{}{\overset{K}{\rightleftharpoons}} [IBr\,Hg^{II}] \qquad \ldots (3)$$

Table 2—Effect of Varying [Substrate] on Average Pseudo-first Order Rate Constants for Oxidation of Hydrazine by IBr in Presence of Hg^{II}

$[IBr]_0 = 5.0 \times 10^{-4}$ mol dm^{-3}, $[Hg^{II}]_0 = 2.5 \times 10^{-3}$ mol dm^{-3}, Solvent = Water-HOAc (10%, v/v); *p*H = 2.8; temp. = 30°C.

$10^3\,[L]_0$ (mol dm^{-3})	$10^4\,k_{obs}$ (s^{-1})	$10^3\,[L]_0$ (mol dm^{-3})	$10^4\,k_{obs}$ (s^{-1})
0.8	0.53	6.7	10.0
1.0	0.75	10.0	16.0
2.0	2.1	20.0	34.0
5.0	7.0	30.0	53.0

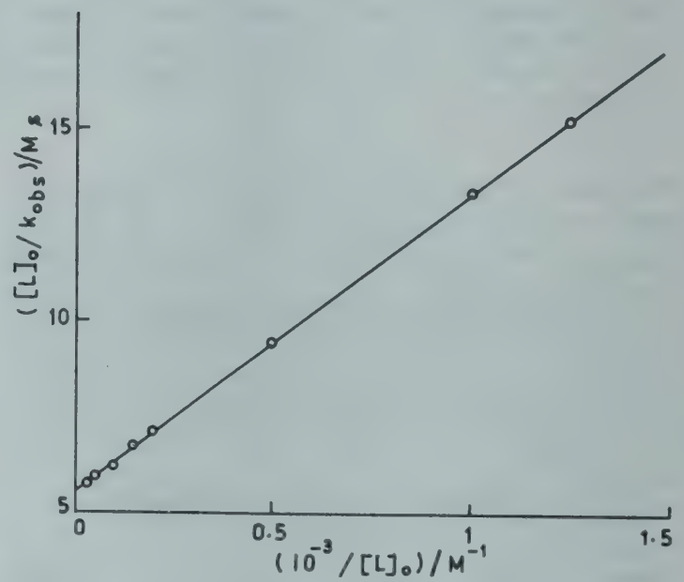

Fig. 2—Plot of $([L]_0/k_{obs})$ versus $([L]_0)^{-1}$. ($[IBr]_0 = 5.0 \times 10^{-4}$ mol dm^{-3}; $[Hg^{II}]_0 = 2.5 \times 10^{-3}$ mol dm^{-3}; solvent = Water-HOAc (10%, v/v); *p*H = 2.8).

$$[IBr\,Hg^{II}] + L \underset{}{\overset{K_1}{\rightleftharpoons}} Hg^{II}L + IBr \qquad \ldots (4)$$

$$Hg^{II}L + L \xrightarrow{k_r} Hg^{II}L_2 \qquad \ldots (5)$$

$$Hg^{II}L_2 \xrightarrow[IBr\,Hg^{II}]{\text{fast}} \text{Intermediate products} \qquad \ldots (6)$$

Scheme 1

$$-\frac{d[IBr]}{dt} = -\frac{d[Hg^{II}L]}{dt}$$

$$= \frac{k_r K K_1 [Hg^{II}][L]^2[IBr]}{[IBr] + K[Hg^{II}][IBr] + KK_1[Hg^{II}][L]} \qquad \ldots (7)$$

In Eq. (7) $(-d[IBr]/dt)/[IBr] = k_{obs}$: k_r, K and K_1 are *p*H-dependent quantities, and the concentration

terms refer to the initial analytical concentrations of various reactants. Fitting the data of Table 1 to Eq. (7) gave the values of k_r, K and K_1 at different pH values; the average values of these constants are presented in Table 1.

The pH-dependent equilibria (8)-(10), were considered for the reactants.

$$LH^+ \underset{}{\overset{K_a}{\rightleftharpoons}} L + H^+; \; K_a = 10^{-8.1} \text{ mol dm}^{-3} \quad \ldots (8)$$

$$Hg^{2+}\cdot aq. \overset{K_{h1}}{\rightleftharpoons} HgOH^+\cdot aq. + H^+;$$

$$K_{h1} = 10^{-3.7} \text{ mol dm}^{-3} \quad \ldots (9)$$

$$HgOH^+\cdot aq. \overset{K_{h2}}{\rightleftharpoons} Hg(OH)_2\cdot aq. + H^+;$$

$$K_{h2} = 10^{-2.6} \text{ mol dm}^{-3} \quad \ldots (10)$$

In the pH region of the study, $[H^+] \gg K_a$ so that the almost exclusive substrate species $= [LH^+] = [L]_0[H^+]$. Moreover, in a predominantly aqueous medium (of acidic pH range), the four-coordinate Hg^{II} would significantly exist[8] as the aqua and hydrolysed aqua forms of $Hg^{2+}\cdot aq.$ $HgOH^+.aq$ and $Hg(OH)_2\cdot aq$, the acetato complexes being possible only in $> 50\%$ acetic acid[9]. (The operation of other equilibria[3a] involving free IBr, such as:

$$2IBr(aq) \rightleftarrows I_2(aq) + Br_2(aq)$$

and

$$IBr + H_2O \rightleftarrows HOI + H^+ + Br^-$$

was not considered as, under the experimental conditions, IBr exclusively existed in a colourless complexed form with Hg^{II} (see ref. 10). The insensitivity of k_{obs} to added halide ions was also a pointer in this regard.

In the light of the above observations, Eq. (7) would then acquire the form (11)

$$k_{obs} \approx \frac{k_r K K_1 [L]_0^2 [H^+]^2 \times [Hg^{II}]_0}{(a[H^+]^2 + b[H^+] + c)} \approx \frac{a'[H^+]^4 + b'[H^+]^3 + c'[H^+]^2}{[H^+]^2 + K_{h1}[H^+] + K_{h1}K_{h2}} \quad \ldots (11)$$

at constant $[IBr]_0$, $[L]$ and $[Hg^{II}]_0$, assuming that $[H^+]$-dependent second and third terms in the denominator of Eq. (7) are negligible in comparison to the first term $[IBr]$; In Eq. (11) a', b' and c' refer to the overall reactivities of the $Hg^{2+}\cdot aq$, $HgOH^+\cdot aq$ and $Hg(OH)_2.aq$ species respectively.

Table 3—Effect of Varying pH on Average Pseudo-first Order Rate Constants for Oxidation of Hydrazine by IBr in Presence of Hg^{II}

$[IBr]_0 = 5.0 \times 10^{-4}$ mol dm^{-3}, $[L]_0 = 5.0 \times 10^{-3}$ mol dm^{-3}, $[Hg^{II}]_0 = 2.5 \times 10^{-3}$ mol dm^{-3}, temp. = 30°C.

pH*	$10^3[H^+]$ (mol dm^{-3})	$10^4 k_{obs}$ (s^{-1})	pH*	$10^3[H^+]$ (mol dm^{-3})	$10^4 k_{obs}$ (s^{-1})
2.4	3.98	21.0	2.85	1.41	6.2
2.5	3.16	16.0	2.9	1.26	6.0
2.6	2.51	13.0	3.0	1.00	4.7
2.65	2.24	12.0	3.2	0.63	2.8
2.75	1.78	9.0	3.6	0.251	2.6
2.8	1.58	7.0	3.8	0.158	1.9
2.82	1.51	6.5	3.9	0.126	1.4

*Solvent = Water-HOAc (10%, v/v); pH adjusted by adding NaOAc.

Treatment of the data of Table 3 in accordance with Eq. (11) furnished the average values of the pseudo-constants a', b' and c' as 1.6 dm^6 mol^{-2} s^{-1}, 0.48 dm^3 mol^{-1} s^{-1} and 3.0×10^{-4} s^{-1} respectively. The calculated values of the pseudo-first order rate constant were in good agreement with the experimental k_{obs} values. an attempt to further resolve each of k_r, K and K_1 into individual constants in terms of separate reactivities of Hg^{2+}, $HgOH^+$ and $Hg(OH)_2$ species [e.g. using Eq. (12)] was not successful.

$$k_r = \frac{k_r^{I}[H^+]^4 + k_r^{II}K_{h1}[H^+]^3 + k_r^{III}K_{h1}K_{h2}[H^+]^2}{[H^+]^2 + K_{h1}[H^+] + K_{h1}K_{h2}} \quad \ldots (12)$$

Discussion

The overall formation of oxidation products of L can probably be formulated in terms of Eqs (13), (15) and (16) which account for the observed stoichiometric ratio of $\Delta[IBr]/\Delta[L] \approx 2$; the product formation steps will presumably be very rapid relative to the rates of the reaction. These results in the present investigation, therefore, do not give any conclusive information regarding a simultaneous two-electron transfer [involving iodine (I) of the IBr acceptor in a polar medium] or two one-electron transfers (involving the Hg^{II} species) in the initial step(s).

$$H_2N\,NH_2 - e^- \rightarrow H_2N\,NH_2^+ \rightarrow H_2N\,NH^\cdot + H^+ \quad \ldots (13)$$

$$2\,H_2N\,NH^\cdot \rightarrow 2\,NH_3 + N_2 \quad \ldots (14)$$

$$H_2N\,NH^\cdot - e^- \rightarrow HN = NH + H^+ \quad \ldots (15)$$

$$HN=NH-2e^- \rightarrow N_2+2H^+ \quad \ldots (16)$$

The mechanism envisages, as most probable steps, the equilibrium formation of Hg^{II}-substrate complex (from the $IBrHg^{II}$ and substrate species) which reacts with another substrate (LH^+) unit in a rate-determining step to form the [Hg^{II}-(substrate)$_2$] species; the latter undergoes interaction with the oxidant or the IBr-Hg^{II} derived complex in very rapid (and kinetically indistinguishable) steps leading to product formation.

Iodine monobromide like the halogens, is known to be involved in charge transfer (CT) complexation with nucleophiles[11,12]. Steps (3) and (4) in that event may be written as (3A) and (4A),

$$L+IBr \rightleftarrows [LIBr] \quad \ldots (3A)$$

$$[LIBr]+Hg^{II} \rightleftarrows [Hg^{II}L]+IBr \quad \ldots (4A)$$

and a rate law similar to Eq. (7) can be derived for the reaction scheme.

In spite of the apparent complexity of the reaction sequence and the rate laws, some reasonably simple mechanistic inferences, give in the sequel, emerge from the study.

(i) It may be pertinent here to remark that in several oxidation reactions of hydrazine and similar substrates, each involving a rate-determining one-electron transfer, the hydrolysed metal ion species oxidizes the substrate much slower than does the unhydrolysed metal ion species[7,13-15].

(ii) Mercury (II) is well known to form complexes with halogens and halides[9] and formation of complexes involving IBr and Hg^{II} is qualitatively seen from the facile formation of a white precipitate in the *p*H range of 2-4 (which dissolves in acid medium of $[H^+] > 1$ mol dm^{-3} giving a brownish red solution with very slow liberation of nitrogen).

Hg^{II}-hydrazine complexes are known[16]. For example, $HgCl_2$ in dilute HCl medium forms complexes with hydrazine under the condition of equivalent concentrations of L and Hg^{II} or a slight excess of L over Hg^{II}; addition of a large excess of L slowly liberates nitrogen[16]. Under conditions of $[HgCl_2] > [LH^+]$, a solid and stable complex of the composition $Hg_2(N_2H_2)Cl_2$ (ref. 11) is formed.

(iii) The observed trend of K_1 (formation constant of Hg^{II}-hydrazine complex) values with *p*H in the present work, is in consonance with the postulation made by earlier workers[7,13,17], i.e. the involvement of protonated species of hydrazine and substituted hydrazines in ligation to metal ions at nitrogen site away from the site of protonation.

Although the mechanism envisaged provides plausible explanation, the exact site of initial electron transfer(s) does not appear so clear-cut. The reported overall redox potentials concerning the free species of the reactants are represented by Eqs (18)-(20).

$$IBr(aq)+e^- \rightarrow Br^- + \tfrac{1}{2}I_2; \quad E^0_{25} = -1.02\ V \ldots (18)$$

$$N_2H_5^+ \rightarrow N_2 + 5H^+ + 4e^-; \quad E^0_{25} = -0.23\ V \ldots (19)$$

$$2Hg^{2+}\cdot aq + 2e^- \rightarrow Hg_2^{2+}\cdot aq, \quad E^0_{25} = -0.92\ V \quad \ldots (20)$$

A qualitative examination of these potential data does not delineate whether the rate-determining step(5) or the subsequent fast step (6) should describe the initial electron transfer(s) in the present redox system. But the following facts: (a) the complexes produced from Hg^{II} and LH^+ have significant successor character [e.g., $Hg_2(N_2H_2)Cl_2$]; (b) slow Hg^{II} oxidation of a large excess of LH^+ in acid medium to produce N_2; (c) rapid evolution of N_2 when IBr is added to the white precipitate of Hg^{II}-hydrazine complex (in the *p*H range of 2-4); and (d) the net [Hg^{II}] remains almost unchanged in the reaction, do indicate that electron transfer might probably have commenced in the rate-determining step(5) and that the electron transfer(s) might be completed in the subsequent very rapid step(s).

Acknowledgement

One of us (LNP) thanks the authorities of Hinjilicut Science College and Berhampur University for permission and facilities for carrying out the work.

References

1 Downs A J & Adams C J, in *Comprehensive inorganic chemistry* edited by J C Bailar, H J Emeleus, R Nyholm & A F Trotman-Dickenson (Pergamon Press, London) 1973, Vol. 2, 1525.

2 Faull J H, *J Am chem Soc*, **56** (1934) 522; Sharpe A G, *J chem Soc*, (1953) 3713.

3 Latimer W M, *Oxidation potentials*, (Prentice-Hall, New Jersy), 1961, (a) p. 65, (b) p. 99, (c) p. 179.

4 Radhakrishna Murti P S, Rath N K & Panda R K, *J chem Soc, Dalton Trans*, 1189 (1986).

5 Bassett J, Denney R C, Jeffery G H & Mendham J in Vogel's *Textbook of quantitative inorganic analysis*, (ELBS and Longman, London) 1978.

6 *Handbook of Analytical Chemistry*, edited by L Meites (McGraw-Hill, New York) 1963, sect. 1, p. 8.

7 Acharya S, Neogi G &Panda R K, *Int J chem Kinet*, **15** (1983) 867.

8 Sanderson R T, *Chemical periodicity* (Reinhold, New York) 1960.

9 The Chemical Society Sptl. Publ. No. 17, *Stability constants of metal-ion complexes*, London, 1964.

10 Gillespie R J & Morton M J, *Quart Rev Chem Soc*, **25** (1971) 553.

11 Andrews L J & Keefer R M, *Adv. inorg Chem Radiochem*, **3** (1961) 91.

12 Mulliken R S & Person W B, *Molecular complexes*, (Wiley, New York) 1969.

13 Acharya S, Neogi G, Panda R K & Ramaswamy D, *Bull*

chem Soc Japan, **56** (1983) 2821; *J chem Soc, Dalton Trans*, (1984) 1477.

14 Morrow J I & Sheeres G W, *Inorg Chem*, **11** (1972) 2606; Ackermann M N, *Inorg Chem*, **10** (1971) 272; Davies G & Kustin K, *J phys Chem*, **73** (1969) 2248.

15 Acharya S, Neogi G, Panda R K & Ramaswamy D, *Bull chem Soc, Japan*, **56** (1983) 2814.

16 Aylett B J in *Comprehensive inorganic chemistry*, edited by J C Bailar, H J Emeleus, R Nyholm & A F Trotman-Dickenson, (Pergamon Press, London) 1973, Vol. 3, p. 301.

17 Sengupta K K, Sen P K & Gupta S S, *Inorg Chem*, **16** (1977) 1396.

Indian Journal of Chemistry
Vol. 27A, November 1988, pp. 974-978

Kinetics of Oxidation of Thiosemicarbazide by Iodamine-T, Iodine Monochloride & Iodine in Acid Medium

B THIMME GOWDA* & J ISHWARA BHAT†
Department of Post-Graduate Studies and Research in Chemistry, Mangalore University, Mangalagangothri 574 199

Received 13 *October* 1986; *rerevised* 1 *February* 1988;*accepted* 7 *March* 1988

Kinetics of oxidation of thiosemicarbazide (TSC) by iodamine-T, iodine monochloride and iodine have been studied in perchloric acid medium. The reaction is first order in [oxidant] and fractional order in [TSC] for all these systems. With iodamine-T, the rate is inverse first order (at $[HClO_4] = 0.02$-0.2 mol dm^{-3}) and inverse fractional order (at $[HClO_4] = 0.2$-2.0 mol dm^{-3}) in $[H^+]$. However in the case of ICl and I_2 the reaction is inverse fractional order in $[H^+]$ over the entire $[H^+]$ range. Increase in ionic strength of medium slightly decreases the rate in all the cases, whereas decrease in dielectric constant of the medium increases the rate in the case of ICl and I_2 oxidations. All oxidations studied follow Michaelis-Menten type mechanism. Rate laws in accordance with the proposed reaction pathways have been deduced. The rate constants predicted from the rate laws are in good agreement with the experimental values.

As a part of our broad program on the use of positive halogens as oxidants in the study of kinetics and mechanism of oxidation of organic substrates, specially thiosemicarbazide (TSC), we report herein the hitherto unreported kinetics and mechanism of oxidation of thiosemicarbazide by iodamine-T, iodine monochloride and iodine in aqueous perchloric acid medium.

Materials and Methods

Iodine and iodine monochloride used were of AR grade. Iodamine-T (N-iodo-potassium-*p*-toluenesulphonamide, RNIK where $R = CH_3C_6H_4SO_2$) was prepared by the iodination of *p*-toluenesulphonamide (PTS) in 10% aq. potassium hydroxide solution and its purity checked by spectral data and estimating the amount of active iodine present in it iodometrically. Stock solutions (~ 0.1 mol dm^{-3}) of iodine (in aqueous potassium iodide solution), iodine monochloride (aqueous) and iodamine-T (in 0.1 mol dm^{-3} aqueous potassium hydroxide) were prepared, standardised by iodometric method and stored in dark coloured bottles. Thiosemicarbazide, TSC (E Merck) were recrystallised from hot water and its aqueous stock solution (~ 0.1 mol dm^{-3}) was used.

The ionic strength of the reaction medium was maintained at 0.5 mol dm^{-3} with sodium perchlorate (E Merck). All other materials and reagents employed were of accepted grades of purity.

Kinetic measurements

The kinetic runs were carried out under pseudo-first order conditions using (5 to 40-fold excess) of [TSC] over [oxidant]. The reactions were initiated by the quick addition of measured amounts of oxidant solution, thermally equilibrated at a desired temperature, to a mixture containing requisite amounts of TSC, perchloric acid and sodium perchlorate solutions and water, pre-equilibrated at the same temperature. The progress of the reactions were monitored for two half-lives by iodometric estimation of unreacted oxidant at regular intervals of time. The pseudo-first order rate constants computed by the method of least squares were reproducible within $\pm 3\%$.

Stoichiometry and product analysis

The stoichiometries of TSC-iodamine-T, TSC-ICl and TSC-I_2 reactions were determined by allowing the reactions to go to completion at different [TSC]/[oxidant] ratios and $[H^+]$ (0.01-2.0 mol dm^{-3}). The presence of solphate and cyanate in the reaction products in iodomine-T and ICl oxidations were detected by standard tests. Further the sulphate was quantitatively determined by gravimetric method (yield: $93 \pm 3\%$). *p*-Toluenesulphonamide (PTS), the reduced product of iodamine-T was detected by paper chromatography using benzyl alcohol saturated with water as solvent and 0.5% vanillin in 1% HCl in ether as spray reagent ($R_f = 0.91$). The observed stoichiometries can be represented by Eqs (1-3).

$$H_2NNHCSNH_2 + 6RNIH + 5H_2O \rightarrow 6RNH_2 + 6I^- + SO_4^{2-} + CNO^- + N_2 + 9H^+ \quad \ldots (1)$$

$$H_2NNHCSNH_2 + 6ICl + 5H_2O \rightarrow 6Cl^- + 6I^- + SO_4^{2-} + CNO^- + N_2 + 15H^+ \quad \ldots (2)$$

$$H_2NNHCSNH_2 + 2I_2 \rightarrow HNCS + N_2 + 4H^+ + 4I^- \quad \ldots (3)$$

† Govinda Dasa College, Suratkal 574 158.

Table 1—Effect of [Reactants] on the Rate of Oxidation of Thiosemicarbazide by Iodamine-T in Perchloric Acid Medium at 303K (μ = 0.5 mol dm^{-3})

10 [$HClO_4$] (mol dm^{-3})	$10^4 k^a_{obs}$ (s^{-1})	10^3 [Iodamine-T]$_0$ (mol dm^{-3})	10^2 [TSC]$_0$ (mol dm^{-3})	$10^4 k_{obs}$ (s^{-1}) at 10 [$HClO_4$] = (mol dm^{-3})				
				0.05	0.1	0.2	0.5	1.0
0.2	21.6	0.5	2.0	7.5	—	2.1	—	—
0.3	12.0	1.0	2.0	7.5	—	2.2	—	—
0.5	7.5	2.0	2.0	7.5	—	2.1	—	—
0.75	4.5	4.0	2.0	7.4	—	2.1	—	—
1.0	3.2	1.0	0.5	4.1	2.0	1.7	0.92	0.71
1.5	2.5	1.0	1.0	5.2	2.6	1.9	1.1	0.78
2.0	2.0	1.0	2.0	7.5	3.2	2.1	1.2	0.80
3.0	1.4	1.0	4.0	9.2	3.8	2.2	1.3	0.85
5.0	1.2	1.0	6.0	12.3	—	2.6	—	—
10.0	0.8							
20.0	0.53							

[a] 10^3[iodamine-T]$_0$ = 1.0 mol dm^{-3}, 10^2 [TSC]$_0$ = 2.0 mol dm^{-3}.

Table 2—Pseudo-first Order Rate Constants for the Oxidation of Thiosemicarbazide (TSC) by Iodine Monochloride and Iodine in Perchloric Acid Medium at 303K

[μ = 0.5 mol dm^{-3}]

10^3 [ICl or I_2] (mol dm^{-3})	10^2 [TSC]$_0$ (mol dm^{-3})	10 [$HClO_4$] (mol dm^{-3})	$10^4 k_{obs}$ (s^{-1})	
			ICl	I_2^a
0.5	2.0	1.0	2.6	3.8
0.75	2.0	1.0	2.7	—
1.0	2.0	1.0	2.6	3.8
2.0	2.0	1.0	2.6	3.9
3.0	2.0	1.0	—	4.1
4.0	2.0	1.0	2.6	—
1.0	0.5	1.0	1.9	—
1.0	0.8	1.0	2.0	3.4
1.0	1.0	1.0	2.1	3.5
1.0	4.0	1.0	3.1	4.2
1.0	6.0	1.0	3.5	4.6
1.0	2.0	0.1	15.4	—
1.0	2.0	0.2	8.9	9.3
1.0	2.0	0.5	4.1	5.4
1.0	2.0	1.5	1.8	3.3
1.0	2.0	2.0	1.5	2.7

[a] [KI] = 0.02 mol dm^{-3}.

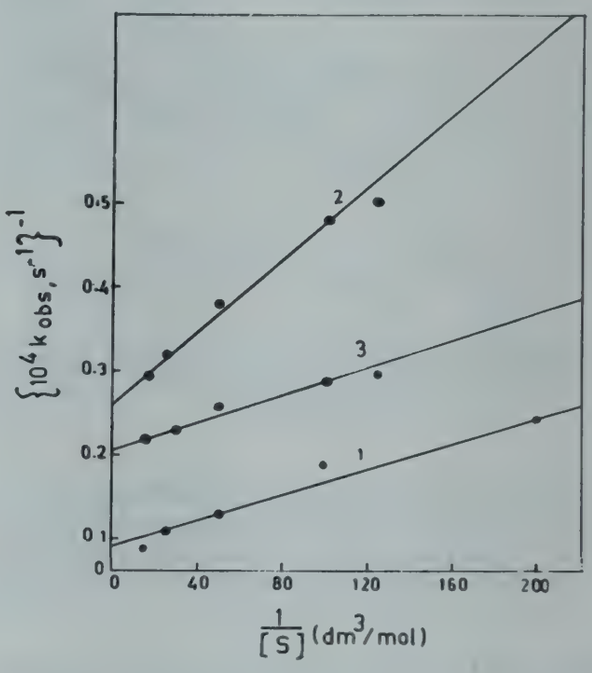

Fig. 1—Plot of $1/k_{obs}$ versus 1/[S]: (1) Iodamine-T (2) ICl (3) I_2 (10^3[oxidant] = 1.0 mol dm^{-3}; 10^2[$HClO_4$] (mol dm^{-3}) = 5.0 (iodamine-T), 10.0 (ICl and I_2(. μ = 0.5 mol dm^{-3}, 10^3 [KI] = 6.0 mol dm^{-3} (with I_2), temp. = 303 K).

Under the experimental conditions employed HNCS produced would be around 0.0005 mol dm^{-3}. It was observed that HNCS produced in reaction 3 did not get oxidised by I_2 at these concentrations.

Results

Kinetics of oxidations of TSC by iodamine-T, iodine monochloride and aqueous iodine were studied at several initial [TSC] and [oxidant] over a wide range of [$HClO_4$] (0.01-2.0 mol dm^{-3}). At constant [$HClO_4$] with several fold excess of TSC (~20 times), the plots of log [oxidant]$_0$/[oxidant] versus time were linear for at least two half-lives with all the oxidants and the pseudo-first order rate constants were unaffected by the changes in [oxidant]$_0$ (Tables 1 and 2), establishing first order kinetics in [oxidant] in all the cases.

The orders in [TSC] and [H^+] were evaluated from the log-log plots of rate constants (k_{obs}) versus [TSC] or [H^+]. At constant [oxidant] and [TSC], the rates decreased with increase in [$HClO_4$] with all the

Table 3—Kinetic Orders and Activation Parameters for the Oxidation of Thiosemicarbazide (TSC) by Iodamine-T, Iodine Monochloride and Iodine

Kinetic orders Observed in	Iodamine-T at $[H^+]$ (mol dm^{-3})					ICl	I_2
	0.05	0.1	0.2	0.5	1.0		
[oxidant]	1.0		1.0			1.0	1.0
[TSC]	0.44	0.3	0.2	0.14	0.1	0.25	0.14
$[H^+]$	−1.0		−0.6			−0.85	−0.53
log A	4.3 ± 0.1					11.3 ± 0.2	10.1 ± 0.3
E_a (kJ mol^{-1})	42.5 ± 2.1					86.2 ± 3.4	80.8 ± 2.8
$\Delta H^{\ddagger}$ (kJ mol^{-1})	40.2 ± 2.0					83.6 ± 5.0	78.3 ± 2.1
$\Delta S^{\ddagger}$ (JK $^{-1}$)	−38.9 ± 1.9					−6.5 ± 0.3	−12.3 ± 0.3
$\Delta G^{\ddagger}$ (kJ mol^{-1})	50.9 ± 3.0					85.8 ± 5.0	81.7 ± 2.1

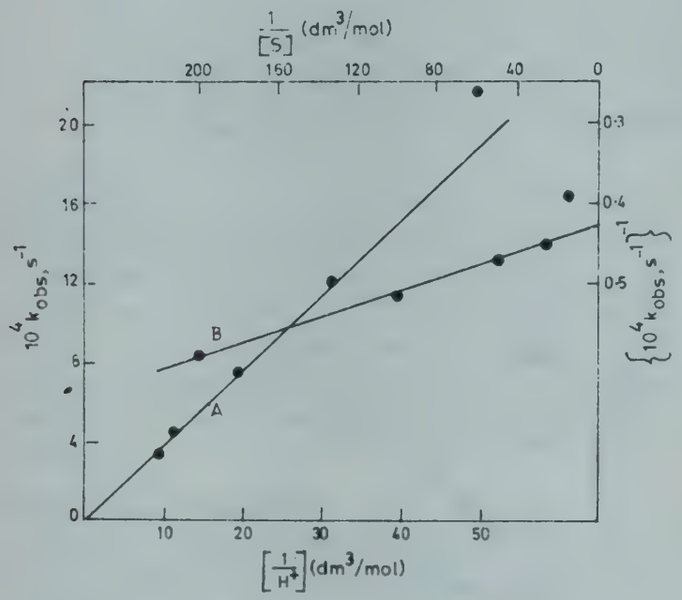

Fig. 2—(A) Plot of k_{obs} versus $1/[H^+]$; (10^3 [iodamine-T] = 1.0 mol dm^{-3}, 10^2 [TSC] = 2.0 mol dm^{-3}, temp = 303 K; μ = 0.5 mol dm^{-3}). (B) Plot of $1/k_{obs}$ versus 1/[S] (10^3[iodamine-T] = 1.0 mol dm^{-3}; $10^2[HClO_4]$ = 2.0 mol dm^{-3}, temp = 303 K; μ = 0.5 mol dm^{-3}).

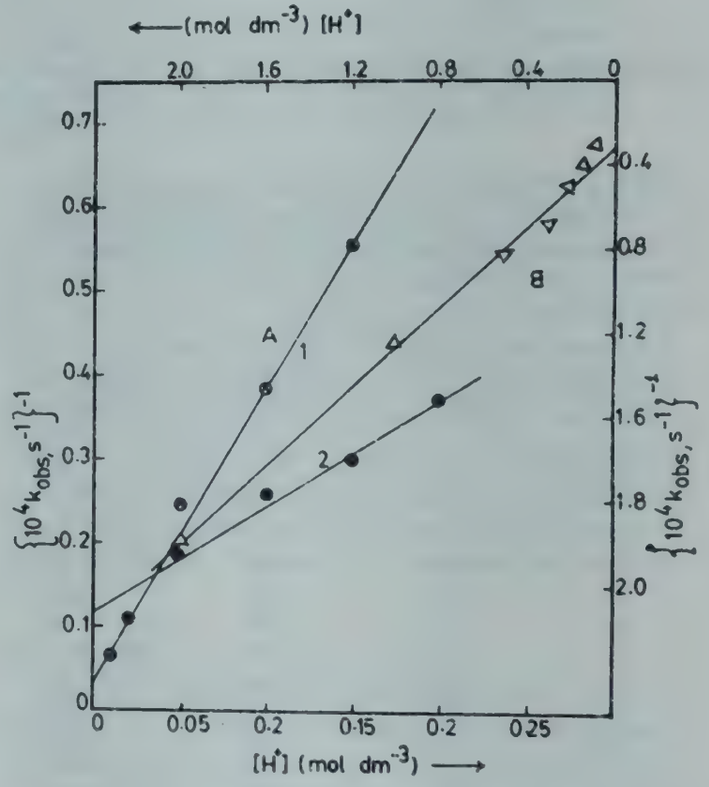

Fig. 3—(A) Plot of $1/k_{obs}$ versus $[H^+]$; (1) ICl (2) I_2. (10^3[OX] = 1.0 mol dm^{-3}; 10^2[TSC] = 2.0 mol dm^{-3}. μ = 0.5 mol dm^{-3}; 10^3 [KI] = 6.0 mol dm^{-3} (with I_2); temp = 303K) (B) Plot of $1/k_{obs}$ versus $[H^+]$ (10^3 [iodamine-T] = 1.0 mol dm^{-3}; 10^2 [TSC] = 2.0 mol dm^{-3}; μ = 0.5 mol dm^{-3}; temp = 303K)

oxidants and the plots of log k_{obs} versus log $[H^+]$ were linear with varying fractional slopes (Table 3). With iodamine-T there were two ranges. The orders in $[H^+]$ were −1.0 and −0.6 in the $[HClO_4]$ ranges, 0.02-0.2 mol dm^{-3} and 0.2-2.0 mol dm^{-3}, respectively. The rates increased with increase in [TSC] with all the oxidants with varying fractional orders (Table 3). Plots of k_{obs} versus [S] were nonlinear in all the cases, attaining limiting values. Double reciprocal plots, $1/k_{obs}$ versus 1/[S] were linear (Fig. 1) with all the three oxidants, indicating the operation of Michaelis-Menten type mechanisms in all these systems. Plots of $1/k_{obs}$ versus $[H^+]$ were also linear (Fig. 3) for all the oxidants except with iodamine-T at low $[H^+]$. Under latter conditions, the plot of k_{obs} versus $1/[H^+]$ was linear passing through origin (Fig. 2).

Increase in ionic strength of the reaction medium slightly decreased the rate (Table 4). But decrease in dielectric constant of the medium (by changing the solvent composition with methanol) slightly increased the rate in the case of TSC-ICl and TSC-I_2 systems but it had no effect in the case of TSC-iodamine-T system. Addition of reaction products I^-, Cl^- (with ICl) and PTS (with iodamine-T) had little or no effect on the rate for all these systems.

The rates of reactions were measured at different temperatures as functions of [TSC] and $[HClO_4]$ and the rate constants for the rate controlling steps were

Table 4—Effect of Added Reaction Products and Variation in Ionic Strength of the Medium on the Rates of Oxidations of Thiosemicarbazide by Iodamine-T, Iodine Monochloride and Iodine in Perchloric Acid Medium at 303K

μ[a] (mol dm^{-3})	$10^4 k_{obs}$ (s^{-1})		
	Iodamine-T	ICl	I_2[b]
0.07	8.2	—	—
0.10	8.1	—	—
0.12	—	3.5	5.4
0.20	7.8	3.1	5.1
0.50	7.5	2.6	3.8
0.80	—	2.3	—
1.00	7.5	1.9	2.4
10^2 [KI][c] (mol dm^{-3})			
0.0	—	2.6	—
0.1	—	2.7	—
0.5	—	—	3.0
0.6	—	2.7	—
1.0	—	2.6	3.5
2.0	—	2.6	3.8
5.0	—	—	5.2
10.0	—	—	6.7

[a] 10^3 [oxidant] = 50 [TSC] = 10 [$HClO_4$] = 1.0 mol dm^{-3}.
[b] Same as (a) and [KI] = 0.02 mol dm^{-3}.
[c] Same as (a) and μ = 0.5 mol dm^{-3}.

calculated at different temperatures from the double receiprocal plots as described under discussion. The constants so computed were used to calculate the activation parameters from the Arrhenius plots, with all the oxidants (Table 3).

Discussion

Iodamine-T (RNIK, where R = $CH_3C_6H_4SO_2$) is analogous to chloramine-T[1-3] and bromamine-B[4] in aqueous solutions and hence the following equilibria exist in its solutions.

$$RNIK \rightleftharpoons RNI^- + K^+ \quad \ldots (4)$$
$$RNI^- + H^+ \rightleftharpoons RNIH \quad \ldots (5)$$
$$RNIH + H_2O \rightleftharpoons RNH_2 + HOI \quad \ldots (6)$$
$$RNIH + H^+ \rightleftharpoons RNH_2I^+ \quad \ldots (7)$$
$$RNH_2I^+ + H_2O \rightleftharpoons RNH_2 + H_2OI^+ \quad \ldots (8)$$

Mechanism of oxidations

(i) With iodamine-T at low [$HClO_4$]: In this case the order of the reaction was dependent on [H^+]; it was -1 at low [$HClO_4$] (0.02 to 0.2 mol dm^{-3}) and less than -1 at high [$HClO_4$] (0.2-2.0 mol dm^{-3}).

At low [$HClO_4$] first order dependence in [iodamine-T], fractional order in [TSC] and inverse first order in [H^+] and no effect on the rate on the addition of reaction product, PTS can be accounted for by the mechanism in Scheme 1.

$$RNHI + S \overset{K_1}{\rightleftharpoons} RNHIS \quad \text{(fast)}$$

$$RNHIS \overset{K_2}{\rightleftharpoons} RNIS^- + H^+ \quad \text{(fast)}$$

$$RNIS^- \overset{k_3}{\rightarrow} S' + RNH_2 + I^- \quad \text{(slow)}$$

$$S' + 5RNHI + H_2O \overset{k_4}{\rightarrow} \text{Products} \quad \text{(fast)}$$

where [RNHI] = [RNIK] and S': $HNNCSNH_2$

Scheme 1

Rate law (8) was deduced in accordance with Scheme 1.

$$-\frac{d[RNIK]}{dt} = \frac{6k_3K_2K_1[RNHI]_{tot}[S]}{[H^+](1 + K_1[S]) + K_1K_2[S]} \quad \ldots (9)$$

or

$$k_{obs} = \frac{6k_3K_2K_1[S]}{[H^+](1 + K_1[S]) + K_1K_2[S]} \quad \ldots (10)$$

Assuming that $[H^+](1 + K_1[S]) \gg K_1K_2[S]$ or K_2 is very small, rate law (10) would be reduced to Eq. (11).

$$k_{obs} = \frac{6k_3K_2K_1[S]}{[H^+](1 + K_1[S])} \quad \ldots (11)$$

or

$$\frac{1}{k_{obs}} = \left\{\frac{1}{6k_3K_2K_1[S]} + \frac{1}{6K_2k_3}\right\}[H^+] \quad \ldots (12)$$

The experimental observation that the plots of $1/k_{obs}$ versus $1/[S]$ and k_{obs} versus $1/[H^+]$ are linear with no and finite intercepts, respectively (Figs 1 and 2), is in conformity with rate laws (11) and (12). The ratio of intercept and slope of the latter plot gave K_1 (113.2 mol^{-1} dm^3). The latter and the product $6k_3K_1K_2$ have been used to predict the rate constants for the variation of [H^+]. At 10^2[$HClO_4$] = 2.0, 3.0, 5.0, 7.5 and 10.0 mol dm^{-3}, 10^4k were calculated to be 20.1, 13.4, 8.1, 5.4 and 4.0 s^{-1} respectively. The corresponding observed values are 21.6, 12.0, 7.5, 4.5 and 3.2 s^{-1}. Reasonable agreement between the predicted the experimental values supports the rate law and hence testifies to the validity of the reaction Scheme 1.

(ii) *With Iodamine-T (at high $[HClO_4]$), ICl and aqueous iodine*

At high $[HClO_4]$ the rate of oxidation of TSC-iodamine-T system was first order in [iodamine-T], fractional order in [TSC] and inverse fractional order in $[H^+]$. Contrary to expections, the order in [TSC] decreased from 0.5 to 0.1 with increase in $[HClO_4]$ from 0.05 to 1.0 mol dm^{-3} (Table 3). At high $[HClO_4]$ most of the substrate would be present in the protonated form and if RNHI continues to be the reactive species even under these conditions, one would expect a pronounced dependence of rate on [TSC], as protonated species (SH^+) are difficult to oxidise than the unprotonated form (S). The decrease in dependence of rate on [TSC] with increase in $[H^+]$ indicates that the reactive oxidising species at high $[HClO_4]$ is different. H_2OI^+ is likely to be the most probable species under these conditions. It is also evident from the identical kinetics observed with the other two oxidants, viz., ICl and I_2. Therefore, observed kinetics in iodamine-T oxidations at high $[HClO_4]$ (0.1-2.0 mol dm^{-3}), and in ICl and aqueous iodine oxidations of TSC may be explained by a common Michaelis-Menten type mechanism shown in Scheme 2.

$$H_2OI^+ \overset{K_6}{\rightleftharpoons} H^+ + HOI \qquad \text{(fast)}$$

$$HOI + S \overset{K_7}{\rightleftharpoons} \text{Complex} \qquad \text{(fast)}$$

$$\text{Complex} \overset{k_8}{\rightarrow} Y \qquad \text{(slow)}$$

$$Y + \&HOI \overset{k_9}{\rightarrow} \text{Final products} \qquad \text{(fast)}$$

Scheme 2

Based on Scheme 2 rate law (13) has been deduced.

$$\text{rate} = -\frac{d[\text{oxidant}]}{dt} = k_8[\text{complex}]$$

$$= \frac{6k_8K_7[\text{oxidant}]_t[S]}{1 + K_6[H^+] + K_7[S]} \qquad \ldots (13)$$

or

$$k_{obs} = \frac{6k_8K_7[S]}{1 + K_6[H^+] + K_7[S]} \qquad \ldots (14)$$

or

$$1/k_{obs} = \frac{1 + K_6[H^+]}{6k_8K_7[S]} + \frac{1}{6k_8} \qquad \ldots (15)$$

The plot of $1/k_{obs}$ versus $1/[S]$ was linear for all the three oxidants with slope $= 1 + K_6[H^+]/6k_8K_7$ and intercept $= (1/6k_8)$. The substrate concentrations were varied at different $[H^+]$ and the slopes of double reciprocal plots (between k_{obs} and [S]) were plotted against $[H^+]$. The plots were linear with slopes and intercepts equal to $K_6/6k_8K_7$ and $1/6k_8K_7$. The values of k_8, K_7 and K_6 were calculated. The activation parameters were computed from k_8 values at different temperatures.

Equation (14) can also be rewritten as Eq. (16) to express the relationship between k_{obs} and $[H^+]$.

$$\frac{1}{k_{obs}} = \frac{K_6[H^+]}{6k_8K_7[S]} + \frac{1 + K_7[S]}{6k_8K_7[S]} \qquad \ldots (16)$$

Plots between $1/k_{obs}$ and $[H^+]$ were linear with intercepts for all the oxidants in conformity with rate law (16) (Fig. 3), thus suggesting the operation of an identical mechanism with all oxidants at high $[HClO_4]$.

References

1 Bishop E & Jennings V J, *Talanta*, **1** (1958) 197.
2 Campbell M M & Johnson G, *Chem Rev*, **78** (1978) 65 and references therein.
3 Gowda B T & Mahadevappa D S, *J chem Soc, Perkin Trans* 2, (1983) 323.
4 Hardy F E & Johnston J P, *J chem Soc, Perkin Trans* 2, (1973) 742.

Indian Journal of Chemistry
Vol. 27A, November 1988, pp. 979-982

Dissociation Constants of Esters of Glycine & Leucine in Different Mixed Solvents

B P DEY & S C LAHIRI*
Department of Chemistry, University of Kalyani, Kalyani

Received 25 *September* 1985; *revised* 29 *July* 1987; *rerevised and accepted* 23 *February* 1988

In order to determine the ratio of zwitterion to neutral forms of the amino acids in different mixed solvents, the dissociations constants of the methyl esters and ethyl esters of glycine and leucine have been determined *p*H-metrically in methanol + water, ethanol + water, isopropanol + water and *t*-butanol + water mixtures. These data have been used to determine the values of the different microscopic constants of the amino acids. The results indicate that the neutral forms are present in negligible amounts even in the high percentages of alcohols.

One of the important features of the amino acids is that they are present predominantly as "zwitterions" in water though the presence of slight amounts of neutral forms is not ruled out. The macroscopic constants (K_1 and K_2) determined experimentally are resultant of the processes actually occurring in the solution (Eqs 1-5)[1]:

$$NH_3^+CHRCO_2H + H_2O \overset{K_A}{\rightleftharpoons} NH_3^+CHRCO_2^- + H_3O^+ \quad \ldots (1)$$

$$NH_3^+CHRCO_2H + H_2O \overset{K_B}{\rightleftharpoons} NH_2CHRCO_2H + H_3O^+ \quad \ldots (2)$$

$$NH_3^+CHRCO_2^- + OH^- \overset{K_C}{\rightleftharpoons} NH_2CHRCO_2^- + H_2O \quad \ldots (3)$$

$$NH_2CHRCO_2H + OH^- \overset{K_D}{\rightleftharpoons} NH_2CHRCO_2^- + H_2O \quad \ldots (4)$$

$$NH_2 \cdot CHR \cdot CO_2H \overset{K_Z}{\rightleftharpoons} N^+H_3 \cdot CHR \cdot CO_2^- \quad \ldots (5)$$

where,

$$K_1 = K_A + K_B$$

$$\frac{1}{K_2} = \frac{1}{K_C} + \frac{1}{K_D}$$

and $$K_Z = \frac{K_A}{K_B} = \frac{K_C}{K_D}$$

Thus, the knowledge of K_Z would be of help not only in determining the ratio of zwitterion to neutral form but also in determining the microscopic constants utilising the values of K_1 and K_2.

Since the neutral amino acid is non-existent, the dissociation constant of the ester of amino acid

$$NH_3^+RCO_2Et \rightleftharpoons NH_2RCO_2Et + H^+ \quad \ldots (6)$$

is regarded to be the K_Z for the reaction (5) and is utilised for the determination of the microscopic constants in water.

In the course of our studies on the effect of solvents on the dissociation constants of the amino acids, we found that the values of K_Z of amino acid esters in aquo-organic mixtures are particularly important in obtaining information regarding the microscopic constants and the ratio of the 'Zwitterion' to neutral form of amino acids in mixed solvents.

The ratio of neutral to zwitterionic forms (K_Z) in a few aquo-organic mixtures has been determined by Edsall *et al*[1] assuming pK_E values of ester amine hydrochloride in water to remain unchanged in aquo-organic solvents.

However, the pK-values of the 'isoelectric reactions' have been found to change with solvent composition[2]. Therefore, it is desirable to determine the pK_E values of esters of the amino acid hydrochlorides in aquo-organic mixtures to get microscopic constants and the extent of conversion from zwitterionic to neutral species. These considerations led us to determine the dissociation constants of methyl and ethyl esters of glycine and leucine in aquo-organic mixtures (methanol + water, ethanol + water, isopropanol + water and *t*-butanol + water mixtures).

Materials and Methods

The methyl and ethyl esters of glycine and leucine hydrochlorides (GR, Sigma Chemicals) were used without further purification. The compounds were analysed by titration of the total amount of the acid present in the ester hydrochlorides. The alcohols were purified and the weight percentages of organic solvents were determined in the usual way[3,4]. The slight traces of water present, if any, in the organic solvents were neglected.

Table 1—The pK_1, pK_2, pK_E and Other Microscopic Constants of Esters of Glycine in Methanol-Water, Ethanol-Water, 2-Propanol-Water and *t*-Butanol-Water Mixtures

Wt% of alcohol	$1/\varepsilon \times 10^2$	Glycine		Glycine Ethyl Ester			Glycine Methyl Ester		
		pK_1	pK_2	pK_E	log K_Z	pK_D	pK_E	log K_Z	pK_D
0	1.27	2.33 (2.34)	9.59 (9.60)	7.70 (7.73)	5.37	4.22	7.65	5.32	4.27
				Methanol-Water					
8.0	1.33	2.57	9.60	8.09	5.52	4.08	7.69	5.12	4.48
16.0	1.40	2.63	9.63	8.12	5.49	4.14	7.72	5.09	4.54
25.2	1.48	2.66	9.67	8.37	5.71	3.96	7.64	4.98	4.69
34.4	1.57	2.90	9.74	8.49	5.59	4.15	7.62	4.72	5.02
44.7	1.69	3.18	9.75	8.43	5.25	4.50	7.60	4.42	5.33
54.2	1.84	3.36	9.78	8.37	5.01	4.77	7.59	4.23	5.55
64.1	2.01	3.50	9.81	8.30	4.80	5.01	7.55	4.05	5.76
75.9	2.25	3.64	9.74	8.28	4.64	5.10	7.38	3.74	6.00
				Ethanol-Water					
8.0	1.35	2.55	9.59	7.74	5.19	4.40	7.73	5.18	4.41
16.4	1.42	2.66	9.68	7.76	5.10	4.58	7.65	4.99	4.69
25.3	1.53	2.70	9.74	7.88	5.18	4.56	7.63	4.93	4.81
34.4	1.71	2.88	9.74	7.86	4.98	4.76	7.61	4.73	5.01
44.0	1.90	3.05	9.75	7.68	4.63	5.12	7.53	4.48	5.27
54.1	2.14	3.38	9.83	7.63	4.25	5.58	7.33	3.95	5.88
64.7	2.44	3.53	9.84	7.59	4.04	5.80	7.25	3.72	6.12
76.0	2.87	3.73	9.73	7.45	3.72	6.01	7.10	3.37	6.36
				2-Propanol-Water					
8.0	1.37	2.40	9.59	7.89	5.49	4.10	7.71	5.31	4.28
16.3	1.50	2.51	9.58	7.98	5.47	4.11	7.68	5.17	4.41
25.1	1.65	2.64	9.59	8.22	5.58	4.01	7.65	5.01	4.58
34.3	1.86	2.81	9.63	8.38	5.57	4.06	7.53	4.72	4.91
43.9	2.13	3.03	9.68	8.10	5.07	4.61	7.46	4.43	5.25
54.0	2.52	3.17	9.74	8.00	4.83	4.91	7.35	4.18	5.56
64.6	3.10	3.49	9.80	7.92	4.43	5.37	7.27	3.78	6.02
75.8	3.87	3.66	9.81	8.14	4.48	5.23	7.19	3.53	6.28
				t-Butanol-Water					
8.0	1.43	2.40	9.55	7.83	5.43	4.12	7.67	5.27	4.28
16.4	1.58	2.50	9.58	8.05	5.55	4.03	7.70	5.20	4.38
25.0	1.80	2.62	9.60	8.15	5.53	4.17	7.58	4.96	4.64
34.2	2.08	2.71	9.61	8.12	5.41	4.20	7.50	4.79	4.82
43.8	2.50	2.73	9.63	8.05	5.32	4.31	7.35	4.62	5.01
54.0	3.18	2.84	9.68	8.00	5.16	4.52	7.25	4.41	5.27
64.5	4.44	2.97	9.78	7.97	5.00	4.78	7.20	4.23	5.55
75.8	5.63	3.27	9.81	7.95	4.68	5.13	7.00	3.73	6.08

Caustic soda was of GR Grade (E Merck). It was standardised in the usual way. Other chemicals were also of guaranteed reagent quality. All solutions were made in water, doubly distilled from all-glass distilling apparatus.

For the determination of the dissociation constants of the methyl and ethyl esters of glycine and leucine hydrochlorides, a known concentration of the ester hydrochloride was neutralised to different extents with caustic soda in different volumetric flasks of known volumes and the hydrogen ion concentrations were measured *p*H-metrically. The process was repeated with diferent concentrations of the ester hydrochlorides. The *p*H-meter readings were taken using a Systronics digital *p*H-meter with a combined glass and calomel electrodes assembly maintained at 298K in the way described in our previous communications[4,5].

Results and Discussion

The pK_E for the reaction,

$$^{+}NH_3CHRCO_2Et + H_2O \rightleftharpoons NH_2CHRCO_2Et + H_3O^{+} \text{ is}$$

$$pK_E = B + \log U_H + \log \frac{[^{+}NH_3CHRCO_2Et]}{[NH_2CHRCO_2Et]}$$

in mixed solvents.

Table 2—The pK_1, pK_2, pK_E and Other Microscopic Constants of Esters of Leucine in Methanol-Water, Ethanol-Water, 2-Propanol-Water and *t*-Butanol-Water Mixtures

Wt% of Alcohol	$1/\varepsilon \times 10^2$	Leucine			Leucine Ethyl Ester		Leucine Methyl Ester		
		pK_1	pK_2	pK_E	log K_Z	pK_D	pK_E	log K_Z	pK_D
0	1.27	2.44 (2.36)	9.59 (9.60)	7.62 (7.63)	5.18	4.41	7.55	5.11	4.48
				Methanol-Water					
8.0	1.33	2.60	9.48	7.71	5.11	4.37	7.60	5.00	4.48
16.0	1.40	2.71	9.48	7.87	5.16	4.32	7.62	4.91	4.57
25.2	1.48	2.83	9.47	8.02	5.19	4.28	7.62	4.79	4.68
34.4	1.57	2.98	9.48	8.12	5.14	4.34	7.54	4.56	4.92
44.7	1.69	3.15	9.49	8.03	4.88	4.61	7.48	4.33	5.16
54.2	1.84	3.30	9.48	8.02	4.72	4.76	7.42	4.12	5.36
64.1	2.01	3.50	9.50	7.95	4.45	5.05	7.30	3.80	5.70
75.9	2.25	3.79	9.51	7.93	4.14	5.37	7.20	3.41	6.10
				Ethanol-Water					
8.0	1.35	2.53	9.55	7.66	5.13	4.42	7.58	5.15	4.40
16.4	1.42	2.60	9.53	7.73	5.13	4.40	7.61	5.01	4.52
25.3	1.53	2.80	9.51	7.89	5.02	4.49	7.50	4.70	4.81
34.4	1.71	2.96	9.53	7.80	4.84	4.69	7.36	4.40	5.13
44.0	1.90	3.13	9.52	7.73	4.62	4.90	7.18	4.05	5.47
54.1	2.14	3.26	9.52	7.61	4.35	5.17	7.08	3.82	5.70
64.7	2.44	3.42	9.54	7.55	4.13	5.41	6.92	3.50	6.06
76.0	2.87	3.68	9.56	7.49	3.81	5.75	6.70	3.02	6.54
				2-Propanol-Water					
8.0	1.37	2.53	9.50	7.88	5.35	4.15	7.69	5.16	4.34
16.3	1.50	2.58	9.50	8.10	5.52	3.98	7.60	5.02	4.48
25.1	1.65	2.81	9.50	8.13	5.32	4.18	7.42	4.61	4.89
34.3	1.86	2.95	9.52	8.17	5.22	4.30	7.28	4.33	5.19
43.9	2.13	3.13	9.52	7.83	4.70	4.82	7.04	3.91	5.61
54.0	2.52	3.37	9.52	7.77	4.40	5.12	6.88	3.51	6.01
64.6	3.10	3.57	9.55	7.84	4.31	5.24	6.77	3.20	6.35
75.8	3.87	3.74	9.58	7.91	4.17	5.41	6.74	3.00	6.58
				t-Butanol-Water					
8.0	1.43	2.53	9.62	7.93	5.40	4.22	7.61	5.08	4.54
16.4	1.58	2.69	9.64	8.15	5.46	4.18	7.45	4.81	4.83
25.0	1.80	2.80	9.62	8.20	5.40	4.22	7.28	4.48	5.14
34.2	2.08	2.91	9.65	8.17	5.26	4.39	7.15	4.24	5.41
43.8	2.50	2.99	9.71	8.15	5.16	4.55	7.00	4.01	5.70
54.0	3.18	3.13	9.75	8.10	4.97	4.78	6.83	3.70	6.05
64.5	4.44	3.28	9.79	8.08	4.80	4.99	6.73	3.45	6.34
75.8	5.63	3.74	9.82	8.07	4.33	5.49	6.65	2.91	6.91

B is the *p*H meter reading in mixed solvents, log U_H is the correction factor to be added algebraically to the *p*H meter reading to have appropriate $[H^+]$ ion concentrations in mixed solvents.

log U_H was determined with each set of measurements in the way described in our previous communications[6-8].

The use of neutral electrolytes was carefully avoided as the solute-solvent interactions of unknown magnitude are likely to mask the 'medium effects' and the ionic strengths were kept low ($3-7\times10^{-3}$ *M*) so that the 'medium effects' could be determined.

The pK_E values of the methyl and ethyl esters of amino acid hydrochlorides are recorded in Tables 1 and 2.

The pK_E values of the esters of glycine hydrochloride and leucine hydrochloride have been found to change with the change int he composition of the solvent, i.e., pK_E values are solvent-dependent. But it is difficult to derive useful conclusions regarding the solvent effect on the pK_E values.

In general, pK_E values of ethyl esters of glycine and leucine change considerably (about 0.7-0.8 and 0.5-0.6 pK_E units respectively) in mixed solvents and pK_E values are higher in mixed solvents com-

pared to those in water except at higher percentages of ethanol and the change in pK_E values is considerably less in ethanol + water mixtures.

The methyl esters, on the other hand, show slight increase in pK_E values initially but these decrease subsequently and the pK_E values are considerably lower in mixed solvents. The changes in pK_E values are about 0.5-0.6 and about 0.8-0.9 pK_E units (for glycine and leucine componds) in mixed solvents (except in methanol + water mixtures where the change in much lower).

The maxima in the pK_E values of the ethyl esters in mixed solvents are: 34 wt% methanol, 25-34 wt% ethanol, 34 wt% isopropanol and 25% *t*-butanol. The maxima in the pK_E values of the methyl esters are usually in the region of 8-16 wt% of organic solvents, though variations exist.

The measurements of *p*H is extremely sensitive task in the region studied and fluctuations in pK_E are expected. The errors in the pK_E values are $\pm$(0.02-0.3) at low percentages of alcohol (about 44 wt%) and $\pm$(0.03-0.04) at higher percentages. Moreover, slight hydrolysis of esters in the *p*H-region cannot be ruled out which may change the pK_E values and the hydrolysis of esters is usually solvent dependent. Moreover, we have not taken into consideration the autoprotolysis constants of water in different mixed solvents to calculate the *p*H values in mixed solvents. Under these conditions, it is not possible to infer much regarding the solvent effect on pK_E of amino acid esters.

The determination of the values of the microscopic constants requires the value of any one of the constants K_Z, K_A, K_B, etc. It is customary to assume that the equilibrium constant for the process, Cation $\rightleftharpoons$ uncharged acid + H^+, is almost equal to the corresponding ionisation constant K_E[9-11] for the basic group of the methyl or ethyl ester of the acid ($pK_E = pK_B$). However, our results suggest that pK_E values of the different esters are not the same but vary considerably in mixed solvents. Bryson *et al.*[12] also suggested the relation $pK_B = pK_E \pm 0.2$ from a study of ten N-arylglycines in aqueous solutions.

K_B has been neglected so that K_1 can be taken equal to K_A. This is justifiable in view of the fact that pK_E (of glycine or leucine ester hydrochloride) is of the order of 7.5-8.0 compared to values of 2.33-2.44 for pK_1 of glycine and leucine. Thus, K_Z (ratio of zwitterionic to neutral forms) can be easily calculated from the reaction,

$$K_Z = \frac{K_1}{K_E}$$

Since, $$\frac{1}{K_2} = \frac{1}{K_C} + \frac{1}{K_D}$$

and $$K_Z = \frac{K_D}{K_C}$$

we have, $$\frac{1}{K_2} = \frac{K_Z}{K_D} + \frac{1}{K_D} = \frac{1}{K_D}(K_Z + 1)$$

$pK_2 = pK_D + \log K_Z$, [neglecting 1 in comparison to K_Z]

$pK_D = pK_2 - \log K_Z$

The value of log K_Z suggests that the percentage of neutral form is very low in water. Though the percentage of neutral form increases in mixed solvents, it is very very small (the ratio i.e. K_Z value changes from 10^5 to 10^3 from water to mixed solvents).

The results also show that pK_D value of the amino acids increase almost continuously with the increase in the [organic solvents], obviously due to the increase in the increase in the concentration of neutral amino acids.

References

1 Edsall J J & Blanchard M H, *J Am chem Soc*, **55** (1933) 2337.
2 Hazra D K & Lahiri S C, *Analyt chim Acta*, **79** (1975) 335; *J Indian chem Soc*, **53** (1976) 787.
3 Bhattacharyya A, Mondal A K & Lahiri S C, *Electrochim Acta*, **25** (1980) 559; *Indian J Chem*, **19A** (1980) 532.
4 Dey B P, Dutta S & Lahiri S C, *Indian J Chem*, **21A** (1982) 886.
5 Pal A, Dey B P & Lahiri S C, *Indian J Chem*, **25A** (1986) 322.
6 Van Uitert L G & Haas C G, *J Am chem Soc*, **75** (1953) 451.
7 Bhattacharya U C & Lahiri S C, *Z phys Chem (N.F.)*, **50** (1966) 131.
8 Lahiri S C & Aditya S, *J Indian chem Soc*, **51** (1974) 319.
9 Ebert L, *Z phys Chem (Leipzig)*, **121** (1926) 385.
10 Greenstein J P & Winitz M, *Chemistry of the amino acids*, Vol I (John Wiley, New York, London) 1961, Chapter 4.
11 Green R W & Tong H K, *J Am chem Soc*, **78** (1956) 4896.
12 Bryson, Davies N R & Serjeant E P, *Nature*, **195** (1962) 996.

Indian Journal of Chemistry
Vol. 27A, November 1988, pp. 983-986

Use of Chelating Ion Exchanger Containing Acetoacetanilide Group in Selective Separation of Beryllium

SWAPAN MAJEE & JYOTIRMOY DAS*
Department of Chemistry, University of Burdwan, Burdwan 713 104

Received 31 *July* 1987; *revised and accepted* 7 *December* 1987

A macroreticular styrene-divinylbenzene based chelating resin having acetoacetanilide as the functional group has been synthesized and characterised. The resin is stable in fairly strong acid or alkaline solution. The sorption patterns of Na(I), K(I), Ca(II), Mg(II), Co(II), Cu(II), Ni(II), Fe(III), Al(III), Ti(IV) and U(VI) have been studied at varying *p*H. The selective nature of the absorption of Be(II) at *p*H 4.0 has been utilized for the separation and concentration of the metal ion in synthetic mixtures and in beryl. Strong H_2SO_4 (6 *N*) has been used for the elution of Be(II) from the resin.

In trace analysis preconcentration of metal ion is often a vital step and various chelating resins having chelating groups like hydroxylamine and its derivatives[1], iminodiacetate[2], thioglycolates[3], dithiozone[4], hydroxyquinoline[5], *o*-hydroxyaldoxime[6], 1-nitroso-2-naphthol[7], 2-nitroso-1-naphthol[8] have been used for the separation of different metal ions.

Acetoacetanilide[9] is a very selective reagent for gravimetric determination of beryllium. So far only one chelating resin containing 1,3-diketo compound[10] has been synthesized. In this work acetoacetanilide has been incorporated in styrene divenylbenzene (DVB) polymer and the resulting ion-exchanger has been characterised. The absorption behaviour of several metal ions on this resin has been studied and a method for the separation and preconcentration of Be(II) has been developed.

Materials and Methods

An atomic absorption spectrophotometer (Shimadzu AA-646) and a double beam UV-visible spectrophotometer (Beckmann 26) were used for measurement of concentrations of the metal ions. Infrared spectra were recorded in KBr matrix on a Beckmann Acculab-10 IR spectrophotometer. Gravity flow columns were made of glass with appropriate reservoirs.

Fresh solution of benzoyl-*m*-nitroacetonilide was prepared by dissolving 0.28 to 0.32 g of the reagent in aqueous ethanol (25 ml). Beryllium solution was prepared from beryllium nitrate (E. Merck) in dilute nitric acid. The metal content was determined gravimetrically[9,11]. Aqueous solutions of the desired diverse metal ions were prepared from their nitrates, chlorides or sulphates and a little acid was added to avoid hydrolysis.

For adjusting the *p*H sodium chloride-hydrochloric acid buffers were used for the *p*H range of 0.5 to *p*H less than 4.0 and sodium acetate-acetic acid buffers were used for the range of *p*H between 4.0 and 6.0. For studying the exchange behaviour of metal ions above *p*H 6.0 to 7.5 buffers were prepared from KH_2PO_4 and Na_2HPO_4.

Synthesis and ion exchange capacity of resin

Styrene-DVB polymer beads (80-100 mesh) containing 8% DVB (Thermax Private Ltd., Poona, India) was nitrated using a mixture of concentrated sulphuric acid and nitric acid. The wet nitrated product was mixed with tin (20 g), industrial ethanol (50 ml) and sufficient amount of conc. hydrochloric acid and refluxed for 12 hr to obtain aminopolystyrene. Finally, the aminated product was condensed with ethyl acetoacetate (4 g for every 3 g of aminopolystyrene) by refluxing the mixture at 110-15° for 24 hr in toluene to get the desired acetoacetanilide resin.

Ion exchange capacity of the resin for metal ions was studied by batch and column operation methods. In batch operation, air-dried resin (0.5 g) was stirred for 24 hr with an excess of the desired metal ion solution of known strength (~ 0.1 *M*) and *p*H controlled by adding suitable buffer; the mixture was filtered and the resin was thoroughly washed with the same buffer until free from the metal ions. The sorbed metal ions were then completely eluted by H_2SO_4 of appropriate strength. The whole process was repeated with buffers of different *p*H. The eluted metal ions were determined by standard methods.

It was found that 50 ml 4 *N* sulphuric acid were sufficient for eluting cobalt(II), copper(II), iron(III), calcium(II), magnesium(II) and nickel(II) while 50 ml 6 *N* sulphuric acid were required for titanium(IV), uranium(VI) and beryllium(II).

In column operation, a glass column (30 cm length and 1 cm i.d.) was packed with ~25 g of air-dried resin (initially swollen with 2 *N* hydrochloric acid for 24 hr). The bed was thoroughly washed with deionised water at a flow rate of 0.5-1.0 ml/min till free from acid. This rate of flow was maintained in all subsequent steps. Known volumes of the desired metal ion (50 ml, ~2 *M*), adjusted to the desired *p*H by adding appropriate buffer, was passed through the column, washed with sufficient amount of deionised water and finally the sorbed metal ions were eluted with sulphuric acid of appropriate strength and determined by appropriate method.

Concentrations of the metal ions before and after elution from the resins were determined by standard procedures. Titanium(IV), uranium(VI), beryllium(II) and copper(II) were determined spectrophotometrically, titanium(IV) was determined with hydrogen peroxide in acid medium[12], beryllium(II) with benzoyl-*m*-nitroacetanilide[13] and copper(II) with sodium diethyl dithiocarbamate[12]. Aluminium(III), iron(III), cobalt(II), sodium(I) and potassium(I) were determined by atomic absorption spectrophotometry. Nickel(II) was determined gravimetrically with dimethylglyoxime[14]. Calcium(II) and magnesium(II) were determined by titration with EDTA using Eriochrome black-T as indicator[14].

Separation procedure

For the separation of Be(II) from its binary mixture with Cu(II), Co(II), Ca(II), Mg(II), Ni(II), Al(III), Fe(III), Ti(IV) or U(VI), the resin column was equilibrated with the buffer solution of *p*H 4.0. The *p*H of the solution containing the mixture of metal ions was adjusted to 4.0 in the presence of EDTA. The solution was then percolated through the resin column, washed thoroughly with the same buffer and eluted with 150 ml 6 *N* H_2SO_4.

It was observed that over 99% beryllium could be recovered using 150 ml of 6 *N* H_2SO_4 as eluant.

Results and Discussion

Characterisation of the resin

The resin was characterised by its water regain value, infrared spectrum, its stability towards acid and alkali, elemental analysis and metal ion exchange capacity.

A sample of dry resin was immersed in deionised water for 48 hr, centrifuged, air-dried and weighed. It was then dried at 100°C for 48 hr and weighed again. Water regain, calculated from the difference in weight, was found to be 0.21 g/g resin.

Infrared spectrum exhibited two bands at 1500 and 1330 cm^{-1} assignable to $-CONH-$ and CH_3CO- groups respectively. The resin was found to be stable in 6 *N* H_2SO_4 and 4 *N* NaOH since no appreciable change in its nitrogen content and sorption capacity for titanium was found.

Estimation of nitrogen and amino group

Small amounts of the air-dried resin of the nitrated polystyrene, aminopolystyrene and the chelating resin containing diketo group (all belonging to the same batch) were thoroughly dried by heating at 80°C for 48 hr and then keeping in a desiccator over phosphorus pentoxide . Nitrogen in each case was determined by micro Duma's method. The amino group content of the aminopolystyrene was determined by titration in nonaqueous medium[15].

The nitrogen content and the capacity for Ti(IV) remained unchanged after treatment with 6 *N* H_2SO_4 or less or with 2*N* NaOH or less. The small value of water regain of the resin indicated that its sorption capacity may not be very high, but experiments showed that the resin had a moderate capacity for beryllium.

The nitrogen content of the nitrated polymer was found to be 5.53%. After reduction, the percentage of nitrogen of the amino resin was found to be 7.1% as total nitrogen and 5.23% as amino nitrogen (from the estimation of amino group) with 1.87% nitrogen as unconverted nitro group. The nitrogen content of the final resin was found to be 5.47%.

In order to study the cation retention capacity of the residual nitro and amino groups of the resin, the capacities of both polynitrostyrene-divinylbenzene and polyaminostyrene-divinylbenzene have been studied and found to be negligible.

Metal absorption capacity and separation

The absorption capacity of beryllium on resin column was slightly lower than that in batch operation (Fig. 1). The total capacity versus *p*H curves for the metals studied, shown in Fig. 1, indicate that the resin exhibits high selectivity for Be(II), which starts getting absorbed by the resin around

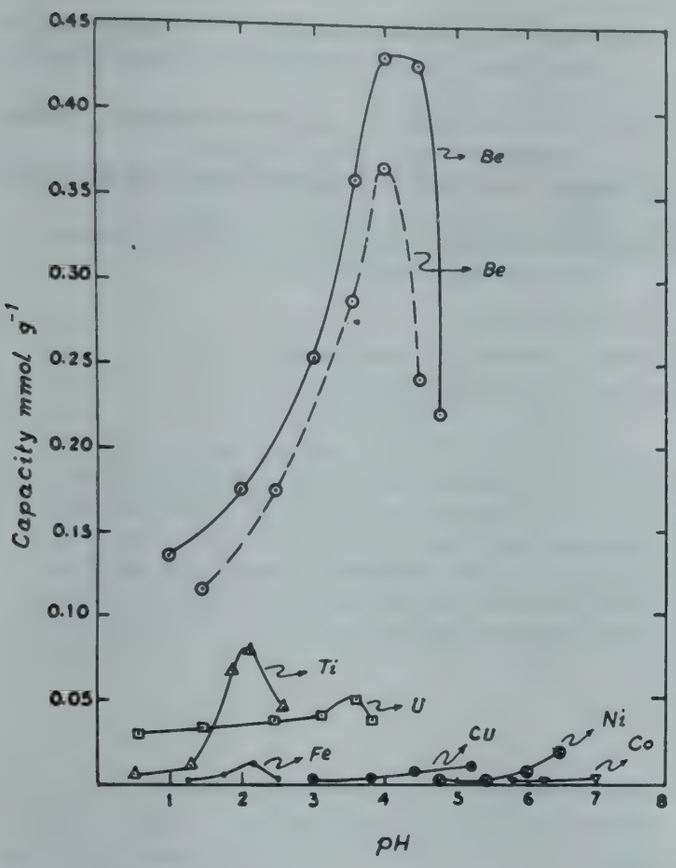

Fig. 1 – Exchange capacity of acetoacetanilide resin for different metal ions as a function of *p*H [———, total exchange capacity; ....., exchange capacity in the resin column].

Table 1 – Separation of Beryllium from Diverse Ions

[Beryllium taken = 45 mg]

Diverse ions	(mg)	Beryllium recovered (%)
Al(III)	100	
Na(I)	50	
K(I)	50	99.77
Ca(II)	50	
Mg(II)	50	
Fe(III)	50	
Ni(II)	100	99.66
Co(II)	100	
Co(II)	100	
Ni(II)	100	99.85
Cu(II)	100	
Al(III)	100	
Fe(III)	50	99.56
Ni(II)	100	

Table 2 – Determination of Beryllium in Beryl Ore

Wt (mg) Beryl ore taken	Be found (mg) by given method*	Be found (%) by given method*	BeO found (%) by given method*	BeO found (%) by standard method*
211.732_4	9.506_7	4.510_8	12.53	12.58
260.421_3	11.692_9	4.496_4	12.49	12.58

*Mean of three determinations.

*p*H 1.5, followed by a maximum with a peak at *p*H 4.0.

Among the other metal ions studied, Fe(III), Co(II), Cu(II) and Ni(II) are only negligibly absorbed by the resin, while Na(I), K(I), Ca(II), Mg(II) and Al(III) are not absorbed at all. So a clear separation of Be(II) from Al(III), Na(I), K(I) Ca(II) and Mg(II) is possible. Separation of Be(II) from Fe(III), Ni(II) and Co(II), separation of Be(II) from Co(II), Ni(II) and separation of Be(II) from Al(III), Fe(III) and Ni(II) are also possible. Addition of 10-20 ml of Na_2EDTA (0.1%) and boiling the mixture for 2 min prevent precipitation of base metals due to hydrolysis at *p*H 4.0. Some examples of separation of Be(II) in synthetic mixture are shown in Table 1.

Separation and determination of beryllium in beryl

Finely powdered beryl (~0.2 g) was decomposed[16] by fusion with NaF, cooled and taken up in conc. H_2SO_4. The mixture was heated to fumes to drive out all the fluoride and transferred into a beaker containing water (~100 ml). A clear solution was obtained by boiling and the volume was made upto 250 ml.

Aliquots of this solution was adjusted to *p*H 4.0 by acetate buffer and passed through resin column (initially adjusted to *p*H 4.0 by the same buffer), when only beryllium was absorbed on the column. The resin column was washed with the same buffer and finally Be(II) was eluted with 50 ml 6 *N* H_2SO_4 and collected in a 100 ml volumetric flask. Beryllium was determined spectrophotometrically using benzoyl-*m*-nitroacetanilide. The results are given in Table 2.

Acknowledgement

We are thankful to M/s. Thermax Private Ltd., Poona for supplying the polystyrene DVB resin beads as gift sample and to Geological Survey of India, Calcutta for supplying the sample of Beryl. One of us (SM) is grateful to the University of Burdwan for the award of a fellowship.

References

1 Vernon F & Eccles H, *Analyt chim Acta*, **77** (1975) 145.
2 Hirsch R F, Gancher E & Russo F R, *Talanta*, **17** (1970) 483.
3 Moyer E M & Fritz J S, *Anal Chem*, **48** (1976) 1117.
4 Tanaka H, Chikuma M, Harad A, Ueda T & Yube S, *Talanta*, **23** (1976) 489.
5 Sugawara K F, Weetall H H & Schucker G D, *Anal Chem*, **46** (1974) 489.
6 Bhattacharyya S & Das H R, *Indian J Chem*, **22A** (1983) 134.

7 Ghosh J P & Das H R, *Talanta*, **28** (1981) 274.
8 Ghosh J P, Pramanick J & Das H R, *Talanta*, **28** (1981) 957.
9 Das J & Banerjee S, *Z anal Chem*, **184** (1961) 110.
10 Majee S, Ray C & Das J, *Indian J Chem*, **27A** (1988) 137.
11 Das J & Shome S C, *Analyt chim Acta*, **24** (1961) 37.
12 Sandell E B, *Colorimetric determination of traces of metals*, (Interscience, New York) 1959, p. 870, 915, 443.
13 Choudhuri N K, *Organic reagents in inorganic analysis, uses of some beta ketoanilides* (Ph.D. Thesis, Burdwan University), 1972, p. 77.
14 Vogel A I, *A text book of quantitative inorganic analysis* (Longman, London) 1978, p. 320, 420.
15 Fichen G E & Lane E S, *Analyt chim Acta*, **16** (1957) 207.
16 Iyer K V, Prakash K A, Iyer S G & Venkateswarlu Ch, *Indian J Chem*, **24A** (1985) 168.

Indian Journal of Chemistry
Vol. 27A, November 1988, pp. 987-990

Spectrophotometric Determination of Gold(III) through Kinetic Reduction of Gold(III)-Gelatin Complex by Hydrazine in Aqueous Medium

TARASANKAR PAL* & ASHES GANGULY
Department of Chemistry, Indian Institute of Technology, Kharagpur 721302

Received 17 *August* 1987; *revised* 4 *November* 1987; *accepted* 1 *February* 1988

An aqueous solution of gold(III)-gelatin complex has been found suitable for the spectrophotometric determination of gold(III) in the range 0.6 μg ml^{-1} – 72 μg ml^{-1} after its reduction to a pink-coloured gold sol with hydrazine. The reduction is found to be first order with respect to [Au(III)complex].The pink coloured gold sol is fairly stable and exhibits molar absorptivity of 3.53×10^3 dm^{-3} mol^{-1} cm^{-1} at λ_{max} 530 nm in alkaline medium. The Sandell's sensitivity for an absorbance of 0.001, relative standard deviation and confidence limit (95%) for 10.30 μg of gold (50 replicates) are 5.58×10^{-2} μg cm^{-2}, 0.82% and 10.285 ± 0.021 respectively. The method shows a remarkable freedom from interferences.

Spectrophotometric methods for the determination of gold(III) generally involve binary complex formation between gold(III) ions and chromogenic reagents[1-5]; however, these methods lack sensitivity. Several extractants for the photometric determination of gold in complex materials have also been reported[6-10]. Conventional methods often involve lengthy procedures due to the necessity of multiple extractions[7], suffer from interference by other metal ions[4], or loss of photometric selectivity arising from the use of reagents such as amides[11], etc.

Long chain proteins have been commonly used for the suppression of polarographic maxima and more recently for the prevention of ion association[11]. This observation has prompted us to re-examine earlier application of gelatin[12,13]. We have now developed a simple and one-step procedure for the determination of gold(III) in water without the use of any toxic or expensive reagent. The various factors which affect the rate of reduction of gold(III)-gelatin have been determined. The method is very selective as well as sensitive and can be used in aqueous phase containing 50 diverse ions and can be applied to more dilute and biological samples without any degradation and pretreatment. Gold may also be reclaimed by this technique of reduction.

Materials and Methods

The absorbance measurements were carried out by the use of a Varian Carry-17D spectrophotometer with 1-cm quartz cell. The *p*H measurements were carried out with a ECIL digital 5652 *p*H meter. The numerical analyses were performed by a HP 1000 computer.

All the reagents used were of AR grade. $AuCl_3.xH_2O$ (1 g) (Johnson Matthey, London) was dissolved in sufficient amount of distilled water, the volume made upto 500 ml and was standardised by the quinol method[14]. A fresh stock solution of hydrazine was prepared by dissolving hydrazine sulphate (E Merck) in distilled water. The solution was then diluted to 10^{-3} *M*. Gelatin solution (1%) was prepared by dissolving gelatin powder (1 g) (Oxo Ltd, London) in 100 ml of warm distilled water. Owing to the obvious microbial degradation of gelatin and the aerial oxidation of hydrazine in water, both the solutions were prepared afresh before the estimation. The hydrazine solution was standardised[15] before use.

Procedure

Aliquots of aqueous solution containing variable amounts of Au(III) and 2 ml of (1%) gelatin solution were mixed together into a series of 10 ml calibrated flasks. The *p*H of the solution was adjusted to about 9.5 using 0.1 *M* NaOH solution. The solution was warmed to about 40°C for 2-3 min and then cooled to room temperature. Hydrazine sulphate solution was added so that the ratio of hydrazine: gold concentrations was 10:1. The mixture was then diluted to 10 ml with distilled water. After 150 min the absorbance was measured at 530 nm against water. For kinetic studies the absorbance values were recorded at different time intervals.

Results and Discussion

Gold(III)-gelatin interaction and effect of reducing agents

A coloured sol was formed by the gold(III)-amino acid complexes in the alkaline *p*H range but the sol particles could not be stabilised by the amino acids as such. However, the sol could be stabilised when carboxymethylcellulose solution was used in alkaline medium. The sol stabilisation property of carboxymethylcellulose solution is known previously[12] also. The complexation and stable coloured sol formation were observed with gold(III) and gelatin or gold(III) and egg albumin systems without adding amino acids. On the other hand, though carboxymethylcellulose solution stabilised the gold sol, the cellulose molecule was not suitable for binding gold(III) ions, like the protein molecules.

Gold(III) ions interact with gelatin in alkaline medium and produce colourless water-soluble gold(III) complexes, but complex formation is considerably affected by *p*H. Below *p*H 6.5, no gold(III)-gelatin complex results as is indicated by the expulsion of total gold(III) ions[12] through a dialysis bag at 30°C. But *p*H > 11.0 is not recommended, as gelatin solution would be hydrolysed at such a high *p*H. The binding of gold(III) ions with an amino group of gelatin may be of similar nature as described earlier[12]. Gold complexes of gelatin are expected to be reduced to gold metal by the strong reducing agents like hydrazine and ascorbic acid, etc. Ascorbic acid was successful in the production of sol at *p*H ~ 9.5, but it needed a longer reduction time as compared to hydrazine. The kinetic aspect of the reaction between gold(III)-gelatin complex and hydrazine was studied by simple spectrophotometric method. Stop flow technique[16] was not necessary in view of the comparatively slower reaction rate. The results were further corroborated by the expulsion of total anions, e.g., Cl^- or I^-, of uncomplexed $HAuCl_4$ or AuI_3 respectively through the dialysis bag at 30°C after the complexation of free gold(III) ions with gelatin. The results show that 1 ml of 1% gelatin can bind 1635 μg of gold(III) ions. Absorbance values were unaffected in the presence of a large excess of gelatin.

Absorption spectra

The particle size of the gelatin-stabilised gold sol was smaller when the reduction of Au(III)-gelatin solution was done at a *p*H above 9.5, but it was larger when reduction was done around *p*H 3.0. The reduction at a lower *p*H produced a blue sol solution (λ_{max} 560 nm) and that at higher *p*H resulted in a pink solution (λ_{max} 530 nm). In both the cases the Au(III)-gelatin complex has negligible absorbance. So, all measurements were done against water blank. The proposed spectrophotometric method gives a solution with a molar absorptivity of 3.53×10^3 l mol^{-1} cm^{-1}. The Sandell sensitivity for an absorbance of 0.001 is 5.58×10^{-2} μg cm^{-2}, with a relative standard deviation of 0.82% and a confidence limit (95%) of 10.285 ± 0.021 for 10.30 μg of gold (50 replicates).

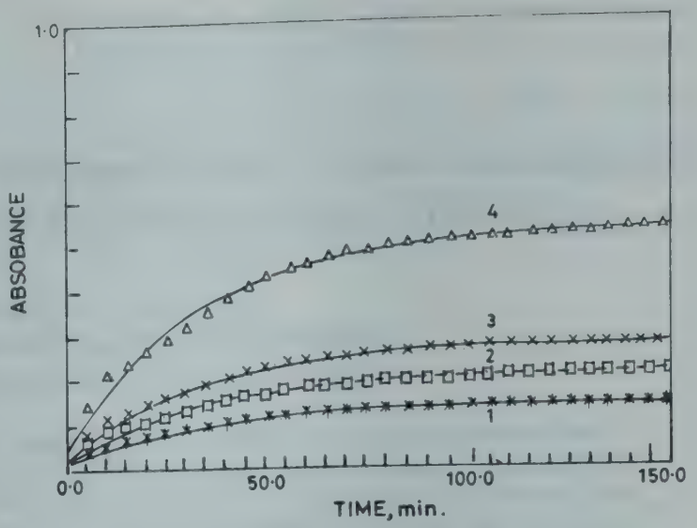

Fig. 1 – Absorbance versus time curves for the reduction of Au(III) to Au(0) by hydrazine (1) 7.9 μg/ml of Au, (2) 11.84 μg/ml of Au, (3) 15.81 μg/ml of Au, (4) 29.55 μg/ml of Au; *p*H 9.5; solid lines correspond to computer generated curves for the proposed kinetic path.

Reduction profile

The reaction rate is dependent on the temperature, but is independent of the concentration of Au(0) in solution. Kinetic analysis of the curve showed (Fig. 1) that the reaction was of first order with respect to the Au(III)-complex concentration in solution. For the first order reaction, monitored via absorbance changes, the absorbance versus time relationship is given by $A_t = A_\infty - (A_\infty - A_0)e^{-kt}$, where, A_0, A_t and A_∞ are initial, intermediate and final absorbances, and k and t are the first order rate constant and time. A computer programme in FORTRAN was developed to generate the change in concentration for each species. Linear regression analysis was used to estimate suitable value of K and A to match the experimental data[17,18]. It follows that the reduction of Au(III)-gelatin complex to Au(0) is a first order process. The K value is 0.0308 min^{-1}. The relationship between concentration and the computed absorbance changes was evaluated with

four solutions. The reaction profile was studied taking the advantage of the comparatively slower reduction rate.

Effect of pH and the sol particle

It was observed that for the quantitative reduction of gold-gelatin complex, a ten-fold excess of hydrazine was needed in the reaction media. The presence of anions, excess hydrazine (more than ten times the amount of gold) and the amount of gold-gelatin complex in the reaction media had no influence on the rate of the reduction reaction. The effect of *p*H on the reaction rate in solution containing 0.1184 mg of Au, 2 ml of (1%) gelatin solution and 1 mg hydrazine was investigated. The hydrogen ion concentration was changed from 1×10^{-6} to 10^{-11} *M* by the addition of NaOH solution. The reaction rate was essentially unaffected in the *p*H range of 9.0-11.0, and between *p*H 6.0 and 9.0 the anomalous absorbance indicated the irregular particle size of the gold sols. In the *p*H range 2.0-3.5 uniform but larger particle size (blue solution, λ_{max} 560 nm) of the gold resulted where gelatin remained only as a sol stabiliser but not as a complexing agent. Owing to the anomalous reduction phenomenon, *p*H-dependent kinetics was not studied. This was authenticated by the reduction of $HAuCl_4$ solution by hydrazine in carboxymethyl cellulose solution.

The time-dependent reduction of gold-gelatin complex with hydrazine was studied keeping all the other factors constant. It was observed that the reduction (99%) was complete only after 120 min but all measurements were done after 150 min.

To further classify the stability of the sol, experiments were performed at different temperatures. Analysis of the rate profiles showed a temperature-dependent reaction path. The temperature dependent reduction was studied at three temperatures (20°, 24° and 32°) showing the activation parameters, $\Delta H^* = 5.6$ kcal mol^{-1}, $\Delta S^* = -234$ JK^{-1}. At a temperature above 40°C, the decrease in absorbance values indicated that the destabilisation of the sol particle in aqueous medium may be due to the precipitation of gold metal by a sol aggregation process or by the denaturation of the polymer used. The gold-gelatin complex in alkaline solution remained stable in the temperature range 20°C – 40°C for a period of four weeks.

The effect of reasonable ionic strength on the reaction rate cannot be studied due to the coagulation of gold sol[13]. However, it has been observed that very low ionic strength (< 0.05 *M*) does not disturb the gold sol and the rate of reduction of gold(III)-gelatin complex.

Effect of diverse ions

Solutions containing 10.30 μg ml^{-1} of gold and various amounts of other ions were mixed and the recommended procedure for gold determination was followed. Alkali and alkaline earth metal ions along with As(III), Mn(II), Zn(II), Cd(II), Sn(II), Bi(III), F^-, Cl^-, NO_3^-, NO_2^-, CO_3^{2-}, SO_3^{2-} do not interfere when present in 500-fold excess. About 100-fold excess of Co(II), Ni(II), Cr(III), Al(III), Hg(II), Pt(II), 50-fold excess of Ag(I), Fe(II) and Fe(III), acetate, tartrate, citrate, 20-fold excess of H_2O_2, 5-fold excess of Cu(II), U(VI), Th(IV) and one-fold excess of Pt(IV), Ra(III), Ru(III), Pd(II), Os(VIII), Ir(III), Re(VII), Mo(VI), W(VI), La(III), V(V) and I^- can be tolerated. The interference due to H_2O_2 can be removed simply by boiling the gold solution before complexation with gelatin. Ba(II), Mn(II), Co(II), Ni(II), Hg(II), Pb(II) could be effectively masked by Na_2-EDTA solution. Therefore, the procedure is very simple, selective and the tolerance limits to diverse ions, except iodide and platinum(IV), are very high. However, the interference due to iodide can be removed effectively by dialysis. Two-fold excess of Ru(III), Rh(III), Os(VIII), Ir(III), Pd(II) and Pt(IV) was tolerated when the calibration curve for Au(0) sol was made at 560 nm after the reduction of Au(III)-gelatin complex at *p*H 2.0-3.5.

In order to confirm the usefulness of the proposed method it was applied to the determination of gold in three synthetic matrices and to a concentrate from low-grade gold ore, overcoming the influence of the interferents. The results are summarised in Table 1 together with the results ob-

Table 1 – Determination of Gold in Various Samples

Sample	Gold found by present method*	Gold found by AAS method*	Relative standard error, %
Synthetic samples (amounts added in mg)			
Au (17.7) + Cu(50) + Al(800) + Fe(100) + Rh(10) + Ir(7)	17.6 μg	17.6 μg	0.56
Au(14.16) + Pt(10) + Pd(10) + Cr(200) + Mn(800)	14.0 μg	14.1 μg	1.12
Au(10.3) + Os(10) + V(10) + Fe(100) + Co(500) + Ni(500)	10.26 μg	10.2 μg	0.38
Gold Ore (Au-0.0024%)	23.8 μg/g	23.6 μg/g	0.83

* Average of five determinations

tained by atomic absorption spectrometry, carried out for comparison. Gelatin-stabilised gold sol in alkaline medium is well suited for preconcentration, recovery and reclaiming of gold from low grade solutions, and platinum metal concentrate. The method is simple, reproducible and can be applied to dilute biological samples without any degradatgion and pretreatment.

References

1 Beamish F E & Van Loon J C, *Analysis of noble metals*, (Academic Press, New York), chapter 3, 1977.
2 Das H R & Bhattacharyya S N, *Talanta*, **23** (1976) 535.
3 Diamantatos A, *Anal chim Acta*, **66** (1973) 147.
4 Anuse M A, Mote N A & Chavan M B, *Talanta*, **33** (1983) 323.
5 Anuse M A, Kuchekar S R, Mote N A & Chavan M B, *Talanta*, **32** (1985) 1008.
6 Mirza M Y, *Talanta*, **27** (1980) 101.
7 Patil P S & Shinde V M, *Mikrochim Acta*, **II** (1973) 331.
8 Mojski M, *Talanta*, **25** (1978) 163.
9 Nesterenko P N & Lomonosov M V, *Zh anal Khim*, (1984) 456.
10 Patel K S & Lieser K U, *Analyt Chem*, **58** (1986) 1547.
11 Jaya S, Rao T P & Ramakrishna T V, *Analyst*, **108** (1983) 1151.
12 Pal T & Maity D S, *Analyst*, **111** (1986) 49.
13 Pal T & Ganguly A, *Analyst*, **112** (1987) 1327.
14 Vogel A I, *A text book of quantitative inorganic analysis* (Longman, London) 1973, pp. 464-465.
15 Pal T, Maity D S & Ganguly A, *Analyst*, **111** (1986) 1413.
16 Taquikhan M M & Martell A E, *J Am chem Soc*, **89** (1967) 4176.
17 Mieling E & Pardue H L, *Analyt Chem*, **50** (1978) 1611.
18 Rao C P, *Piecewise constant orthogonal functions and their application to systems and control* Lecture notes on Control and Information Sciences Series-55, Springer Verlag), 1983.

Indian Journal of Chemistry
Vol. 27A, November 1988, pp. 991-993

Notes

Prototropic Equilibria of Electronically Excited Molecules: 9-Phenylcarbazole & 1,4,5,8,9-Pentamethylcarbazole

MANNAM KRISHNAMURTHY
Department of Chemistry, Andhra University,
P.G Extension Centre, Nuzvid 521 201
and
SNEH K DOGRA*
Department of Chemistry, Indian Institute of Technology,
Kanpur 208 016

Received 10 *November* 1987; *revised and accepted*
14 *January* 1988

Electronic absorption and fluorescence spectra of 9-phenylcarbazole and 1,4,5,8,9-pentamethylcarbazole have been studied in different solvents and at various $[H^+]$. These spectra are nearly insensitive towards the nature of the solvent, as depicted by both band maxima and fluorescence quantum yields. Monocation of these molecules are non-fluorescent and prototropic equilibrium is established in S_1 state, indicating that carbon centre becomes more basic.

The weekly basic characteristics of the aromatic hydrocarbons towards strong Bronsted acids have been recognised[1]. Most of the theoretical studies[2,3] have predicted that in the excited singlet states these aromatic hydrocarbons become more basic as compared to those in the ground state. Though pK_a^* values agree qualitatively with those predicted by the Förster cycle method, the fluorimetric titrations of the prototropic reaction (monocation-neutral) give only the ground state pK_a values[4-6]. This indicates that the prototropic equilibria are not established in the excited singlet state during the lifetimes of these conjugate acid-base pairs. On the other hand, prototropic equilibria are established in the protonation reaction of heterocyclic hydrocarbons, e.g. indole[7,8], carbazole[9,10] etc. The only problem is that the monocations of these hydrocarbons are non-fluorescent. Recently we have observed that monocation of 2-hydroxy- and 2-methoxy-carbazoles[10] are fluorescent and the prototropic equilibrium is established in the S_1 state. Presently we have studied the prototropic equilibria for the protonation reactions of 9-phenylcarbazole (9PC) and 1,4,5,8,9-pentamethylcarbazole (PMC) in order to see the effect of electron withdrawing and electron donating groups on these equilibria.

9PC and PMC (Aldrich Chemicals, England) were recrystallised from methanol. Solvents were purified before use. Calculations were made as reported in recent papers[10,11].

The absorption and fluorescence spectra of carbazole, 9PC and PMC were recorded in different solvents and at different $[H^+]$ and spectral characteristics are recorded in Table 1. The relevant data agreed with the literature values[12,13]. The data in Table 1 clearly indicate that the phenyl group at the position-9 of 9PC is not in the same plane as carbazole in S_0 and S_1 states. This is manifested in the near similarity of the vibrational frequencies in the S_0 and S_1 states, matching of the O − O band and the mirror image symmetry observed in the absorption and fluorescence spectra. This agrees with the earlier results[13] as well as that observed in 9-phenylanthracene[14]. The larger red shift observed in PMC is consistent with the behaviour of methyl groups. The absorption and fluorescence spectra of carbazole and 9PC are insensitive towards solvents whereas the fluorescence spectrum of PMC gets little bit red shifted, e.g. Stokes shift increases from 410 cm^{-1} (in cyclohexane) to 900 cm^{-1} (in water). This is further manifested by the fluorescence quantum yields observed in different solvents.

The effect of varying $[H^+]$ on the spectrum of carbazole is similar to that observed by Capomacchia and Schulman[9], i.e. absorption spectrum is insensitive to any variation in $[H^+]$ in the range of *p*H 14 to H_0 −4 and the molecule decomposes with increase in $[H^+]$ as revealed by change of colour of carbazole. Behaviour of 9PC and PMC is similar to that of carbazole except that changes in the absorption and fluorescence spectra occur at different $[H^+]$.

Solubility of 9PC is very small in water and thus it is not easy to locate the band maximum in absorption spectrum but saturated solution if 9PC in water does confirm the fluorescence spectrum. The intensity of the fluorescnece band starts decreasing below $H_0 \sim 0$ and completely vanishes at $H_0 - 4$, without the appearance of a new fluorescence band. This could be either due to proton-induced fluorescence quenching of the neutral molecule or due to the formation of non-fluorescent monocation. The formation of latter species is only an excited state phenomenon as this species does not exist in the S_0 state in this acid concentration range. As observed earlier[10], the monocation of carbazole is non-fluorescent, but the similar species of 2-hydroxy- and 2-methoxy-carbazoles are fluorescent, with a red shifted fluorescent band in comparison to the neu-

Table 1—Long Wavelengths Absorption Maxima (λ_a), Molar Extinction Coefficients (ε), Fluorescence Maxima (λ_f) and Fluorescence Quantum Yields (ϕ_f) for Carbazole, 9-Phenylcarbazole and 1,4,5,8,9-Pentamethylcarbazole in Different Solvents

Solvent	Carbazole		9-Phenylcarbazole		1,4,5,8,9-Pentamethylcarbazole	
	λ_a, nm (log ε)	λ_f, nm (ϕ_f)	λ_a, nm (log ε)	λ_f, nm (ϕ_f)	λ_a, nm (log ε)	λ_f, nm (ϕ_f)
Cyclohexane	331 (3.34)	329 (0.40)	339 (3.49)	335 (0.25)	347 (3.54)	352 (0.47)
	318 (3.45)	343	326 (3.58)	352	335 (3.57)	366
	306 (3.52)	359	313 sh	368		388 sh
1,4-Dioxane	333 (3.49)	336 (0.50)	340 (3.57)	339 (0.28)	348 (3.57)	335 (0.50)
	322 (3.53)	352	327 (3.53)	356	337 (3.68)	371
	310 (3.41)	363	313 sh	365		395 sh
Ether	333 (3.50)	336 (0.38)	339 (3.62)	339 (0.25)	348 (3.55)	356 (0.46)
	321 (3.54)	351	326 (3.57)	357	336 (3.62)	370
	309 sh	363	313 sh	367		
Acetonitrile	334 (3.48)	336 (0.36)	340 (3.63)	340 (0.26)	349 (3.55)	358 (0.44)
	321 (3.59)	352	326 (3.60)	359	339 (3.63)	372
	309 sh	365	313 sh	371		
Methanol	335 (3.50)	338 (0.41)	339 (3.68)	340 (0.26)	349 (3.60)	358 (0.46)
	323 (3.54)	354	325 (3.63)	358	336 (3.64)	373
	310 sh	367	313 sh	373		
Water, *p*H 8	335 (3.52)	347	—	354	346 (3.82)	369
	319 (3.52)	363		369	332 (3.84)	385
				385		
H_2SO_4, $H_0 - 8$	377 (3.40)	—	—	—	382 (4.09)	—
	364 (3.72)				368 (4.07)	

tral species. Further pK_a^* values obtained from the fluorimetric titrations are -1.3, for the former and 0.1 and 0.0 for the latter species respectively. Since the pK_a^* obtained for 9PC from the fluorimetric titrations are not very different (see later) it can be concluded that the monocation of 9PC is also non-fluorescent. Similar behaviour is observed for PMC and thus the results obtained can be explained in a similar fashion.

The ground state pK_a value for 9PC could not be calculated spectrophotometrically as the formation of monocation is not complete even at $H_0 - 10$ and thus can be $< H_0 - 8$, whereas the pK_a value for the similar reaction of PMC is -4.7. This behaviour is consistent with the fact that the electron withdrawing groups (e.g. phenyl) decrease the pK_a value, whereas the electron donating (methyl) groups increase the pK_a value of the parent molecule, i.e. carbazole (-6.2)[9]. The pK_a^* values obtained from the fluorimetric titrations also follow a similar trend and a similar explanation also holds for these reactions. The values obtained are -2.0 and 0.1 for 9PC and PMC, respectively. The pK_a^* value for the PMC is also calculated using Förster cycle method and absorption data only (1.0), since the monocation is non-fluorescent. The agreement between the two values is not that bad. This is because (a) the absorption and fluorescene spectra are nearly insensitive to solvents, (b) mirror image symmetry is observed and (c) the vibrational spacing with ground and excited singlet states is nearly same for both the conjugate acid-base pairs.

Finally, it is difficult to point out the exact site of protonation, but based on the fact that the electrophilic attack in carbazole occurs in succession at position-3, 6 and 1 (see reference 15), it can be concluded that the protonation will take place at position-3. The following cannonical structures (I and II)

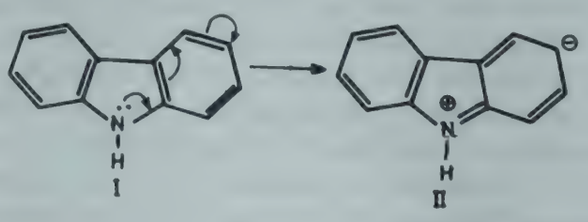

I II

can be written for carbazole. The presence of phenyl group at position-9 and methyl groups at positions 1, 4 and 9 supports our results.

It can be concluded that basicity of carbon centre increases on excitation and unlike carbocyclic aromatic hydrocarbons, the prototropic equilibria are established in 9PC and PMC in the S_1 state during the lifetimes of these species, similar to the results observed for 2-hydroxy- and 2-methoxy-carbazoles[10], carbazole[9] and indole[7] molecules.

The authors are thankful to the Department of Science and Technology, New Delhi, for financial support.

References

1 Hammett L P, *Physical organic chemistry* (McGraw Hill Book Co., New Delhi), 1940.

2 Flurry (Jr) R L, *J Am chem Soc*, **88** (1966) 5393.

3 Manoharan R & Dogra S K, *J Photochem Photobiol A Chem*, **43** (1988) 81.

4 Flurry R L (Jr) & Wilson R K, *J phys Chem*, **71** (1967) 589.

5 Mason S F & Smith B E, *J chem Soc (A)*, (1969) 325.

6 Colpa J P, Maclean C & Macka E L, *Tetrahedron*, **9**(Suppl 2) (1963) 65.

7 Remers W A, *The chemistry of heterocyclic compounds*, Vol. 25, edited by W.J. Houlihan (Wiley-Interscience, New York), 1972, pp. 11, 19, 24.

8 Vander Doncket E, *Prog React Kinet*, **5** (1970) 275.

9 Capomacchia A C & Schulman S G, *Anal chim Acta*, **59** (1972) 401.

10 Krishnamurthy M & Dogra S K, *Spectrochim Acta*, **59** (1972) 401.

11 Krishnamurthy M & Dogra S K, *J Photochem*, **32** (1986) 235; *Chem Phys*, **103** (1986) 325; *J chem Soc Perkin Trans*, **2** (1986) 1247; *Photochem Photobiol*, **44** (1986) 571; *Indian J Chem*, **26A** (1987) 215, 587.

12 Samanta A, Chattopadhyay N, Nath D, Kundu T & Chowdhury M, *Chem phys Lett*, **121** (1985) 507.

13 Retting W & Zander M, *Chem phys Lett*, **87** (1982) 229.

14 Werner T C, *Modern fluorescence spectroscopy*, Vol. 2, edited by E.L. Wehry (Plenum Press, New York), 1976, pp. 296.

15 Jaffe H H & Orchin M, *Theory and applications of ultraviolet spectroscopy* (Wiley, New York), 1962, pp. 356.

Indian Journal of Chemistry
Vol. 27A, November 1988, pp. 994-996

Spectrophotometric Studies on Electron-Donor-Acceptor Complexes of Aromatic Hydrocarbons with Tetrabromophthalic Anhydride

P C DWIVEDI*, NISHI SHARMA & ARCHANA SRIVASTAVA

Department of Chemistry, H.B. Technological Institute, Kanpur 208 002

Received 16 *October* 1987; *revised* 17 *January* 1988; *accepted* 27 *January* 1988

Electron donor-acceptor interactions between aromatic hydrocarbons, namely acenaphthene, pyrene, hexamethylbenzene, naphthalene, mesitylene, biphenyl and benzene as electron donors and tetrabromophthalic anhydride as electron acceptor have been examined by electronic spectroscopy in carbon tetrachloride solution. The spectral and thermodynamic parameters of the complexes are reported. The $h\nu_{CT}$-ionisation potential plot is found to be linear.

Electron donor-acceptor (EDA) complexes between tetrachlorophthalic anhydride (TCPA) and tertiary amines initiate polymerization[1]. It was felt that EDA complexes of tetrabromophthalic anhydride (TBPA) with a variety of electron donors may also act as initiators. Unfortunately, reports on EDA interactions of TBPA are scanty[2,3]. The present study on the interaction of aromatic hydrocarbons with TBPA forms a part of a broad programme aimed at developing new EDA complexes as initiators in polymerisation.

All the aromatic hydrocarbons, viz, benzene, biphenyl, mesitylene, naphthalene, hexamethylbenzene, pyrene and acenaphthene, were purified by crystallisation or fractional distillation. TBPA (Aldrich Chemicals, USA) was repeatedly crystallised from benzene till identical absorption spectra were obtained in CCl_4 with samples from successive crystallisation. Carbon tetrachloride (BDH, A R) was dried and distilled before use.

Spectral measurements were made on a Beckman D U spectrophotometer fitted with variable temperature cell compartment and matched silica cells of 1 cm pathlength. Equilibrium formation constants (K) and molar extinction coefficients (ε) of the EDA complexes were calculated graphically using the modified Scott equation[4]. In evaluating K, Person's criteria[5] regarding donor concentrations were satisfied. The enthalpies of formation (ΔH) were evaluated from the equilibrium constants at different temperatures in the range of 293-313 K.

All the aromatic hydrocarbons and TBPA have appreciable absorption in the CT region. Therefore, CT bands of all the EDA complexes were obtained by difference spectra. The spectral and thermodynamic data of the EDA complexes studied presently are given in Table 1. The ν_{CT} is linearly related to the ionization potential (I_p) for most of the donors studied (Fig. 1), indicating the validity of the Mulliken's original relationship[6] $h\nu_{CT} = I_p - E + C + \sigma/(I_p - E + C)$ to all the complexes studied (ν_{CT} is the absorption frequency of CT band, I_p is the ionization potential of the donor, E is the electron affinity of the acceptor and the term $C + \sigma/(I_p - E + C)$ takes into account the stabilization energy of the ion pair). It is evident from Table 1 that CT absorption maxima of EDA complexes generally decrease with increase in I_p of the donor. While uncertainties in the determination of ΔH in systems with small K-values would be large, the ΔH values are estimated to be well within $\pm$ 10% even after accounting for all possible sources of error.

If the electron donors in Table 1 are considered in three separate groups of methyl substituted (Group I), phenyl substituted (Group II) and polynucelar hydrocarbons (Group III), the complex stability order (as measured by K and ΔH) is: hexamethylbenzene > mesitylene > benzene (Group I) biphenyl > benzene (Group II) acenaphthene > pyrene > naphthalene > benzene (Group III) The above orders satisfy the condition that lower the I_p higher is the stability of the complex.

The half-band widths ($\Delta\nu_{1/2}$) increase with increase in complex strength (as measured by ΔH) and follow the above order with the exception of pyrene in Group III. This direct relationship between $\Delta\nu_{1/2}$ and the strength of complexes was earlier[7,8,9-12] attributed to the large resonance interaction in the complexes. The values of ε and the oscillator strength (f) of

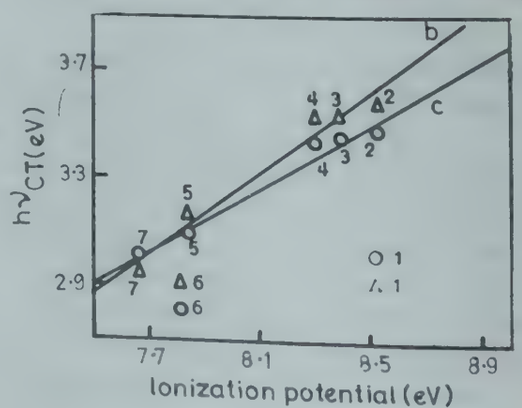

Fig. 1—$h\nu_{CT}$ versus ionization potential (I_p) plots for EDA complexes of aromatic hydrocarbons with (a) TBPA and (b) TCPA (the numbers refer to donors listed in Table 1)

Table 1—Spectral and Thermodynamic Data for EDA Complexes of Aromatic Hydrocarbons with TBPA and TCPA[a] in CCl_4 Solution

Electron Donor	Ionisation potential	Electron acceptor[b]	λ_{CT} (nm)	K[c] (dm^3, mol^{-1})	ε ($dm^3\ mol^{-1}cm^{-1}$)	$-\Delta H$ (kcal mol^{-1})	$\Delta\nu_{1/2}$	f	$\Delta\nu$[d] $\times 10^{-2}$ (cm^{-1})
Benzene	9.24	(i)	350	1.48	666	0.24	1243	0.003	8
		(ii)	340	0.42	704	0.36	1115	0.003	
Biphenyl	8.53	(i)	345	1.40	1071	1.4	1741	0.006	10
		(ii)	357	0.63	1666	2.9	2032	0.015	
Mesitylene	8.39	(i)	350	3.3	1500	1.6	2152	0.014	8
		(ii)	360	5.2	978	3.9	2164	0.019	
Naphthalene	8.30	(i)	350	3.8	1000	3.0	2003	0.009	10
		(ii)	362	2.3	1667	2.0	3409	0.026	
Hexamethylbenzene	7.85	(i)	390	13.4	1409	7.0	4536	0.028	6
		(ii)	400	12.1	1833	5.9	4845	0.038	
Pyrene	7.82	(i)	425	9.0	1300	5.0	3323	0.013	8
		(ii)	440	5.6	1333	2.8	6945	0.023	
Acenaphthene	7.66	(i)	420	9.3	778	5.8	3652	0.012	6
		(ii)	410	8.4	821	3.5	5403	0.019	

[a] Data from references (7) and (8)
[b] (i) TCPA, (ii) TBPA
[c] At 26°C; data are given at one temperature only for the sake of brevity.
[d] The difference in the ν_{CT} values of TCPA and TBPA.

EDA complexes, which provide a measure of the intensity of CT band, follow the above order in the case of donors of Groups I and II. However, in the case of the donors of Group III these values are in the order: benzene < acenaphthene < pyrene < naphthalene.

It is, thus, seen that the intensity of CT band increases for donors of Groups I and II as the strength of interaction (as measured by ΔH) increases. However, intensity of CT band decreases as the strength of interaction increases in the case of donors of Group III (with the exception of benzene). Similar observations have been made earlier in some instances[8,10]. This exceptional behaviour may possibly be due to the difference in the overlap parameter (σ) of the Mulliken's original relationship for the three groups of donors.

It is known that for a series of EDA complexes of donors of like structure with acceptors of, also of like structures, the shift ($\Delta\nu$) should be constant. In Table 1, the $\Delta\nu$ values of corresponding CT bands of TCPA and TBPA complexes ($\Delta\nu$ represents the difference in ν_{CT} values of TCPA and TBPA) are nearly constant indicating that the mode of interaction of both the acceptors in these complexes is the same. Similar observations have been made on structurally identical chloranil and 2,3-dichloro-5,6-dicyano-*p*-benzoquinone as acceptors[10,13].

Nagy and coworkers[14] have estimated the electron affinity (E) of TBPA to be 0.7 eV in a series of EDA complexes with a common electron donor and closely related electron acceptors. This value, being higher than that for TCPA (0.58 eV) seems to suggest that TBPA should be a better electron acceptor than TCPA. Accordingly, the stability of the naphthalene + TBPA complex has been reported[3] to be higher than that of naphthalene + TCPA complex. The values of λ_{CT}, $\Delta\nu_{1/2}$, ε and f in Table 1 are generally higher for the TBPA complexes than those for TCPA complexes. The slope of the $h\nu_{CT}$ versus I_p plot, a, is smaller for TBPA (0.6) than that for TCPA (0.75) (see Fig. 1). It may be mentioned here that the values of $\Delta\nu_{1/2}$, ε and f are known to increase with increase in the strength of interaction for a number of EDA complexes[7,8,9–12,15,16]. Also, the smaller the a and the ν_{CT} values the stronger is the resonance interaction[17]. Based on these observations, TBPA appears to be a better electron acceptor than TCPA. However, the K and ΔH values (which are measure of the stability of the EDA complexes) are generally higher for the TCPA complexes. This may be due to larger uncertainty in the measurement of K and ΔH values in these systems.

References

1 Medvedev S S, Stavrova S D & Chikhacheva I P, *Polim Simp*, **1** (1971) 144.
2 Chakrabarti S K, *Spectrochim Acta*, **24A** (1968) 790.
3 Christodouleas N & McGlynn S P, *J chem Phys*, **40** (1964) 166.
4 Scott R L, *Recl Trav chim Phys-Bas Belg*, **75** (1956) 787.
5 Person W B, *J Am chem Soc*, **87** (1965) 167.
6 Mulliken R S, *J Am chem Soc*, **74** (1952) 811.
7 Dwivedi P C & Banga A K, *Indian J Chem*, **19A** (1980) 158.
8 Dwivedi P C & Gupta A, *Proc Indian Acad Sci (Chem Sci)*, **93** (1984) 29.
9 Dwivedi P C & Banga A K, *Indian J Chem*, **19A** (1980) 908.

10 Dwivedi P C, Gupta A & Banga A K, *Curr Sci*, **51** (1982) 651.
11 Dwivedi P C, Gupta A & Banga A K, *Curr Sci*, **51** (1982) 1152.
12 Mulliken R S & Person W B, *Molecular complexes* (Wiley Interscience, New York) 1969.
13 Dwivedi P C & Agarwal Rama, *Indian J Chem*, **24A** (1985) 1015.
14 Nagy J B, Nagy O B & Bruylants A, *J phys Chem*, **28** (1974) 980.
15 Daisey J M & Sonnessa A J, *J phys Chem*, **76** (1972) 1895.
16 Dwivedi P C & Banga A K, *J inorg nucl Chem*, **42** (1980) 1767.
17 Foster R, *Organic charge-transfer complexes* (Academic Press, New York) 1969, pp 46.

Indian Journal of Chemistry
Vol. 27A, November 1988, pp. 997-998

Kinetics of Iron(II) Reduction of *trans*-Bromoammine- & *trans*-Bromo(N)glycine-cis(dimethylglyoximato)cobalt(III)

G BALASUBRAMANIAN,
T THOTHADRI & V R VIJAYARAGHAVAN*

Department of Physical Chemistry, University of Madras, Guindy Campus, Madras 600025

Received 31 *October* 1987; *revised and accepted* 6 *January* 1988

The kinetics of iron(II) reduction of *trans*-bromoammine- and *trans*-bromo(N)glycine-bis(dimethylglyoximato)cobalt(III) were studied at 30°C and 1.0 mol dm^{-3} ionic strength ($LiClO_4$ + $HClO_4$) in the $[H^+]$ range of 2.3×10^{-3} to 0.1 mol dm^{-3}. The rate of reduction of the bromoammine is sensitive to $[H^+]$ variation. This behaviour is explained in terms of the presence of protonated and unprotonated forms of the complex in equilibrium, the unprotonated form being more reactive than the protonated form. The kinetics of reduction of the bromoglycine complex show a poor sensitivity to $[H^+]$ variation. This is attributed to the coordinated glycine which coordinates to Fe(II) through the free carboxyl group and hence inhibits bridging by the oxime.

Kinetic studies on the iron(II) reduction of cobaloximes(III), reported from this laboratory, have indicated the presence of equilibria involving protonated and unprotonated species of the cobaloximes, the protonated forms reacting at a slower rate than the unprotonated forms[1,2]. This behaviour could be explained as due to a lower formation constant for the formation of a precursor complex between the protonated species and Fe(II). Herein we report the results of studies on the kinetics of iron(II) reduction of *trans*-bromoammine- and *trans*-bromo(N)glycine-bis(dimethylglyoximato)cobalt(III) complexes, the objective being to obtain information on the effects of nonbridging ligands.

trans-Bromoamine bis(dimethylglyoximato)-cobalt(III), *trans*-$[Co(dmgH)_2(NH_3)Br]$, was prepared from *trans*-$H[Co(dmgH)_2Br_2]$ as reported in literature[3,4] the latter being prepared using cobalt(II) bromide as the starting material. *trans*-Bromo(N)glycinebis(dimethylglyoximato)cobalt(III), *trans*-$[Co(dmgH)_2$(N-hlycine)Br] was prepared by stirring glycine with *trans*-$H[Co(dmgH)_2Br_2]$ in a 1:1 molar ratio at 60°C. The dark brown precipitate of *trans*-$[Co(dmgH)_2$(glycine)Br] was crystallised from ethanol, washed with ether and dried. The complex was characterised by UV-visible and IR spectra, and elemental analyses. The similarity between the UV spectra of the two complexes suggests that the complex was *trans*-$[Co(dmgH)_2$(N-glycine)Br].

The kinetics of iron(II) reduction of the complexes was studied spectrophotometrically under psuedo-first order conditions with an excess of iron(II) perchlorate, prepared by dissolving pure iron powder (Sarabai M) in perchloric acid under nitrogen atompshere. The reaction mixture was kept in a thermostated cell compartment of a Shimadzu UV-visible-260 recording spectrophotometer. An atmosphere of nitrogen was maintained using serum caps to seal the cells. The reaction was monitored at 300 nm for both the complexes. Perchloric acid was used as the source of H^+, and glycine buffer was used above *p*H 2. Lithium perchlorate was used for adjusting the ionic strength.

The stoichiometry of the reaction was determined to be 1:1 [Co(III):Fe(II)]. The reaction mixture containing a ten-fold excess of Fe(II) over complex was acidified with excess $HClO_4$ (1 *N*) after completion of reaction and Co(II) and Fe(III), separated by ion-exchange, were estimated spectrophotometrically[5] as $CoCl_4^{2-}$ and Fe(III)-NCS^- complex, respectively.

The second order rate constant for the Fe(II) reduction of *trans*-$[Co(dmgH)_2(NH_3)Br]$ at 30°C in the $[H^+]$ range of 0.0023-0.1 mol dm^{-3} at $\mu = 1.0$ mol dm^{-3} are presented in Table 2. It is seen that the rate constant decreases with increase in $[H^+]$ and reaches a limiting value at $[H^+] = 0.08$ mol dm^{-3}. This kinetic behaviour suggests the presence of protonated and unprotonated forms of the complex in equilibrium, the protonated form reacting at a slower rate. The data could be fitted into the rate equation (1)

$$k = (k_1 K[H^+] + k_2)(1 + K[H^+])^{-1} \quad \ldots(1)$$

where $k = k_{obs}/[Fe(II)]$, is the second order rate constant, k_1, the limiting rate constant due to the protonated form and K, the protonation constant. The constants k_1 and k_2 were determined using a *p*H-metrically determined value of K, (650 ± 230 $dm^3 mol^{-1}$) in Eq. (1). The values are: $k_1 = 0.068 \pm 0.01$ $dm^3\,mol^{-1}s^{-1}$ and $k_2 = 0.90 \pm 0.35$ $dm^3 mol^{-1}s^{-1}$.

The second order rate constants for the reduction of *trans*-$[Co(dmgH)_2$(N-glycine)Br] are also given in Table 1. While there is a seven-fold increase in k for the reduction of *trans*-$[Co(dmgH)_2(NH_3)Br]$ as $[H^+]$ is varied from 0.1 to 0.003 mol dm^{-3} there is only a two-fold increase under similar conditions in the case of *trans*-$[Co(dmgH)_2$(glycine)Br], the rate constant being nearly the same for both the complexes at high $[H^+]$. Under these conditions, the latter complex should be mainly in the form

Table 1—Rate Constants[a] for Iron(II) Reduction of *trans*-$[Co(dmgH)_2(NH_3)Br]^b$(I) and *trans*-$[Co(dmgH)_2(N\text{-glycine})Br]^c$(II)

$[H^+]$ 10^3 mol dm^{-3}	$k \times 10$ (dm^{3}mol^{-1}s^{-1})	
	I	II
2.3	4.41	—
3.0	—	1.5
3.4	3.62	—
5.0	2.91	1.43
6.0	2.62	—
7.5	2.30	1.31
10.0	1.89	1.25
13.0	1.68	—
20.0	—	1.06
30.0	1.12	—
50.0	—	0.74
60.0	0.81	—
80.0	—	0.60
100.0	0.71	0.57

(a) $I = 1.0$ mol dm^{-3} ($LiClO_4$); temp. = 30°C
(b) [Complex] = 3.14×10^{-5} mol dm^{-3}; [Fe(II)] = 6.62×10^{-4} mol dm^{-3}
(c) [Complex] = 9.2×10^{-5} mol dm^{-3}; [Fe(II)] = 9.2×10^{-4} mol dm^{-3}

$[Co(dmgH)(dmgH_2)(NH_2CH_2COOH)Br]$ in the $[H^+]$ range employed. The acid dissociation constants for the complex were measured *p*H-metrically[6], the values being $pK_1 = 3.2$ and $pK_2 = 5.8$. The first protonation step should be due to the oxime ($pK = 5.8$) and the second, to the glycine ($pK = 3.2$). Extensive protonation of the oxime should inhibit precursor formation with Fe(II), while at the same time, Fe(II) binds to the free carboxylato group of the glycine, thus strongly reducing the ease of electron transfer, since glycine is not an electron mediator. It may be noted that there is a marked increase in the protonation constant of the oxime when glycine replaces the ammine at the axial position of the complex.

References

1 Balasubramanian P N & Vijayaraghavan V R, *Inorg Chim Acta*, **38** (1980) 49.
2 Arunachalam M K, Balasubramanian P N & Vijayaraghavan V R, *J inorg nucl Chem*, **43** (1981) 753.
3 Ablov A V & Samus N M, *Russ J inorg Chem*, **5** (1960) 410.
4 Ablov A V & Filippov M P, *Russ J inorg Chem*, **4** (1959) 1004.
5 Kitson R E, *Anal Chem*, **22** (1959) 664.
6 Irving H & Rossotti H S, *J chem Soc*, (1953) 3397.

Indian Journal of Chemistry
Vol. 27A, November 1988, pp. 999-1001

Iron ⇌ Calcium Ion Exchange Reaction in Cement Hydration Phase, 11 Å Tobermorite

NITIN LABHASETWAR & O P SHRIVASTAVA*

Department of Chemistry, Dr H S Gour Vishwavidyalaya, Sagar 470003

Received 23 *October* 1987; *revised and accepted* 28 *January* 1988

An important phase formed during the hydration reaction of cements is identical with the mineral tobermorite, a calcium silicate hydrate close to $Ca_5Si_6O_{18}H_2.4H_2O$. The crystalline synthetic 11Å tobermorite undergoes exchange with iron to give tobermorites having 0.93-14.12 wt% of Fe when placed in a dilute solution containing initially 100-1800 ppm of Fe^{3+} ions at 25°C. The equilibrium is reached after 7-10 days. The $3Ca^{2+} \rightleftharpoons 2Fe^{3+}$ exchange reaction of this calcium silicate hydrate is very much similar to that of clays and zeolites. The free energy of exchange reaction is −498.6 cal/equiv.

Barrer[1] has pointed out that the structure of several layer silicates should favour ion exchange due to their typical anionic frame work. The calcium silicate hydrate $Ca_5Si_6O_{18}H_2.4H_2O$, has been identified as a cation exchanger[2-5]. This compound is identical with silicate mineral 11Å tobermorite, an important phase in hydration reaction of portland cement. Previous studies have confirmed that the ion-exchange reaction takes place in 11Å synthetic tobermorite, but the thermodynamics and mechanism of such exchange reactions are not yet fully understood. We present here quantitative data on the iron ⇌ calcium exchange reaction in 11Å tobermorite with a view to understanding the thermodynamics of the exchange reaction.

Tobermorite was synthesized by the method described by Kalousek[6]. Calcium oxide was obtained by igniting pure reagent grade calcium carbonate (Analar) in a platinum crucible at 1000°C; silicondioxide was obtained from optical grade quartz (0.90% non-volatile with hydrofluoric acid) which has been ground in an agate-lined micronizing mill. To promote batch reactivity, additional aluminium oxide was added at the rate of 0.2 g aluminium oxide per 100g of reactants. The mixed reagents were treated in a stainless-steel autoclave at the saturated steam pressure for 48hr at 175°C. The product thus obtained was washed in water and acetone and dried in CO_2-free air. When placed in water, it gave a *p*H of ~8.0. Examined with the electron microscope, the synthetic product was found to consist of thin platy crystals having maximum lengths of 0.5-5.0 μm. The dried product gave an X-ray powder diffraction pattern which contained 18 prominent reflections having *d*-spacings between 11.3Å and 1.627Å which matched the standard in both position and intensity[7]. The additional reflections are also listed in Table 1.

The calcium ions of the 11Å tobermorite are not exchanged by monovalent ions like Na^+, K^+ or divalent ions larger than Ca^{2+} (e.g. Sr^{2+} Ba^{2+}). However, the Ca^{2+} ions are exchanged partially by Mg^{2+}, Ni^{2+}, Co^{2+} at *p*H = 8. The exchange reaction with iron was effected by shaking 100ml of Fe^{3+} solution (100-1800 ppm) with 1g synthetic

Table 1—X-ray Powder Diffraction Data for Tobermorite and Iron-exchanged Tobermorite

S.	11 Å Tobermorite		Iron exchanged Tobermorite		
S.	*d*-spacings (Å)	I/I_{max} (%)	*d*-spacings (Å)	I/I_{max}	*hkl*
1	11.2103	9.18	11.1397	4.00	002
2	7.0292	3.88	7.0223	20.25	011
3	5.4878	19.31	5.4493	14.54	201
4	Abs*		5.1773	7.91	013
5	Abs		4.4808	9.00	210
6	4.2554	4.29	4.2348	74.39	105
7	3.6344	14.35	3.6355	26.91	115
8	3.5136	11.79	3.5085	16.00	205
9	3.3250	8.58	3.3388	31.64	016
10	Abs		3.2399	30.25	007
11	3.0840	100.00	3.0835	95.06	220
12	Abs		3.0347	38.29	313
13	2.9747	37.35	2.9725	13.14	222
14	2.8138	45.80	2.8084	60.06	400
15	2.7035	6.38	2.7089	11.82	224
16	2.4213	7.17	Abs		027
17	2.3447	8.58	2.3477	12.69	132
18	Abs		2.2824	14.54	209
19	2.2482	14.35	2.2449	14.06	308
20	2.1433	8.88	2.1404	9.38	423
21	2.0697	10.12	Abs		513
22	2.0295	17.15	2.0288	30.25	332
23	1.9996	8.29	Abs		319
24	1.9510	4.94	1.9531	14.06	037
25	Abs		1.8753	9.77	600
26	1.8421	29.75	1.8397	27.56	040
27	1.8164	11.11	Abs		0.112
28	1.7208	8.00	1.6852	44.72	435
29	1.6730	11.79	1.6698	10.56	239
30	1.6122	2.61	1.6019	4.0	4111
31	1.5411	6.63	1.5246	6.89	048
32	Abs		1.5072	23.16	2213

*Peak absent.

tobermorite in each of the nine sealed bottles for 7-10 days. After a steady state had reached, both solution and the solid were analysed. Table 2 summarises the mass balance calculations of the exchange reaction. The data have been collected from the calcium and iron estimations from the solution phase after filtration. The weight per cent of iron has been determined from the solid exchanged product. The ion exchange reaction in 11Å tobermorite can be summarised by the following equilibrium:

$$2Fe^{3+}_{solution} + 3Ca^{2+}_{Tobermorite} \rightleftharpoons 2Fe^{3+}_{Tobermorite} + 3Ca^{2+}_{solution} \quad \ldots (1)$$

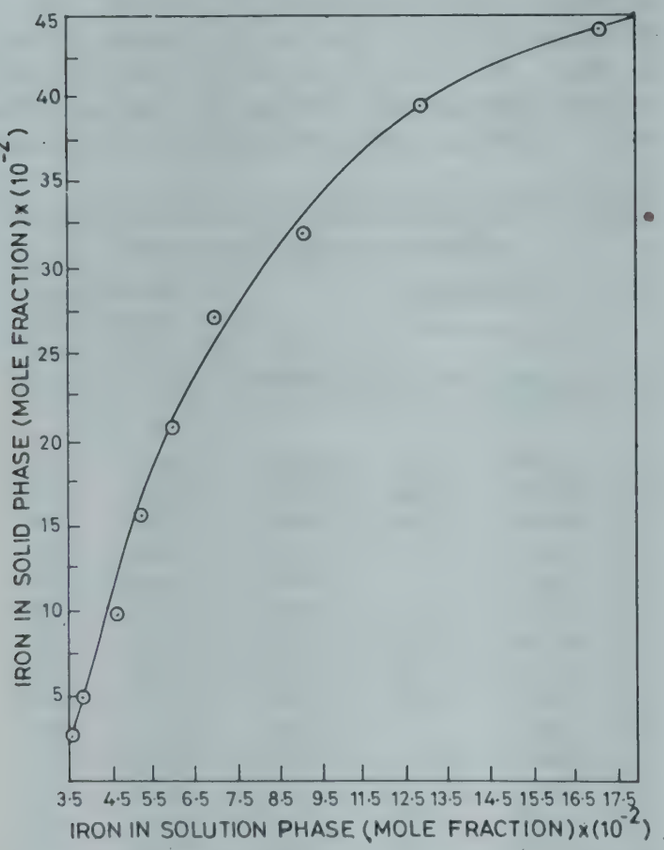

Fig. 1—Ion exchange isotherm for $3Ca^{2+} \rightleftharpoons 2Fe^{3+}$ system in 11Å tobermorite.

The selectivity coefficients have been listed in Table 2. The thermodynamics of this exchange reaction can be worked out on the basis of that already developed for zeolite exchangers by Gaines and Thomas[8] and other workers[9-13]. Fig. 1 shows the ion exchange isotherm for $2Fe^{3+} \rightleftharpoons 2Ca^{2+}$ system in 11Å tobermorite. The plot of $\log_{10} K_d$ against mole fraction of the entering ion in solid phase enabled us to determine the value of equilibrium constant K from the following equation proposed by Gaines and Thomas:

$$\ln K = (b - a) + \int_0^1 \ln K_d . dZ_M$$

where b = charge of the relasing ion from solid phase, a = charge of the incoming ion in solid phase, K_d = selectivity coefficient and Z_M = equivalent fraction of the introduced metal ion in solid phase.

Substitution of $\ln K$ in the relation $\Delta F_T = -RT \ln K$ gave the free energy of the exchange reaction. These free energy calculations have been made for set 6 (1000 ppm Fe^{3+}, marked with asteric in Table 2). Within the limits of experimental error, the best fit value of $\ln K_d$ is 6.796 leading to $\Delta F_{289} = -498.46$ cal/equiv. The plot of $\log_{10} K_d$ against the fractional atomic replacement of Ca^{2+} is linear. The linear relationship breaks down only when the exchanger becomes almost saturated with Fe^{3+} (i.e. beyond 1800 ppm). The mass balance data reveal that the calcium iron molar ratio is about 1.5:1 which agrees with the expected value of molar ratio Ca/Fe for the exchange reaction represented by Eq. (1). The X-ray powder diffraction data of tobermorite and those of iron exchanged tobermorite reveal that the crystallinity of the exchanger remains intact after the cation exchange. The empiri-

Table 2—$3Ca^{2+} \rightleftharpoons 2Fe^{3+}$ Exchange in Synthetic 11Å Tobermorite

Intial [Iron] (mmol/dm³)	Iron in solid phase		Iron in soln. after equilibrium (mmol/100 ml)	Selectivity coeff. K_d†	Calcium released (mmol/g)	Mol Ca^{2+} released / Mol Fe^{3+} in solid	Empirical formulae of iron-exchanged products
	wt%	mmol/g					
1.79	0.93	0.166	0.009	1860.0	0.242	1.46	$Ca_{4.82}Fe_{0.12}Si_6 \cdots\cdots nH_2O$
3.58	1.82	0.326	0.0181	1802.0	0.463	1.42	$Ca_{4.66}Fe_{0.24} \cdots\cdots$
7.16	3.62	0.648	0.0460	1408.5	0.939	1.45	$Ca_{4.31}Fe_{0.47} \cdots\cdots$
10.74	5.41	0.969	0.0760	1276.0	1.366	1.41	$Ca_{4.00}Fe_{0.71} \cdots\cdots$
14.32	7.25	1.298	0.1180	1100.0	1.804	1.39	$Ca_{3.68}Fe_{0.95} \cdots\cdots$
17.90*	8.99	1.609	0.1799	894.5	2.301	1.43	$Ca_{3.31}Fe_{1.18} \cdots\cdots$
21.48	10.45	1.871	0.2740	683.0	2.619	1.40	$Ca_{3.08}Fe_{1.37} \cdots\cdots$
26.85	12.51	2.240	0.4240	527.8	3.136	1.40	$Ca_{2.70}Fe_{1.64} \cdots\cdots$
32.23	14.12	2.528	0.6610	382.6	3.412	1.35	$Ca_{2.50}Fe_{1.85} \cdots\cdots$

K_d is defined as the ratio of the amount of iron sorbed per gram of sample to the amount of unsorbed iron per ml solution.

cal formulae for different exchange products are listed in Table 2. A comparison of TG curves of the exchanger and that of cation-exchanged products between 320 and 1230K shows that the water loss in the exchanged samples follows identical pattern. The TG curves show two regions of water loss, first region or rapid water loss at 323-483K and second extending from 483 to 998K.

Tobermorite has shown remarkable capacity to act as an ion exchanger for iron. Its exchange properties can be compared with those of two other well known families of silicate minerals: clays and zeolites. The complete thermodynamics of tobermorite exchange reaction could be developed for divalent and trivalent ions. A preliminary methematical treatment of exchange properties reveals that a formal analogy exists between this exchange and zeolitic exchange reactions.

The crystal structure of mineral 11Å tobermorite has been studied in detail by Hamid *et al.*[14,15] Examination of exchange properties in the light of crystal structure of tobermorite lead us to believe that the 'interlayer' calcium content is the most favourable site for substitution. Mössbauer studies on the sample are in progress.

The authors are greatful to the M P Council of Science and Technology for providing funds for this work. Thanks are due to Prof. F P Glasser for his valuable suggestions. We also thank the Head, Department of Chemistry, Dr H S Gour Vishwavidyalaya, Sagar for providing facilities.

References

1 Barrer R M, *Zeolites and clay minerals as sorbents and molecular sieves*, (Academic Press, London, New York) (1978) 497.
2 Shrivastava O P & Glasser F P, *J React Solids*, 2 (1986) 261.
3 Srivastava O P & Glasser F P, *J Mat Sci Lett*, **4** (1985) 1122.
4 Komarneni S, Roy D M & Roy R, *Cem Concr Res*, **12** (1982) 773.
5 McCulloch C E, Angus M J, Crowford R W, Rahman A A & Glasser F P, *Min-Mag*, **49** (1985) 211.
6 Kalousek G L, *J Am ceram Soc*, **40** (1957) 74.
7 *JCPDS powder diffraction file*, (Inorganic Press, Mineral Section, File No. 19-1364) (1983).
8 Gaines G L & Thomas H C, *J chem Phys*, **21** (1953) 714.
9 Rosseinsky, *Chem Rev*, **65** (1965) 467.
10 Barrer R M & Meiser W M, *Trans Faraday Soc*, **55** (1959) 130.
11 Barrer R M, Ress L V C & Ward D J, *Proc Roy Soc (London)*, **A-273** (1963) 180.
12 Ames L L, *J Am Mineralogist*, **49** (1964) 1099.
13 Sherry H S & Walton H F, *J phys Chem*, **70** (1966) 1158.
14 Hamid S, *Z Fur Kristallogr*, **154** (1981) 189.
15 Megaw H D & Kelsey C, *Nature*, **177** (1956) 390.
16 Mitsuda T & Taylor H F W, *Min-Mag*, **42** (1978) 229.

Indian Journal of Chemistry
Vol. 27A, November 1988, pp. 1002-1004

Synthesis & Characterisation of Di- & Tri-telluratoferrate(III) Complexes

H G MUKHERJEE* & (Miss) SHYAMALI DE
Department of Chemistry, University College of Science, Calcutta 700 009
and
L C W BAKER
Georgetown University, Washington D C, U S A

Received 6 *September* 1985, *revised* 11 *August* 1986; *rerevised and accepted* 7 *March* 1988

$Li_7[Fe(H_2TeO_6)_2(OH)_2].3H_2O$ and $Li_6Fe_4Te_3O_{24}H_{12}.2H_2O$ or $[Li_6Fe_4Te_3O_{18}, 6H_2O]$, $2H_2O$ have been prepared by the reaction of telluric acid, ferric nitrate and lithium sulphate in different alkaline media. These compounds have been characterised by chemical analyses, oxidation state determination, magnetic moment measurements, thermal analyses, electronic and infrared studies. Probable structures of these compounds have been suggested.

Tellurate can function as a heteropoly addendum like periodate, because it contains Te(VI) which has small size, high positive charge and ability to take tetrahedral and octahedral geometry with oxygen donors. Furthermore, tellurate ion is a good oxidising as well as stabilising agent. Like periodate it can stabilise unusual oxidation states of many transition metal ions[1-3].

Nyman and Campbell[4] reported two periodates of iron(III), $Na_5Fe(H_2IO_6)_2(OH)_2$ (1:2 type) and $H_3Fe_4I_3O_{24}H_{12}$ (4:3 type) similar to the corresponding cobalt(III) compounds[5,6]. This inspired us to prepare the corresponding tellurato complexes of iron(III), $Li_7[Fe(H_2TeO_6)_2(OH)_2].3H_2O$ (in weak alkaline medium) and $Li_6Fe_4Te_3O_{24}H_{12}.2H_2O$ (in strong alkaline medium). The complexes have been characterised by various physico-chemical studies.

Lithium bis(dihydroxo dihydrogentellurato)ferrate(III) trihydrate

Ferric nitrate (1 g, 0.002 mol) dissolved in 25 ml of water and telluric acid (1.3 g, 0.004 mol) dissolved in 25 ml of water were heated separately to 70-80°C. Telluric acid solution was added to the ferric nitrate solution with stirring. A brown solution was formed to which was added 50 ml of 1.5 *N* potassium hydroxide solution with stirring. The yellow solution so formed was allowed to settle and filtered off. To this filtrate an aqueous solution of lithium sulphate (2 g, 0.02 mol) was added with stirring. A light yellow compound was precipitated; it was filtered through a sintered bed and washed several times with water-methanol (1:1) mixture to remove excess alkali. The compound was finally washed with ether and dried *in vacuo* over fused calcium chloride for 48 hr.

Lithium tris(tellurato)tetrakis-ferrate(III) dihydrate

Telluric acid (1.3 g, 0.004 mol) dissolved in 25 ml of water was mixed with 50 ml of 3 *N* potassium hydroxide solution and warmed at 70-80°C. To it 25 ml of an aqueous solution of ferric nitrate (1 g, 0.002 mol), warmed at 70-80°C, were added with constant stirring. A dark brown solution was formed. The solution was filtered off and to the filtrate an aqueous solution of lithium sulphate (2 g, 0.02 mol) was added with stirring; the compound thus obtained was filtered and collected as above.

Tellurium was estimated gravimetrically[7]. Iron was estimated by dichromate as usual[8]. Lithium was estimated using a Varian Techtron AA6 spectrophotometer. Water was determined by the weight loss of the compound at 120°C for 4 hr.

The magnetic moment of the di(tellurato)ferrate(III) compound was measured by the Gouy method at 300°K using copper sulphate pentahydrate as the calibrant. The magnetic susceptibility of the compound was corrected using Pascal's constants.

Magnetic susceptibilities and magnetic moments of the tritellurato tetraferrate(III) compound were measured in the temperature range 83-302°K using a Curie type Faraday balance.

Thermograms of the compounds were recorded with a Shimadzu Thermal Analyser DT-30 at the rate of 10° per minute from room temperature (30°) to 600°C in the nitrogen atmosphere. Simultaneously, DTA curves were also recorded with the same instrument. The decomposition products in each step were isolated and their percentage compositions were determined by chemical analyses.

Reflectance spectra of the solid compounds were recorded on a Cary 17D spectrophotometer, using magnesium carbonate as standard, in the range of 800-200 nm. The compounds were poorly soluble in water and the electronic spectra were recorded with the alkaline mother liquor using the same instrument.

Infrared spectra of the complexes were recorded on a Perkin-Elmer 357 spectrophotometer in cesium iodide phase in the range 4000-200 cm^{-1}.

Analytical data of the complexes are given in Table 1.

Oxidation states of tellurium and iron were determined iodometrically[9]. The following reactions in-

Table 1—Analytical Data of the Complexes

Compound	Found (Calc.),%			
	Li	Fe	Te	H_2O
$Li_7[Fe(H_2TeO_6)_2(OH)_2].3H_2O$	7.35 (7.54)	8.75 (8.67)	39.80 (39.65)	8.34 (8.38)
$Li_6Fe_4Te_3O_{24}H_{12}.2H_2O$	3.78 (3.78)	20.67 (20.68)	35.79 (35.45)	3.37 (3.33)

Table 2—Results of Magnetic Studies of Tri(tellurato)tetraferrate(III)

Temp (K)	$\chi_M \times 10^6$ (cgs) [$\chi_d = 253.70 \times 10^{-6}$]	$1/\chi_{Fe} \times 10^{-2}$	$\mu_{eff.}$ (B.M.)
302.3	18,980	2.10	3.401
287.5	19,960	2.00	3.394
265.3	20,843	1.92	3.339
213.3	23,882	1.67	3.105
195.2	26,628	1.50	3.237
136.8	36,040	1.11	3.152
102.9	44,962	0.89	3.054
83.7	55,159	0.72	3.050

dicate that the di(tellurato)ferrate(III) and tri(tellurato)tetraferrate(III) complexes require 5 and 10 equivalents of sodium thiosulphate respectively.

$$Li_7[Fe(H_2TeO_6)_2(OH)_2].3H_2O + 5I^- + 10\,H^+ = 7Li^+ + Fe^{2+} + 2TeO_3^{2-} + 5/2I_2 + 11H_2O$$

$$Li_6Fe_4Te_3O_{24}H_{12}.2H_2O + 10I^- + 18H^+ = 6\,Li^+ + 4Fe^{2+} + 3TeO_3^{2-} + 5I_2 + 17H_2O$$

The experimental magnetic moment value of di(tellurato)ferrate(III) compound is found to be 5.93 B.M. which is very close to the expected value of 5.9 B.M. for the high-spin (sp^3d^2) octahedral iron(III) complexes.

Magnetic susceptibility and magnetic moment values of the tritellurato tetraferrate(III) compound are given in Table 2.

The spin only $\mu_{eff.}$ value ($S = 5/2$) should be equal to 5.92 B.M., but the experimental value obtained is nearly 3.40 B.M. at room temperature ($\sim 302°K$). This low value of $\mu_{eff.}$ may be attributed to the presence of oxygen bridge between iron atoms, analogous to those of the dimer $Fe_2(OH)_2^{4+}$ or of the enneacarbonyl, $Fe_2(CO)_9$, which were found to be diamagnetic[10]. Similar observations were found in many other polynuclear iron complexes[11]. Moreover, the reciprocal magnetic susceptibilities per iron atom calculated for different temperatures showed that the compound deviated widely from Curie-Weiss behaviour. These results are highly suggestive of polynuclear structure of tri(tellurato) tetraferrate(III) compound.

The di(tellurato)ferrate(III) compound loses three molecules of water of crystallisation within 140°C, and has a corresponding DTA peak at 100°C. The second step of decomposition (140°-330°C) involves the elimination of three molecules of water with the formation of an intermediate product $Li_7FeTe_2O_{11}$. The compound completely decomposes at 570°C with the formation of Li_2TeO_3, Li_2O and $LiFeO_2$ and elimination of oxygen. DTA shows corresponding decomposition at 545°C.

The tri(tellurato)tetraferrate(III) compound starts to decompose below 100°C with the release of two molecules of loosely held water of crystallisation and is decomposed within 170° with the release of six molecules of coordinated water which is also supported by DTA data. It is endothermic reaction and takes place at peak temperature of 80°C. The decomposition at 170°C is a slow process and continues upto 480°C with the formation of an intermediate product, $Li_6Fe_4Te_3O_{15}$ and liberation of oxygen molecules. The final decomposition step completes at 700°C with a sharp peak for DTA at 540°C. The final products are found to be Fe_2O_3, Li_2O and TeO_2 (formed at 600°C or above)[12].

The reflectance spectra of the compounds are characterised by three bands at 200-240, 350-370 and 470 nm. The band at 200-240 nm is due to TeO_6 octahedron[2] and the bands at 350-370 and 470 nm are due to *d-d* transition $^6A_{1g} \rightarrow {}^4T_{2g}$ and $^6A_{1g} \rightarrow {}^4T_{1g}$, ^4E_g respectively which indicate the six-coordinated high-spin (sp^3d^2) octahedral state of iron(III)[13].

The electronic spectra of the mother liquor are characterised mainly by two bands: one around 220-230 nm due to TeO_6 octahedron and other at 470 nm due to $^6A_{1g} \rightarrow {}^4A_{1g}$, ^4E_g transition of six-coordinated Fe(III)[13]. Some deviation of the bands in electronic spectra may be due to solvation effect.

The infrared spectra of both the compounds are more or less identical. A band appearing at 3550-3000 cm^{-1} (b,s) is due to ν_{OH} mode of the water molecules[14] and TeOH hydroxo group. The band at 2370 cm^{-1} (ms) is the first harmonic of Te−OH band around 1210 cm^{-1} while the band at 1670 cm^{-1} (ms) is due to δHOH of coordinated water. The absorption spread around 1075 cm^{-1} (ms) is due to δ_{Te-OH} and Fe−OH bridging vibrations[15]. The medium strong band at 860 cm^{-1} in the case of tri(tellurato)tetraferrate(III) is due to Fe−O−Fe bridging[16] present in this type of polynuclear complexes. Absorption at 660 cm^{-1} (ms) in both the complexes is due to ν_{Te-O} vibration whereas the ν_{M-O} appears at 525 cm^{-1} (ms)[17,18] and the band at 450 cm^{-1}(ms) is due to δ_{O-Te-O} (as compared to O−I−O)[19] and FeO_6 octahedron[18]. The weak absorption that appears at 310 cm^{-1} may be assigned as δ_{O-M-O} and δ_{M-O-Te} vibrations[17] and the bands appearing in the lower ranges are due to lattice vibrations[18].

The authors thank Dr. N. Roychoudhury, Prof. M. Choudhury, (Mrs) D. Ghosh and D. Das of the Indian Association for the Cultivation of Science, Calcutta; Dr. N. Roy of G.S.I., Calcutta; S. Maikap of Bose Institute, Calcutta; and Dr. B. Mondal and Dr. B.K. Das of Science College, Calcutta for their kind help and cooperation.

References

1 Lister M W, *Can J Chem*, **39** (1961) 2330.
2 Balikungeri A, Pelletier M & Monnier D, *Inorg chim Acta*, **22** (1977) 7.
3 Lister M W & McLeod P, *Can J Chem*, **43** (1965) 1720.
4 Campbell M J M & Nyman C J, *Inorg Chem*, **1** (1962) 842.
5 Baker L C W, Mukherjee H G & Chaudhury B K, *Indian J Chem*, **19A** (1980) 589; *J Indian chem Soc*, **57** (1980) 16.
6 Baker L C W, Lebioda L, Gromouski J & Mukherjee H G, *J Am chem Soc*, **102** (1980) 3274.
7 Hornberger A W, *J Am chem Soc*, **30** (1908) 387.
8 Vogel A I, *A text book of quantitative inorganic analysis* (Longmans Green, London), 1962, 310.
9 Lister M W & Yoshino Y, *Can J Chem*, **38** (1960) 45.
10 Selwood P W, *Magnetochemistry*, 2nd Edn (Interscience, New York), (1956) 216.
11 Bancroft G M, Maddock A G & Randi R P, *J chem Soc A*, (1968) 2939.
12 Duval C, *Inorganic thermogravimetric analysis*, 2nd Edn (Elsevier Publication, New York), 1963, 520.
13 Lever A B P, *Inorganic electronic spectroscopy* (Elsevier, Amsterdam, London, New York) 1968, 294.
14 Siebert V H, *Z anorg allg Chem*, **301** (1959) 161.
15 Nakamoto K, *Infrared spectroscopy of inorganic and cordination compounds* (John Wiley, NY), 1963, 82.
16 Collins R L & & Pettit R, *J chem Phys*, **39** (1963) 3433.
17 Siebert H, *Z Naturforsch*, **27B** (1972) 1299.
18 Nyqist R A & Kagel R O, *Infrared spectra of inorganic compounds* (Academic Press, N Y) 1971.
19 Baker L C W, Mukherjee H G, Sarkar S B & Chaudhury B K, *Indian J Chem*, **21A** (1982) 618.

Indian Journal of Chemistry
Vol. 27A, November 1988, pp. 1005-1007

Thorium(IV) Nitrate Complexes with Some Substituted Pyrazol-5-ones

BABU KUNCHERIA & P INDRASENAN*
Department of Chemistry, University of Kerala,
Trivandrum 695 034

Received 31 *August* 1987; *revised* 4 *February* 1988;
accepted 16 *February* 1988

Nine new complexes of thorium(IV) nitrate with some pyrazol-5-one derivatives such as 3-methyl-1-phenylpyrazol-5-one, 3-methyl-4-phenacyl-1-phenylpyrazol-5-one, 4-benzoyl-3-methyl-1-phenylpyrazol-5-one, 3-methyl-4-nitroso-1-phenylpyrazol-5-one, 3-methyl-4-nitrosopyrazol-5-one, 2,3-dimethyl-4-nitroso-1-phenylpyrazol-5-one, 1-carbimido-3-methylpyrazol-5-one, 2,3-dimethyl-1-phenyl-4-(2,4-dihydroxyphenylazo)pyrazol-5-one and 2,3-dimethyl-1-phenyl-4-(2-hydroxynaphthylazo)-pyrazol-5-one have been synthesised and characterised on the basis of elemental analyses, IR spectral, conductance, magnetic moment and molecular weight data.

Pyrazolone and substituted pyrazolones form stable complexes with lanthanides and actinides[1-8]. Herein we report the preparation and characterisation of nine new stable complexes of thorium(IV) nitrate with some pyrazolone derivatives, viz. 3-methyl-1-phenylpyrazol-5-one (MPP), 3-methyl-4-phenacyl-1-phenylpyrazol-5-one (MPPP), 4-benzoyl-3-methyl-1-phenylpyrazol-5-one (BMPP), 3-methyl-4-nitroso-1-phenylpyrazol-5-one (MNPP), 3-methyl-4-nitrosopyrazol-5-one (MNP), 2,3-dimethyl-4-nitroso-1-phenylpyrazol-5-one (DNPP), 1-carbimido-3-methylpyrazol-5-one (CMP), 2,3-dimethyl-1-phenyl-4-(2,4-dihydroxyphenylazo)pyrazol-5-one (DPDP) and 2,3-dimethyl-1-phenyl-4-(2-hydroxynaphthylazo)pyrazol-5-one (DPHP).

Thorium(IV) nitrate (BDH, 99.9% pure) was used as such. The ligand MPP was obtained commercially (BDH, AR) and all other ligands were prepared by literature methods[9-14]. The solvents such as methanol, ethanol, chloroform, acetone, acetonitrile and ether were dried by the usual methods. The complexes were prepared as described below.

A solution of thorium nitrate (2 mmol) and the ligand (4 mmol for DNPP, CMP and DPDP; 6 mmol for other ligands) in methanol (for MPP and MPPP), ethanol (for BMPP and DNPP), acetone (for MNPP, MNP and DPHP) and acetonitrile (for CMP and DPDP) was refluxed for 3 hr. In the case of BMPP sodium acetate (1 g) was also added. The resulting solution was concentrated (i) to a viscous mass in the cases of MPP, MPPP, MNPP, MNP and DPHP, (ii) to half the volume to get crystals of the complexes of BMPP, CMP and DPDP and (iii) to one quarter of its volume to get crystals of DNPP complex. The viscous masses obtained for MPP, MNPP, MNP and DPHP were stirred repeatedly with hot benzene to remove excess ligands leaving behind solid complexes. The MPP complex was recrystallised by dissolving in minimum quantity of methanol and adding ether, while the complexes of MNPP, MNP and DPHP were recrystallised from acetone after adding ether. The complex of MPPP obtained as a viscous mass was washed several times with chloroform to remove excess ligand and the complex was recrystallised from methanol after adding chloroform. All the complexes were filtered and dried *in vacuo* over phosphorus(V) oxide.

Room temperature ($28 \pm 2°C$) molar conductivities of 10^{-3} *M* solutions of the complexes in acetonitrile, methanol and nitrobenzene were measured using an ELICO conductivity bridge type CM 82 fitted with dip type cell (type-CC-03) having platinum electrodes (cell constant, 1.28 cm^{-1}). Room temperature magnetic susceptibilities were measured by the Gouy method using mercury(II) tetrathiocyanatocobaltate(II) as the calibrant. The IR spectra of the ligands and the complexes were recorded in KBr in the range 4000-400 cm^{-1} on a Perkin-Elmer 397 IR spectrophotometer. Molecular weights of the complexes ($\sim 10^{-3}$ *M* solutions) were determined by the cryoscopic method using nitrobenzene as the solvent[15].

All the complexes are coloured non-hygroscopic crystalline solids (Table 1). Analytical and molecular weight data of the complexes (Table 1) indicate the general compositions as $ThL_3(NO_3)_4$ (L = MPP, MPPP and MNPP), $Th(BMPP)_3NO_3$, $ThL_2(NO_3)_4$ (L = MNP, DNPP and CMP) and $ThL_2(NO_3)_2$ (L = DPDP and DPHP). Amongst the nine complexes, $Th(CMP)_2(NO_3)_4$ and $Th(DPDP)_2(NO_3)_2$ are insoluble in almost all the common solvents and hence their molecular weights and molar conductivities could not be determined.

Molar conductances of the complexes in acetonitrile, methanol and nitrobenzene (Table 1) are in the ranges expected for nonelectrolytes indicating that nitrate ions are coordinated to the metal ions[16]. However, in acetonitrile and methanol slightly higher values than those expected for nonelectrolytes are observed for some of the complexes. This is probably due to partial replacement of the coordinated nitrate groups by the solvent molecules. All

Table 1—Analytical, Molecular Weight and Conductance Data of Thorium(IV) Nitrate Complexes with Some Pyrazol-5-one Derivatives

Complex	Colour	Found (Calc), %				Mol. wt found (Calc)	Λ_M of 10^{-3} *M* solutions		
		Metal	C	H	N		Aceto-nitrile	Methanol	Nitro-benzene
$[Th(MPP)_3(NO_3)_4]$	Pale yellow	23.1 (23.0)	36.1 (35.9)	3.2 (3.0)	13.7 (13.9)	1017 (1002)	42.2	113.2	7.9
$[Th(MPPP)_3(NO_3)_4]$	Brown	17.1 (17.0)	47.5 (47.7)	3.5 (3.5)	10.4 (10.3)	1330 (1356)	41.4	97.3	8.7
$[Th(BMPP)_3(NO_3)]$	Yellow	20.4 (20.6)	54.3 (54.4)	3.5 (3.5)	8.2 (8.7)	1096 (1125)	—	45.8	2.4
$[Th(MNPP)_3(NO_3)_4]$	Yellow	21.0 (21.3)	32.9 (33.1)	2.6 (2.5)	16.4 (16.7)	1038 (1089)	15.9	—	2.3
$[Th(MNP)_2(NO_3)_4]$	Yellow	31.7 (31.6)	13.0 (13.1)	1.5 (1.4)	19.0 (19.1)	752 (734)	23.6	63.2	2.3
$[Th(DNPP)_2(NO_3)_4]$	Brown yellow	25.4 (25.4)	28.6 (28.9)	2.9 (2.4)	15.3 (15.3)	952 (914)	48.2	94.3	6.5
$[Th(CMP)_2(NO_3)_4]$	Pale pink	30.3 (30.4)	15.3 (15.7)	1.8 (1.8)	18.2 (18.4)	— (762)	—	—	—
$[Th(DPDP)_2(NO_3)_2]$	Red orange	23.0 (23.1)	40.2 (40.7)	2.9 (3.0)	13.6 (13.9)	— (1002)	—	—	—
$[Th(DPHP)_2(NO_3)_2]$	Red orange	21.5 (21.7)	47.2 (47.1)	3.3 (3.2)	13.0 (13.1)	1041 (1070)	61.3	113.7	8.5

the complexes, as expected for Th^{4+} ion, are diamagnetic.

The IR spectra of the ligands exhibit $\nu C=O$ modes (ring carbonyl) at 1600 (BMPP), 1605 (for MPP and MPPP), 1610 (DPDP), 1640 (CMP), 1660 (DPHP), 1680 (DNPP), 1690 (MNPP) and 1700 cm^{-1} (MNP). This band is shifted to lower wavenumber in the complexes of seven ligands (except those of MPP and MPPP) indicating that the ring carbonyl group is bonded to the metal ion in these seven complexes. While the solution spectra of MPP and its complex show that the ring carbonyl of MPP is coordinated to the metal ion, those of MPPP indicate that the ring C=O of MPPP is not coordinated. The apparent non-shift of $\nu C=O$ of MPP complex in the solid state is due to the presence of strong hydrogen bonding[3,17]. The side chain $\nu C=O$ modes of MPPP (1675 cm^{-1}), BMPP (1640 cm^{-1}) and CMP (1700 cm^{-1}) are shifted to 1640, 1610 and 1660 cm^{-1}, respectively on complexation. Therefore, in the complexes of these ligands the side carbonyl group is also participating in coordination. The doubly split band in the region 3500-3450 cm^{-1} observed in the spectrum of CMP due to νNH_2 is not appreciably shifted in the complex indicating noninvolvement of the $-NH_2$ group in coordination.

The $\nu N=O$ modes in the spectra of MNPP, MNP and DNPP appearing in the region 1420-1410 cm^{-1} are shifted in the complexes and appear in the range 1400-1390 cm^{-1}, indicating participation of $-N=O$ group in coordination with the metal ion. The comparatively small shifts (~20 cm^{-1}) in $\nu N=O$ modes may be due to coupling of $\nu N=O$ vibration with other stretching vibrations of the ligand.

The ligand BMPP, DPDP and DPHP exhibit a broad band in the regions 2900-2300, 2900-2400 and 3600-2900 cm^{-1}, respectively, assignable to H-bonded νOH modes. On complexation this band vanishes suggesting that the hydroxy group is coordinated to the metal ion via deprotonation. The deprotonation is further supported by the elimination of the NO_3^- ions in the complexes of BMPP, DPDP, and DPHP. The band at 1220 cm^{-1} in the spectrum of DPDP is assigned to $\nu H-O...H$. This mode is slightly shifted to a higher wavenumber (1230 cm^{-1}) in the complex showing that the Th^{4+} ion is substituted for H^+ ion in the $H-O...H$ system. The $\nu N=N$ modes of DPDP and DPHP appearing at 1480 cm^{-1} are shifted to 1440 cm^{-1} in the complexes of these ligands indicating the participation of π bond of N=N system in complexation with the Th^{4+} ion.

IR spectra of all the nine complexes exhibit three additional bands at 1420, 1280 and 1020 cm^{-1}. The bands at 1420 and 1280 cm^{-1} are the two split bands ν_4 and ν_1, respectively of the coordinated nitrate groups. The third band at 1020 cm^{-1} is attributed to ν_2 mode of NO_3 group. Since the magni-

tude of splitting, $\nu_4 - \nu_1$ is of the order of 140 cm^{-1}, nitrate groups are coordinated monodentately in all the complexes[18], which is supported by the nonelectrolytic behaviour of the complexes.

The above observations and discussion suggest that the present complexes have the formulae shown in Table 1. The ligands MPP and MPPP act as monodentate ones coordinating only through the ring carbonyl group. The ligands BMPP, MNPP, MNP, DNPP and CMP are bonded to the metal ion in a bidentate fashion, while DPDP and DPHP act as tetradentate ones. Of the nine complexes, the complexes $[Th(BMPP)_3(NO_3)]$, $[Th(DPDP)_2(NO_3)_2]$ and $[Th(DPHP)_2(NO_3)_2]$ have anionic ligands resulting in the removal of the some of the nitrate ions via deprotonation. Thus, in the first three complexes the metal ion has a coordination number of seven. All the other complexes except $[Th(MNPP)_3(NO_3)_4]$ have a coordination number of eight for the metal ion, while in $[Th(MNPP)_3(NO_3)_4]$ a coordination number of ten is suggested for Th^{4+} ion.

The authors are grateful to Prof. C G R Nair for his helpful suggestions and also to the UGC, New Delhi for awarding a teacher fellowship under the FIP to one of them (BK).

References

1 Koppikkar D K, Sivapullaiah P V, Ramakrishnan L & Soundarajan S, *Structure and bonding*, **34** (1978) 135.
2 Okafor E C, *J inorg nucl Chem*, **42** (1980) 1155.
3 Nair C G R & Radhakrishnan P K, *Proc Indian Acad Sci*, **90** (1981) 541.
4 Giri V & Indrasenan P, *Polyhedron*, **2** (1983) 573.
5 Radhakrishnan P K, Indrasenan P & Nair C G R, *Polyhedron*, **3** (1984) 67.
6 Jacob Chacko, *Synth react inorg met-org Chem*, **12** (1982) 361.
7 Sobhanadevi G & Indrasenan P, *Inorg chim Acta*, **133** (1987) 157.
8 Babu Kuncheria & Indrasenan P, *Polyhedron*, **7** (1988) 143.
9 Das N B & Mittra A S, *Indian J Chem*, **16B** (1978) 638.
10 Jensen B S, *Acta chem Scand*, **13** (1968) 1668.
11 Nanda N, Padmanavan S, Tripathy B & Mittra A S, *J Indian chem Soc*, **52** (1975) 533.
12 Podder S N, Sankar A K & Adhya J N, *Z anal Chem*, **203** (1964) 333.
13 Vogel A I, *A textbook of practical organic chemistry* (Longmans, London), 1968, pp. 479 & 622.
14 Gopalakrishnan Nair M R & Prabhakaran C P, *J inorg nucl Chem*, **43** (1981) 3390.
15 Palmer W G, *Experimental physical chemistry* (The University Press, Cambridge), 1954, pp. 119.
16 Geary W J, *Coord chem Rev*, **7** (1971) 81.
17 Katritzky A R & Maine F W, *Tetrahedron*, **20** (1964) 304, 307.
18 Curtis N F & Curtis Y M, *Inorg Chem*, **4** (1965) 804.

Indian Journal of Chemistry
Vol. 27A, November 1988, pp. 1008-1009

Ternary Complexes of Some Lanthanides with Cyclopentanetetracarboxylic Acid, L-Histidine or Methionine as Primary Ligand & Hydroxyquinoline as Secondary Ligand

S K AGRAWAL & K C GUPTA*

Department of Chemistry, B S A College, Mathura 281 004

Received 5 *October* 1987; *revised* 16 *November* 1987; *accepted* 29 *February* 1988

The stability constants and thermodynamic parameters of La^{3+}, Ce^{3+}, Pr^{3+} and Nd^{3+} complexes of *cis*-1,2,3,4-cyclopentanetetra-carboxylic acid (CPTA), L-histidine (Hist) and methionine as the primary ligands and 8-Hydroxyquinoline (HQ) as the seccondary ligand have been determined *p*H-metrically at 30, 40 and 50°C and at an ionic strength $\mu = 0.2$ *M* ($NaClO_4$) by Irving and Rossotti method. The stability constants follow the order: $La^{3+} < Ce^{3+} < Pr^{3+} < Nd^{3+}$.

In the present note, ternary complexes of the type M(A)(B) have been investigated where M = La^{3+}, Ce^{3+}, Pr^{3+} and Nd^{3+}, A = *cis*-1,2,3,4-cyclopentanetetracarboxylic acid (CPTA), histidine (Hist) and methionine and B = hydroxyquinoline (HQ). The modified method of Irving and Rossotti[1,2] has been applied to study the formation constants corresponding to the reaction, MA + B ⇌ MAB.

CPTA (Matheson, Colemon and Bell Co) and other chemicals used were BDH reagents of AR grade. Fresh solutions of metal ions were prepared by dissolving the lanthanum oxide, cerium nitrate, praseodymium nitrate and neodymium nitrate in perchloric acid (AR) and were estimated by standard methods[3]. The solutions of CPTA, L-histidine and methionine were prepared in conductivity water while the solution of HQ was prepared in hydrochloric acid.

The titrations were carried out with a digital Philips *p*H meter model PP 9045.

The following mixtures of solutions were prepared and the total volume was kept 50 ml by adding the required amount of conductivity water:

(A) 0.02 *M* $HClO_4$ + 0.18 *M* $NaClO_4$,

(B) 0.02 *M* $HClO_4$ + 0.002 *M* secondary ligand + 0.18 *M* $NaClO_4$,

(C) 0.02 *M* $HClO_4$ + 0.002 *M* metal perchlorate + 0.002 *M* primary ligand + 0.176 *M* $NaClO_4$,

(D) 0.02 *M* $HClO_4$ + 0.002 *M* metal perchlorate + 0.002 *M* primary ligand + 0.002 *M* secondary ligand + 0.176 *M* $NaClO_4$.

The ionic strength was maintained by adding requisite amount of neutral solution of sodium perchlorate and the ratio of M:A:B was kept 1:1:1. The solutions were titrated against 0.2*M* NaOH and titrations were repeated for accuracy.

The *pK* values of hydroxyquinoline were calculated using the Martell and Chaberek[4] method and are in agreement with the literature values[5]. The values of $\bar{n}$ (the average number of secondary ligand molecules attached to primary complex) were calculated from the equation,

$$\bar{n} = \frac{(V_3 - V_2)(N + E^\circ)}{(V_0 + V_1)\bar{n}H.T^\circ cm}$$

where T°cm = total concentration of metal ion in solution, N = molarity of alkali, E° = initial strength of acid in the system, V_0 = total volume of the mixture taken initially, V_1 = the volume of alkali required in the titration of mineral acid (mixture A). V_3 and V_2 are the differences in volumes of alkali added between curves (D) and (C) and (B) and (A) respectively (Fig. 1) at the same *p*H. $\bar{n}$H is the average number of protons attached to secondary ligand at the same *p*H. Further, *pL* values (free ligand exponent) have been calculated at $\bar{n} = 0.5$. A typical plot of *p*H versus alkali added is presented in Fig. 1 for Ce(III)-L-histidine-HQ system. The calculation shows that the primary complex is formed at a lower *p*H and is stable even at a higher *p*H value. The primary complex curve (C) and mixed ligand curve (D), overlap each other upto *p*H 4.75. This indicates that in this *p*H range,

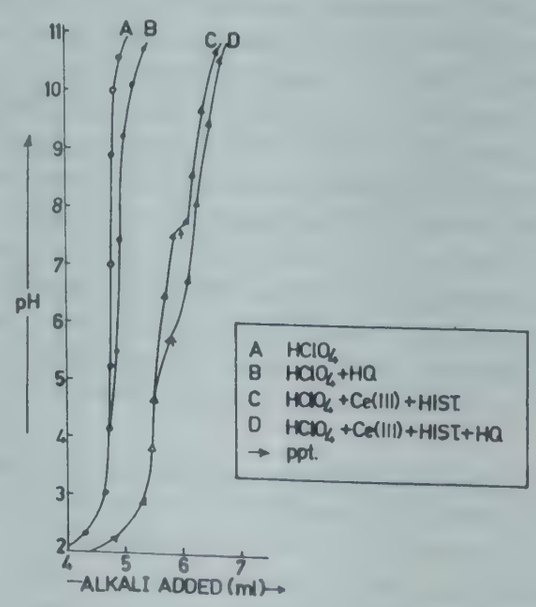

Fig. 1—Titration curves for Ce(III)-L-Hist-HQ mixed ligand system at 30°C

Table 1—Stability Constants and Thermodynamic Parameters of Mixed Ligand Complexes at Different Temperatures [$\mu = 0.2M$ $NaClO_4$]

System	Temp. (°C)	log K^{MA}_{MAB}	$\Delta G°$ (kcal mol^{-1})	$\Delta H°$ (kcal mol^{-1})	$\Delta S°$ (kcal mol^{-1})
	30°	6.36	−8.82		
La(III)-CPTA-HQ	40°	5.88	−8.42	−15.67	−23.16
	50°	5.66	−8.37		
	30°	6.25	−8.67		
Ce(III)-Hist.-HQ	40°	6.08	−8.71	−5.82	9.23
	50°	5.99	−8.85		
	30°	6.30	−8.74		
Pr(III)-Hist.-HQ	40°	6.16	−8.82	−5.37	11.02
	50°	6.06	−8.96		
	30°	6.33	−8.80		
	40°	6.21	−8.89	−5.60	10.05
Nd(III)-Hist.-HQ	50°	6.10	−9.02		
	30°	6.59	−9.13		
Pr(III)-Methionine-HQ	40°	6.17	−8.84	−15.00	−19.68
	50°	5.92	−8.75		
	30°	7.04	−9.76		
Nd(III)-Methionine-HQ	40°	6.52	−9.34	−19.25	−31.66
	50°	6.18	−9.13		

where primary ligand combines with metal, combination of the secondary ligand does not take place. Curve (D) diverges from curve (C) after *p*H 4.75. In this *p*H range combination of the secondary ligand with primary complex starts. The horizontal distance (V_2) between curve (A) and (B) and that (V_3) between curves (C) and (D) indicate the proton released due to self-dissociation of secondary ligand plus the release of proton due to the formation of mixed ligand complex. Thus (V_3-V_2) accounts for the total protons released due to the formation of mixed ligand complex. By using these values, $\bar{n}$ was calculated. The *pL* values were calculated at $\bar{n} = 0.5$ and are summarized in Table 1. The error limit is 0.06 log units.

The values of the change in free energy ($\Delta G°$), enthalpy ($\Delta H°$), and entropy ($\Delta S°$) have been calculated at three different temperatures and at a constant ionic strength $\mu = 0.2M$ ($NaClO_4$) by the temperature coefficient method using Gibb's Helmhlotz equation[6] (Table 1). The higher values for $\Delta S°$ in the M-Hist-HQ systems indicate that the complexation is faster as compared to that in the other systems.

The stability constants of the metal ions follow the order; $La^{3+} < Ce^{3+} < Pr^{3+} < Nd^{3+} < Nd^{3+}$. The above trend is further confirmed by the values of $\Delta G°$ obtained during the course of the investigation.

The authors are thankful to Dr T C Sharma, Principal, Central School, Mathura Cantt for providing computer facilities and to the U G C New Delhi for providing financial assistance to one of them (K C G).

References

1 Irving H M & Rossoti H S, *J chem Soc*, (1954) 2904.

2 Chidambaram M V & Bhattacharya P K, *J inorg nucl Chem*, **32** (1970) 3271.

3 Vogel A I, *A text book of quantitative inorganic analysis* (Longmans Green, London) 1978.

4 Chaberek S & Martell A E, *J Am chem Soc*, **77** (1955) 1477.

5 Louis Meites, *Hand book of analytical chemistry* (McGraw-Hill, New York) 1982.

6 Yatsimirskii K B & Vasi'l eV V P, *Instability constants of complex compounds* (Pergamon, New York) 1960.

Indian Journal of Chemistry
Vol. 27A, November 1988, p. 1010

Formation Constants of Al(III), In(III), Ga(III), Oxovanadium(IV) & Dioxouranium(VI) Chealtes with 8-Formyl-7-hydroxy-4-methyl-2H-1-benzopyran-2-one

P KAMANNARAYANA* & K RAGHAVACHARI
Department of Chemistry, JNTU College of Engineering, Kakinada 533 003

Received 3 *August* 1987; *revised* 12 *November* 1987; *accepted* 19 *February* 1988

Proton-ligand and metal-ligand formation constants of 8-formyl-7-hydroxy-4-methyl-2H-1-benzopyran-2-one chelates with Al(III), In(III), Ga(III), oxovanadium(IV) and dioxouranium(VI) have been determined *p*H-metrically in 70% (v/v) aqueous ethanol at 35°C and $I = 0.1$ *M* ($NaClO_4$). The order of formation constant (log β_2) is: oxovanadium(IV) > dioxouranium(VI) and Ga(III) > In(III) > Al(III).

8-Formyl-7-hydroxy-4-methyl-2H-1-benzopyran-2-one (FHMB) is known to act as a bidendate chelating agent towards bivalent transition metal ions[1] and trivalent lanthanides[2]. In the present note we now report the formation constants of FHMB with Al(III), In(III), Ga(III), oxovanadium(IV) and dioxouranium(VI) in 70% (v/v) ethanol-water medium at 35°C and $I = 0.1$ *M* ($NaClO_4$).

All the chemicals used were of AR grade. The ligand FHMB was prepared by the procedure given in the literature[3]. The *p*H was recorded with an Elico digital *p*H meter model LI-120 equipped with a glass-calomel electrode assembly. The electrode system was calibrated with suitable standard buffers and necessary temperature corrections were made. The *p*H meter readings (B) in 70% (v/v) ethanol-water were corrected by the method suggested by Van Uitert and Haas[4].

Proton-ligand and metal-ligand formation constants have been determined using Irving-Rossotti *p*H titration technique[5]. The following mixtures (total vol 50 ml) were titrated against standard carbonate-free NaOH solution (0.1 *M*) in an inert atmosphere of nitrogen: (i) 5×10^{-3} *M* $HClO_4$; (ii) 5×10^{-3} *M* $HClO_4 + 2 \times 10^{-3}$ *M* FHMB solution; (iii) 5×10^{-3} *M* $HClO_4 + 2 \times 10^{-3}$ *M* FHMB + 4×10^{-4} *M* metal ion solution maintaining a constant ionic strength at 0.1 *M* $NaClO_4$ in 70% (v/v) ethanol-water.

The metal-ligand titration curves were well below the metal ion hydrolysis curves indicating the completion of chelation (as evident from maximum $\bar{n}$ values) before the onset of metal ion hydrolysis. A perusal of the metal-ligand formation curves ($\bar{n}$ versus *p*L) indicates the formation of both 1:1 and 1:2 metal chelates ($0.1 < \bar{n} < 1.8$) with these metal ions. Refined values[6] of the metal-ligand formation constants are presented in Table 1. The standard deviations for proton-ligand and metal-ligand systems are within ± 0.03. The closeness in log K_1 and log K_2 values reveals simultaneous formation of both 1:1 and 1:2 complexes.

Table 1—Proton-Ligand and Metal-Ligand Formation Constants of FHMB in 70% (v/v) Ethanol-Water

[$I = 0.1$ *M* $NaClO_4$; temp. = 35°C]

	H	Al^{3+}	In^{3+}	Ga^{3+}	VO^{2+}	UO^{2+}
log K_1	7.13	6.83	6.56	7.26	6.98	6.86
log K_2	—	5.39	6.32	6.92	6.54	5.54

The order of formation constants of the metal-ligand complexes in the case of oxo ions is oxovanadium(IV) > dioxouranium(VI), while that with respect to trivalent ions is Ga(III) > In(III) > Al(III). The higher stabilities of oxovanadium(IV) complexes as compared to those of dioxouranium(IV) complexes may be attributed to the participation of '3*d*' orbitals in the former in coordination in contrast to behaviour of 5*f* orbitals in dioxouranium(VI). The increase in stability from Al(III) complexes to Ga(III) complexes is in accordance with the decreasing order of charge density and heats of hydrations of these metal ions.

The authors thank the authorities of JNTU College of Engineering, Kakinada for providing the necessary facilities during the course of this investigation.

References

1 Jagannadha Charyulu K, Omprakash K L, Chandrapal A V & Reddy M L N, *J Indian chem Soc*, **60** (1983) 236.
2 Ettaiah P, Jagannadhacharyulu K, Omprakash K L, Chandrapal A V & Reddy M L N, *Indian J Chem*, **24A** (1985) 890.
3 Parikh S H & Thakur V N, *J Univ Bombay*, **36** (1954) 37.
4 Van Uitert L G & Haas C G, *J Am chem Soc*, **75** (1953) 451.
5 Irwing H & Rossotti H S, *J chem Soc*, (1953) 3397; (1954) 2904.
6 Block B P & McIntyre (Jr) G H, *J Am chem Soc*, **75** (1953) 5667.
7 Basalo F & Pearson R G, *Mechanism of inorganic reactions* (John Wiley, New York), 1958, 16.

Indian Journal of Chemistry
Vol. 27A, November 1988, pp. 1011-1012

Ion Selective Membrane Electrodes Based on Precipitated Nitron Halides & Nitron Thiocyanate

RAJESH CHANDRA MISRA & M C CHATTOPADHYAYA*
Department of Chemistry, University of Allahabad, Allahabad 211 002

Received 11 *May* 1987; *revised* 29 *December* 1987; *accepted* 14 *January* 1988

The preparation of new electrodes for Br^-, I^- and SCN^- ions based on precipitated nitron bromide, nitron iodide, nitron thiocyanate as electroactive materials and silicon rubber as inert binder is described. The working *p*H ranges for bromide, iodide and thiocyanate selective electrodes are 2-13, 2-10 and 3-8, respectively. Both the bromide and iodide selective electrodes show linear response in the concentration range of $1 \times 10^{-1} M$ to $1 \times 10^{-5} M$. The thiocyanate selective electrode shows linear response in the concentration range of 1×10^{-1} to $5 \times 10^{-6} M$. The response times of the bromide, iodide and thiocyanate selective electrodes are 10 sec, 20 sec and 15 sec, respectively. The selectivity coefficients for different anions for all the three electrodes have been evaluated. These electrodes are found to be useful in electrometric titrations.

Nitron can be precipitated by various monovalent anions[1]. In this laboratory a nitrate selective electrode based on precipitated nitron nitrate was prepared[2] and found suitable for direct determination of NO_3^- in the presence of other anions, except I^- which caused interference. The present work was undertaken to see if precipitated nitron bromide, iodide and thiocyanate could be used for the preparation of ion selective membrane electrodes for the determination of Br^-, I^- and SCN^-, respectively and to see to what extent other halides and other anions interfere in the working of such electrodes. The characteristics of these electrodes have been examined in detail.

Preparation of master membranes

Brown coloured nitron bromide, ash coloured nitron iodide and black coloured nitron thiocyanate precipitates were obtained by adding respectively Br^-, I^- and SCN^- to a solution of nitron (0.5g) in 20% (v/v) acetic acid. After washing and drying the precipitates, the master membrane with each precipitate was prepared[2] by mixing each of the precipitates (100 mg) with silicon rubber (400 mg).

Preparation of electrodes

A small portion from each nitron halide and nitron thiocyanate membranes was cut and plugged at one end of the glass tube (outer diameter 0.8 cm, inner diameter 0.5 cm) with the help of Araldite (Ciba-Geigy). These tubes were filled with 0.1 *M* solution of KBr, KI and KSCN, respectively. In each of these tubes was added a 0.1 *M* solution of KCl. A saturated calomel electrode was inserted for electrical contact. A separate saturated calomel electrode was used as an external reference electrode. Thus the three electrode systems can be represented as follows:

SCE $Cl^-(0.1M) \times (0.1M)$ Membrane Sample SCE

where X is Br^-, I^-, SCN^-

Before taking measurements each electrode system was kept immersed for six days in 0.1 *M* solution of respective anion.

Three separate sets of solutions of KBr, KI and KSCN were prepared in which the concentration was varied in the range of $1 \times 10^{-1} M$ to $1 \times 10^{-6} M$ and the potential was recorded with respective ion selective electrode with the help of Philips *p*H meter PR-9405M at room temperature ($25° \pm 2°C$). The response of each electrode was plotted against the concentration of respective ion in a semilog graph paper and it was observed that in the case of bromide and iodide selective electrodes, a linear response was obtained down to $1 \times 10^{-5} M$ concentration of the respective ion and for the thiocyanate selective electrode linear response was observed down to thiocyanate concentration of $5 \times 10^{-6} M$. Other properties like response time, *p*H range, age of the membrane of all the three electrodes were determined (Table 1). The selectivity coefficients were determined by mixed solution method[3-5] (Table 2).

Though the iodide ion interfered with the bromide selective electrode, the reverse was not true. There was no interference of iodide ion on thiocyanate selective electrode. The presence of nitrate ion had very

Table 1—Characteristics of Ion Selective Membrane Electrodes

Ion selective electrode	Lower detection limit (*M*)	Per decade change in potential (mV)	Response time (sec)	Working *p*H range	Life of electrode
Bromide	1×10^{-5}	60	10	2-13	Over 6 months
Iodide	1×10^{-5}	50	20	2-10	8 months
Thiocyanate	5×10^{-6}	40	15	3-8	Over 6 months

Table 2—Selectivity Coefficients of Ion Selective Membrane Electrodes at 25 ± 2°C

Ion selective electrode	Selectivity coefficient in presence of interfering anion (0.001 *M*)											
	F^-	Cl^-	Br^-	I^-	NO_3^-	NO_2^-	SCN^-	AC^-	SO_4^{2-}	CO_3^{2-}	$C_2O_4^{2-}$	PO_4^{3-}
Bromide	5.0×10^{-2}	5.0×10^{-2}	–	1.0	5.0×10^{-2}	5.0×10^{-2}	~0[a]	5.0×10^{-2}	1.6×10^{-3}	1.6×10^{-3}	1.6×10^{-2}	5.0×10^{-4}
Iodide	5.0×10^{-2}	5.0×10^{-2}	1.0×10^{-2}	—	1.0	5.0×10^{-2}	~0[a]	~0[a]	3.2×10^{-3}	3.2×10^{-3}	3.2×10^{-2}	5.0×10^{-4}
Thiocyanate	5.0×10^{-2}	5.0×10^{-1}	1.0×10^{-2}	~0[a]	~0[a]	1.0	—	~0[a]	3.2×10^{-3}	1.6×10^{-3}	~0[a]	~0[a]

a selectivity coefficient value of ~0 indicates there is no interference at all concentrations

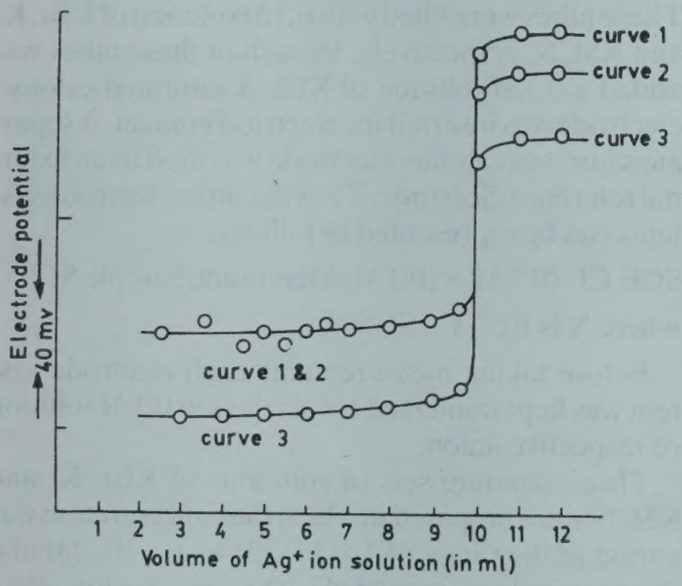

Fig. 1—Precipitation titrations of halide and thiocyanate ions against 0.001 *M* silver nitrate. [Curves 1-3 represent titration of 10 ml of 0.001 *M* potassium iodide, thiocyanate and bromide solutions respectively]

little influence on the selectivity coefficients value of either bromide or thiocyanate selective electrode, althoug it had a marked influence on the working of iodide selective electrode. The presence of other ions either caused very little or no interference on the working of all the three electrodes. Out of the three electrodes, thiocyanate selective electrode was found to be the best, for which the selectivity coefficient values are very small for all the anions studied.

In commercially available Br^- selective electrodes[6] the interference due to iodide is much larger as compared to the present electrode. For Philips and Orion electrodes K_{BrI} values are 20 and 5×10^3 respectively. A comparison of K_{SCNX} values for halide ions for present thiocyanate electrode with those for solid state thiocyanate electrode[7], reveals that with respect to Br^- and I^- interferences, the present electrode is definitely better in performance.

Application

In order to explore the utility of these electrodes in potentiometric titrations, precipitation titrations of soluble silver salt against halide ion was performed using all the three selective electrodes as indicator electrodes.

For titration standard solutions of halide ion (potassium salts) and silver ion were prepared. Usually three sets of solutions for each halide ion were titrated in which concentrations were varied from 0.01 *M* to 0.001 *M*. In all cases there was a sharp increase in the value of electrode potential at the equivalence point (Fig. 1).

The authors are thankful to State Council of Science and Technology, U P, Lucknow for financial help.

References

1 Vogel A I, *Quantitative inorganic analysis* (Longman-ELBS, London) 1969.
2 Lal U S, Chattopadhyaya M C, Dey A K, *Michrochim Acta*, (1980) 417.
3 Pungor E, *Analyt Chem*, **39** (1967) 28A.
4 Overman Robert F, *Analyt Chem*, **43** (1969) 616.
5 Moody G J & Thomas J D R, *Talanta*, **18** (1971) 1251.
6 Lakshinaryaniah N, *Membrane electrodes* (Academic Press, New York) 1976 pp 144.
7 Mascini M, *Anal chim Acta*, **62** (1972) 29.

THE WEALTH OF INDIA

An Encyclopaedia of Indian Raw Materials and Industrial Products, published in two series :
(i) Raw Materials, and **(ii) Industrial Products.**

RAW MATERIALS

The articles deal with Animal Products, Dyes & Tans, Essential Oils, Fats & Oils, Fibres & Pulps, Foods & Fodders, Drugs, Minerals, Spices & Flavourings, and Timbers and other Forest products. Names in Indian languages, and trade names are provided.

For important crops, their origin, distribution, evolution of cultivated types and methods of cultivation, harvesting and storage are mentioned in detail. Data regarding area and yield and import and export are provided. Regarding minerals, their occurrence and distribution in the country and modes of exploitation and utilization are given. The articles are well illustrated. Adequate literature references are provided.

Eleven volumes of the series covering letters A–Z have been published.

Vol. I : A (Revised) Rs. 300.00; Vol. I (A-B) Rs. 120.00; Vol. II (C) Rs. 143.00; Vol. III (D-E) with index to Vols. I-III Rs. 158.00; Vol. IV (F-G) Rs. 150.00; Vol. IV Suppl. Fish & Fisheries Rs. 84.00; Vol. V (H-K) Rs. 171.00; Vol. VI (L-M) Rs. 135.00; Vol. VI : Suppl. on Livestock including poultry Rs. 153.00; Vol. VII (N-Pe) Rs. 150.00; Vol. VIII (Ph-Re) Rs. 129.00; Vol. IX (Rh-Sc) Rs. 200.00; Vol. X (Sp-W) Rs. 338.00; Vol. XI (X-Z) with Cumulative Index to Vols. I-XI Rs. 223.00.

INDUSTRIAL PRODUCTS

Includes articles giving a comprehensive account of various large, medium and small scale industries. Some of the major industries included are : Acids, Carriages, Diesel Engines, Fertilizers, Insecticides & Pesticides, Iron & Steel, Paints & Varnishes, Petroleum Refining, Pharmaceuticals, Plastics, Ship & Boatbuilding, Rubber, Silk, etc.

The articles include an account of the raw materials and their availability, manufacturing processes, and uses of products, and industrial potentialities. Specifications of raw materials as well as finished products and statistical data regarding production, demand, exports, imports, prices, etc. are provided. The articles are suitably illustrated. References to the sources of information are provided.

Nine volumes of the series covering letters A–Z have been published.

Part I (A-B) Rs. 87.00; Part II (C) Rs. 111.00; Part III (D-E) with Index to Parts I-III Rs. 150.00; Part IV (F-H) Rs. 189.00; Part V (I-L) Rs. 135.00; Part VI (M-Pi) Rs. 42.00; Part VII (Pl-Sh) Rs. 90.00; Part VIII (Sl-Tl) Rs. 99.00; Part IX (To-Z) with Index to Parts I-IX Rs. 120.00.

HINDI EDITION : BHARAT KI SAMPADA—PRAKRITIK PADARTH

Vols. I to VII and two supplements of Wealth of India—Raw Materials series in Hindi already published.

Published Volumes :

Vol. I (अ-औ) Rs. 57.00; Vol. II (क) Rs. 54.00; Vol. III (ख-न) Rs. 54.00; Vol. IV (प) Rs. 125.00; Vol. V (फ-मेरे) Rs. 90.00; Vol. VI (मेल-रू) Rs. 120.00; Vol. VII (रे-वाटा) Rs. 203.00; Vol. VIII (वाय-सीसे) Rs. 300.00.

Supplements :

Fish & Fisheries (Matsya & Matsyaki) Rs. 74.00;
Livestock (Pashudhan aur Kukkut Palan) Rs. 51.00

Vols. IX to XI under publication.

Please contact :

SENIOR SALES AND DISTRIBUTION OFFICER

PUBLICATIONS & INFORMATION DIRECTORATE, CSIR
Hillside Road, New Delhi 110 012

RN 7090/63

CSIR PUBLICATIONS

WEALTH OF INDIA

An encyclopaedia of the economic products and Industrial resources of India issued in two series

RAW MATERIALS SERIES – Contains articles on plant, animal and mineral resources.

	Rs.	$	£
Vol. I(A) (Revised)	300.00	94.00	74.00
Vol. I (A-B)	120.00	60.00	26.00
Vol. II (C)	143.00	66.00	34.00
Vol. III (D-E)	158.00	64.00	40.00
Vol. IV (F-G)	98.00	54.00	24.00
Supplement (Fish & Fisheries)	84.00	32.00	21.00
Vol. V (H-K)	171.00	68.00	42.00
Vol. VI (L-M)	135.00	68.00	30.00
Supplement (Livestock including Poultry)	153.00	68.00	39.00
Vol. VII (N-Pe)	150.00	60.00	38.00
Vol. VIII (Ph-Re)	129.00	64.00	28.00
Vol. IX (Rh-Se)	156.00	70.00	38.00
Vol. X (Sp-W)	338.00	150.00	85.00
Vol. XI (X-Z)	223.00	77.00	44.00

INDUSTRIAL PRODUCTS SERIES – Deals with major, Small-Scale and Cottage Industries

Part I (A-B)	87.00	40.00	22.00
Part II (C)	111.00	48.00	28.00
Part III (D-E)	150.00	67.00	39.00
Part IV (F-H)	189.00	84.00	48.00
Part V (I-L)	135.00	46.00	34.00
Part VI (M-Pi)	42.00	16.00	5.60
Part VII (Pl-Sh)	90.00	36.00	12.00
Part VIII (Si-Ti)	99.00	54.00	20.00
Part IX (To-Z)	120.00	68.00	24.00

BHARAT KI SAMPADA (Hindi Edition of Wealth of India, Raw Materials):

Vol. I (अ-औ)	57.00	32.00	13.00
Vol. II (क)	54.00	30.00	12.00
Vol. III (ख-न)	54.00	30.00	12.00
Vol. IV (प)	125.00	68.00	32.00
Vol. V (फ-मेरे)	90.00	44.00	20.00
Vol. VI (मेल-रू)	120.00	54.00	26.00
Vol. VII (रे-वाटा)	203.00	80.00	50.00
Vol. VIII (वाय-सीसे)	300.00	80.00	50.00
Livestock (Kukkut Palan)	51.00	30.00	12.00
Fish & Fisheries (Matsya aur Matsyaki)	74.00	42.00	10.00
A Dictionary of Generic & Specific Names of Plants & Animals Useful to Man	45.00	22.00	10.00

Please Contact :

SENIOR SALES & DISTRIBUTION OFFICER
PUBLICATIONS & INFORMATION
DIRECTORATE, CSIR
HILLSIDE ROAD, NEW DELHI - 110012

OTHER PUBLICATIONS

	Rs.	$	£
The Useful Plants of India	192.00	64.00	48.00
A Dictionary of the Flowering Plants in India by H. Santapau & A.N. Henry	63.00	28.00	16.00
Glossary of Indian Medicinal plants by R.N. Chopra, S.L. Nayar & I.C. Chopra	93.00	32.00	20.00
Supplement to Glossary of Indian Medicinal Plants by R.N. Chopra, I.C. Chopra & B.S. Verma	51.00	18.00	12.00
The Flora of Delhi by J.K. Maheshwari	42.00	16.00	5.50
Illustrations to the Flora of Delhi by J.K. Maheshwari	105.00	44.00	26.00
Herbaceous Flora of Dehra Dun by C.R. Babu	216.00	120.00	44.00
Gnetum by P. Maheshwari & Vimla Vasil	30.00	12.00	4.00
Marsilea by K.M. Gupta	62.00	27.00	16.00
Aquatic Angiosperms	30.00	12.00	4.00
Indian Fossil Pteridophytes by K.R. Surange	99.00	44.00	25.00
Cedrus by P. Maheshwari & Chhaya Biswas	63.00	28.00	16.00
Proteaceae by C. Venkata Rao	108.00	48.00	27.00
Pinus by P. Maheshwari & R.N. Konar	45.00	22.00	16.00
Loranthaceae by B.M. Johri & S.P. Bhatnagar	83.00	37.00	21.00
Abies & Picea by K.A. Chowdhury	21.00	12.00	4.20
Indian Thysanoptera by T.N. Ananthakrishnan	39.00	16.00	5.20
The Millipede Thyropygus by G. Krishnan	18.00	7.00	2.40
Indian Sardines by R.V. Nair	33.00	14.00	4.40
Drug Addiction with special Reference to India by R.N. Chopra & I.C. Chopra	19.00	7.00	2.40
Diosgenin & other Steroid Drug Precursors by L.V. Asolkar & Y.R. Chandha	54.00	26.00	12.00
Cholera Bacteriophages by Dr. Sachimohan Mukerjee	45.00	20.00	12.00
Cottonseed Chemistry & Technology by K.S. Murti & K.T. Achaya	116.00	64.00	26.00
Corrosion Map of India	27.00		3.60
Rural Development and Technology: A Status Report-cum-Bibliography by PR Bose and V.N. Vashist	150.00	76.00	34.00
Termite Problems in India	14.00	6.00	1.80
Research & Development Management	38.00	20.00	
Proceedings of the Seminar on Primary Communications in Science & Technology in India by R.N. Sharma & S. Seetharama	78.00	35.00	68.00

Packing and Postage Extra

Printed & Published by Shri S.S. Saksena, Editor, Publications & Information Directorate (PID)
Hillside Road, New Delhi 110012, at PID Photocomposition-cum-Printing Unit

Regd No. D(C)-1018